CESIUM DODECYL SULPHATE PHASE BEHAVIOR IN AQUEOUS SOLUTIONS AND COMPARISON WITH THE SODIUM DODECYL SULPHATE/WATER PHASE DIAGRAM

A MASTER'S THESIS SUBMITTED TO THE FACULTY OF THE GRADUATE SCHOOL OF THE UNIVERSITY OF MINNESOTA
BY

APOSTOLOS NIKOLAOU VAGIAS

IN PARTIAL FULLFILLMENT OF THE REQUIREMENTS FOR THE DEGREE OF MASTER OF SCIENCE

ADVISORS: H.TED DAVIS (+), ALON McCORMICK, YIANNIS KAZNESSIS

FEBRUARY 2010

ACKNOWLEDGEMENTS

First and foremost, I would like to thank the Department of Chemical Engineering and Materials Science at the University of Minnesota, Minneapolis and the University of Minnesota for the acceptance and continuous support in the program all these years. I would like to thank the faculty members of my department. The knowledge acquired through the graduate courses has been really valuable. Thanks to the teaching assistants, who tried to do the best they could do. Special thanks to the Director of Graduate Studies, Professor David J. Norris for his guidance on the program these 2 years and to the 'head' of the Department, Professor Frank S. Bates. Professors F. S. Bates and H. T. Davis had the marvelous idea to investigate the effect of the alkali metal counterion change on the dodecyl sulphate phase behavior. I would like to deeply thank my advisor H. Ted Davis whose mentorship and faith to me in my program in these 2 years has been really admirable. I know he would be proud of me now. I would also like to thank my other 2 advisors Alon McCormick and Yiannis Kaznessis for their time, support and guidance on the experiments and the ongoing scientific and research cooperation. I would also like to thank my first mentor at the Chemical Engineering And Materials Science Department, Professor Lorraine Falter Francis. Working under her guidance I had the chance to learn many things of the academic and research life in the most prestigious department in the United States in the summer of 2006, as an undergraduate intern.

Special thanks to Professor Jayesh Ramesh Bellare, world expert in Cryo-TEM and CEVS inventor, who inspired me with enthusiasm in the field of TEM and Cryo-TEM during his sabbatical at the University in 2008, as well as the post doctorate fellow Arunagirinathan 'Arun' Manickham, for their support in the Cryo-TEM studies of the surfactant nanostructures.

I would also like to thank for his scientific collaboration on the surfactant project the world expert in Electron Microscopy, Professor Yeshayahu 'Ishi' Talmon, Professor at the Technion Institute of Technology in Haifa, Israel.

Professor Raul Caretta deserves special gratefulness, both for his contribution in the ion exchange experiment, as well as in the Lab Safety issues that he so diligently explained to me.I want to thank professor Michael Tsapatsis for the valuable knowledge of his reactor course.

I should not omit to thank the Characterization Facility for their patience. Special thanks to Prof. Greg Haugstad for the scientific collaboration in AFM during the summer of 2008, to Maria Torija for her scientific collaboration in my project in XRD and SAXS and the TEM trainers for their patience and time: Dr. Bob Hafner and Dr. Ozan Ogurlu. Last but not least, I want to thank Chris Frethem at the Characterization facility for his support in various moments at Niels Hasselmo Hall.

Additionally, I would like to thank the research fellow Wieslaw Suszynski, whose contribution in the optical visualizations with cross polarized light has been significant. It has been a real pleasure to work with him these 2 years. Also, the postdoctorate research fellow Tobias Foster for his scientific cooperation, the graduate student Xiaobo Gong and the graduate students of Professor McCormick group: Hanseung Lee, Giovanni Cocchi, Karan Jindal and Daniel O' Neal. Also the friends from the Graduate Program; David Nare, Nan Zhang, Dawud Tan and Damien Brewer.

I should not forget to thank Julie Prince, Mary G.Nissen, Teresa Bredahl, Connie Galt, 'Sue', Danny Williams, Larry Storey, C. J. Stone and of course, Jim Pirie. They have always been very helpful and supportive in every moment and the Department should be proud of all of them.Thanks to anyone that I did not mention.

I want to deeply thank in the School of Chemical Engineering at the National Technical University of Athens, Greece, my first advisor Professor Miltiadis Statheropoulos, all the Professors that have been a good bridge of communication overseas and especially the following Professors: Professor Doros Theodorou for his support in many cases, Professor Kyriakos Masavetas and Professor Aggelos Papaioannou and Andreas Boudouvis

.

I could not omit to thank my family: my mother Eleni, my father Nikolaos and my brother Ilias, whose real love and purity anyone would desire and crave for. I also want to especially thank my aunt, Professor Alexandra Gogou, in the scientific formatting of my thesis.

DEDICATIONS

This thesis is dedicated to my family, as well as my advisor H. Ted Davis.

ABSTRACT

The goal of this Master's Thesis has been to interpret the phase behavior of the cesium dodecyl sulphate/water system and compare the findings with the analogous findings of the SDS/water system. The synthesis of CsDS has been examined through 2 different methods: recrystallization and ion exchange. The phase behavior of the CsDS/water system has been examined, using several characterization methods. Macroscopic observation with cross-polarized light was used to interpret the solubility curve in the concentration region 1 wt % - 30 wt % CsDS. X-ray Diffraction was used in order to identify the unit cell crystal structure of CsDS and deduce conclusions about similarities and differences among different CsDS samples, unheated and heated. Cryo-TEM was used in order to observe the CsDS micellar nanostructures in an aqueous CsDS solution at a concentration higher than the CMC of CsDS for the given temperature. Optical microscopy with cross-polarized light was used in order to check for presence of liquid crystals, as well as to verify the solubility curve observed by the macroscopic observation. Small Angle X-ray Scattering was used in order to identify the phase of the liquid crystal structure (hexagonal or lamellar) in the intermediate concentration region (30-50 wt %).This study also includes the examination of possible organic and/or inorganic impunities in the CsDS/water phase behavior in the low concentration region (5-40 wt%) using macroscopic observation with cross-polarized light. The studies have indicated certain differences between the Cs^+ and the Na^+ system. The solubility curve of the CsDS/water system in the concentration region 1 wt % - 40 wt % CsDS is relatively flat, characterized by higher Krafft temperatures than the SDS/water system, for the same concentration region. This can be explained by the differences in the hydrated radii between the alkali metals, Cs^+ and Na^+ .The larger ionic radius of Cs^+ attracts weaker the electrons of the water molecules. This corresponds to a smaller hydrated radius for Cs^+ compared to Na^+ and therefore to less hydrophilicity and lower solubility (higher Krafft temperature) for a given concentration, for the CsDS/water system compared to the SDS/water system. Another difference is the width in terms of concentration of the two-phase region of liquid crystals and micelles. This is larger for the Cs^+ system and it indicates stronger van der Waals forces between the less ordered micellar phase and the more ordered liquid crystal phase. Both ellipsoidal micelles and threadlike structures were observed on the same grid in a CsDS/water solution, using Cryo-TEM. The ellipsoidal micelles that were observed for the CsDS/water system are twice as large as the ones observed for the SDS/water system, while it is very likely that the threadlike structures are related to some birefringent, intermediate liquid crystals that were observed by the macroscopic observation with cross–polarized light, when the heating rate was larger than 0.2[°C/min]. Therefore, it is concluded that heating rates larger than that value can affect the structures observed macroscopically, as well as microscopically. The X–ray Diffractograms of all CsDS samples had similar 2θ diffraction angles which may indicate similar unit cell crystal structures. The diffractograms of the unheated CsDS and SDS crystals also exhibit similarities in their diffraction angles in the diffraction angle examined.

TABLE OF CONTENTS

Table of Contents iv
List of Tables vii
List of Figures viii
Scientific purpose & techniques 1
Organization of the thesis 3
CHAPTER 1: INTRODUCTION - FUNDAMENTALS OF MICROSTRUCTURED FLUIDS 4
1.1. Introduction to Colloids: A definition 5
1.2. Amphiphiles and surfactants 6
1.2.1. Amphiphiles 6
1.2.2. Surfactants 7
1.3. Micelles, bilayers, liquid and solid crystals, phase behavior 8
1.3.1. Micelles and critical micelle concentration (CMC) 8
1.3.2. Reasons behind micelle formation - the hydrophobic effect 11
1.3.3. Definition of crystal classes 14
1.3.4. Liquid crystals 15
1.3.5. Critical Packing Parameter (P) 17
1.3.6. Phase behavior 19
1.3.6.1.The phase diagram 19
1.3.6.2.The lever rule 22
1.4.Summary 23

CHAPTER 2: MATERIALS & METHODS 25
2.1. Preparation methods 26
2.2.1. Recrystallization 26
2.2.1.1. Introduction to recrystallization 26
2.2.1.2. Ethanolic recrystallization in the purification of SDS 27
2.2.1.3. Aqueous recrystallization in the synthesis of CsDS: The synthesis of CsDS by dissolution of solid SDS into an aqueous CsCl solution 28
2.2.2. Ion exchange 29
2.2.2.1. Introduction to ion exchange 29
2.2.2.2. Materials and methods 32
2.2.2.3. How to secure feed purity 37
2.3. Characterization methods 38
2.3.1. Introduction 38
2.3.2. Cryo-TEM experiments 39
2.3.2.1. Goal 39
2.3.2.2. Technique 39
2.3.2.3. Materials and methods 40
2.3.2.4. Limitations 42
2.3.3. Macroscopic observation using cross-polarized light (Concentration region 1 %wt - 30 %wt) 44
2.3.3.1. Goal 44
2.3.3.2. Technique 44
2.3.3.3. Materials and methods 47
2.3.3.3.1. 1st Cycle: periodic heating and cooling only (no seed added) 50
2.3.3.3.2. 2nd Cycle: the correction by a tiny solid seed 51
2.3.3.4. Limitations 52
2.3.4. X-ray diffraction analysis (by permission of Maria Torija Juana) 54
2.3.4.1.Goal 54
2.3.4.2.1. Technique 1: The powder method 55
2.3.4.2.2. Technique 2: The Debye - Scherrer Method 56
2.3.4.3. Materials and methods 57
2.3.4.4. Limitations 58
2.3.5. Optical Microscope experiments 58
2.3.5.1. Goal 58
2.3.5.2.Technique 59
2.3.5.3. Materials and methods 61

2.3.5.4. Limitations 62
2.3.6. Small angle X-ray Scattering experiment 63
2.3.6.1.Goal 63
2.3.6.2.Technique 63
2.3.6.3.Materials and methods 64
2.3.6.4. Limitations.. 65

CHAPTER 3: THE CsDS/WATER SYSTEM AND A DESCRIPTION OF THE SDS/WATER SYSTEM 67
3.1.Preface 68
3.2. The CsDS/water phase diagram 68
3.3. The SDS/water phase diagram 71

CHAPTER 4: RESULTS OF THE EXPERIMENTS FOR THE CsDS/WATER SYSTEM 76
4.1. Preface 77
4.2. Results 77
4.2.1.Results on the macroscopic observation with cross-polarized light. Solubility curve and Krafft temperatures (concentration region 1 wt % - 40 wt %); macroscopic experiments. 77
4.2.1.1. 1st Cycle - Periodic heating and cooling only (no seed added). 77
4.2.1.2. 2nd Cycle - The correction by a tiny solid seed 83
4.2.2. Cryo-TEM experiments; the micellar nanostructures. 89
4.2.3. Possible metastabilities and the results of the X-ray Diffraction experiments 91
4.2.4. Results of the optical microscope 104

CHAPTER 5: DISCUSSIONS AND ANALYSIS 106
5.1. Preface 107
5.2. Discussions on the macroscopic experiments with cross-polarized light 107
5.2.1. The effect of the heating rate selection on the phase behavior 107
5.2.1.1. Intermediate liquid crystals 112
5.2.2. The solid crystal dispersion in water 118
5.3. Discussions on the Cryo-TEM experiments 118
5.4. Discussions on the XRD experiments 119
5.4.1. Limitations 119
5.4.2. Discussion about the X–ray diffractograms and the Debye rings 121
5.4.3. Discussion about impurity in the crystals 124
5.5. Impurities and their effect in the phase behavior in the region 1 wt % - 40 wt % CsDS 125
5.5.1. The effect of organic impurities 125
5.5.2. The effect of inorganic impurities 128
5.6. The Gibbs Phase rule, intraparticle and interparticle forces and a definition of phase transitions for both CsDS/water and SDS/water systems 128

5.6.1. The application of the Gibbs Phase rule in the CsDS/water system and the SDS/water system 128
5.6.2. Interparticle and intraparticle forces in the two systems 129
5.7. Discussions on the CsDS/water system 130
5.8. An analysis of the SDS/water system 132
5.9. A comparison between the CsDS/water and the SDS/water systems 134
CHAPTER 6: CONCLUSIONS 145
CHAPTER 7: ONGOING WORK AND FUTURE PERSPECTIVES 149
7.1. Preface 150
7.2. SAXS experiments 150
7.3. Optical microscope 152
7.4. X-ray Diffraction experiments 154
7.5. Macroscopic observations 155
7.6. Impurities in SDS and their effect in the CsDS/water phase behavior 155
7.6.1. Organic impurities 156
7.6.2. Inorganic impurities 156
7.7. CsDS micellar nanostructures at 0.34 [M] concentration and comparison with existing studies 157
BIBLIOGRAPHY 159

APPENDIX A:SYNTHESIS RESULTS 172
APPENDIX B: 5 wt % - 55 wt % CsDS CONCENTRATION TABLE 179
APPENDIX C: 5 wt % - 40 wt % IMPURE and PURIFIED CsDS/WATER EXPERIMENTS - CONCENTRATIONS & FIGURES 181
APPENDIX D: CsDS/WATER CONCENTRATIONS FOR INTERMEDIATE LIQUID CRYSTAL EXPERIMENT 188
APPENDIX E: STATISTICAL TOOL.....190
APPENDIX F: BILAYERS.....193
APPENDIX G: PERMISSIONS AND LICENSE AGREEMENTS 195

LIST OF TABLES

Page

Table 1.1. Various solid and liquid-like lamellar phases with their corresponding geometric order and phase structure……17
Table 2.1. Parameters for the Cryo-TEM sample preparation of a 12 wt % (0.34 [M]) CsDS/water solution at VITROBOT (micellar region)……42
Table 2.2. Different concentrations and types of samples analyzed at the Bruker AXS-MicroDiffractometer……. 57
Table 3.1. Krafft temperatures for the 5 wt % - 25 wt % concentration region……73
Table 4.1. Heating and cooling rates for the 1st cycle with comments; water tank temperatures…....79
Table 4.2. Heating and cooling rates of the 1st cycle with comments; sample temperatures……...80
Table 4.3. Differences between the 1st-4th thermal treatment compared to the 5th thermal treatment (1st cycle); water tank temperatures…….81
Table 4.4. Differences between the 1st-4th thermal treatment compared to the 5th thermal treatment (1st cycle); sample temperatures……...81
Table 4.5. 25 wt % - 40 wt % CsDS region. Candidate Krafft T [ºC] without seed addition……...83
Table 4.6. Krafft temperatures of the 3 independent samples at each concentration, before and after the addition of seed. Concentration region 5 wt % - 20 wt % CsDS (2nd cycle)……85
Table 4.7. Comments on the heating runs for experiments in the concentration region 25 wt % - 40 wt % (2nd cycle)……..88
Table 4.8. Different concentrations and types of samples analyzed at the Bruker-AXS MicroDiffractometer……. 95
Table 4.9. Raw data for the unheated 5% wt purified CsDS sample…….97
Table 4.10. Raw data for the 15% wt impure CsDS sample……..…….98
Table 4.11.Raw data for the 40% wt (initially superheated and then naturally cooled) purified CsDS sample……..99
Table 4.12.Raw data for the 45% wt (initially heated and then naturally cooled) purified CsDS sample……...……100
Table 4.13.Raw data for the 45% wt 40% wt (initially heated then supercooled and naturally warm-up) purified CsDS sample ……101
Table 4.14. 2·θ values for the five CsDS samples in the 2·θ region 0 - 35º); four purified CsDS samples (supercooled, superheated, heated, unheated) and one impure……102
Table 5.1. Comparison between the 1st cycle and 2nd cycle of experiments in the concentration region 5 wt % - 20 wt % CsDS……110
Table 5.2. Krafft temperature for impure CsDS in the region 1 wt % - 40 wt % ……...128
Table 5.3. A summary of certain differences between SDS and CsDS……...144
Table7.1.Instrumental methods used for analysis of the impurity in the sample……...157
Table A.1. ICP Results of each process……176
Table A.2. Time for each process……177
Table B.1. Concentrations before and after seed insertion, 5-55 wt % CsDS, 2nd cycle…… 180
Table C.1. Weighed concentrations for the impure samples in the region 5 wt % - 20 wt %CsDS…182
Table C.2. Weighed concentrations for the impure samples in the region 25 wt % - 40 wt % CsDS..183
Table D.1. CsDS concentrations in water – intermediate liquid crystal experiment…….. 189
Table D.2. SDS concentrations in water - intermediate liquid crystal experiment……..189

LIST OF FIGURES

Page

Figure 1.1. CTAB Molecule…….8
Figure 1.2. SDS Molecule……8
Figure 1.3. Mobility of the solute (chloropyridine) vs. the SDS concentration……10
Figure 1.4. Tetrahedral conformation for water……..13
Figure 1.5. Critical Packing Parameters and the corresponding aggregate shape……18
Figure 1.6. The lever rule……22
Figure 2.1. Continuous setup for the ion exchange synthesis method……...35
Figure 2.2. The Transmission Electron Microscope……...40
Figure 2.3. Macroscopic observation with cross-polarized light……46
Figure 2.4. Thermodynamic equilibrium approach for the 2nd cycle…….51
Figure 2.5. The X-ray Diffraction technique for the Powder Method……...56
Figure 2.6. Optical microscope setup……59
Figure 2.7. The X-ray Scattering concept……...63
Figure 3.1. The CsDS/water phase diagram……...68
Figure 3.2. The SDS/water phase diagram……71
Figure 3.3. The SDS/water phase diagram……72
Figure 3.4. Cryo-TEM image of an 8 wt % SDS solution forming spherical micelles……74
Figure 4.1. Solubility curves estimation in the region of 5 wt % - 20 wt % pure CsDS, 1st Cycle (water tank temperatures). ……78
Figure 4.2. Solubility curve estimation for the 5 wt % - 20 wt % CsDS concentration for three independent samples examined at each concentration and heated by the 2nd cycle……86
Figure 4.3. Typical appearance of two-phase coexistence (liquid crystalline phase and micellar phase) at T > 35 [°C]……..87
Figure 4.4. Cryo-TEM image of a 0.34 [M] CsDS aqueous solution, on the same grid……90
Figure 4.5. Cryo-TEM image of a 0.34 [M] CsDS aqueous solution, on the same grid……90
Figure 4.6. Possible metastabilities……...91
Figure 4.7. Supercooled sample……92
Figure 4.8. Superheated sample…….....93
Figure 4.9. Solid crystals in aqueous solution (stable state) created by solute or solvent jump…. 94
Figure 4.10. The Debye rings of the four purified samples……....96
Figure 4.11. The Debye rings of the impure CsDS sample……...96
Figure 4.12. Diffractograms for the 5 wt % purified CsDS unheated sample……..97
Figure 4.13. Diffractogram for the 15 wt % impure CsDS unheated sample…….....98
Figure 4.14. Diffractogram for the 40 wt % purified CsDS……...99
Figure 4.15. Diffractogram for the 45 wt % purified CsDS sample……...100
Figure 4.16. Diffractogram for the 40 wt % purified CsDS sample ……101
Figure 4.17. 15 wt % and 50 wt % samples at T = 50 [ºC]……..……..104
Figure 4.18. 30 wt % CsDS sample at various temperatures…….105
Figure 5.1. DSC Graph Intensity (Arbitrary units) vs. Temperature for the SDS/water system at 50 wt % SDS concentration ……111
Figure 5.2. The application of the lever rule application for the coexisting phases, in a CsDS/water system in the concentration region 1wt % - 30 wt % CsDS……...113
Figure 5.3. Intermediate, birefringent liquid crystals at T>40 [ºC], for the case of 38% (left) and 20% (right) of CsDS/water system……115
Figure 5.4. 30 %, 20 %, 10 wt % CsDS micellar and intermediate liquid crystalline phases ……. 116
Figure 5.5. 40 %, 30 %, 20%, 10 wt % CsDS water and solid crystals heated…….117
Figure 5.6. 30 wt %, 15 wt % purified CsDS at T > 35 [ºC]. Intermediate, birefringent liquid crystals observed in both samples ……117
Figure 5.7. Solubility curve in the region 1 wt % - 40 wt % for purified and impure CsDS…….127
Figure 5.8. The SDS/water phase diagram and the CsDS/water phase diagram……...134
Figure 5.9. X-ray Diffraction Analysis for SDS crystals at T = 25 [ºC]……141
Figure 5.10. Time for the dissolution of intermediate liquid crystals vs. surfactant concentration-same

heating rate ……142
Figure 7.1. Typical hexagonal pattern with certain interstructural spacings……...151

Figure A.1. Ion exchange equilibrium constant K_H^{Na} vs. mole fraction of Na^+ in the resin for different divinylbenzene crosslinkage degrees……..173
Figure A.2. Rotameter calibration at T = 25 [ºC] ……...174
Figure A.3. Breakthrough curves for a NaCl 0.19 [M] solution……..175
Figure A.4. Reduced cost of CsDS produced……..177
Figure A.5. Time for every different method in the production of CsDS……...178
Figure C.1. 5, 10, 15, 20 wt % impure CsDS seeded…….183
Figure C.2. 5, 10, 15, 20 wt % impure CsDS…….184
Figure C.3. 5 and 10 wt % impure CsDS……...184
Figure C.4. 5, 10, 15, 20 wt % impure CsDS……..185
Figure C.5. Liquid crystals in a 60 wt % purified CsDS…….185
Figure C.6. 45 wt % impure CsDS - ongoing transition from solid to liquid crystal…….186
Figure C.7. Solid crystals (stable state) created by solute or solvent jump……186
Figure C.8. Solid crystals (stable state) created by solute or solvent jump……187

Scientific purpose & techniques

The goal of this Master's Thesis is to investigate the phase behavior of Cesium Dodecyl Sulphate/water system at different temperatures and concentration. At first, the study involved the synthesis of the CsDS surfactant through aqueous recrystallization and ion exchange. Then, the phase behavior of the CsDS/water system was explored, using a variety of characterization techniques. The exploration of the CsDS/water phase behavior comprised of the following goals:

1. To identify the solubility curve (transition of solid crystals and micelles to neat micellar solution).

2. To interpret the size and shape of the micellar structures.

3. To locate the concentration and temperature for the onset of liquid crystals.

4. To identify the liquid crystal phases.

There has also been an attempt to identify the CsDS solid crystal structure characteristics; the unit cell type, space group, unit cell angles and unit cell volume.

The characterization techniques that were used, are the following:

- Macroscopic observation using cross-polarized light, in order to interpret the solubility curve (region 1 wt% - 40 wt% CsDS), as well as to explore the presence of birefringent liquid crystals in the system.
- Microscopic observation using cross-polarized light, in an attempt to verify the findings of the macroscopic observations regarding the solubility curve (region 1 wt% - 40 wt %), as well as to check the possibility of presence of birefringent liquid crystals in the system.
- Cryo Transmission Electron Microscopy experiments, performed by Arunagirinathan M.A. and Bellare J.R. and the instrument was operated by both Arunagirinathan M.A. and Bellare J.R., in order to observe the micellar structures of the CsDS/water system in the region 1 wt% - 30 wt% CsDS.
- Small Angle X-ray Scattering, performed by Torija M.J., in an attempt to identify the concentration and temperature where the liquid crystal phase first appears in the

CsDS/water system.

- X-ray Diffraction experiments, performed by Torija M.J., which would help to explore the unit cell crystal structure of impure and purified, unheated and heated CsDS (see sections: 2.2.1.2, 2.2.1.3., 5.5 and 7.6).

Having accomplished the above goals for the CsDS/water system, certain features of the CsDS/water system are compared with the analogous features of the SDS/water phase diagram. A reason of interest is to explore if the change in the alkali metal counter ion might affect the phase behavior of the corresponding surfactant/water system. This is because a change in the counterion might result in weaker or stronger interaction with the Dodecyl Sulphate chain upon binding, depending on its ionic radius.

Organization of the thesis

Chapter 1 provides a theoretical background in colloidal systems. Certain nanostructural concepts are defined; the terms colloid, amphiphile, surfactant, liquid and solid crystal and the phase behavior are presented.

Chapter 2 includes a presentation of the materials and methods used to synthesize CsDS, as well as the characterization techniques that were used to interpret the CsDS/water phase behavior in the various regions.

The estimation of the resulting CsDS/water phase diagram is reported in chapter 3. This diagram depicts certain structures formed at the analogous concentration and temperature regions. A summarized report of the results is also provided. Analogous features of the SDS/water system are also outlined, as reported by **[1]**, **[2]** and **[3]**.

Chapter 4 presents the results of each characterization method used for a certain concentration and temperature region, more elaborately.

Chapter 5 includes the discussions of the results presented in chapter 4 and the connection with their physical meaning. A comparison between the CsDS/water system and the SDS/ water system is also provided.

Chapter 6 is a conclusion of the discussions on the CsDS/water system and its comparison with the SDS/water system, while chapter 7 is an assembly of future perspectives and future ideas about these experiments. Following this conclusion, the bibliography is reported.

After the bibliography, the appendixes are provided. These appendixes include theories not directly related with the thesis, tables with calculations for experiments of the thesis and experiments that were not part of the thesis, but have helped to gain a further insight about future perspectives.

CHAPTER 1 - INTRODUCTION

FUNDAMENTALS OF MICROSTRUCTURED FLUIDS

In the introductory chapter, certain fundamental principles of nanostructured fluids are defined. The chapter begins with the definition of a colloidal substance. Having defined what a colloidal substance is, the description proceeds in the definition of the amphiphile, a subcategory of which are the surface active agents, or 'surfactants'.

As the surfactant concentration in water increases, the nanostructural order of the surfactants in the solution increases correspondingly. The surfactants self-assemble into micelles, which are single-layered, enclosed cavities (Scriven, 1990). As surfactant concentration increases, the order for the surfactant molecules also increases and intermediate mesophases appear; the hexagonal phase, the mesomorphic phase, the cubic phase, the tetragonal phase and the lamellar phase **[4].** These mesophases have been reported by Kekicheff et al. (1981), (1987) in their studies about the SDS/water phase diagram [1**], [2]** and **[3]**. The same authors report that at even higher surfactant concentrations, the nanostructures that formed are solid crystal polymorphs with variable degree of hydration **[2]**, **[3]**.

This chapter also includes a definition of the phase diagram and certain mathematical equations that are used to interpret phase diagram characteristics. A relation of the phase diagram with the concept of thermodynamic equilibrium (equality of chemical potentials) is also provided.

1.1. Introduction to colloids: A definition and classification into categories

The definition of colloid by Graham is a fundamental definition that is referred here for scientific history purposes. Graham (1861) was the first to introduce the term 'colloids' **[5]**. According to what Norde (2005) has reported, Graham defined as 'colloids' (in Greek the word means gluish), systems that are comprised of a continuous phase and a dispersed phase **[5]**. A more precise definition for the colloid has been given by Davis (1990), who defined the colloid as a 'fluid-bounded, persistent structure that is submicroscopically small in at least one dimension'. The definition of a microstructure is reported in Peter Kelley Kilpatrick's PhD Thesis (University of Minnesota, 1983) as 'the spatial variation in chemical

composition for a substance which is larger than the molecular dimensions, but smaller than the macroscopic dimensions (i.e. less than 0.5[μm])' **[6]**. Another definition of colloid has been provided by Hiemenz, who stated that 'a colloid is a particle whose one linear dimension is between 10^{-6} to 10^{-9} [m]' [**7].**

The colloids were classified by Ostwald and Perrin (beginning of the 20th century) into lyophilic and lyophobic. According to Ostwald and Perrin (early1900s'), 'lyophilic colloids are the ones for which the dissolution in solvent is favored, while the opposite holds for the lyophobic colloids' **[5]**.

Another category consists of the association colloids (Mukerjee, 1967), which are colloidal systems where each molecule of the dispersed phase consists of a lyophilic part and a lyophobic part **[8]**. Because of their binary properties, when the molecules of the dispersed phase are dispersed into the continuous phase, they tend to satisfy the properties of each compartment and they associate into larger compartments, called aggregates **[8]**. These structures consist of two parts. One part has incorporated all the hydrophobic moieties, while all hydrophilic moieties have been oriented towards the hydrophilic part **[8]**. An example of such an association formation can be a micelle (see 1.2 and 1.3), with a hydrophilic core and a hydrophobic shell **[8]**. Following Mukerjee (1967), 'in the association colloids, the molecules of the dispersed phase are soluble in the continuous phase and spontaneously self–assemble to form micelles in the colloidal size range' **[8]**. As it has been reported in the PhD Thesis of Kilpatrick P. (1982), when the solvent is water, the terms 'lyophilic' and 'lyophobic' become 'hydrophilic' and 'hydrophobic', respectively **[5]**.

1.2. Amphiphiles and Surfactants

1.2.1. Amphiphiles

According to Mukerjee et al. (1967), the amphiphilic solutions represent a subcategory of colloidal systems **[8]**. Following Mukerjee' s report, the amphiphiles are molecules which are composed of a hydrophilic part and a hydrophobic part (polar head group and

hydrocarbon chain, respectively) **[8]**. In presence of water, as presented by Mukerjee et al. (1967), amphiphiles self-assemble into structures, called micelles, in order to reduce contact between polar head groups and non-polar environments, or vice-versa (see 1.3.1) **[8]**.

1.2.2. Surfactants

Following Zuchen Lin's description (PhD Thesis, University of Minnesota,1993), 'the surfactants (contracted word for 'surface active agents') are amphiphilic molecules that decrease the surface free energy of the system they comprise, by lowering the surface tension of the continuous medium in which they become dissolved (environment) and the interfacial tension between liquid phases' **[9].**

The surfactants are a representative subclass of the amphiphiles. Surfactants have a breadth of applications in cosmetics **[10]**, pharmaceuticals **[11]**, drug delivery [**12**], water ultra filtration [**13**] and nanoscale particle production **[14]**. Based on the charge of the polar head group of the surfactant, they can be classified into the following categories: anionic, cationic, non-ionic and zwitterionic [**15**].

An anionic surfactant has a negative charge on its polar head group; two examples can be both sodium dodecyl sulfate, as reported by Kekicheff et al. **[2]** and cesium dodecyl sulfate **[16]**. Similarly, a cationic surfactant has a positive charge on the polar head group, such as in cetyl trimethylammonium bromide (the polar head group is an ammonium cation) **[17].** According to Holmberg K. (2003), 'a zwitterionic surfactant consists of two compartments that have opposite charge with each other; a cationic (usually an amine group) and an anionic (for example, carboxylate) compartment' **[18]**. In zwitterionic surfactants, each compartment can be considered an ionic, polar head group. Holmberg K.(2003) also claims that glycine (NH_2CH_2OOH), which is a molecule with two ionic groups that carry opposite charges, might be considered an example of a zwitterionic surfactant **[18]**.

A nonionic surfactant's polar head group has no net charge, following Kalfayan L. **[19]**. According to Makievski A.V. et al., alkyl dimethyl phosphine oxides (for example, decyl dimethyl phosphine oxide) belong to nonionic surfactants **[20]**.

Molecular structures with the individual compartments of a typical cationic and an anionic surfactant are presented in Figures 1.1 **[17]** and 1.2 **[21]** respectively. These compartments include the hydrocarbon chain, the polar head group and the bound counter ion.

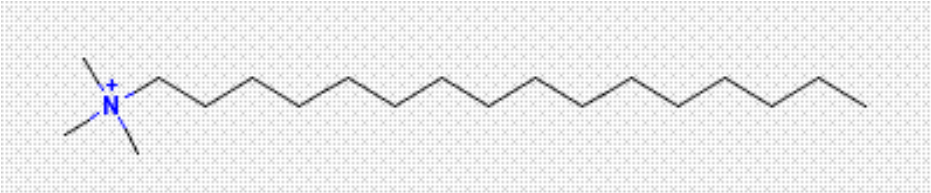

Fig.1.1. CTAB molecule reported by **[17].** The Figure has been reproduced with permission that has been granted from the copyright holder (see Appendix G for permission).

.

Figure 1.1 depicts the CTAB (Cetyl Trimethyl Ammonium Bromide) molecule as a cationic surfactant where the polar head group has a positive sign and the counterion has a negative sign **[17]**.

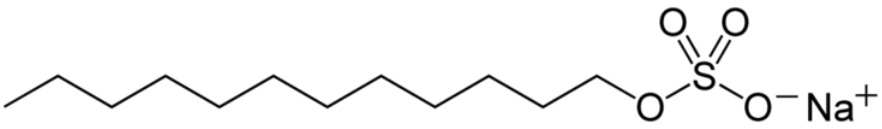

Fig.1.2. SDS Molecule adapted from **[21]**.No permission is required to reproduced the Figure, according to **[21]**.

Figure 1.2 is an example of an anionic surfactant (Sodium Dodecyl Sulphate) where the polar head group has a negative sign and the counter ion has a positive sign **[21]**.

1.3. Micelles, bilayers, liquid and solid crystals, phase behavior

1.3.1. Micelles and critical micelle concentration (CMC)

As mentioned in 1.2.1 according to Mukerjee (1967), surfactant solutions belong to association colloids **[8].** The cooperative association of the surfactant molecules, following

the description by Zuchen Lin (PhD Thesis, University of Minnesota, 1993), is related with favorable free energies of association of the molecules into certain structures**[9]**. As it has been reported by Zuchen Lin (1993), the structure with the most favorable association energy is the micelle, where lyophobic parts are not exposed to water and lyophilic parts come into contact with water **[9]**. A definition has been given by Scriven (1990), according to which 'the micelle is defined to be a cooperative association of amphiphilic molecules or ions into an enclosed single-layered structure at equilibrium' **[9]**. 'The micelles represent a thermodynamically equilibrated, stable phase that remains steady, independent of preparation history and treatment', as Scriven (1990) has stated**[9]** and according to Mukerjee (1967) they (micelles form in dynamic equilibrium with 'n' surfactant monomers from the bulk solution **[8].** As such, micelles:

i. Adsorb at the interfaces.

ii. Form association colloids in organic and aqueous bulk phases.

Since CsDS/water is an alkali metal anionic sulfate surfactant, it might be useful to provide the definition of the Krafft temperature for the sodium soaps by R.G. Laughlin (1994), as it has been reported by Lin et al. (2005) **[24].** According to the definition of Laughlin (1994), the Krafft temperature for a sodium soap solution represents the temperature, at which the solubility of the surfactant in water is 1 wt % **[24]**. 'Since the Critical Micelle Concentration for a surfactant in water is far less than 1 wt %', R. G. Laughlin continues, 'the Krafft temperature is defined as an upper boundary value, where the solubility equals the Critical Micelle Concentration' **[23]**, **[24]** and **[25]**. At concentrations lower than the Critical Micelle Concentration (CMC), according to Candau (1990), no micelles are formed, while above the CMC, any additional 'n' surfactant molecules will either incorporate themselves into an aggregate with aggregation number 'n', or dynamically equilibrate with the micellar unit **[26]**.

The surfactant molecules, following Hiemenz (1997), arrange themselves into a micellar configuration, according to the reaction scheme:

$$n \cdot M \leftrightarrows M_{n,}$$

where the index “n” at the right part of the reaction is the micelle aggregation number **[27]**.

For the SDS/water system, Shah et al. (2001) have reported that the aggregation number ‘n’ is between 40 and 60, where ‘n’ kinetically independent surfactant molecules self-assemble to form a larger kinetically independent colloidal unit (the micelle), comprised of these n surfactant molecules **[28]**. When certain physical properties of an aqueous surfactant system (such as the electrical/equivalent conductivity, the mobility or the surface tension) are plotted versus the surfactant concentration, they indicate a sudden breakup (discontinuity), at the CMC [**22]**.

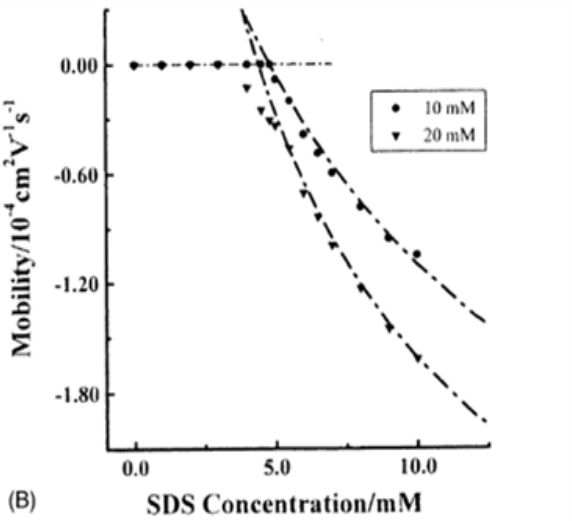

Fig.1.3. Mobility of the solute (chloropyridine) vs. SDS concentration in the solution, reported by C. Erh –Lin et al. and references therein [**22]**. The Figure has been reproduced with permission (license agreement) that has been granted from the Copyright Clearance Center, Inc. (see Appendix G for permission)

Figure 1.3 depicts the mobility curve (a physical property of the system) of chloropyridine (a solute) versus the surfactant concentration (SDS is another co-solute). In the corresponding system, the surfactant (SDS Sodium Dodecyl Sulfate) interacts with the other solute (chloropyridine, in this case) [**22]**. The Critical Micelle Concentration of the surfactant can be estimated, as the concentration where the curve of the diagram exhibits a sudden discontinuity and decrease [**22]**. For the given system (Figure 1.3), the CMC of SDS is about 5 [mM] [**22]**.

The reason why the mobility exhibits this sudden decrease at the CMC region is related with the surfactant molecules' aggregation into micelles. When the surfactant molecules aggregate, they self-assemble into micelles and the kinetically independent surfactant units decrease from n to 1. This corresponds to an increase in the radius of the kinetically independent unit (which is now the micelle), as described by the equilibrium reaction**[27]**:

$$nM \leftrightarrows M_{n,}$$

As the surfactant molecules self-assemble into a micelle, the radius of the charged unit becomes larger as well; the mobility 'V' of the colloidal particles will decrease correspondingly [**22]**. The surfactant molecules are more mobile than the micelle, according to the following formula by Hiemenz et al. (1997) for the mobility:

$$V=q\cdot E / [6\cdot \pi \cdot \eta \cdot R_s]$$

where R_s is the radius of the colloidal particle, E is the electrical potential of the solution, q is the charge of the colloidal particle and η is the viscosity of the medium (water) **[29]**.

The discontinuity of the mobility curve at the CMC is due to the fact that the micellization process of the surfactants is a thermodynamic transition of 1st order. When the 1st derivative of the system's Gibbs free energy over the number of moles - the chemical potential - is plotted versus a certain thermodynamic quantity, as Linder has stated (2004), the graph exhibits a discontinuity, at exactly the CMC. For instance, when the chemical potential ($\mu = [\partial \Delta G / \partial \Delta n_\alpha]_{T, P}$), is plotted versus the temperature of the solution the graph exhibit a discontinuity at the transition temperature and this can be assigned to the Krafft temperature, if the transition is the micellization process **[30]**.

1.3.2. Reasons behind micelle formation - the hydrophobic effect

According to Mukerjee (1967), in order for the hydrophobic moieties to minimize interaction with water, the surfactants self-assemble into micelles, which (micelles) have a hydrophobic core (hydrocarbon tails) and two hydrophilic compartments; a hydrophilic shell and the

hydrophilic polar head groups**[8]**. The cause for the micellization from a thermodynamic point of view, as it has been reported in the notes of Class #104: 'Physical Chemistry of Macromolecules' at the Biochemical Engineering Graduate Program at Brandeis University, is the increase in the solvent entropy and the micelle formation can be explained by the hydrophobic effect **[31]**.

Practically, when a surfactant is dissolved in water, its hydrophobic tails do not favor interaction with water molecules **[31]**.

As it has been presented in the notes of the class #104: 'Physical Chemistry of Macromolecules' at the Biochemical Engineering Graduate Program at Brandeis University, in an aqueous solution with water neighbors only, each water molecule is considered to be inscribed into a tetrahedron, where the oxygen atom lies in the center and the two hydrogen molecules point towards the 2 apex of the tetrahedron (The 2 hydrogen molecules weakly attract 2 other water molecules through Van der Waals forces) **[31]**. The 2 unbound electrons of the oxygen atom, as reported in these notes, form hydrogen bonds with another 2 hydrogen molecules, each bond with a different water molecule **[31]**. Therefore, according to the notes from Brandeis University, in an aqueous solution, each water molecule has four nearest neighbors and forms hydrogen bond with only two of them, having totally six different ways to make bonds with two of its nearest neighbors (six different ways, for three neighbors) **[31]**.

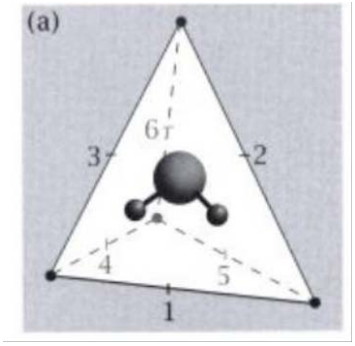

Fig.1.4. Tetrahedral conformation for the water molecule in the water network; Figure reported in the Class #104: 'Physical Chemistry of Macromolecules', at the Biochemistry Graduate Program, at Brandeis University **[31]**. The Figure has been reproduced with permission that has been granted from the copyright holder himself: Professor Gregory A. Petsko (see Appendix G for permission).

Following the notes of the class #104: 'Physical Chemistry of Macromolecules' at the Biochemical Engineering Graduate Program at Brandeis University, 'if one water molecule is replaced by a hydrophobic compound, then, the number of available bonds decreases by one; three water neighbors and one hydrophobic neighbor' **[31]**. The smaller number of available neighbors for bonding, changes the geometric configuration from a tetrahedron to a triangle, which reduces the number of conformations in terms of different possible bonds that a water molecule can have, from six to four **[31]**. This is an entropic penalty for water, because this presence of hydrophobic molecules will also result in some hydrophobic cavity formations (unfavorable interactions with water) **[31]**.

As presented by Alberts (1989), in the case of pure water, each water molecule is inscribed in a tetrahedron and is connected with other water molecules, through hydrogen-bond network **[32]**. In this network, the molecules can have 3 degrees of freedom; rotational, vibrational and translational **[32]**. Because of thermal motion ($k_B \cdot T$) of some water molecules, the degrees of freedom of some other water molecules might be temporarily reduced and also because of the formation of each hydrophobic cavity at first, when a hydrophobic molecule will be inserted in the water network, the solvent entropy

seems to decrease (entropic loss) **[32]**. The hydrogen network is strong enough, however, that, as Alberts has reported (1989) it will outbalance any of these perturbations (decreases in the number of conformations) in the long term **[32]** and will increase the solvent entropy and minimize the Gibbs Surface energy.

This entropy gain is larger compared to the entropic losses, as they were described by the reasons that Albert (1989) has reported and they were mentioned above **[32].**The solvent will force the hydrophobic units to cluster together into an enclosed single unit assembly, where the interfacial area between solvent and solute will decrease (smaller than the sum of the surface areas of the multiple individual cavities) **[32]**. This conformation will minimize interactions between water molecules and hydrophobic groups, as the water molecules will have to arrange themselves around fewer kinetically independent units (n surfactant molecules will comprise a kinetically independent unit of aggregation number, n) **[33]**. Therefore, the water molecules had lost some of their degrees of freedom, will regain them.

This micellization action will result in an overall increase in solvent entropy, as there will be more space available for the water molecules to move and this will assist the corresponding water molecules to gain again their lost degrees of freedom **[33]**, **[34]**, **[35]**, **[36]**, **[37]**. Therefore, the micellization process is a spontaneous process.

1.3.3. Definition of crystal classes

A crystal class can be fully defined by a Latin letter followed by a Greek subscript, according to Tardieu et al. (1973), where the Latin letter depicts the long-range organization (space group, 1-dimensional, 2-dimensional or 3-dimensional lattices) for the different crystalline structures:

L is used for 1-dimensional lamellar phase (1-dimensional order)

H is used for 2-dimensional hexagonal phase (2-dimensional order)

P for 2-dimensional oblique or centered phase

M for 2-dimensional monoclinic phase

R for rhombohedral phase

Q, cubic phase

C, 3-dimensional crystal phase

Always according to Tardieu et al. (1973), the Greek letter (subscript) characterizes the short-range conformation of the hydrocarbon chain (if it is a liquid-like, or a solid-like conformation), where 'α' (alpha) corresponds to liquid-like state, whereas β, β', δ (vita, vita-prime, or delta), correspond to partial order of matter (more ordered than the alpha state) **[39]**.

Various crystal classes have been reported by Kekicheff et al. (1981), (1987) for the SDS/water system at surfactant concentrations higher than 70 wt%, where these classes are indicated by the symbols (C, C′, C′′, and C′′′)**[2], [3]**. These symbols correspond to different 3-dimensional crystal structures (polymorphs), where the superscripts '′', '′′', '′′′' indicate different organization of the surfactant molecules in space (unit cell crystal structure) and the subscript (C_x, $C_{1/8}$, and C2) corresponds to different degrees of hydration in the 3-dimensional hydrated crystal structures **[2], [3]**. For example, the subscript '1/8' means that in the hydrated crystal network, there will be 1 water molecule per 8 SDS molecules.

1.3.4. Liquid crystals

Following the description by Kilpatrick (1983), the liquid crystals exhibit intermediate behavior between solid crystals and liquid state of matter and the difference between solid and liquid crystals lies at the molecular level order (the order consists of positional and orientational order), where solid crystals possess positional as well as orientational order; liquid crystals possess orientational order, but do not always possess positional order. According to the description presented by Kilpatrick (1983), the lack of positional order for the liquid crystals means that they can flow and they can be subject to deformation of flow (shear forces) **[6]**. Macroscopically, the liquid crystals can possess 1-dimensional or 2-dimensional order, in terms of how the pattern is formed. From the liquid crystals, the lamellar structures possess 1-dimensional geometric order, while the hexagonal structure possesses 2-dimensional geometric order **[6]**.

The liquid crystals are also called mesomorphic crystals. According to Stegemeyer (1994), there are two types of liquid crystals; the thermotropic liquid crystals, which result upon heating of the surfactant system, as well as the lyotropic liquid crystals, which are formed upon addition of solvent **[40]**.

Two examples of lyotropic liquid crystals are the hexagonal liquid crystal (which is an aggregate of 6 rod-like micelles assembling a hexagon) and the lamellar liquid crystal. According to Kilpatrick (1983), the hexagonal liquid crystal has 2-dimensional geometric order and only orientational order, while the lamellar liquid crystal has 1-dimensional geometric order (as well as both 1-dimensional positional and orientational order) and consists of a parallel set of two surfactant monolayer sheets, sheets that are separated by a water layer **[6]**. Surfactant molecules within the bilayer structure are prone to thermal fluctuations, but they cannot escape the bilayer (see Appendix F). This is because of the surfactant positional order in the bilayer, as has been mentioned above **[6]**. Moreover, all liquid crystal phases but the cubic phase (Q_{α}) are optically anisotropic, which means that all phases but the cubic, exhibit birefringence and magnetic and electric polarization, when these phases are observed through cross-polarized light see **[38]**, **[40]**, **[41]**, **[42]** and**[43]**.

According to the classification by Ranck et al. (1974), the lamellar phases can be either:

i. Type L_{α}, which has a “liquid-like” chain conformation. In that conformation, the bilayers are separated by water molecules. The structure exhibits 1-dimensional periodicity as it consists of repeating surfactant bimolecular lamellae. These lamellae can be parallel, curved or semi-planar.

ii. Of type $L_{\beta'}$, which has a gel-like chain conformation.

iii. Of type L_{δ}, which has a coil-like chain conformation **[41]**.

The phases L_{β}, $L_{\beta'}$ and L_{δ} exhibit more order in their short-range conformation compared to the L_{α} phase **[41]**.

Table 1.1.Various solid and liquid-like lamellar phases with their corresponding geometric order and phase structure **[41], [44]**

Intermediate phase type	Geometric order, in dimensions	Phase structure
L_{β}	1-D	Untilted gel
$L_{\beta'}$	1-D	Tilted gel
L_{δ}	2-D	2-D crystal
L_{α}	1-D	Fluid lamellar
H	2-D	Hexagonal

1.3.5. Critical Packing Parameter (P)

In dilute aqueous solutions, as presented by Zuchen Lin (1994), the packing of surfactant molecules into larger aggregates consists of the following three terms:

i. A favorable lyophilic contribution, due to Van der Waals attractive forces between the polar head groups and water. **[9].**

ii. A surface term that reflects the opposing trends between the crowding of the surfactant head groups closer together to minimize hydrocarbon/water contacts and their splitting apart due to steric (excluded volume effects) and electrostatic repulsion**[9]**.

iii. A packing term which requires that water molecules and polar head groups are excluded from the hydrophobic interior of the aggregate - (limitation of geometrically accessible forms available to aggregates) **[9].** The opposite holds for reverse micelles, where the hydrophilic core does not allow lyophobic groups to approach it **[9]**.

According to Israelachvili J.N (1992), **t**hese three factors can be summarized into a single parameter, the Critical Packing Parameter, 'P' and P can predict the corresponding shape of the aggregate conformation **[45]**.:

$$P = V_{-t} / [a_{\_\ o} \cdot l_{\_c,\,t}]$$ **[45]**

, where V_t is the volume of the hydrocarbon chain,

$a_{\_\ o}$ is the optimal head group area

$l_{c,t}$ is the critical hydrocarbon chain length

The value of the critical packing parameter ‘P’, can predict the form that the surfactant aggregate will have. For example,

i. A regular spherical micelle (single-layered) with hydrophobic interior and hydrophilic environment

ii. A rod-like micelle (single-layered).

iii. A planar or curved bilayer

iv. An inverted micelle with hydrophobic environment and hydrophilic interior

The parameter ‘P’ may be used to explain differences in the phase behavior between the SDS/water system and the CsDS/water system in general, but especially as far as the micellar behavior is concerned (see 5.7, 5.8 and 5.9).

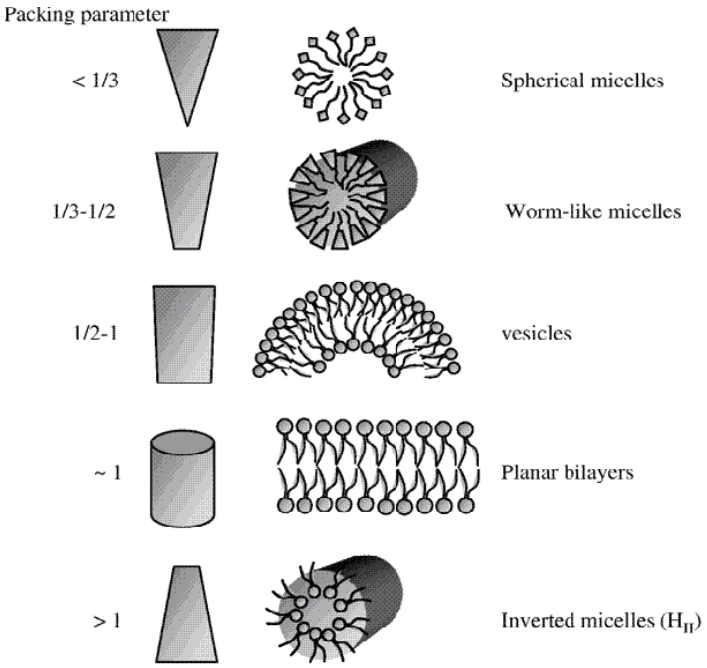

Fig.1.5. Critical Packing Parameters and the corresponding aggregate shape adapted with permission that has been granted from the copyright holder himself: Professor Israelachvili J.N. **[45]**. (see Appendix G for permission)

1.3.6. Phase behavior

1.3.6.1. The phase diagram

As it is presented by Stølen, S. et al. (2004) –and their definition has been mentioned in the introductory paragraphs of this first chapter-, 'the phase diagram is a map that displays potential space regions where the various phases of the system are stable. The potential space is given by the following system variables: temperature, pressure and composition' **[46]**.

In the case of this study, a surfactant/water system is represented by a temperature vs. concentration phase diagram. The various regions of the diagram represent stable phases of the components **[46]**. Regarding a phase and its properties, Stølen, S. et al (2004) have defined as phase, a state that has particular composition and definite physicochemical properties. Stølen, S. et al. (2004) in their discussion about phases indicate that different phases might be identical in composition, but may have different physical properties **[46]**. As Lavis D.A. et al. have stated (1999): 'each phase results in different molecular arrangements. This difference in arrangements, in turns, results in differences in the spatial or orientational order' **[47]**. Some characteristic phases for a surfactant/water system that are indicated can be the micellar phase, the hexagonal phase and the lamellar phase **[48]**.

For a two-phase region in a surfactant/water system, the thermodynamic equilibrium between the two corresponding phases can be mathematically described as an equality in chemical potentials between a phase 'α' and a phase 'β', for the 2 coexisting phases 'α' and 'β', where $T_\alpha = T_\beta$, as well as $P_\alpha = P_\beta$ **[46]**:

$$[\partial \Delta G / \partial \Delta n_\alpha]_{T,P} = [\partial \Delta G / \partial \Delta n_\beta]_{T,P} = \mu_{i,\alpha} = \mu_{i,\beta}$$

'i' represents a single component in the 2 phase region.

In equation 1, ΔG is the Gibbs free energy of the mixture and $[\partial \Delta G / \partial \Delta n_\alpha]_{T,P}$ is the partial molar Gibbs Free Energy of the mixture with respect to a certain phase (a phase α, or a phase β) at constant temperature and pressure. The partial molar Gibbs free energy of the mixture with respect to the phase α is equal to the chemical potential of that phase in the mixture. In the case of thermodynamic equilibrium between two phases, molecules or aggregates travel from one phase to another, but the net flux of molecules in each phase is

zero **[49]**.

Following Stølen S. et al. (2004), 'the phases 'α' and 'β' can be any two coexisting phases in thermodynamic equilibrium with each other' **[49]**. The system lies at its thermodynamic equilibrium, when the partial molar Gibbs free energy has a global minimum in the potential space. Another way to express the thermodynamic minimum is to express that, having been perturbed by its thermodynamic equilibrium via one of the following methods: dilution, condensation, heating, cooling

The system will revert to its initial thermodynamic state. In the case of thermodynamically metastable states, the system might initially lie in a local thermodynamic Gibbs free energy minimum. The initial state of thermodynamic minimum is local, because any perturbation of the system by this thermodynamic minimum, via one of the above mentioned methods, will not bring the system back to this same initial state but it will drive it to a different, more stable state. The new final state might macroscopically look different than the initial (local minimum of Gibbs free energy) and for sure, the system in the initial, metastable state will have a higher chemical potential value than the analogous chemical potential value of the global thermodynamic minimum state. The definition of metastabilities is necessary, as samples were examined for their metastability (see 4.2.3, 5.4.2, 5.7 and 5.9).

Certain examples of 2 phase region (phases α and β in phase equilibria) can be:

i. Micellar aggregates (phase 'α') and hexagonal phase aggregates (phase 'β'), in a two-phase coexistence region of α and β

ii. Coexistence of two different liquid crystal aggregates (for example, hexagonal phase and cubic phase)

iii. Coexistence of liquid crystal aggregates and solid crystals (for example, hexagonal phase coexisting with some solid crystal)

iv. Coexistence of different polymorphs (solid crystals with different unit cell crystal structures) and/or different degree of hydration in the unit cell **[2].**

Following the description about phase transitions by Lavis, D.A. and McDonald Bell,

G. (1999), the boundary lines that separate different phases in a phase diagram, indicate thermodynamic transitions **[47]**. When a thermodynamic transition occurs, the thermodynamic order of state in the system changes, as presented by Lavis, D.A. and McDonald Bell, G., (1999) and the system exhibits different degree of order in the phase regions that the phase transition spans **[47]**. With increasing temperature, the order decreases. When it is heated, the system moves from anisotropic state of ordered crystals to some less ordered state, such as a neat micellar solution (see the SDS/water phase diagram that has been reported by Kekicheff et al**. [1]**). Certain thermodynamic variables, such as the chemical potential or the entropy, exhibit a discontinuity in their curve, when these variables are plotted versus another independent variable (temperature and pressure, respectively), as presented by Stølen, S. and Grande, T., (2004) **[46]**. And as shown by the same authors, the slope that is defined as the chemical potential versus the systems' temperature is the entropy of the system. A change in entropy occurs at the temperature of phase transition.

As indicated by Israelachvili J.N. (1992), the following series depicts an arrangement of surfactant nanostructures in terms of increasing packing **[45]**. As the packing of more surfactant molecules with each other into aggregate s increases, the order in the corresponding phases also increases. The interactions between surfactant molecules and water molecules become weaker and the spatial degrees of freedom for the surfactant molecules decrease as one moves from left to right**:**

Ellipsoidal micelles << Rod-like micelles << liquid crystals << lamellae **[45]**

This series of increasing order is presented at this point, to connect with the discussion about certain features of the CsDS/water phase diagram and its comparison with the SDS/water phase diagram that is presented in sections 5.7 and 5.9. Certain differences in the discussion of these sections will be explained according to this series. The term 'ellipsoidal' corresponds to micelles that have either spherical shape or their shape corresponds to an ellipsis.

1.3.6.2. The lever rule

In a two-phase coexistence region of ‘α’ and ‘β’ and a given temperature, the lever rule will determine the amounts of each phase (phases ‘α’ and ‘β’) for a certain composite concentration.

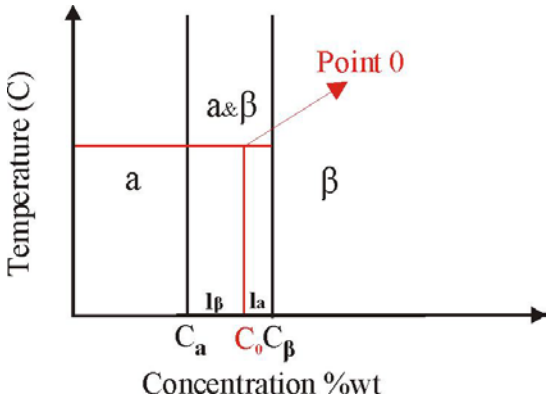

Fig.1.6. The lever rule. The figure has been constructed from scratch, based on the lever rule’s description provided by Stølen, S. and Grande, T., (2004) in their book with title: ‘Chemical thermodynamics of materials: macroscopic and microscopic aspects’ **[46].**

Figure 1.6 shows the lever rule in the case of a two-phase region in a surfactant /water system. A horizontal line of constant temperature (tie line) will intersect the 2-phase region (coexisting phases ‘α’ and ‘β’). The perpendicular intersections at the edges of the two phase region will provide the corresponding concentration for each single phase (C_α and C_β). The concentration of the mixture that corresponds to that tie line is given by a perpendicular projection from point O. When the total number of moles in the system (n_o) is known, the corresponding mole fractions χ_α and χ_β, can be determined. The number of moles in each phase can be determined, using the concentrations C_α and C_β ($C_\alpha = n_\alpha /V$, where V is the solution volume) and the mole fractions $\chi_{\alpha \text{ and }} \chi_\beta$, The relations that have been used are:

$$C_o = \chi_\alpha \cdot C_a + \chi_\beta \cdot C_\beta$$

$$\chi_\alpha = n_\alpha / n_o$$

$$\chi_\beta = n_\beta / n_o$$

$$\chi_\beta + \chi_\alpha = 1$$

The Gibbs phase rule is written as: F = C – P +2, where ‘F’ are the degrees of freedom, ‘C’ is the number of components and ‘P’ the number of phases and the value of ‘2’ represents the two independent potential space variables (pressure and temperature). Using the Gibbs phase rule, one can identify the number of degrees of freedom in the system for a fixed number of phases and components **[49]**. The phase diagram of a surfactant/water system can predict how many phases and what types of phases coexist at certain regions of temperature and concentration; for example, micellar phase and/or other mesophases. This is one way of using the Gibbs phase rule, where the number of components in the mixture and the number of degrees of freedom are known. Another way to use the Gibbs rule would be to identify the number of phases in a region for a fixed number of degrees of freedom and a fixed number of components. As it was mentioned before, the lever rule can provide the relative amounts of each compound in a two-phase region, for a certain composite concentration of the mixture. For the surfactant/water systems, the phase diagram can also provide the location of the solubility curve. This curve represents the thermodynamic transition line from solid crystals and micelles (two phase region) to neat micellar solution (one phase region), as temperature increases. Also, the phase diagram can depict the concentration width for any two-phase region, such as the coexistence region of liquid crystals and micelles.

A characteristic example of an anionic surfactant/water phase diagram is the SDS/water system, where studies have been reported by Fontell et al., Kekicheff et al. **[1]**, **[2]** and **[3]**. Similarly to SDS, CsDS is a single tail anionic sulfate surfactant where the anionic polar head group is a sulfate group and the single hydrocarbon chain consists of 12 carbon atoms **[16]**. Another group of anionic surfactants are the carboxylic surfactants **[50].**

1.4. Summary

Certain concepts of nanostructured fluids have been defined in this 1st chapter; the terms of the colloidal substance, of the amphiphile and the surfactants. As the concentration of surfactant in water increases, the nanostructural order of the surfactants in the solution increases accordingly. At first, the surfactants self assemble into micelles. The micelles are

single-layered enclosed cavities. As order increases, intermediate mesophases appear; the hexagonal phase, the mesomorphic phase, the cubic phase, the tetragonal phase and the lamellar phase. At very high surfactant concentrations in the system, solid crystal polymorphs with variable degree of hydration are expected. For all liquid and solid crystals, their name is given by a Latin letter followed by a Greek subscript, indicating long range order and short range hydrocarbon chain conformation, respectively. The phase diagram is a diagram with potential space variables as its coordinates. In this diagram, certain phases coexist in thermodynamic equilibrium. The chemical potentials are equal and the net flux of the chemical potential between the two phases in thermodynamic equilibrium is zero.

CHAPTER 2

MATERIALS AND METHODS

Chapter 2 presents the materials and experimental methods used to synthesize CsDS and to characterize its phase behavior in water. Specifically, section 2.2 outlines the methods of synthesis of CsDS. Section 2.2.1.3. presents the recrystallization (of SDS in an aqueous CsCl solution into CsDS) and section 2.2.2. the ion exchange of SDS into HDS and the neutralization with CsOH into CsDS. The sample preparation method, the goal of each experiment, the analogous technique of each characterization experiment, as well as limitations of the instruments, are described in this chapter.

2.1. Preparation methods

Two methods have been examined for the preparation of Cesium Dodecyl Sulphate, in this project. These are:

- Recrystallization of aqueous CsCl solution with SDS into CsDS. All CsDS samples that were examined in this phase behavior study were synthesized by recrystallization.
- Ion exchange of SDS into HDS followed by neutralization of HDS with CsOH into CsDS (batch processes and a continuous process (see appendix A for the continuous process)).

2.2.1. Recrystallization

2.2.1.1. Introduction to recrystallization

Recrystallization, according to Anne Marie Helmenstine, is a purification method of solid crystals **[51]**. In a solution where solid crystals (‘A’) have already been dissolved, different solid crystals (‘B’) are added and new solid crystals form (‘C’ and ‘D’) **[51]**. For the one type of new crystals formed (‘C’), precipitation is favored and for the other type (‘D’), it is more favorable to dissolve in the solvent **[51]**. The purification principle of (‘A’) into (‘C’) is based on the different solubility of these crystals in the solvent, at certain temperature **[51]**.

The following reaction represents the recrystallization:

$$A + B \rightarrow C + D$$

New solid crystals form (‘C’ and ‘D’) and they keep forming, until all the old crystals (‘A’ and ‘B’) have been completely dissociated **[51]**. It should be mentioned that the term “recrystallization” is used to define two different processes in this thesis; ethanolic recrystallization in the purification of SDS and aqueous recrystallization in the synthesis of CsDS.

2.2.1.2. Ethanolic recrystallization in the purification of SDS

All the CsDS samples that were used to examine the phase behavior were purified according to this method, as it is described in 2.2.1.2. As Kekicheff et al (1981) and Muramatsu et al. (1976) have reported by relative studies on SDS, organic impurities can be present in SDS **[2]**, **[52]**. The yield in purified SDS is reported in 5.5. and the results of the comparison in the phase behavior between purified and impure CsDS in the concentration region 1 wt% -40 wt% CsDS, as they has been observed by the macroscopic experiments with cross-polarized light, are presented and discussed in sections 5.5. and 7.6. Because of the solubility difference in ethanol between possible organic impurities and SDS, the organic impurities can be dissolved and SDS can precipitate in the ethanolic solution **[51]** .

The SDS (Sigma-Aldrich, Inc.) had the following identity:

L4509 (Product number) Sigma-Aldrich Sodium dodecyl sulfate Reagent Plus®, 98.5 wt % pure (Gas Chromatography Analysis).

The purification process of organic impurities from SDS involved:

i. Dissolution of 40.5572 [g] of SDS into 400 [ml] of ethanol at T=25 [ºC]. The solubility of SDS in methanol is equal to the solubility of SDS in water. The latter is about 10% [wt/v] at T=25 [ºC]. The solubility of SDS in ethanol at T=25 [ºC] is the same.

ii . The solution is heated up to 50 [ºC] and stays at that temperature for 1’. The system is cooled down to T=0 [ºC] for 8 [hrs].

iii. The suspension is vacuum filtered at 0 [ºC] with cold water at around 0 [ºC]. The filtrand is collected, while the filtrate is thrown.

iv. The filtrand is stored in the desiccator for 2 days.

2.2.1.3. Aqueous recrystallization in the synthesis of CsDS: the synthesis of CsDS by dissolution of solid SDS into an aqueous CsCl solution.

Regarding the CsDS preparation, the aqueous recrystallization is represented by the reaction:

$$Cs\ Cl\ (aq) + NaDS\ (aq) \rightarrow CsDS\ (aq) + NaCl\ (aq)$$

Recrystallization was selected as a method to synthesize CsDS in order to be able to compare the purity of the produced CsDS with an existing study (see Appendix C). A reason of interest for synthesizing CsDS is to compare the micellar nanostructures of CsDS that are formed at the Krafft temperature of the system at certain concentration above the critical micelle concentration value, with existing studies **[53]** and **[54]**. The materials and preparation method are presented below:

*Materials used (*All the reagents were ordered by Sigma Aldrich Corporation)*:*

C3011 (Product number) Sigma - Aldrich Cesium chloride Grade I, ≥ 99.0 wt %; L4509 (Product number) Sigma - Aldrich Sodium dodecyl sulfate Reagent Plus®, 98.5 wt % (GC)

*Preparation method (t*ime: 8 hours)*:*

a. Dissolution of 0.377 moles of CsCl into 200 ml of water (solution A).

b. Addition of 0.0377 mol of SDS into Solution A, which is 10 % of the quantity of CsCl in the solution, or, 0.1 [mol] Na^+ ions for 1 [mol] Cs^+ in the solution.

c. In case of a transparent solution at T=25 [ºC], the solution would be cooled down to 0 [ºC].

d. In case if a non-transparent solution at T=25 [ºC], the suspension would be heated up to 60 [ºC]. Then, it would be cooled down to 0 [ºC].

e. The suspension would be vacuum filtered at 0 [ºC]. During vacuum filtration, the filtrand was washed thoroughly with 4 batches of cold water at about 0 [ºC] - 150 ml each batch. Since the recrystallization' s efficiency, for the procedure from step 'a' to 'e', is defined as: ([moles of CsCl] –[Moles of SDS])/[moles of CsCl], 0.0377 [mol] SDS would

recrystallize 0.0377 [mol] of CsCl into 0.0377 [moles] CsDS. In other words, for 1 [mol] of Cs^+ in the solution after recrystallization, the recrystallized CsCl sample that dissolves in water again, would be the 90 wt % of the initial feed of CsCl. The purity in the CsDS product would be 90 wt %. Proportionally, the experiment would produce a CsDS product 90 wt % pure.

f. The filtrand, that contains 90 wt% recrystallized, purified product, is received and is dissolved into a flask that contains 0.377 [moles] of CsCl; steps a through e are repeated.99 wt % of the CsCl of the feed is recrystallized and likewise, the purity of the CsDS product would be 99 wt % in CsDS).

g. The filtrand is stored in the desiccator for 2 days.

2.2.2. Ion exchange

The ion exchange is a mass transfer process between a liquid stream and a solid surface. Solid is the ion exchange bed and the liquid is the aqueous solution that is ion exchanged **[55]**.

2.2.2.1. Introduction to ion exchange

Both for the batch and the continuous processes, the ion exchange mechanism involves the following mechanism:

i. Ions that are supposed to be exchanged, undergo simultaneous diffusion and convection from the bulk solution region to the interface between the bulk solution and the surface of the resin particles.

ii. The ions diffuse from the resin surface (outside) towards the macropores of the ion exchange resin (inside). It is assumed that the only pores towards which the ions diffuse, are the macropores of the resin.

iii. Then, the ions react at the sites of the functional groups within the matrix of the resin and ion exchange takes place.

iv. Finally, the ion exchanged product moves with coupled diffusion and convection back to the interface between the surface of the resin and the bulk solution **[55]**.

The ion exchange is an equilibrated process, described by the following equilibrium reaction scheme:

$$R^{-}\text{-}H^{+}\ (s) + Na^{+}\text{-}DS^{-}\ (l) \leftrightarrow R^{-}\text{-}Na^{+}\ (s) + H^{+}\text{-}DS^{-}\ (l)$$

The indices (l) and (s) correspond to the liquid phase and the solid phase, respectively. The resin that has been used, was initially in the protonated form (H^{+}).The following equilibrium reaction scheme is characterized by its equilibrium constant:

$$K_{H}^{Na} = [\ R^{-}\text{-}Na^{+}] \cdot [\ H^{+}\text{-}DS^{-}] / ([\ R^{-}\text{-}H^{+}] \cdot [\ Na^{+}\text{-}DS^{-}])$$

where the quantities in the brackets "[]" can be expressed by one of the following quantities: activity coefficients, mole fractions, and/or concentrations – the concentrations are expressed as molalities.

As K_{H}^{Na} becomes larger than 1, the resin - Na^{+} attraction is favored more, compared to the resin - H^{+} attraction. In this case, it becomes favorable for the solid resin particles to uptake Na^{+} and release H^{+} in the solution. The efficiency of the ion exchange process at equilibrium, described in the scheme above, depends on a number of factors, such as:

i. The percent of divinylbenzene cross-linkage in the resin **[55]**. According to Harland C. E. (1994), the resin particles are constituted by a network of polystyrene molecules, called a 'polystyrene matrix'. Divinylbenzene molecules have been inserted by the manufacturer between the styrene molecules (within the 'polystyrene matrix'), in order to increase the cross-linkage within the polystyrene network **[55]**. These divinylbenzene molecules are linked with each other with sulfonic groups, forming sulphur bridges **[55]**. Due to these bonds between the divinylbenzene molecules, the resin network forms the so-called 'cross-linkage' **[55]**. According to the description provided by Harland C. E. (1994), by adding more divinylbenzene molecules, the cross-linkage between the divinylbenzene molecules increases **[55]**. With increasing divinylbenzene cross-linkage, the resin matrix becomes denser, the porosity of the bed is decreased and the mobility of ions inside the resin matrix is also decreased **[55]**. To relate with the experiment provided in Appendix A (where

Na^+ ions are adsorbed by the resin and H^+ ions are released in the solution), the percent of divinylbenzene cross-linkage in Amberlyst 15-Wet is about 12% wt. The larger the value of K_H^{Na}, the higher the ion exchange efficiency will be (or the higher the release of H^+-DS^- in the aqueous solution).For a given amount of ions adsorbed onto the polystyrene matrix of the resin, a larger degree of divinylbenzene cross-linkage would be related to a larger K_H^{Na} value (See Figure A.1, Appendix A). Another way to interpret Figure A.1. is that for a fixed value of divinylbenzene cross-linkage, the smaller the mole fraction of ions adsorbed on the resin, the larger the value of K_H^{Na} will be.

ii. In general, the ion exchange efficiency may be related with the bead size (resin particle's characteristic diameter). As the bead size becomes smaller, there is less resistance for the ions to diffuse towards the macropores in the interior of the particles and the ions will diffuse faster onto the active sites of the bead.

iii. The size of the ions that are exchanged. An example can be the case of ion exchange for alkali metals. This factor (size of the alkali metal ions that are exchanged) is related with the thesis and can be used to estimate the most efficient method to use ion exchange, in an attempt to retrieve CsDS as the final product (section 7.7 and Appendix A). The lyotropic series of the alkali metals can help to explain the effect of the ionic size on the ion exchange process: Na^+ is a cation with a larger charge density compared to Cs^+, so the former has a larger ionic radius than the latter **[56]**. This difference in ionic radii means that, in an aqueous solution, the former attracts the electrons of neighboring water molecules stronger than the latter, resulting in a larger hydrated ionic radius for Na^+ compared to Cs^+**,** eventually **[56]**. As the hydrated Na^+ ion is a larger cation compared to the hydrated Cs^+, the former is attracted weaker by the resin compared to the latter **[56]**.

iv. The acidic strength of the resin. To relate this with the experiment that is presented in Appendix A, a resin with a stronger acidic character has more H^+ ions available at the active sites, compared to a resin of a weaker acidic character.

v. The feed concentration. The concentration of SDS in the solution feed should be carefully selected, in order to maximize K_H^{Na} and to receive the largest possible yield of HDS. One thing that should be considered is that if the concentration of SDS in the solution increases, the equilibrium of the ion exchange reaction presented in point 'i' (previous page) will be shifted to the right, according to Le Chatelier' s principle **[57]**. In an attempt to select the correct concentration of SDS in the feed solution, another thing that should be taken into account is the set of data regarding the equilibrium constant in the ion exchange reaction (see Figure A.1. in Appendix A). According to these data of Appendix A and the stoichiometry of the ion exchange reaction, in order for the yield of HDS at equilibrium to be maximized, the concentration of SDS in the feed solution should be about 0.1 [M] (or less than 0.1 [M]). Moreover, when the feed concentration of SDS is 0.1 [M] or less, the possibility for the ion exchanged product in the solution to contain Na^+ ions is minimized. Finally, certain studies of polystyrene–divinylbenzene resin applications have been included in the bibliography; **[58]**, **[59]** and **[60]**.

2.2.2.2. Materials and methods

The following materials were bought from Sigma-Aldrich Inc:

Amberlyst 15 - Wet (strongly acidic, Industrial Grade Strongly Acidic Polymeric Resin); C8518 (Product number) Sigma - Aldrich Cesium hydroxide hydrate ≥ 90 wt %; L4509 (Product number) Sigma-Aldrich Sodium dodecyl sulfate Reagent Plus®, 98.5 wt % pure (Gas Chromatography).

Preparation method:

For the batch experiments, the mass balance can be written as:

$[\partial c/\partial t]$ = [rate of the ion exchange reaction] $\neq 0$, (transient process) (no flow into or outwards from the reactor) **[61]**.Two different batch experiments are described below: one in a single flask and one in three flasks in series.

1. In a single conic flask

50 [g] of new (unused) Amberlyst 15-Wet resin is weighed on an analytical balance. This unused mass of resin is inserted in a conic flask. Deionized water is added in 7 batches of 100 [ml], in order to wash the quantity several times for any ultra fine particles to be removed- particles with size less than the acceptable size according to the manufacturer's standards (cutoff particle characteristic dimension: less than 0.355 [nm]) **[62]**. During this step 'a', the resin also increases to its final swollen volume, where solvent molecules would swell the polymer matrix of the resin.

a. A volume of 250 [ml] of a HCl 1.88 [M] solution (~7% v/v) is added to the flask with the resin for a contact time of about 30'. During that time, slight agitation by hand is used. The HCl supernatant is discarded.

b. Totally 7 batches of 100 [ml] deionized water each, are added to the flask with the resin, where each batch stays for a contact time of 20'. Over that time, slight agitation by hand is used. The total time that the resin is in contact with water is 2 hours 30'.

c. A volume of 100 [ml] SDS 0.04 [M] solution is added to the ion exchange resin, for a contact time of 30'. During that time, slight agitation by hand is used.

d. The supernatant is poured off and it is collected. This is the received product (HDS). Vacuum filtration is avoided, to overcome the possibility of foaming by expansion of the dodecyl sulfate acid, an acid with low surface tension.

The time for a complete experiment is 3 hours 30'.

2. Three consecutive conic flasks; A, B and C

The 3 flasks in series scheme represents a batch process where the ion exchange efficiency is expected to be larger compared to the single flask experiment (see Appendix A). The process might be also considered as a semi - batch process. The product as supernatant is collected every time from the first flask and added in the consecutive flask, without using the first flask again for the same experiment **[63]**.

Preparation method:

a. This is the same step, as step 'a' for the preparation method of the single flask. This step is followed for the flasks B and C.

b. 7 batches of 100 [ml] deionized water are added to flask A. Each batch stays for a contact time of 20' – the total contact time is 2 hours 30'. The same step is followed for flasks B and C, simultaneously.

c. A volume of 100 [ml] SDS 0.04 [M] solution is added in flask A, for a contact time of 8 hours. During that time, slight agitation by hand is used.

d. The supernatant - ion exchanged solution - is poured off from flask A and is inserted into flask B. Vacuum filtration is avoided, to overcome foaming by expansion of the dodecyl sulfate acid, because it is an acid with low surface tension.

e. Steps 'd' and 'e' are followed for flask B. Then, the supernatant is inserted in flask C.

f. Steps 'd' and 'e' are followed for flask C. Then, the supernatant is collected.

The supernatant from flask C is the final product - the ion exchanged HDS solution. The time for a complete run is 55 hours 30'.

3. Continuous experiment design (basic design provided by Professor Raul Caretta). A continuous ion exchange experiment is provided in Appendix A, where NaCl solution is used as the feed solution and HCl is collected as the product. The reason why NaCl was selected as the feed solution, is because NaCl is a chemical reagent relatively available in every laboratory. In contrast to the batch experiments, the mass balance for the continuous experiment is written as:

$[\partial C/\partial t]$ = [rate of the ion exchange reaction] + $[C_{in}]$ - $[C_{out}] \neq 0$ (transient process), where C is the concentration of the feed **[61]**.

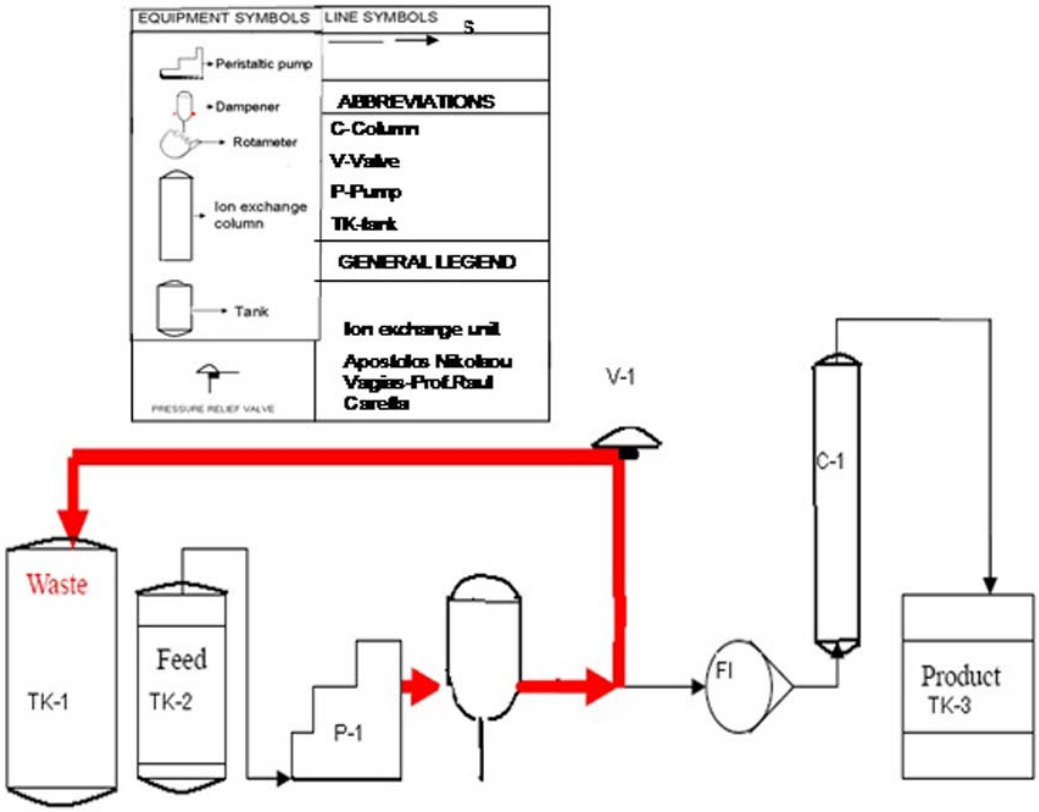

Fig.2.1. Continuous setup for the ion exchange synthesis method.

Description of the equipment:

A waste tank (TK-1) is used to remove excess solution from the equipment.

A feed tank (TK-2) holds the feed solution.

A peristaltic pump (P-1) is used to pump fed solution from the feed tank (TK-2).

A dampener (next to the peristaltic pump) absorbs the oscillations of the peristaltic pump and helps to provide a smooth pulsation of the peristaltic pump.

A pressure relief valve directs air bubbles to the atmosphere and excess solution to the waste tank (TK-1).

A rotameter (flow indicator, FI) measures the flow rate in the equipment.

An ion exchange column (C-1) is the column filled with the ion exchange resin particles.

A tank (TK-3) collects the product (ion exchanged solution).

The column (C-1) was loaded with swollen resin. The resin swelling ratio is 50%. This

means that a quantity of 10 [g] fresh resin, for example, would swell to a final mass of 15 [g] after washing. In that experiment, 25.5 [g] of swollen mass was measured, as wet bed (Certain studies for the swelling of polymeric resins are provided; **[55]** and **[66]**). Having loaded the column with that mass of wet bed, the next step involved the calculation of the setup parameters.

Resin properties:

- Surface Area = 53 [m^2 / gram]
- Total Pore Volume = 0.4 [ml / gram]
- Shipping weight = 770 [g / L]
- Porosity = 0.20
- Active sites = 4.7 [meq / ml]
- Moisture holding capacity = 50 wt %
- Particle diameter, d_p = {6·V_p / [surface area of a particle]}=147 [nm]

Column dimensions:

- height of the column, H = 30 [cm]
- diameter of the column, D = 2.2 [cm]

Given the above mentioned values for the resin properties and the column dimensions, the following parameters were calculated:

- Aspect ratio, L = H/D = 15
- Wet bed volume = 26.17 [ml]
- Active sites of the bed used = 122 [meq]
- Hold-up volume of the Tygon® tubing = 52 [ml]

Finally, having operated at a flow rate of 2.3 [ml/sec] (measured with the calibrated rotameter -see Appendix A), the following parameters were also calculated:

- Residence time of the system = 26.17 [ml] / 2.34 [ml/sec] = 12 [sec]
- Superficial Velocity = 2.34 [cm^3/sec] · 30 [cm] / 26.17 [cm^3] = 2.68 [cm/sec]
- Reynolds Number = 0.005 (Laminar flow, for the given Superficial Velocity)

Procedure:

1. The peristaltic pump (P-1) starts and pumps solution from the feed tank (TK-2). A pulsation dampener absorbs oscillations of the peristaltic pump and guarantees smooth pulsations **[64]**.

2. The pumped solution travels through the tubing and it arrives at the pressure relief valve.

3. At the pressure relief valve, air bubbles and excess liquid volume (more liquid volume than what volume the tube can hold) are sent back to the “waste” tank (TK-1).

4. Solution, which has not been sent to the “waste” tank (TK-1) will pass through the rotameter (FI). Then, it will enter the ion exchange column (C-1) - see Appendix A for the calibration of the rotameter.

5. The product is collected at the outlet into a product collection tank (TK-3).

In all the connections, Tygon® tubing was used **[65]**.

2.2.2.3. How to secure feed purity

Figure 2.1 demonstrates the setup of the continuous experiment for the ion exchange synthesis process. This setup, however, has not been used in the CsDS synthesis for the CsDS/water phase behavior (section 7.7). This setup was used in an experiment that was performed to retrieve HCl solution from an initial NaCl feed solution (see Appendix A).

The advantage behind the use of the waste tank (TK-2) with the relevant tubing is the prevention of feed pollution (see red line, Figure 2.1). Feed pollution could be caused by excess liquid being held up in the Tygon® tubing between the positive displacement pump and the pressure relief valve **[65]**. The following example illustrates the significance of the problem of feed pollution.

Assuming that there is no waste tank and a single feed tank is used, feed from (TK-2) supplies the system with HCl (during activation of the resin). When the pump (P-1) shuts down temporarily, in order for the system to be washed with deionized water, the hold-up volume of the liquid on the Tygon® tubing in the red region contains a strong acid; HCl. When the feed solution in tank (TK-2) is switched to deionized water, the hold-up volume in

the red marked region will enter the tank (TK-2) and the initial solution contained in the feed tank (TK-2) will be polluted by HCl. The use of the waste tank (TK-1) will prevent possible contamination of the tank (TK-2), as tank (TK-1) collects any excess liquid being held up along the way of the red tubing. The problem of pollution is avoided by directing the excess liquid volume to the 'waste' chamber, (TK-1).

2.3. Characterization Methods

2.3.1. Introduction

The phase behavior of CsDS/water has been explored with various characterization techniques. Each technique was used to provide information about the phase behavior at different concentration and temperature regions. The techniques attempted to provide information about the micellar structures (single phase region), the two-phase region of solid crystal and micelles, the two-phase region of liquid crystals and micelles, the liquid crystal phase (single phase region), as well as information about the unit cell crystal structure. The techniques that were used have been:

- Macroscopic observation with cross-polarized light, in order to identify the solubility curve and to check the existence of birefringence.
- Optical microscopy with cross-polarized light, to examine multiple phase transitions on a single slide, simultaneously.
- Cryo-TEM that has been performed by Arunagirinathan M.A. and Bellare J.R., in order to observe CsDS micellar nanostructures in aqueous solutions **[16]**.
- X-ray Diffraction that has been performed by Torija M.J., in an attempt to examine the unit cell crystal structure of CsDS.
- Small-Angle X-ray Scattering that has been performed by Torija M.J., in an attempt to identify the type of some liquid crystal phase.

In all these techniques, the association of certain research fellows was helpful. Specifically, Suszynski W. has provided help in the setup of the equipment and the camera

in the macroscopic observation with cross-polarized light. The same fellow has also contributed to a major extend in the visualization experiment, by helping to design the visualization slide and by providing the camera, the slides of the analyzer and the polarizer, as well as the actual optical microscope. Bellare J.R. and Arunagirinathan M.A. performed the Cryo-TEM sessions **[16]**, while Torija M. J. performed the X-ray Diffraction and Small Angle X-ray Scattering experiments.

2.3.2. Cryo-TEM experiments (These experiments were performed by Arunagirinathan MA. and Bellare J.R. and the instrument was operated by both Arunagirinathan M.A. and Bellare J.R. and the results are provided by their permission)

2.3.2.1. Goal

The goal of these experiments was to identify the representative micellar nanostructures of CsDS in water at certain concentration and temperature (higher than the CMC of CsDS for the given temperature (a related study about critical micelle concentrations is provided by Mukerjee (1967) **[16]**) and, after having identified them, to compare these structures with the analogous structures of the SDS/water system, at the same concentration and temperature. Cryo-TEM is a characterization technique that provides the possibility to observe directly the existing micellar nanostructures at a given temperature, by preserving the aqueous samples through ice vitrification.

2.3.2.2. Technique

The electron beam is produced in the filament source (indicated yellow) and is driven from the top of the column to the bottom of it, by the action of an accelerating voltage. The voltage is produced between the anode and the cathode of a bias shield **[68]**. On its way down the column, the beam passes through pairs of gun alignment coils and sets of apertures. The set of coils ensures that the beam is symmetrical, while the apertures magnify and illuminate the specimen’s image on the fluorescent screen **[68]**.

Figure 2.2 presents parts of the Transmission Electron Microscope; 'Transmission' means that the electron beam penetrates into the specimen's structure. The resulting image on the fluorescent screen is the 2-dimensional projection of a 3-dimensional structure.

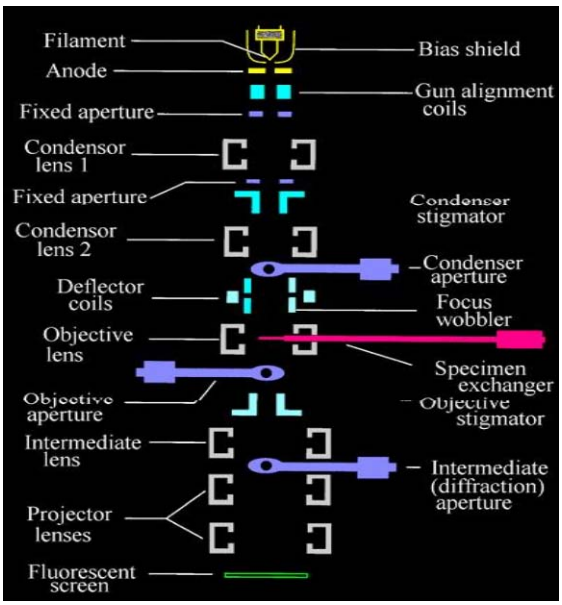

Fig.2.2. The Transmission Electron Microscope. The Figure has been reported by Robert Hafner **[68]**. The permission to reproduce the figure has been granted by Robert Hafner.

2.3.2.3. Materials and methods

Sample preparation:

The CsDS was synthesized by recrystallization of an aqueous CsCl solution into CsDS, using SDS (analyzed in 2.2.1.3). The crystals were initially weighed in order for the sample to reach 12 wt % CsDS final concentration of the suspension (or 0.34 [M]). Then, the crystals were dissolved in water at T =25 [ºC], to a 12 wt % CsDS final concentration of the suspension (or 0.34 [M]). At that temperature, the sample was not a neat solution, but was instead a 2 phase system (solid crystals and micelles). The sample was then heated to a temperature, where the system would become a single phase isotropic micellar solution.

Methods (Performed by Arunagirinathan, M.A.; Bellare, J.R. and included with their permission):

1. A 0.34 [M] CsDS solution was prepared at T =25 [ºC]. The samples were taken to

Niels Hasselmo Hall, at the Biomedical Engineering School of the University of Minnesota (part of the Characterization Facility). They were heated in a heating water bath from T=25 [ºC] to T >35 [ºC] (the heating rate was not mentioned).

2. Part of the solution was transferred in a microcentrifuge tube. The tube was inserted in the VITROBOT device that has a CEVS (Controlled Environment Vitrification Chamber) **[48]** at T=35 [ºC] and Relative Humidity =100%. Having stayed for 30' at these conditions, the sample became a neat solution and was ready for the next step of the sample preparation. A lacey formvar carbon coated grid by Ted Pella® was mounted on a pair of tweezers which (tweezers) were inserted in the VITROBOT.

3. The tweezers (with the grid mounted) were dipped into the microcentrifuge tube that contained the sample. The time over which the sample is in contact with the Cryo-TEM grid, is called plunge time. The grid was lifted from the sample solution, allowed to wait for 1 [sec] (wait time) and blotted for a certain period of time (blot time). During the blotting process, blotting drums with filter papers mounted on them forced the sample to compress (shear forces that cause shear flow). The strength of the blotting forces is represented by the blot offset parameter in table 3.1. By blotting, the excess liquid was removed, from the front and the rear sides of the grid. The blotting process resulted in a thinned solution with an average thickness of about 100 [nm], as Hansen et al. (1993) have reported **[69]**. The blotted film lies only within the holes of the grid **[69]**.

4. Then, a drain time was maintained that would allow for any shear forces, which had been applied during blotting on the compressed sample, to relax **[48]**.

5. A polymer vessel, with a small brass cap in the center of it, was used. The polymer vessel was filled with liquid nitrogen at its boiling point, while the brass cap was filled with liquid ethane at its freezing point **[16]**. Then, the grid was plunge frozen into liquid ethane at its freezing point (plunge time). The large heat capacity of liquid hydrocarbons enables the sample to be rapidly vitrified to liquid ethane solidification temperature (ultra rapid freezing of water with cooling rates of about 1000000 [K/sec]) **[69]**. Almost instantly, the grid is transferred into the liquid nitrogen chamber of the same brass cap, in order for

the sample to reach the boiling temperature of liquid nitrogen, a temperature which is lower than the solidification temperature of liquid ethane **[69]**. The transfer from the brass cup into the liquid nitrogen is fast, in order to avoid any humidity from the environment to condense on the sample. That would cause, according to Arunagirinathan M.A. and Bellare J.R., formation of ice layer above the vitrified region of the sample and the ice formation would result in problem during the visualization of the sample, during Cryo-TEM **[16]**.

6. The grids were then inserted in a Cryo grid box. This device helps to transfer the grids into a liquid nitrogen dewar or into a small thermo flask **[16]**.

7. The grids were carefully transferred from the small thermo flask onto the Cryo Transfer station. This transfer should also be fast enough, so that ice crystallization (from water in the form of humidity in the environment), is prevented, here as well. The sample (grid) was consecutively loaded from the Cryo Transfer station onto the Cryo Grid holder. Then, the grids were directly loaded onto the microscope cold stage (T ~ -175 [°C]) **[69]**.

Table 2.1. Parameters for the Cryo-TEM sample preparation of a 12 wt % (0.34 [M]) CsDS/water solution at VITROBOT (micellar region)

Blot Tim e (sec)	5
Wait Time (sec)	1
Blot Offset (mm)	-1
Drain Time (sec)	25
Plunge Time (sec)	5

2.3.2.4. Limitations

The sample preparation of the Cryo-TEM session can experience certain difficulties due to:

1. Ice crystallization. Ice crystallization (instead of vitrification) may happen during the several transfers of the grid; from the VITROBOT to the dewar, from the dewar to the

station and from the station to the microscope. The water has to be vitrified in order for the actual nanostructures (that are formed at the sample preparation temperature) to be preserved. Liquid ethane is used as a cryogen, in order for bubble formation to be avoided; bubble formation would retard the sample's freezing rate. Therefore, ultra-fast vitrification is used (freezing rates on the order of 1000000 [K/sec] are used) **[69]**. Moreover, crystalline ice that is present in the grid holes might melt after the grid has been loaded on the microscope. The ice that melts can cause drifting of the grid **[16]**. This makes more difficult to focus on a certain location of the grid with the Digital Microscope Camera, because the grid is moving **[16]**. Crystallized water and other impurities absorbed by the grid during the multiple transfer processes might also affect the vacuum quality in the instrument, as it might not be possible to reach the high vacuum needed for the operation of the microscope ($10^{\wedge\text{-}11}$Torr) **[68]**. It might be also possible to induce severe problems on the pumping system **[16]**.

2. Menisci formation. The film blotting procedure might cause a thickness gradient across the holey polymer grid. As Hansen et al. (1993) have reported, depending on the amount of dispersion in the grid holes after blotting, different menisci might be formed; biconcave, biconvex or biplanar **[69]**. In biconcave menisci, surface tension effects cause segregation of particles towards the outer edge of the sample hole **[69]**. On the contrary, biplanar and biconvex menisci form thicker films that do not cause particle segregation, but a more uniform distribution of particles in the hole **[69]**.

3. Radiation damage and low contrast. Radiation damage is caused by electrons impinging on the sample. This process generates heat and free radicals **[69]**. As mentioned in **[69]**, vitreous ice is 10 times more resistant to beam damage than crystalline ice. An explanation is that free radicals, which have been generated by the interaction of the electron beam with the sample, diffuse faster in the case of the amorphous ice compared to the crystalline ice, in which case (crystalline ice) they become trapped at crystal boundaries and the sample warms up. This is why ice crystallization should be avoided. One way to decrease electron beam damage is to operate the microscope in a dark room

(lights turned off) in order to decrease the electron beam current. A way to decrease radiation is by operating the microscope at low beam current (high acceleration voltage). This will ensure that the beam will neither heat the sample, nor distort the microstructures **[69]**.

Regarding phase contrast enhancement, this is important for systems that exhibit low phase contrast, because of water presence, such as the surfactant/ water systems. In these systems, the microscope should be operated in slight defocus (**[69]**, **[16]** and **[48]**).

4. Instrument resolution. A very important parameter for the Cryo-TEM experiments is the microscope's resolution. For the microscope that was used for the experiments, the resolution is less than 1 [nm] **[68]**.

2.3.3. Macroscopic observation using cross-polarized light (concentration region 1 wt % - 30 wt %)

2.3.3.1. Goal

The macroscopic observation using cross-polarized light would help to:

- determine the exact location of the solubility curve (identification of the transition temperature from solid crystals and micelles to neat micellar solution)
- identify the presence of anisotropic crystals using cross-polarized light
- define the concentration boundaries between the neat micellar solution (single phase region) and the two-phase region of liquid crystals coexisting with micelles

2.3.3.2. Technique

The description (Figure 2.3) starts from the light source (back) towards the camera (front):

1. A uniform, white light beam is emitted from a regular light source (lamp). It is assumed that the horizontal level represents the reference plane and that the light bulb (source) has an inclination with respect to the horizontal level. The several light beams will

be scattered away from the source in a semi-circular fashion, towards the air. Apart from the beam that propagates along the horizontal level (parallel to the reference plane), the angle with respect to the horizontal level that all the other light beams form, beams which are transmitted from the light source (from the air) and become incident onto the glass surface of the water tank, is the same with the back reflecting angle, as Snell's law governs the interaction of the media (air/glass and/or sample) with beams that come at an angle with respect to the horizontal level **[70]**.

2. The light beam first passes through a polarizer. The polarizer is a glass filter that allows wavelengths that propagate along certain planes only, to pass through.

3. Refraction 1. At the air/glass interface, Snell's Law for refraction holds:

$$n_{1/}\, n_2 = \sin\theta_2 / \sin\theta_1$$

where n_1 and n_2 are the refractive indices of air and glass, respectively **[70]**. The wavelengths of light propagate along different planes. Different planes have different refractive indices. The plane-polarized light arrives at the glass surface of the water tank, where part of it gets transmitted, another part of it gets refracted for the 1st time (air/glass refraction) and the remaining part of it gets back-reflected towards the air.

The angle of the light beam, which is formed between the horizontal axis and the incident light beam that passes through the air/glass surface, is larger compared to the analogous angle - with respect to the horizontal level - that the refracted beam forms. The refracted beam converges more towards the horizontal axis compared to the light beam that passes through the air/glass (water tank) surface.

4. Next refractions. On its way to the sample, the plane-polarized light that has been first refracted at the air/glass container interface (2nd refraction), passes through the glass container/tank water interface (3rd refraction). Next, the beam passes through the tank water/glass Pyrex® tube/sample interface (4th refraction) and finally this refracted plane-polarized light beam enters the sample. If the sample is anisotropic, it will exhibit birefringence. Birefringence is a physical property of materials that are optically anisotropic. The optical properties of anisotropic materials vary along different crystallographic

directions and the polarized beam is split in two wavelengths, where each wavelength propagates along a different crystallographic plane (these planes are perpendicular with each other).All liquid crystal phases but the cubic phase (the cubic phase is isotropic) are anisotropic. Solid crystals can also be anisotropic and therefore birefringent, as well. Some examples of inorganic birefringent solid crystals are the calcite **[71]** and the barium titanate ($BaTiO_3$) **[72]**, while an example of an anisotropic, organic birefringent solid crystal is a coordination polymer based on terpyridine and dicyanoaurate anion **[73]**.

5. While propagating towards the camera, the two split light beams undergo several refractions (the reverse process with respect to step 4). They undergo a 1st refraction at the glass Pyrex ® tube/sample interface, then a 2nd refraction at the glass Pyrex ® tube/water tank interface, a 3rd refraction at the tank water/glass container interface and a 4th one at the interface between glass and air.

6. When they are at the air and as they approach the camera, the two split light beams arrive at the analyzer (2nd polar filter). The analyzer, which is mounted on the camera, will recombine the two light beams into a single beam, according to constructive and destructive interference. Constructive interference means that wavelengths propagating with the same phase will add up in magnitude, while destructive means that waves out of phase will cancel out each other **[74]**.

7. The total, recombined beam (the two split beams that have been interfered constructively) arrives at the camera for visualization **[74]**.

8. If the structure is an anisotropic crystal, the sample will exhibit birefringence.

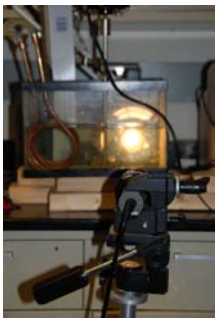

Fig.2.3. Instrument setup of the macroscopic observations. Size scale: The height of the water tank is 8 [inches] and the width is 12 [inches].

2.3.3.3. Materials and methods

Sample preparation:

The CsDS was synthesized by recrystallization of an aqueous CsCl solution with SDS (see 2.2.1.3) **[16]**, **[42]**. The samples used in these experiments were manually ground CsDS crystals, inserted in Glass Pyrex® Tubes (Internal Diameter = 15 [mm], Length = 80[mm]).

Then, water was added at T = 25 [ºC] and the samples were sealed with screw caps. In certain cases, the sample preparation involved that the solid crystals be manually ground using a grinding mortar and pestle, by which process the solid crystal size would be more finely dispersed in water and this process would increase the chances that the system could approach thermodynamic equilibrium (See 5.2.2.) it is also likely that with increased dispersion in water, the solid crystal size have satisfied the powder limit in size, as well(particle size: 0.8 - 75 [μm]) **[75]**.The powder limit is a necessary condition for the X-ray Diffraction experiments and is mainly discussed in sections 2.4.3 and 5.4.2., 5.7. and 5.9 The sealed tubes would be ready for visualization.

Methods:

The tubes were submerged in a water tank at T = 25 [ºC]. The tank was connected with a heating source. An agitator had a spinning speed at 45 [rpm]. This ensured uniformity in the tank temperature. Cross-polarized light would used to check for birefringence (because of presence of anisotropic crystals in the samples).

At this point, certain terms that are used throughout in the thesis are defined; these are the terms: ‘run’, ‘cycle’ and ‘set’. According to their usage throughout the thesis, a ‘cycle’ is the thermal protocol that was used for the samples. A ‘run’ is a single experimental session, at which at least one set was examined. A ‘set’ is the number of samples examined at each concentration, simultaneously. In cases where there was a single sample at a concentration, the terms ‘sample’ and ‘set’ coincide.

Two different cycles of experiments have been included:

The 1st cycle involved periodic heating and cooling (no seed added). In fact, a certain

time needed to elapse for the temperature of the water tank to be the same as the temperature of the glass Pyrex® tube. Later on, however, this was taken into account. Both in the methods in Chapter 2 and in the results reported in Chapter 4, the actual sample temperatures as well as the water tank temperature have been included (see 4.2.1 and 5.2).

In the 2nd cycle the samples were heated, at first. Then, they were cooled and seed was added in them. The samples were then heated again (in fact, this is the correct way for the system to approach thermodynamic equilibrium). The time needed to elapse, for the temperature difference between the water tank and the glass Pyrex® tube to become zero, has been taken into account. The temperatures that are mentioned for that cycle are the temperatures of the glass Pyrex® tube.

The differences between the 1st and the 2nd cycle are described in Chapter 5.2. The major difference, however, between the 1st and the 2nd cycle is the use of a tiny solid seed. The use of a seed helps to prove that the system has reached thermodynamic equilibrium (see 4.2.1, 5.2.1). As mentioned previously in brief, in a more careful examination of the Krafft temperature for the 1st heating cycle in the 5 wt % - 20 wt % concentration region, the estimation for the time needed for the center of the glass Pyrex ® tube to reach the temperature of the water tank was included. To find that time, dimensionless heat transfer charts were used (Heisler diagrams) **[76]**. The temperature field within the control volume of the glass tube is described as a function of the radial distance and time, T = T(r, t).The Pyrex® tube is considered an intersection of an infinite cylinder and an infinite slab. Using the Heisler Diagrams **[76]**, the time is calculated for each object (once for the infinite cylinder and once for the infinite slab). Using superposition, the solution for the finite cylinder will be the product of the 2 above solutions. When the Fourier Number for the system at a certain dimensionless temperature Y is known, that time can be found.

By using the following constants:

Density = 1000 [kg /m^3] (density of water) **[77]**

Cp = 4.05 [kJ/Kg] (thermal heat capacity of the medium - water) **[77]**

R = 0.5 [cm] (radius of the glass tube)

$\alpha = 1.36 \cdot 10^{-3}$ [cm^2/sec] = k /[density · Cp] (thermal diffusivity of a glass) **[78]**

the Biot Number and the dimensionless Temperature Y for the system were calculated. For these values, the time (either for the infinite slab or for the infinite cylinder) for the center of the control volume to reach the temperature of the water tank was estimated to be about 12'.

As far as the time needed for the center of the sample to reach thermodynamic equilibrium at certain temperature, it is assumed that this time is about 30 minutes, after the center of the sample has reached the water tank temperature.

The digital thermometer (thermometer 'A'), which was used, had been bought at the stockroom of the Chemistry Department at the University of Minnesota. This thermometer had an accuracy of ±0.1 [ºC]. Before inserting in the water tank, thermometer 'A' measured the ambient temperature, at T = 25[ºC]. This measurement was compared with the temperature, measured by a thermometer in the ambient space (thermometer 'B'). The measurements of the 2 thermometers were in good agreement. After having inserted thermometer 'A' and another thermometer (thermometer 'C') in the water tank, thermometers measured the temperatures within the following temperature regions: T < 25 [ºC] and at T > 25 [ºC]. In either temperature region (at T < 25 [ºC] and at T > 25 [ºC]), the temperature, that was measured by either thermometer 'A' or 'C' simultaneously, was the same. The comparison between thermometers 'A', 'B' and 'C', at different temperatures and different environments, showed that the indications of the thermometers match.

Thermometer 'A' has also measured the temperature of an ice/water bath, a mixture where its temperature is a superior standard. Considering the thermometer's accuracy of ±0.1 [ºC], this thermometer measured the ice/water mixture within its accuracy (0.2±0.1 [ºC]). This effective comparison between the three thermometers, as well as the accuracy of thermometer 'A' in the determination of the ice/water bath temperature, are two facts that strengthen the support of the measurements of thermometer 'A' and, therefore, the findings of these experiments.

2.3.3.3.1. 1st Cycle: periodic heating and cooling only (no seed added)

Concentration region: 5 wt % - 20 wt % CsDS

A single run was performed, with one sample at every concentration 5 wt %, 10 wt %, 15 wt % and 20 wt % CsDS. All 4 samples were thermally treated simultaneously. In this experiment, periodic cooling and heating were performed in this temperature region with the same heating and cooling rates. The samples were prepared at T = 25 [ºC] and they were submerged in the immersion bath, at T = 31±0.1 [ºC] (water tank temperature). Starting from T = 25 [ºC], the samples were heated with a large heating rate (0.2 [ºC/min]) up to T ~ 31 [ºC] (solution temperature) and T = 34.2±0.1 [ºC] (water tank temperature). Then, a lower heating rate (0.05 [ºC/min]) was selected in the temperature region between T ~ 31 [ºC] (solution temperature) and T = 34.2±0.1 [ºC] (water tank temperature), to T ~ 35 [ºC] (solution temperature) and T = 38.2±0.1 [ºC] (water tank temperature).

Concentration region: 25 wt % - 40 wt % CsDS

The time needed for the temperature of the tank to be the same as the temperature of the glass Pyrex® tube, was taken into account. The samples started as solid crystals dissolved in water at T = 25 [ºC]. In this intermediate concentration region 25% wt - 40% wt CsDS, two independent sets were performed, each set consisted of one sample at every concentration; 25%, 30%, 35%, 40 wt % CsDS.

Concentration region: 45 wt % - 60 wt % CsDS

The time needed for the temperature of the water tank to become the temperature of the glass Pyrex® tube was taken into account. Three independent sets have been performed, each set consisted of one sample at every concentration; 45%, 50% and 55 wt % CsDS. For the concentration 60 wt %, a single sample was examined in a different run. At T = 25 [ºC], all samples consisted of two phases (solid crystals and micelles), mainly solid crystals. The samples were heated from T = 26 [ºC] up to T = 39.2 [ºC], with a heating rate of $\Delta T/\Delta t$ = 0.08 [ºC/min]. The heating rate to approach thermodynamic equilibrium was the same as the one used by Kekicheff et al. **[2]** in their findings for the SDS/water phase diagram.

2.3.3.3.2. 2nd Cycle: the correction by a tiny solid seed

The 2nd cycle involved: heating, cooling with seed addition and reheating. This protocol provides more chances for the system to approach thermodynamic equilibrium - which is a necessary condition to calculate the Krafft temperature at the corresponding concentration. The process is provided below:

1. A 1st heating had a measured transition temperature T1 (candidate Krafft temperature) at which temperature the teeny tiny solid crystal has disappeared (at least for the macroscopic observation).

2. Cooling with seed addition; the sample was cooled to a certain temperature (T < T1). At that same temperature, the seed that had been added did not dissolve after certain time (~30').

3. A 2nd heating followed, where a transition temperature T2 was measured (at which temperature the teeny tiny solid crystal had disappeared).

The matching of the 2 temperatures with each other (T1 = T2), suggests that this temperature is indeed the Krafft temperature.

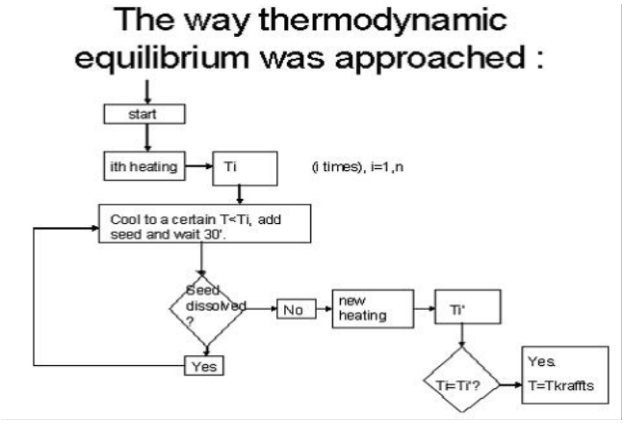

Fig.2.4. Thermodynamic equilibrium approach for the 2nd cycle.

Concentration region 5 wt % - 20 wt % CsDS

A single run was performed, with a set of three samples at every concentration; 5%, 10%, 15% and 20 wt % CsDS. At T = 25 [ºC], the samples consisted of two coexisting

phases (solid crystals and micelles). The samples were heated with a rate of 0.2 [ºC/min], from T = 25 [ºC] to T = 37.5 [ºC]. At the last temperature, the sample stayed for 40'.

The cooling rate that was used, was 0.05 [ºC/min], from 38 [ºC] down to 34.8 [ºC] and 0.1 [ºC/min], from 34.8 [ºC] to 32 [ºC]. According to the protocol of Figure 2.4, the samples would reach a certain temperatures, lower than the transition temperature of the 1st heating treatment. At that same temperature, a seed would be added in all of them and they would stay at that temperature for a certain period of time (in these experiments, for example, the samples stayed at T = 34.8 [ºC] for 12'.). If the seed (that had been added) was dissolved at a certain temperature, the system would be cooled down by 1 [°C]. A new seed would be added and the sample would stay at that same temperature. This process would be repeated, until the seed was not dissolved. The mass of solid seed that had to be added, had to be small enough, so that the concentration of the CsDS/water system does not practically change. Indeed, the mass of the seed that was added, was in the order of 3 [mg] in all cases, while the mass of the solid crystals was about 20 [mg].The mass of the crystals, was an order of magnitude higher (see Appendix B). The heating rate was in the same order of magnitude with the one used by Kekicheff et al. **[2]** in their findings for the SDS/water phase diagram.

Concentration region 25 wt % - 40 wt % CsDS

The thermal protocol was the same, as the one described above for the concentration region 5 wt % - 20 wt % CsDS. Assuming that the time for the seed to dissolve does not depend on the concentration, the waiting time at a certain temperature (to observe phase transitions and for the seed to dissolve) is the same with the lower concentration region between 5 wt % and 20 wt %.

2.3.3.4. Limitations

Some of the major limitations for the macroscopic experiments using cross-polarized light are:

1. Sample impurity.

The CsDS impurity is a major concern for these macroscopic observations. The impurities could be due to the reagents, such as SDS (organic and/ or inorganic) or CsCl. Certain parameters could affect the sample's concentration and its purity, such as improper screw cap sealing, drastic humidity changes (if the screw cap were loose) and dust and dirt from the outside environment. This example might be helpful to illustrate a case, when impurities might affect the sample: A glass tube, which had previously been washed with deionized water and had not been washed thoroughly, was inserted in an oven for several hours for the remaining water droplets to evaporate. When the glass tube was removed from an oven, water droplets might still be in the glass tube). The sample's purity (and impurity) was first described in sections 2.2.1.2 and 2.2.1.3; sample purity is also discussed in sections 5.5 and 7.6.

2. Sample inhomogeneity.

The sample has to be as homogeneous as possible. The dispersion of solid crystals in water is a parameter that can affect the approach of thermodynamic equilibrium for the system. The more finely dispersed the solid crystal in water, the faster the approach of thermodynamic equilibrium. A more elaborate analysis of the solid crystal dispersion in water follows in 5.2.2.

3. Heating rate selection

This is a very important independent variable. Only the proper selection of heating rate is going to provide representative results. There should be a balance between heating rate selection and experimental time. This has been shortly discussed in 2.3.3.3. and is thoroughly analyzed in 5.2.1.

4. Temperature uniformity

The immersion bath temperature uniformity is necessary, in order for the results to be more reliable. As mentioned in 2.3.3.3, an agitator with a spinning speed of 45 [rpm] was used, to make sure that the temperature is uniform throughout the tank. A thermometer (thermometer C) was immersed in the tank to measure the temperature. The temperature of the sample was calculated, by correcting the water tank temperature, using the Heisler Charts

(mentioned in 2.3.3.3.) **[76]**. The reliability of the temperature measurements (using three independent thermometers), is discussed in section 2.3.3.3, as well.

5. Surface roughness

No glass Pyrex® tube was deliberately scratched. Microcracks on the inner surface of the glass tube might enhance the effect of surface roughness of the glass tube on the observations. These microcracks create an interfacial area for nucleation and growth of a new solid phase. Unfortunately, this is a parameter that it is difficult to control. It is also difficult to have glass tubes with no internal surface roughness.

2.3.4. X-ray diffraction analysis (Experiments performed by Torija M.J. and the results are provided by her permission)

2.3.4.1. Goal

The X-ray Diffractograms of the samples would help:

- To examine the unit cell crystal structure of the purified CsDS samples (unheated, heated, superheated, supercooled) and the impure CsDS (Impurities in SDS that was used to synthesize CsDS, were mentioned in 2.2.1.2. and they are also analyzed in 5.5 and in 7.6).
- By comparing the purified CsDS X-ray Diffractogram with the analogous Diffractogram of SDS, to deduce conclusions about similarities and/ or differences regarding the unit cell crystal structure of the 2 crystals. All the samples were tested at T = 25 [ºC].
- To examine whether possible impurities present in the impure CsDS, have affected its unit cell crystal structure compared to the purified CsDS (see 5.5, 7.6. and 2.2.1.2).
- To check if the initially superheated and initially supercooled samples (macroscopically different samples) that have already been naturally cooled and warmed to T = 25 [ºC], respectively, represent metastable states or not. This can be done by comparing the diffractograms of all the purified CsDS samples. This would be the first step towards the identification of the unit cell crystal structure characteristics.

Specifically, using some software (such as the software Jade, found at the Characterization Facility of the University of Minnesota, Minneapolis **[79]**), the information

provided by the X-ray diffractograms can help to identify the following information for the CsDS crystal:

1. Cell type (monoclinic, triclinic etc.)
2. Space group (C2, P1 etc.)
3. unit cell edges a, b, c
4. unit cell angles α, β, γ
5. 'd' spacing
6. Unit cell volume and density

The set of X-ray Diffraction experiments have taken place at the Characterization Facility using the instrument Brucker –AXS MicroDiffractometer **[79]**. The reason why the MicroDiffractometer and not a regular powder diffractometer was used, was because of the small angle diffraction region that Kekicheff et al have suggested in their study of the SDS/water system **[4].**The same diffraction angle region was used for the CsDS samples.

Two methods, which can be used to collect the data set of Intensity vs. 2·θ and the Debye rings at certain angles, are presented:

1. The powder method **[80]**.

2. The Debye - Scherrer method **[81]**.

2.3.4.2.1. Technique 1 - The powder method

1. CsDS crystals are ground to powder and are inserted in the center of a rotating stage **[75]**.According to Torija M.J., 'the instrument was a diffractometer with horizontal platform, area detector and collimator of 0.8 [mm] diameter.'

2. An X-ray beam is excited from a metal (copper) sealed tube with a certain voltage 45 [kV] and certain electrical current intensity 40 [mA]. The X-ray beam passes through a crystalline monochromator where only the most abundant wavelength - K_{α} - is allowed to pass through. Then, this wavelength is scattered towards the specimen.

3. The monochromated X-ray beam encounters the powder sample. The sample is rotated and the diffraction angles of the given material are measured. An area detector is used

to measure the diffracted beam intensity, at diffraction angles between 0 - 2·θ degrees, or, between 5° and 75° **[81]**. Following Torija M.J., 'the frames are centered at 15 degrees.'

4. Diffractograms with coordinates Intensity vs. 2·θ are formed **[81]**. Based on the information provided by the diffractograms, the interplanar spacing d can be estimated, according to Bragg's Law for a certain diffraction angle, θ: $n \cdot \lambda = 2 \cdot d \cdot \sin\theta$ **[82]**.

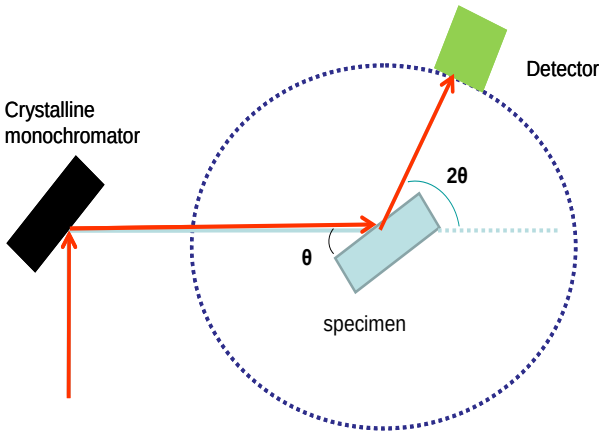

Fig.2.5. The X-ray Diffraction technique for the Powder Method, reported by Alen T. **[75]**. The Figure has been reproduced with permission that has been granted from the Copyright Clearance Center Inc. (see Appendix G for permission)

2.3.4.2.2. Technique 2: The Debye - Scherrer Method

1. The crystalline sample is ground to powder. Then, the ground sample is inserted in a glass tube in the center of a Debye - Scherrer camera **[75]**.

2. Monochromated X-ray beam interacts with the sample and based on the orientation of the crystallographic planes, diffraction cones at certain diffraction angles (2·θ) are formed.

3. The conical shape is based on the rotational symmetry of the diffraction for the crystals, as long as the Bragg's law is satisfied for the certain angles **[82]**.

4. A circular film strip surrounding the particle exhibits the diffraction patterns as concentric rings. These rings are the result of the interaction of the light beam cones with the film. Rings are formed at planes, where constructive interference of wavelengths takes place (wavelengths diffracting at particular interplanar crystal spacing - d_{hkl}).

5. Debye rings are formed **[80]**.

2.3.4.3. Materials and methods

CsDS crystals for all five samples (purified and impure) were prepared by recrystallization **[16]**, **[51]** (regarding purification mentioned in this thesis, see sections: 2.2.1.2, 2.2.1.3, 5.5 and 7.6). The sample preparation differs between the four purified CsDS samples and the impure CsDS. For the purified samples, the purification included removal of possible impurities from SDS, as described in section 2.2.1.2. The SDS, which had been used in the synthesis of the impure CsDS, was not purified in ethanol. On the other hand, the purity of the SDS, which had been used in the synthesis of CsDS by aqueous recrystallization, was the one claimed by the vendor. The following steps have been the same for all five samples:

1. SDS was dissolved in an aqueous solution of CsCl, where SDS was recrystallized into CsDS, as described in 2.2.1.3.

2. The samples were brought at the Characterization Facility in glass Pyrex® tubes. From this point on, Torija M.J. at the Characterization Facility of the University of Minnesota performed the next steps of the experiment. The X-ray Diffraction analysis was performed at T = 25 [ºC], with a q range between 1.4 and 1.6. The quantity q is a dimensionless number called 'wave vector'. This quantity ('q') indicates the propagation direction of the X-ray wavefront and is defined as the vector difference between the incident and the diffracted beam **[83]**. The parameter 'q' is used to interpret the particle size, d_p, according to the following formula: $q = 2 \cdot \pi \cdot \lambda / d_p$ **[83]**.

Table 2.2. Different concentrations and types of samples analyzed at the Bruker AXS-MicroDiffractometer. (The colors are simply a convention) **[79].**

'Red'	**'Green'**	**'Yellow'**	**'Grey'**	**'Sample B'**
45% liquid crystalline, unheated	40% supercooled (candidate Metastable)	40% superheated (Candidate Metastable)	5% room temperature, solid crystals and water	15 wt % Unheated
Purified CsDS	Purified CsDS	Purified CsDS	Purified CsDS	Impure CsDS

2.3.4.4. Limitations

1. Powder limit

In order for the X–ray Diffraction experiment to succeed, any particle of the material under examination (on average) has to satisfy the powder limit. The powder limit range for a particle size is between 0.8 [μm] and 75[μm] **[75]**.

2. Sample purity

The purity of CsDS is a very fundamental parameter that should be concerned. The impurities could be organic and/or inorganic. The sample's purity (and impurity) is discussed in 2.2.1.2, 2.2.1.3, 5.5 and 7.6.

3. Sample inhomogeneity

The sample has to be as homogeneous as possible, in order for the diffractogram to be representative. The dispersion of solid crystals in water is a parameter that can affect the approach of thermodynamic equilibrium. There is more elaborate analysis of the solid crystal dispersion, in 5.2.2.

4. Instrument limitations

The preselected $2 \cdot \theta$ range where the diffractogram is obtained, is another limiting parameter of the instrument. It is possible that the $2 \cdot \theta$ range that had been selected was not able to capture the whole spectra of the sample. This scattering angle regime has to be carefully selected in order to demonstrate the diffractogram of the crystal.

2.3.5. Optical Microscope experiments (by the aid of Suszynski W., who helped in the design of the slide and who provided the polar filters)

2.3.5.1. Goal

A set of experiments was designed at the Coatings Process Fundamentals Laboratory at the University of Minnesota, with the help of the Research Engineer in charge of the Laboratory, Suszynski W. These experiments were performed, in order to:

1. Observe multiple phase transitions of different samples representing a wider concentration region (5 wt% - 100 %wt). These samples were heated simultaneously with the

same heating rate, under a single glass slide (see method).

2. Prove if anisotropic liquid crystals exist, in samples at the intermediate concentration region (30 wt % - 45 wt % CsDS). It should be verified if mosaic structures or other 'liquid-crystal'-type structures (representative of anisotropic materials) are formed **[84],** in proving that anisotropic liquid crystals exist or not, apart from checking the presence of birefringence through cross-polarized light.

3. Double-check the transition temperatures that have been observed in the macroscopic experiment, for the solubility curve (concentration region: 1 wt% - 30 wt % CsDS).

4. Get images of solid and liquid crystals of CsDS.

2.3.5.2. Technique

The optical microscope setup consisted of an optical microscope and a pair of polar filters; a polarizer and an analyzer.

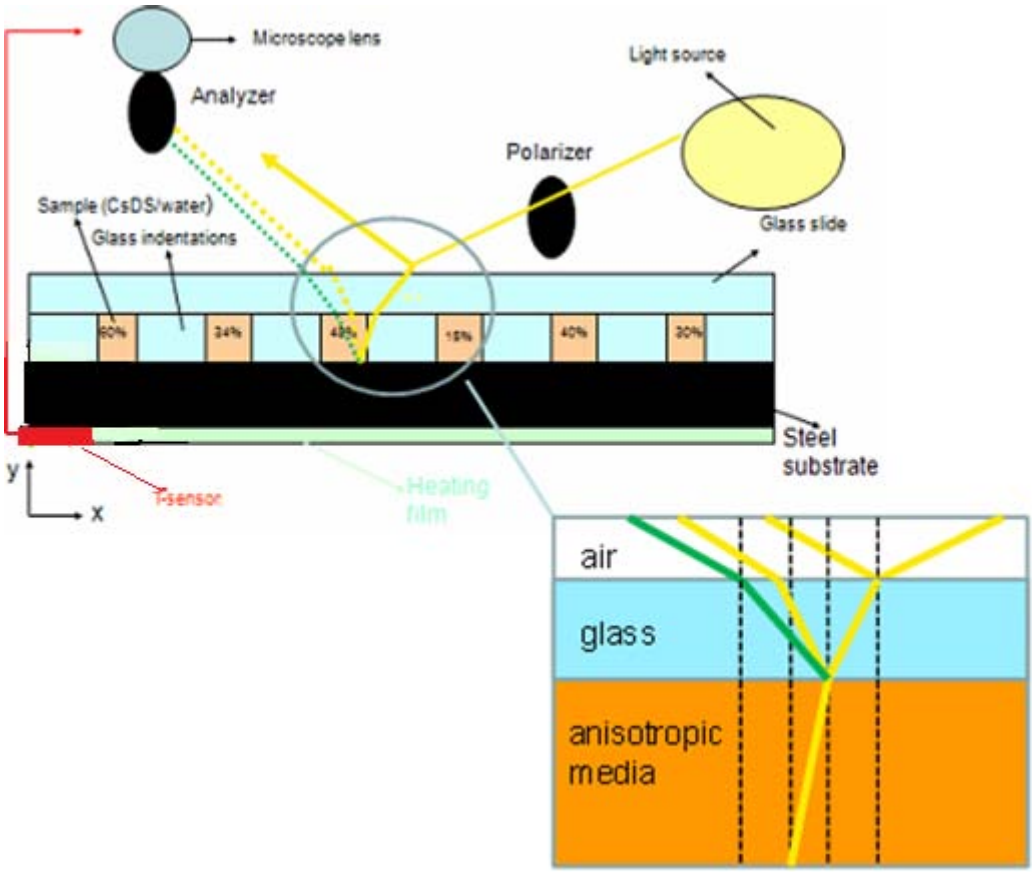

Fig.2.6. Optical microscope setup.

The operation setup is described below:

1. A uniform, white light beam comes at an angle to the reference y-axis from the fiberoptic light illuminator and is shown in Figure 2.6. as a yellow beam.

2. The light beam first passes through a polarizer. The polarizer is a glass filter that allows for wavelengths that propagate along certain planes only, to pass through.

3. The plane-polarized light arrives at the glass surface. The interaction of the light beam with the media, whether the media is air, glass and/or sample, is governed by the Snell's law **[70]**. The light wavelengths that propagate from the air towards the glass slide (the propagation direction forms a nonzero angle with respect to the y-axis) arrive at the air/glass interface. Since air and glass are different media, they have different refractive indices. A part of the transmitted beam gets back-reflected. Another part of the transmitted beam refracts through the glass.

4. Part of the already refracted (at the air/glass interface) beam gets again back-reflected and refracted, at the glass/sample interface. If the sample is anisotropic, the back-reflected beam will split in two wavelengths that propagate along two different planes that are perpendicular with each other. Certain solid crystals are anisotropic, such as $BaTiO_3$ **[72].** Also, all liquid crystal phases but the cubic phase, are anisotropic. In anisotropic materials, the optical properties of the material vary along certain crystallographic directions. The anisotropy of a material is also related to its birefringence. Birefringence means that the polarized beam, which has already interacted with an anisotropic sample, will back-reflect and split in two beams. These two beams (indicated with green and yellow colors in Figure 2.6.) propagate along two different crystallographic planes on the sample that are perpendicular with each other (see the magnified image on the down-right part of Figure 2.6). The dotted black lines, which are located at the down-right image of Figure 2.6 represent the perpendicular axis (y-axis).

5. The rest part of the beam that has arrived at the air/glass interface, gets back-reflected. On the way to the CCD camera (see Method), these two light beams will undergo a 3^{nd} refraction (and back-reflection) at the glass/sample interface and a 4^{th} refraction (and

reflection) at the air/glass interface. As mentioned before, the corresponding light waves propagate along different planes. Since the planes are different, each plane is characterized by different refractive indices.

6. The two split light beams will arrive at the analyzer (2^{nd} polar filter). The analyzer is a light filter that recombines the two light beams into a single beam, according to constructive and destructive interference. Constructive interference means that wavelengths propagating with the same phase will add up in magnitude, while destructive means that waves out of phase will cancel out each other **[74]**.

7. After constructive interference, the recombined beam (the superimposed beam of the two split beams) arrives at the microscope for visualization **[74]**.

8. If the observed structure is an anisotropic liquid crystal, characteristic patterns of anisotropic liquid crystals could be observed, such as fan-like structures **[42]**, Schlieren textures and/or oily streaks **[42]** and mosaic texture **[84]**.

2.3.5.3. Materials and methods

Sample preparation:

1. The CsDS crystals were synthesized by recrystallization of an aqueous CsCl solution with SDS (see 2.2.1.2, 2.2.1.3, 5.5 and 7.6) **[16]**, **[51]**. Both purified SDS and impure SDS was used to synthesize CsDS.

2. The crystals were weighed on an analytical balance. They were deposited on a 5 [cm] x 5 [cm] sheet of paper. This is a typical paper with glossy texture that is used to weigh materials on an analytical balance and it has been bought at the Chemistry Stockroom at the University of Minnesota. The sheet of paper was folded to reduce its surface to one fourth of its initial surface and it was pressed using a hand fist, in order to smash the crystals into finer particles. This ‘smashing’ process lasted for about a minute.

3. The ground solid crystals were inserted into the glass indentations of the glass slide that had been used for these experiments. Water was added in order to make the samples slurries. A glass stick was used to homogenize the dispersion adequately.

4. The indentations with samples inside were covered by a glass slide.

Method:

On the bottom of the assembly, a resistor wire (red box, in Figure 2.6) is sandwiched between two thin plastic films and forms a heater, according to Suszynski W. The resistor wire acts as a heating element. A thermocouple (insulated in a small silicone mold) was attached to the resistor wire heater, but not connected to the wire itself, as this would cause the current to flow from high voltage circuit to low voltage circuit, according to Suszynski W. and would consequently damage the heater control unit. The thin steel plate placed on top of the heater is used to uniformly distribute the generated heat to the samples. Right above the steel plate, small glass chambers with samples inside are located. The small glass chambers have been built on a standard microscope slide base by adhering to it (with epoxy) smaller, rectangular glass pieces. These pieces were roughly 2 [cm] in length and 0.5 [cm] in width. The samples in a slurry form were inserted into these chambers (glass indentations), as described in the sample preparation section. The heater and the thermocouple (red box, in Figure 2.6) are connected to the digital heater controller. The thermocouple provides steel plate top surface temperature feedback to the controller. The sample chambers are covered by a glass slide. The slide, which acts as an insulator that reduces heat loss, allows for the light to pass and provides optical access for observation. A fiberoptic light source is placed close to the samples. The light that is produced by the fiberoptic source goes through a fiberoptic guide. The guide end is mounted at a fixed incident angle and has a polarizer attached to it.

2.3.5.4. Limitations

1. Instrument resolution

The light microscope's resolution is 200[nm] **[68]**. So, particles with dimensions less than 200 [nm] cannot be visualized under the optical microscope.

2. Sample purity

The CsDS purity is a major concern. The impurities could be organic and/or inorganic. The sample's purity (and impurity) is described in sections 2.2.1.2, 2.2.1.3.3 and is also discussed in 5.5 and in 7.6. In this experiment, however, the impure CsDS was also inserted

in the indentations for visualization.

3. Sample inhomogeneity:

Within the indentations, the suspension (slurry) has to be as homogeneous thin film as possible, in order for the measured temperature to be representative. As mentioned in all the experiments, the dispersion of the solid crystals in water is a parameter that can affect the approach of thermodynamic equilibrium for the system. There is more elaborate analysis of the solid crystal dispersion in 5.2.2.

2.3.6. Small angle X-ray Scattering experiment (Experiments performed by Torija M.J. and the discussion is provided by her permission)

2.3.6.1. Goal

1. To check if some liquid crystal phase is present in a CsDS/water sample, at a certain temperature and concentration (T = 45 [ºC] and 32 wt % concentration).

2. To identify the type of the liquid crystal phase (hexagonal, lamellar or other), if liquid crystal phase exists.

2.3.6.2. Technique

The following schematic depicts the basic light scattering principle. An explanation of that schematic follows.

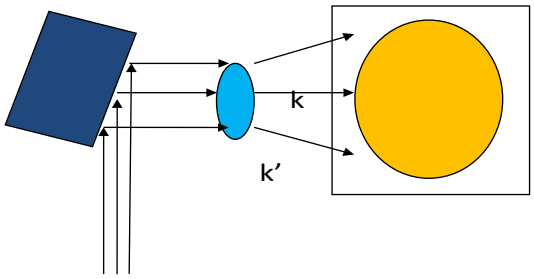

Fig.2.7. The X-ray Scattering concept. The original Figure has been reported by Paul F. Fewster **[85]**. The Figure has been reproduced with one-time and non-exclusive permission that has been granted from the World Scientific Publishing Company, Mrs. Ning Tu (ntu@wspc.com.sg) (see Appendix G for permission).

1. Electrons are excited from certain orbitals of a metal (copper). These electrons

produce an unfiltered X-ray beam (black arrows). The beam interacts with the monochromator (indicated dark blue in Figure 2.7). The most abundant X-ray wavelength will pass through the monochromator and will be scattered.

2. The monochromated X-ray beam interacts with the sample (indicated light blue in Figure 2.7). Some part of the beam is scattered after the interaction with the particle, while another part of it is not scattered (The wavevectors k' are the ones with the maximum perpendicular deviation in direction with respect to the propagation direction of the unscattered wavevector k).

3. After the interaction with the sample, the scattered beam travels in a flight tube. Then, the scattered and unscattered beams arrive at the 2-dimensional surface detector. A photomultiplier measures the intensity of the scattered X- ray beam **[85]**.

4. The scattered electron beam is absorbed by the detector and a circular 2-dimensional projection (indicated bright orange in Figure 2.7.) of the scattered electron beam is formed.

The scattered and unscattered electron beams (k' and k respectively), the scattering wavevector q, the scattering angle θ and the particle size d_p are all related to each other with the following relations:

(i) $q = k-k'$ **[83]**

(ii) $q = 4 \cdot \pi \cdot \sin\theta/\lambda$ **[83]**

(iii) $q = 2 \cdot \pi/d_p$ **[83]**

2.3.6.3. Materials and methods

Sample preparation:

1. The purified (see 7.6, 5.5, 2.2.1.2. and 2.2.1.3.) CsDS crystals were synthesized by recrystallization of aqueous CsCl solution with SDS **[16]**, **[51]**.

2. A weighed quantity of crystals was added in a glass capillary of 1 [mm] diameter (provided by Charles Supper Company). Then, water was added at T = 25 [ºC] to reach the desired concentration of 32 wt % CsDS. At T = 25 [ºC], the system was heterogeneous (2 phases).

3. The sample was sealed with Teflon tape and was heated to a temperature higher than 40 [ºC] instantly, with large heating rate (larger than 1 [ºC/min]). The reason for that heating

was, as Torija M.J. had suggested, to check if the macroscopically two different phases would look different at T=25 [ºC], after the sample had already been cooled down to T=25[ºC]. The sample looked heterogeneous and biphasic, when it was cooled down again.

4. The sealed, naturally cooled capillary was brought to the Characterization Facility at the University of Minnesota, at T=25 [ºC], where Torija M.J. performed the rest of the analysis at T=25 [ºC]. The idea was to re-heat the samples from T=25 [ºC] to a temperature higher than 40 [ºC].

Methods (by permission of Torija M.J.)

The capillary was inserted in the Chamber of the SAXS instrument. The analysis was done at T = 25[ºC], with a q range between 1.4 and 1.6 ($q = 2 \cdot \pi / d_p$), where d_p is the particle size. A single sample was examined. The sample was heated from T = 25[ºC] to T > 50 [ºC] (the heating rate is unknown) for more than 45'. Intensity vs. $2 \cdot \theta$ values for this sample were provided at T = 45[ºC], where the sample has stayed at that temperature for 45' and 60'.

The outcome of this attempt to identify the liquid crystal phase is discussed in section 7.2, in the bounds of a future work.

2.3.6.4. Limitations

1. Instrument limitation

Data can be collected within the following $2 \cdot \theta$ regime: between 0.10 and 15 degrees, depending on the detector to sample distance. This corresponds to structural features that span the dimension range between 0.25 and 80 [nm] **[86]**.

2. Sample homogeneity

The sample has to be as homogeneous as possible, in order for the scattering data to be representative. The dispersion of solid crystals in water is a parameter that can affect the approach of thermodynamic equilibrium for the system. There is more elaborate analysis of the solid crystal dispersion in 5.2.2.

3. Powder limit

When a crystal sample is analyzed, any particle of the material (on average) has to satisfy the powder limit. This would increase the reliability of the scattering data. As has been mentioned in 2.3.3.3, the particle size range is between 0.8 [μm] and 75[μm] **[75]**.

4. Sample purity

The CsDS purity is a major concern. The impurities could be organic and / or inorganic. The sample's purity (and impurity) is discussed in 2.2.1.2, 2.2.1.3.3, 5.5 and in 7.6.

CHAPTER 3

THE CsDS/WATER SYSTEM AND A DESCRIPTION OF THE SDS/WATER SYSTEM

3.1. Preface

Chapter 3 presents the major experimental results that have been performed in order to investigate the phase behavior of the CsDS/water system. It also includes a brief report on some of the analogous features of the SDS/water system, where the SDS/water system is reported by Fontell et al., Kekicheff et al. **[1]**, **[2]** and **[3]**. The results of the experiments by each method that was used to explore the CsDS/water phase behavior, are reported in Chapter 4 and are analyzed in Chapters 5 (Discussion) and 7 (Ongoing work and future perspectives). The CsDS/water phase diagram follows a brief discussion that explains the various structures depicted.

3.2. The CsDS/water phase diagram

Figure 3.1 includes almost all the structures that have been observed at various temperatures and concentrations, with the analogous characterization techniques that were used.

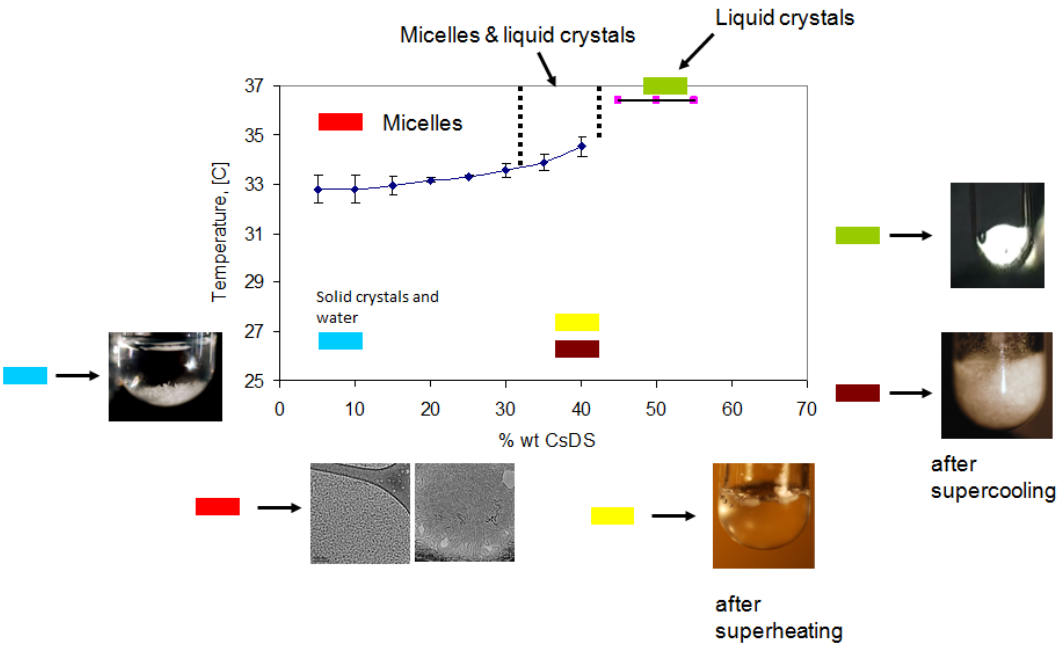

Fig.3.1. The CsDS/water phase diagram **[16]**.

Specifically, the macroscopic observations with cross-polarized light in the concentration region 5 wt % - 30 wt % CsDS have resulted in the solubility curve estimation (transition of CsDS solid crystals and water to isotropic micellar solution). The solubility curve is relatively flat at temperatures around 33 [ºC]. The standard deviation in the solubility curve is calculated with respect to the average of the transition temperatures at a certain concentration, for a single heating cycle. The system at temperatures between 25 [ºC] and 33[ºC] is represented by the solid crystal and water as a two-phase region (blue legend - The photograph was captured at T = 25 [°C]).

At temperatures higher than 33 [ºC] and in the concentration region 5 wt % - 30 wt % CsDS, the system is in the region of one-phase isotropic micellar solution. Using Cryo-TEM (by permission of Arunagirinathan, M.A.; Bellare, J.R. who operated the instrument), ellipsoidal and threadlike nanostructures have been observed (bright pink legend-TEM images captured at T=33 [°C]). The ellipsoidal structures had the following characteristic dimensions: semi-major axis: 7 [nm] and semi–minor axis: 5 [nm] and the threadlike structures had a diameter of about 15 [nm] **[16]**.

At temperatures higher than 34 [ºC] and in the concentration region 30 wt % - 45 wt% CsDS, the results of the macroscopic experiments with cross-polarized light suggest that the system lies in a two-phase region, where micelles coexist with some birefringent crystal phase. All birefringent phases that have been observed macroscopically with cross-polarized light should probably be liquid crystals and not some anisotropic solid crystals. The arguments that the birefringent phase and is a liquid crystal – and not a solid crystal - are several. First, this birefringent crystal appears macroscopically the same for temperatures higher than 34 [°C], up to more than 50 [°C]. Second, for heating rates higher than 0.2 [°C/min] in a different concentration region (less than 30 wt %), the same birefringent structures have also appeared, macroscopically. These structures, however, shrink over the time, when the system stays for certain time at certain temperatures (see 5.2.1.1 and 5.9). So, these birefringent structures do not represent a stable phase in the concentration region less than 30 wt %. Third, it is less likely for birefringent solid crystals to have appeared in these

temperatures examined (lower than 50 [°C]). Arguments to support the 3rd reason can be found in the analogous SDS/water system, where for the analogous concentration and temperature region, only anisotropic liquid crystals have been reported **[1]**, **[2]** and **[3]**. Therefore, the already observed birefringent crystals in the CsDS/water system should represent some liquid crystal structures. Finally, the optical microscope experiments with cross-polarized light were performed in order to prove the existence of birefringent liquid crystals. These experiments are discussed in section 7.3.

In the concentration region 30 wt % - 45 wt% CsDS, the exact concentration boundaries of the two-phase region of liquid crystals and micelles have not exactly been identified. This is suggested to be part of a future study. At 40 wt % (yellow legend - The photograph was captured at T = 25 [°C]) the figure represents a sample that looked relatively viscous by naked eye when the photograph was captured (at T = 25 [°C]) but had been treated as follows: It had been initially superheated (the heating rate was larger than 0.2 [ºC/min] from T = 25 [°C] to T = 55 [°C]). After natural cooling to T = 25 [°C], the sample looked relatively viscous. Then, a solid CsDS seed was inserted. At T = 25 [°C] and at the same concentration (~40 wt %), an initially supercooled sample (brown legend) is also depicted. The sample had been heated to 55 [°C] with heating rate 0.2 [ºC/min]. Then, the sample was cooled faster than 0.2 [ºC/min] to 0 [°C]. Finally, it was left to warm up naturally at T = 25 [°C]) (The photograph with the brown legend was captured at T = 25 [°C]).

At temperature higher than 37 [°C] and at concentrations higher than 45 wt % CsDS, birefringent (most likely liquid) crystal sample (green legend) appears. A more elaborate discussion on the CsDS/water system and its comparison with the analogous features of the SDS/water system follow in section 5.9.

Figure 3.1 does not include the results of the XRD, the SAXS and the optical microscope experiments. Both the results of the XRD experiments and some images captured by the optical microscope experiments are presented in Chapter 4. Discussion about all the experimental findings follows in Chapters 5, 6 and 7.

3.3. The SDS/water phase diagram (the features of the SDS/water phase diagram have first been reported by Fontell et al. and Kekicheff et al.) [1],[2] and [3]

Below are presented certain features of the SDS/water phase diagram, which has been reported by Kekicheff et al. and Fontell et al. **[1]**, **[2]** and **[3]**. Section 3.3 includes the results of a Cryo-TEM experiment that was designed to interpret the micellar nanostructures formed by the SDS/water system, in a 0.3 [M] solution. The experiment was done by Arunagirinathan, M.A.; Bellare, J.R. and the permission to use the material was granted by Arunagirinathan, M.A.; Bellare, J.R. **[16]**.

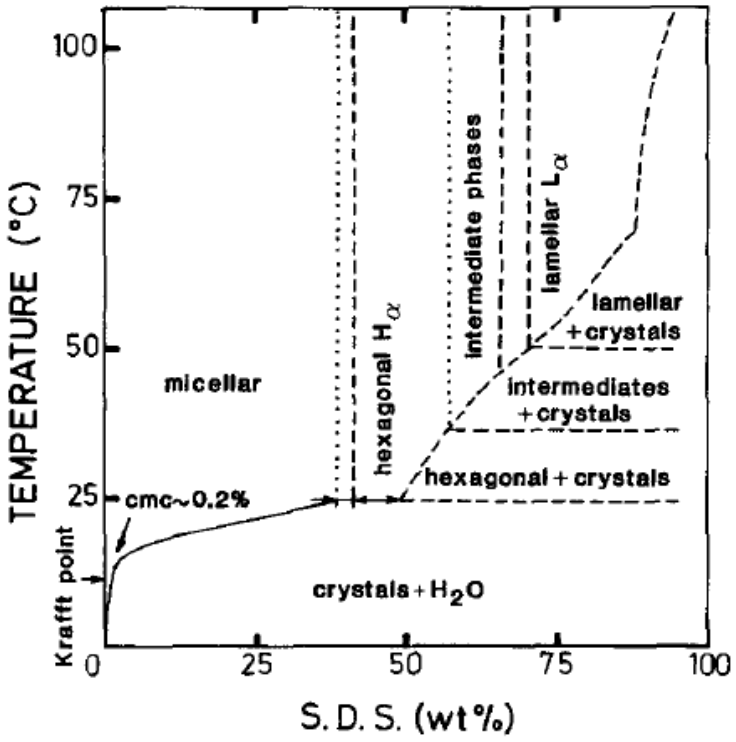

Fig.3.2. The SDS/water phase diagram reported by Fontell et al **[1]**. The Figure has been reproduced with permission that has been granted from Taylor and Francis Group and the Copyright Clearance Center Inc. (see Appendix G for permission)

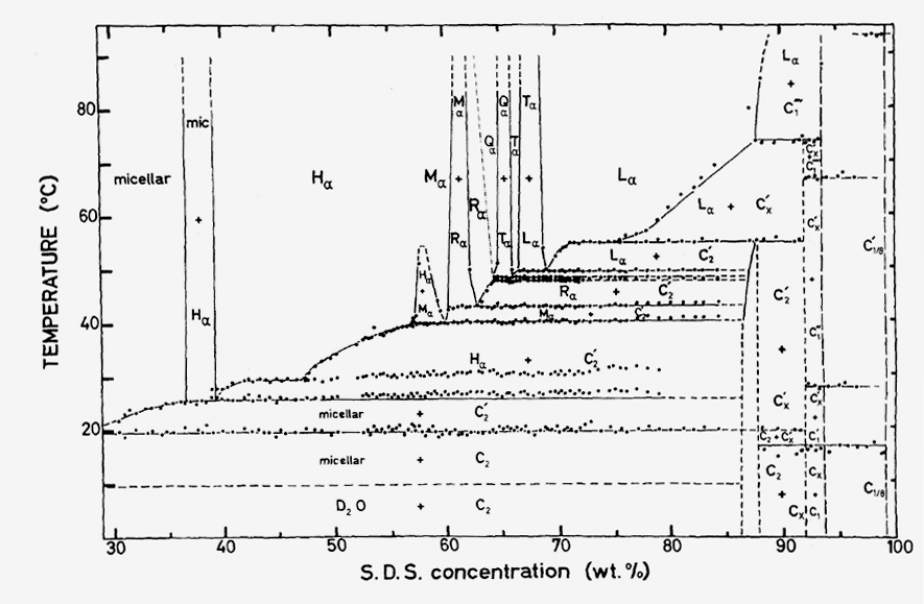

Fig.3.3. The SDS/water phase diagram, as it has been reported by Kekicheff et al **[2]**. The Figure has been reproduced with permission that has been granted from Taylor and Francis Group and the Copyright Clearance Center Inc. (see Appendix G for permission)

Seven certain features of the SDS/water system as they were explored by Kekicheff et al. and Fontell et al. are presented below. These features do not include part of this thesis' exploration and the sentences that are provided, were used to describe these features. They have been included in order to be compared briefly with the analogous features of the CsDS/water system, a system which has been explored with the experiments of this thesis.

1. Solubility curve and Krafft temperatures; concentration region 1 wt % - 35 wt % SDS; reported by Fontell et al. **[1]**

The Krafft temperatures for concentrations less than 25 wt % are lower than 25[ºC]. Table 3.1 presents these temperatures at the corresponding concentrations. These temperatures have been interpolated from the data provided by Fontell et al **[1]**. As far as the solubility curve is concerned, which separates the isotropic micellar region from the anisotropic two-phase micellar and solid crystal region, this exhibits a non-zero slope. As concentration increases, the Krafft temperature increases as well.

Table 3.1. Krafft temperatures for the 5 wt % - 25 wt % concentration region **[1]**

wt % SDS	**T [ºC]**
5%	18
10%	20
15%	21.5
20%	23
25%	23.5

2. Solid crystal structure at temperatures below 19 [ºC]; concentration region 1 wt % - 70 wt% SDS; reported by Kekicheff et al. **[2]**.

For temperatures between 19 [ºC] and 10 [ºC] and in the concentration region 1-70 wt % SDS, the system forms micelles and solid crystals with hydrophobic environment and hydrophilic core (C_2) **[2]**. Crystal polymorph transitions - transformations between solid crystals with differences in their unit cell crystal structure - as well as the actual transition temperatures were both measured using High Sensitivity Differential Scanning Calorimetry **[2], [3]**.

3. Micellar nanostructures of the SDS/water system; concentration region 1 – 35 wt % SDS **[16]**

Cryo-TEM experiments have been conducted by Bellare J.R. and Arunagirinathan M.A. **[16]** for a 0.3 [M] SDS solution and the following VITROBOT parameters: Temperature = 30 [ºC] and Relative Humidity = 100 %. As shown in Figure 3.4, regular spherical micelles of 5 [nm] diameters have been observed **[16]**. The Krafft temperature for this concentration is about 19 [ºC] **[1]**.

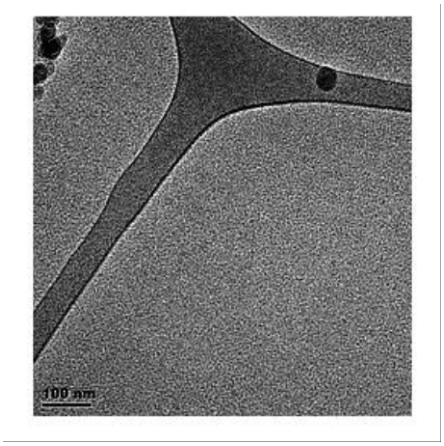

Fig.3.4. 8 wt % SDS solution forming spherical micelles. Size scale: 100 [nm]. Cryo-TEM image has been reproduced with permission from both Bellare J.R. and Arunagirinathan M.A. who both performed the experiments, as well as operated the instrument **[16]**.

4. Intermediate concentration region; 35 wt % - 40 wt % SDS **[2]**

At temperatures higher than 25 [ºC], the system lies in an anisotropic two-phase region; hexagonal phase with liquid-like core (H_α) coexists with a micellar phase. At temperatures lower than 25 [ºC], a two-phase system exists, C_2 solid crystals and micelles. This description is based on the data provided by High Sensitivity Differential Scanning Calorimetry **[2]**.

5. Concentrations between 40 wt % and 55 wt % SDS; studies reported by Kekicheff et al. **[2]** and **[3]**

At temperatures higher than 30 [ºC], the system forms hexagonal phase with liquid-like core (H_α). The transition enthalpies have been calculated, using High Sensitivity Differential Scanning Calorimetry **[2]**. At concentrations higher than 48 wt % SDS, the same authors have explored the phase transitions using X-ray Diffraction and as Deuterium Nuclear Magnetic Resonance **[3]**. Deuterium Nuclear Magnetic Resonance is used to identify the anisotropy of the material. The deuterium nucleus has a quadrupole moment, which interacts with the nuclear electrical environment and perturbs the energy levels of the nuclei **[3]**. In a DMR spectrum - plotted as Intensity vs. Frequency -, the quadrupole of an anisotropic phase

will be split in 2 distinct peaks. This quadrupole appearance is true for all liquid crystal phases but the cubic. The cubic, is a highly viscous, isotropic phase, which gives a single peak in its DMR spectrum **[3]**.

6. Concentrations higher than 55 wt %; studies reported by Kekicheff et al. **[2]**, **[3]**

At temperatures higher than 30 [ºC], the system forms intermediate mesophases with liquid-like core; mesomorphous M_α, rhombohedral R_α, tetrahedral T_α, cubic Q_α. The temperatures, where the phase transitions took place, were obtained using High Sensitivity Differential Scanning Calorimetry – all these experiments were conducted by Kekicheff et al. **[2]**. The same authors also conducted X-ray Diffraction experiments, to identify the concentrations and temperatures, at which phase transitions occur **[3]**. As the concentration of surfactant in the system increases to values higher than 60 wt %, lamellar phase with liquid-like core appears (L_α).

7. Crystal polymorphs - Different unit cell crystal structures **[2]**, **[3]**

High Sensitivity Differential Scanning Calorimetry was used by Kekicheff et al. to measure the transition temperatures precisely, for the case of different polymorphs for SDS **[2]**. As mentioned before, the polymorphs are solid crystals with variable degree of spatial ordering of the unit cell crystal structure. These include: C_x, $C_{1/8}$, $C_{1/8}$', C_1', C_1'', C_1''', C_x', C_x'', C_x''', C_2', C_2'', C_2'''. The superscripts (primes) refer to different unit cell classes, while the subscripts refer to different degrees of hydration in the unit cell crystal structure.

CHAPTER 4

RESULTS OF THE EXPERIMENTS FOR THE CsDS/WATER SYSTEM

4.1. Preface

This chapter includes the results of the experimental methods and the materials used to explore the phase behavior of the CsDS/water system. At first, the results of the macroscopic observation with cross-polarized light are presented. Then, follow the results of the Cryo-TEM images of the CsDS/water solution at concentration close to the concentration of the SDS/water system -0.3 [M] **[16]** (see section 3.3). Consecutively, the results of the following techniques are presented, namely the X-ray Diffraction, Optical Microscopy and Small Angle X-ray Scattering.

4.2. Results

4.2.1. Results on the macroscopic observation with cross-polarized light. Solubility curve and Krafft temperatures (concentration region 1 wt % - 40 wt %); macroscopic experiments.

As mentioned in Chapter 2 (2.3.3.3), two different cycles (thermal protocols) of experiments were performed:

1st cycle: The samples were periodically heated and cooled (no seed was added).

2nd cycle: The samples had been heated at first. Then, they were cooled and a seed was added. The samples were then reheated.

It is more likely that the 2nd cycle has approached thermodynamic equilibrium. Both results of the 1st and the 2nd cycle are presented, for comparison.

4.2.1.1. 1st Cycle - Periodic heating and cooling only (no seed added)

In this experiment, the samples were periodically heated and cooled in this temperature region with the same heating and cooling rates. For this cycle, as mentioned in the 2nd chapter, tables 4.1 and 4.2 report data referring to the sample temperature and to the water bath temperature, respectively. The samples were submerged in the immersion bath, with

immersion bath temperature at T = 31±0.1 [ºC]. Starting from T = 25 [ºC], the samples were heated with a large heating rate (0.2 [ºC/min]) up to solution temperature of T = 31±0.1 [ºC] and a water tank temperature of T = 34.2±0.1 [ºC]. Then, a lower heating rate (0.05 [ºC/min]) was selected for the following temperature region:

- solution temperature of T = 31±0.1 [ºC] and water tank temperature at T = 34.2± 0.1 [ºC]
- solution temperature of T = 35±0.1 [ºC] and water tank temperature at T = 38.2± 0.1 [ºC].

For the given heating rates, it was possible to observe liquid crystal phase up to the solution temperature of T = 34.5±0.1 [ºC] and water tank temperature of T = 37.5±0.1 [ºC]. The sample had stayed at that temperature for about 9 minutes, before becoming a neat solution.

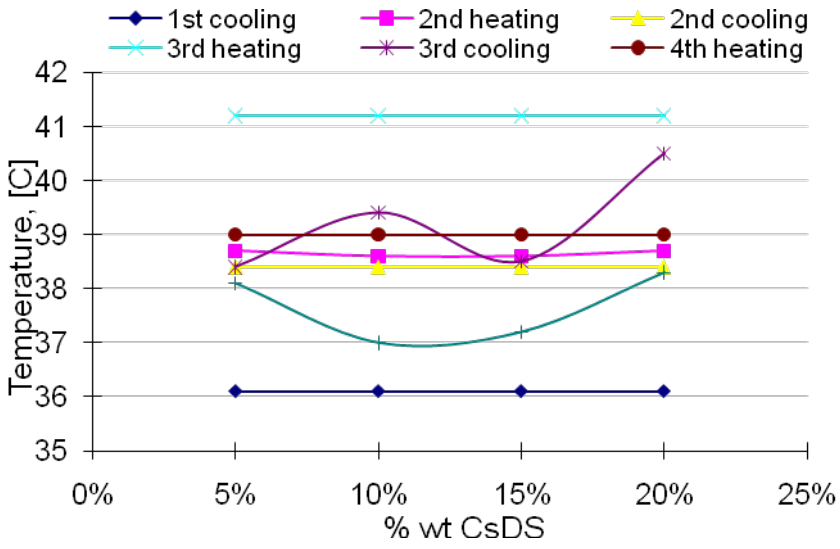

Fig.4.1. Solubility curve estimations in the region of 5 wt % - 20 wt % pure CsDS, for the 1st Cycle (water tank temperatures).

In these experiments, transition was only observed during the 1st heating process (1st disappearance of the solid crystals). In any other cooling or heating process of the same cycle, it was not possible to observe transitions. This suggests that the cooling rates used have been too large for the sample to approach thermodynamic equilibrium. Heating rates in

the range 0.2-0.5 [ºC/min] allowed the observation of liquid crystalline intermediates. These intermediate liquid crystals can dissolve after the end of the experiment into a neat micellar solution. In some cases, these intermediate liquid crystals might not disappear (5.2.1.1). In all thermal treatments demonstrated in Figure 4.1, the samples were first heated fast from T = 25 [ºC] up to T = 36 [ºC] (~0.2 [ºC/min]). Then, they were slowly heated (~0.02-0.05 [ºC/min]) between 36[ºC] and 40 [ºC].

Comments and differences between the first four thermal treatments and the fifth thermal treatment are presented in the following tables; table 4.1 and table 4.2 depict the comments, while tables 4.3. and 4.4. depict the differences.

Table 4.1. Heating and cooling rates for the 1st cycle with comments; water tank temperatures

Heating and cooling rates/1st Cycle	1st cooling	2nd heating	2nd cooling	3rd heating	3rd cooling	4th heating	4th cooling	5th heating	5th cooling
Heating rate (ΔT/Δt), [ºC/min]	0.2 [ºC/min] between 25 and 36 [ºC]. Then, 0.05 [ºC/min] between 36 and 40 [ºC].	0.2 [ºC/min] between 25 and 36 [ºC]; 0.05 [ºC/min] between 36 and 40 [ºC].	0.02 [ºC/min]	0.2 [ºC/min] between 25 and 36 [ºC]; 0.06 [ºC/min] between 36 and 40 [ºC].	0.11 [ºC/min]	0.2 [ºC/min] between 25 and 36 [ºC]; 0.06 [ºC/min] between 36 and 40 [ºC]	0.12 [ºC/min]	0.2 [ºC/min] between 25 and 36 [ºC]; 0.05 [ºC/min] between 36 and 40 [ºC]	0.02 [ºC/min]
Comments	At 36.1 [ºC], wait 4'.	At 38.7 [ºC], wait 9'.	0.1 [ºC/min], stayed for 10' at each temperature.	At 38 [ºC] there was some ordering of needle-like structures.	Larger deviation of estimated tempe-ratures	At 39 [ºC]: disappearance of solid crystals		Starting at T = 35 [ºC], stay for 20' at each tempera-ture up to 40 [ºC].	

Table 4.2. Heating and cooling rates of the 1st cycle with comments; sample temperatures

Heating and cooling rates-1st Cycle	1st cooling	2nd heating	2nd cooling	3rd heating	3rd cooling	4th heating	4th cooling	5th heating	5th cooling
Heating rate [°C/min], as average (=ΔT/Δt)	0.2 [°C/min] between 25 and 36 [°C]. Then, 0.05 [°C/min] between 36 and 40 [°C].	0.2 [°C/min] between 25 and 36 [°C], 0.05 [°C/min] between 36 and 40 [°C].	0.02 [°C/min]	0.2 [°C/min] between 25 and 36 [°C]. Then, 0.06 between 36 and 40 [°C].	0.11 [°C/min]	0.2 [°C/min] between 25 and 36 [°C] .Then, 0.06 [°C/min] between 36 and 40 [°C].	0.12 [°C/min]	0.2 [°C/min] between 25 and 36 [°C] .Then,0.05 [°C/min] between 36 and 40 [°C]	0.02 [°C/min]
Comments	At 36.1 [°C], wait 4'.	At 38.7 [°C], wait 9'.	At each 0.1[°C/min], stayed 10'.	At 38 [°C], there was some ordering of needle-like structures	Larger deviation of estimated Temperatures	At 39 [°C], disappearance of solid crystals		At 35 [°C], stay at each temp for 20', up to 40 [°C].	

Table 4.3. Differences between the 1st-4th thermal treatment and the 5th treatment (1st cycle); water tank temperatures

1st- 4th thermal treatment	5th thermal treatment
❖ Fast heating up to 35 [ºC] (~0.2 [ºC/min]) ❖ Slow heating/cooling rates (~0.05[ºC/min]) ❖ Stayed at 35.9 [ºC] for 9'; intermediates observed. ❖ Easier to check the solubility temperatures while heating.	❖ Fast heating up to 35 [ºC] (~0.2 [ºC/min]) ❖ Starting from 35 [ºC] and rising up 1 [ºC] each time, the sample stays at each temperature for a period of 20'; slower heating and similar cooling rates (~0.006 and 0.02[ºC/min], respectively). ❖ Stayed at 35.9 [ºC] for 30'; intermediates observed. ❖ Easier to check the solubility temperatures while heating.

Table 4.4. Differences between the 1st-4th thermal treatment and the 5th thermal treatment (1st cycle); sample temperatures

1st- 4th thermal treatment	5th thermal treatment
❖ Fast heating up to 32 [ºC] (~0.2 [ºC/min]) ❖ Slow heating/cooling rates (~0.05[ºC/min]) ❖ Stayed at 35.9 [ºC] for 9'; intermediates observed. ❖ Easier to check the solubility temperatures while heating.	❖ Fast heating up to 32 [ºC] (~0.2 [ºC/min]) ❖ Starting from 32 [ºC] and rising up 1 [ºC] each time, the sample stays at each temperature for a period of 20'; slower heating/similar cooling rates (~0.006 and 0.02[ºC/min], respectively). ❖ Stayed at 35.9 [ºC] for 30'; intermediates observed. ❖ Easier to check the solubility temperatures while heating.

Concentration region: 25 wt % - 40 wt % (1st cycle):

Two runs were performed. Each run consisted of a set of 3 independent samples-one set at each concentration. The process involved only heating, neither cooling nor seed addition. These measurements of 1st cycle in the concentration region 25 wt % - 40 wt % CsDS have suggested that the transition temperature from solid crystals and micelles to a neat micellar solution - or micellar solution in coexistence with liquid crystals - should be around 35 [ºC].

The transition temperatures observed by the 2nd cycle are much lower than those which have been estimated by the 1st cycle. The use of a seed serves to locate the Krafft temperature and prove that the system has reached thermodynamic equilibrium. As will be shown below, the temperatures indicated by the 2nd cycle are lower than those which have been estimated by the 1st cycle.

Concentration region: 45 wt % - 60 wt % CsDS (1st cycle):

At room temperature, the samples consisted of 2 phases -solid crystals dissolved in water. What has been observed through the macroscopic observation with cross-polarized light in all these samples (heated according to 1st cycle), is that a transition starts at T=35±1 [ºC], where liquid crystals appear on the boundary of solid crystals. When the samples were heated, they looked birefringent and relatively viscous (when the tubes were tilted, the suspension did not flow). This suggests that in the concentration region 45 wt % - 55 wt % CsDS, the samples belong to some pure liquid crystal state.

The macroscopic observation with cross-polarized light did not provide evidence about the specific type of the liquid crystal in that region (whether it is hexagonal, lamellar, or some other phase).The crystal looked birefringent when the sample was heated. This indicates that this phase cannot be cubic. Small Angle X-ray Scattering (SAXS) was used to examine the liquid crystal structure type in that concentration of the phase diagram. A relative discussion follows in section 7.2.

Table 4.5. 25 wt % - 40 wt % CsDS region. Candidate Krafft T [ºC] without seed addition

Run	wt % CsDS before seed	T1 [°C] / Candidate Krafft Temperatures (1st cycle)
(1st run)	25	33.7±0.1
		33.4±0.1
		33.4±0.1
	30	33.7±0.1
		34.3±0.1
		34.4±0.1
	35	33.7±0.1
		34.1±0.1
		34.4±0.1
	40	33.7±0.1
		34.1±0.1
		34.4±0.1
(2nd run)	25	34±0.1
		34±0.1
		34±0.1
	30	34±0.1
		34±0.1
		34±0.1
	35	34±0.1
		35.7±0.1
		35.7±0.1
	40	34±0.1
		35.7±0.1
		35.7±0.1

4.2.1.2. 2nd cycle -The correction by a tiny solid seed

All the temperatures reported for the 2nd cycle, correspond to the temperature in the center of the glass tube (sample temperature). For the concentration region 1 wt % - 40 wt % CsDS, the results of this cycle of experiments suggest that the solubility curve is a flat line with respect to the concentration, at temperature 33 ± 1 [ºC].

A low enough heating rate (0.08[°C/min]) was used in the sodium dodecyl sulphate system, so that the system approaches thermodynamic equilibrium **[1]**, **[2]**. The selection of a proper heating rate is very important at temperatures around the Krafft temperature, for the system to reach thermodynamic equilibrium.

Section 5.2.1 includes a more elaborate discussion about how important it is to select carefully the heating rate. The heating rate selection can influence the corresponding appearance of the system.

Concentration region: 5 wt % - 20 wt % CsDS (2nd cycle)

Some of the description has been included in Chapter 2 (materials and methods). The samples were heated with a rate of 0.2 [ºC/min], from 25 [ºC] up to 37.5 [ºC]. The sample stayed at T= 37.5 [ºC] for 40'. In these experiments, the onset of a thin boundary of liquid crystal on the solid crystals appears at T_sample = 33.2 [ºC] (for T_tank = 34.7 [ºC]). At about 33.2 [ºC], the liquid crystal disappeared in all the samples that were examined. So, a candidate Krafft temperature is T = 33.2 [ºC].

A cooling rate of 0.05 [ºC/min] was used between 38 [ºC] and 34.8 [ºC]. The samples stayed at that temperature for 12' and then seed was added in all of them. The seed mass added was very small compared to the mass of crystals in the sample.

The seed mass was on the order of 3 [mg], while the mass of the solid crystals was about 20 [mg] - an order of magnitude higher). The samples remained at T = 34 [ºC], for about 3 hours. The seeds were completely dissolved in the samples. Then, the samples were cooled down to 32 [ºC] with a cooling rate of 0.1 [ºC/min] and stayed there for 12'. A seed was added in all of them and they stayed there for 1 hour. The crystals first remained undissolved, at T = 31.8 [ºC]. This indicates that this temperature was close to the Krafft temperature for the given concentration.

A final heating cycle was performed, in order to verify that the candidate temperature is indeed the Krafft temperature. The water tank was heated from 31.8 [ºC] to 32.7 [ºC], with a heating rate of 0.05 [ºC/min]. Then, the water tank remained at 32.7 [ºC] for 16' and then heated up to 32.9 [ºC], where it remained for 50 minutes. Then, the tank was heated with 0.1 [ºC/min] up to 33.2 [ºC], where it remained for another 25'.The crystals dissolved in all the samples, with a small deviation in temperature, for the concentrations.

Table 4.6 includes the estimated Krafft temperatures for the sets of 3 independent

samples at every concentration, in the region 5 wt % - 20 wt % CsDS. As can be seen in Figure 4.2, the Krafft temperature difference between the 1st heating and the 2nd heating (after cooling, where seed was added) is less than 1 [ºC]. This is not a significant difference, considering the fact that this is the first estimation of the solubility curve of the CsDS/water system that is reported so far.

Table 4.6. Krafft temperatures of the 3 independent samples at each concentration, before and after the addition of the seed. Concentration region 5 wt % - 20 wt % CsDS

Run	**% wt CsDS_ before seed addition**	**Seed addition**	**Candidate Krafft T [°C], 3 samples**	**Candidat Krafft T [°C] after seed 3 samples**
(1st run)	5	Seed added at 31.8±0.1 [°C]	33.2±0.1	Between 31.8±0.1 and 32.4 ±0.1
	5	Seed added at 31.8±0.1[°C]	33.2±0.1	Between 31.8±0.1 and 32.4 ±0.1
	5	Seed added at 31.8±0.1[°C]	33.2±0.1	Between 31.8±0.1 and 32.4 ±0.1
	10	Seed added	33.2±0.1	32.4 ±0.1
	10	Seed added	33.2±0.1	32.4 ±0.1
	10	Seed added	33.2±0.1	32.4 ±0.1
	15	Seed added	33.2±0.1	32.7 ±0.1
	15	Seed added	33.2±0.1	32.7 ±0.1
	15	Seed added	33.2±0.1	32.7 ±0.1
	20	Seed added	33.2±0.1	32.9 ±0.1
	20	Seed added	33.2±0.1	33.2 ±0.1
	20	Seed added	33.2±0.1	33.2 ±0.1

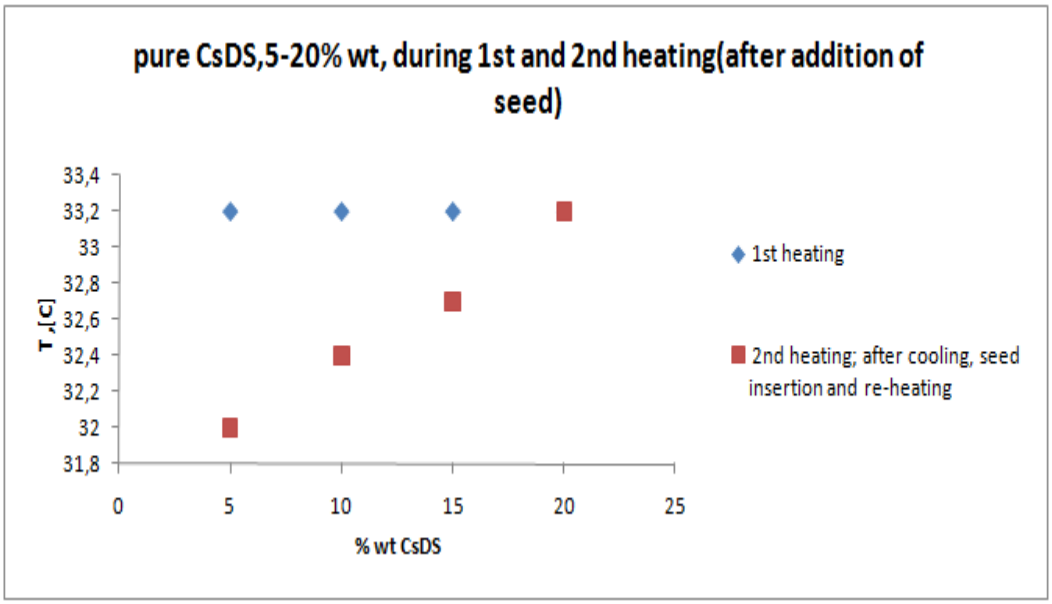

Fig.4.2. Solubility curve estimation for the 5 wt % - 20 wt % CsDS concentration region. 3 independent samples examined at each concentration and heated by the 2nd cycle.

Figure 4.2 depicts the solubility curve estimation for the 5 wt% - 20 wt % region for the 3 independent samples. The Krafft temperatures that were found during the 1st heating, deviate less than 1 [º C] from the temperatures that were found during the 2nd heating; after cooling and seed insertion. The solubility curve in the region 5 wt % - 20 wt % seems pretty flat, ($(\Delta T)_{max}$ = (33.2-32) = 1.2 [ºC]) compared to the solubility curve for the SDS/water system in the same region of concentration (which has a positive slope as suggested by Fontell et al. **[1]** and Kekicheff et al. **[2]**).

It can be suggested for the reheating (red squares in Figure 4.2), that the identification of the Krafft temperature of the 20 wt % CsDS sample has been more accurate. This is because the system has stayed long enough at a certain temperature to relax at its thermodynamic equilibrium (~30'). Also, heating rates between 0.2 and 0.5 [ºC/min] were used. These heating rates led to the formation of liquid crystalline intermediates, intermediates that can dissolve after the end of the experiment (giving place to a neat micellar solution). These liquid crystals might not always disappear (read about the intermediate liquid crystals in 5.2.1.1).

Concentration region: 25 wt % - 40 wt % CsDS (2nd cycle)

The cooling with seed addition and reheating has ensured approach of thermodynamic equilibrium. Figure 4.3 depicts a typical example of a two – phase region of liquid crystals and micelles in this concentration region.

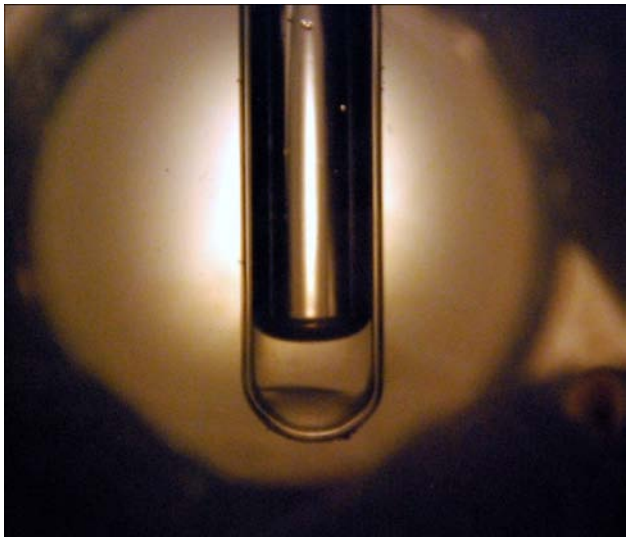

Fig.4.3. Typical appearance of two-phase coexistence (viscous structure and micellar phase) at T > 35 [°C].No cross–polarization. Size scale: *the t*ube diameter is 15[mm].

Table 4.7.Comments on the heating runs; 25 wt % - 40 wt % (2^n cycle)

Run	wt % CsDS	Seed addition	Candidate Krafft , T [°C] 3 sets
(1^{st} run)	25	1^{st} seed added at 34.5±0.1 [°C] and dissolved. 2^{nd} seed added at 32.5±0.1 [°C] and did not dissolve.	33.7±0.1
			33.7±0.1
			32.6±0.1
	30	1^{st} seed added at 34.5±0.1 [°C] and dissolved. 2^{nd} seed added at 32.5±0.1 [°C] and did not dissolve.	33.7±0.1
			33.7±0.1
			33.2±0.1
	35	Seed added at 31.8± 0.1 [°C].	33.5±0.1[°C] -pure micellar solution (14’ at 33.8±0.1[°C])
			33.7±0.1 [°C] - micellar & liquid crystal (14’ at 33.8±0.1 [°C])
			33.7-pure liquid crystal (14’ at 33.8±0.1 [°C])
	40	1^{st} seed added at 34.5±0.1 [°C] and dissolved.	<35.8± 0.1 [°C] (one of the three samples is referred, as the other 2 tubes were broken).

At concentrations between 30 % and 45 % wt CsDS and for temperatures higher than 34 ± 1 [ºC], the findings of either the 1st or the 2nd cycle suggest that there is a two-phase region of liquid crystals and micelles (The reasons why these structures are considered liquid crystals have been reported in section 3.2). This is suggested indirectly by the results of the through macroscopic observation with cross-polarized light. For 3 independent samples at 35% wt CsDS (all of which were heated according to the 2nd cycle, one looked as a neat micellar solution, another one looked pure liquid crystalline and the last one looked as micellar solution with a tiny liquid crystal.

The number of independent samples that need to be treated according to the 2nd cycle should be increased. This will increase the confidence about the findings in the region 25% wt - 40% wt CsDS. As the concentration increases from 35% wt to 45% wt, a trend in the transition temperature has been observed. This trend corresponds to an increase in the transition temperature of about 2 [ºC], from 34 [ºC] to 36 [ºC] over this concentration region (35% - 45%). It might be helpful to review the CsDS/water phase diagram in Chapter 3 at this point. At concentrations higher than 40% wt CsDS, the samples were treated according to the 1st cycle (heating only); the samples had a highly viscous, liquid crystalline appearance during the experiment (8 hours).

At concentrations higher than 45% wt CsDS, observations from some samples treated according to the 2nd cycle (1st heating, cooling and seed addition and 2nd heating) suggest that the system should form pure liquid crystal phase only (1 phase region) at temperatures about 35±1 [ºC].Within the time frame of these experiments, no complete melting of the tiny solid crystal was observed. The observed transition temperatures, were the transition temperatures of the 1st heating cycle only (transition of solid crystals to liquid crystals).

4.2.2. Cryo-TEM experiments; the micellar nanostructures (performed by **Arunagirinathan M.A.; Bellare J.R.)**

The importance of the heating rate was first observed in the macroscopic observations with cross-polarized light. For the same reasons as presented in chapter 4.2.1, the heating rate during the sample preparation of Cryo-TEM is very important. It should be carefully

selected in order to observe the representative shape and size of the nanostructures. A discussion on the heating rate is presented in 5.2.1.

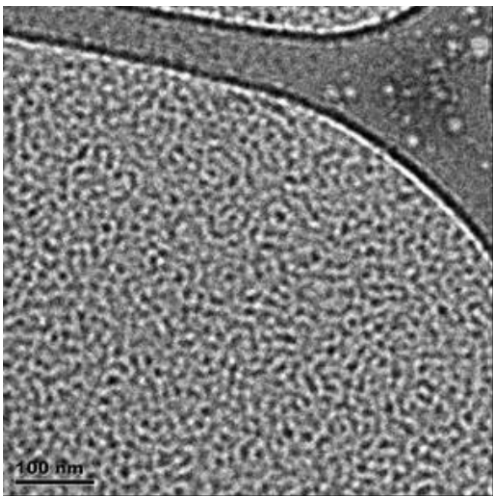

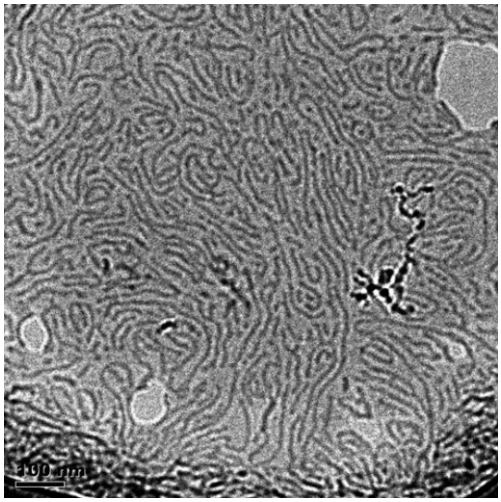

Fig.4.4, ***left;*** **Fig.4.5,** ***right.*** Cryo-TEM images of a 0.34 [M] CsDS aqueous solution. The TEM images represent the same grid. (Sample Preparation: T = 35 [ºC] and Relative Humidity = 100%). Samples heated from T = 25 [ºC]. Scale size in either figure: 100 [nm] – The TEM images (Fig.4.4. and Fig.4.5.) have been reproduced with permission from Arunagirinathan M.A. who both performed the experiment and operated the instrument **[16]**.

Figures 4.4 and 4.5 depict the observed nanostructures on the same grid for a CsDS/water solution at concentration 0.34 [M], using Cryo-TEM. At T = 25 [ºC], the system was an aqueous solution of solid crystals. Then, the sample was inserted in the VITROBOT, where the following parameters were used: T = 35 [ºC] and Relative Humidity =100 %. During that sample preparation session (see the sample preparation for the Cryo-TEM experiment in Chapter 2), the heating rate from T = 25 [ºC] to T = 35 [ºC] was not measured.

On the same grid, both ellipsoidal and threadlike structures were observed. This fact can be related to the selection of heating rate (see 5.2.1.). The ellipsoidal structures had a semi-major axis of 7 [nm] and a semi-minor axis 5 [nm]. The threadlike structures had a diameter of about 15 [nm] and their length varied from 200 [nm] to more than 1000 [nm].

4.2.3. Possible metastabilities and the results of the X-ray Diffraction experiments (X-ray diffraction experiments performed by **Torija M.J.)**

At concentrations higher than 30 wt % CsDS, the system at T = 25 [ºC] looked as solid crystals dispersed in water. Heating and cooling rates higher than 0.2 [°C/min] resulted in the appearance of macroscopically different states of the samples. The dispersion of solid crystals in water has not been taken into account in these experiments.

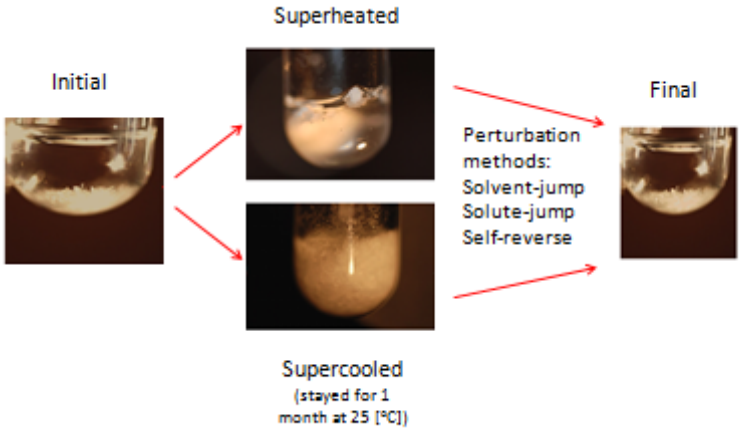

Fig.4.6. Possibility for metastabilities; s*ize scale*, tube diameter: 15 [mm]. No cross–polarized light was used. *Left*, unheated sample at T = 25 [ºC]; *above in the middle*, superheated (from T = 25 [ºC] to T = 55[ºC] with a heating rate higher or equal than 0.2 [ºC/min] and then naturally cooled to T = 25 [ºC]); *below in the middle*, supercooled sample (heated from T = 25 [ºC] to T = 55[ºC] with a heating rate higher or equal than 0.2 [ºC/min]; then, cooled down to 0 [ºC] for an hour; then, warmed naturally at T = 25 [ºC]) that had been naturally cooled to T = 25 [ºC]; *right*, sample already reversed to the initial state at T = 25 [ºC] (right).

Different macroscopic states were formed. These states were formed when the samples were:

1. Had been heated up to 55 [ºC] at a heating rate higher or equal than 0.2 [ºC/min]. Then, they were left to cool down naturally to T = 25 [ºC] over long time and stayed there for more than 8 hours - superheated samples (*above in the middle*, Figure 4.6*)*.

2. Had been heated up to 55 [ºC] at a heating rate higher or equal than 0.2 [ºC/min] (superheated samples). Then, left to cool down to T = 25 [ºC] naturally over long time and stayed there for more than 8 hours. The samples were then cooled down to 0 [ºC], for a period of an hour and then they were brought again at T = 25 [ºC] to warm naturally (*below in the middle,* Figure 4.6).

3. Had been heated up to 55 [ºC] and directly cooled at 0 [ºC], for a period of a few minutes and then they were brought again at T = 25 [ºC] to warm naturally (also, *below in the middle*, Figure 4.6).

The system would remain in any of the three states for a long period of time; a week up to a month. After that time, there were cases that the system would not revert to the initial state. In other cases, the system would revert to the initial state, after a week. The samples were monitored frequently within the 8 hours of the experiments. After natural warm up, the samples were left at T = 25 [ºC] for another 8 hours. Then, they were observed again.

Fig.4.7. Initially supercooled sample. Initially heated from T = 25 [ºC] to T = 55[ºC] with a heating rate higher or equal than 0.2 [ºC/min]. Then, the sample was cooled down to 0 [ºC] for an hour and then brought again at T = 25 [ºC] to warm naturally). Figure captured at T = 25 [ºC] after natural warm - up. No cross–polarized light was used. *Size scale,* tube diameter: 15 [mm].

Figure 4.7 depicts the crystalline state for a sample that had been heated with the following temperature history" Initially, has been heated from 25 [ºC] to 55 [ºC] with a heating rate of 0.2 [ºC/min] and then, the sample would be either:

- cooled down naturally at 25 [ºC] for a period of 8 hours at first. Subsequently, cooled at 0 [ºC] for 1 hour, or
- directly stored in the fridge for a period of 1 hour at 0 [ºC].

Fig.4.8. Initially superheated sample (from T = 25 [ºC] to T = 55[ºC] with a heating rate higher or equal than 0.2 [ºC/min] and then naturally cooled to T = 25 [ºC]). Figure captured at T = 25 [ºC] after natural cool down. *Size scale,* tube diameter: 15 [mm]. No cross–polarized light was used. Solid crystals form at the boundary of the seed.

Figure 4.8 represents a sample which has been initially superheated and then left to cool down naturally to T = 25 [ºC] for a certain period of time; a week up to a month. At the time the figure was captured, the system had been perturbed by tiny solute addition (concentration). Within 8 hours after the addition of a tiny solid seed, a macroscopically different interface at the boundary of the solid crystal would have been created. It has been observed that dilution or addition of a tiny solid seed of nuclei (solvent and solute jumps, respectively **[88]**, **[89], [35]**, **[36]**, **[37]**, **[87], [90]**) would almost always return the system to the ‘initially-observed’ macroscopic appearance (unheated sample).

Fig.4.9. Solid crystals in aqueous solution (stable state) created by solute or solvent jump at a 10 wt % CsDS sample at T = 25 [ºC]. *Size scale*, tube diameter: 15 [mm]. No cross-polarized light was used. The figure was captured at T = 25 [ºC] **[87]**, **[88]**, **[89]-[35]**, **[21]**, **[37]**, **[90]**).

Figure 4.9 represents a system after it has been perturbed by dilution or addition of a tiny solid seed of nuclei (solvent and solute jumps, respectively **[87]**, **[88]**, **[89]-[35]**, **[36]**, **[37]**, **[90]**) to the initially observed (unheated) macroscopic appearance.

This rarely has been observed to happen, in the cases of natural reverse without perturbation. Specifically, if no seed had been added into the sample, it has been observed that in some cases the sample would revert to the initially observed macroscopic state (natural reverse) and in other cases it would not.

The different macroscopic appearance could lead to the following hypothesis: that the macroscopically different, thermally treated samples represent metastable states. X-ray Diffraction Experiments were carried out to examine if the samples that looked macroscopically different than the unheated sample (superheated and supercooled samples, respectively), represent metastable states or not.

X- ray Diffraction Results

Following Torija M.J., ‘the instrument that was used was a diffractometer with horizontal platform, area detector and collimator of 0.8 [mm] diameter. The X-ray source

was a Cu (copper) sealed tube with 45 [kV] and 40 [mA]. The frames were centered at 15 degrees. As mentioned in chapter 2, the diffractograms I vs. $2\cdot\theta$ are a valuable source towards the identification of the unit cell structure. The Diffraction ring patterns (Debye rings) help to estimate how amorphous or crystalline the material is, as well as to have a qualitative estimation about the crystal size of the material. A larger crystal size would correspond to smaller number of crystals that may not satisfy the powder limit **[75]**. Large crystals favor the formation of a more weakly defined diffraction ring and following Torija M.J, 'a lower concentration can favor the formation of a more weakly-defined Debye ring'.. These diffraction rings (Debye rings), which are presented in Figures 4.10 and 4.11, correspond to the dried byproduct of the following samples that are depicted in table 4.8. (regarding the discussion about the dried byproduct, see sections 5.4, 5.7 and 5.9).

Table 4.8. Different concentrations and types of samples analyzed at the Bruker-AXS MicroDiffractometer. The color is simply a convention **[79]**

'Red'	'Green'	'Yellow'	'Grey'	'B sample'
45 wt %, liquid crystalline	40 wt %, supercooled, pure - state 2b	40 wt %, superheated, pure -state 2b	5 wt %, unheated	15 wt %, unheated
Pure CsDS	Pure CsDS	Pure CsDS	Pure CsDS	Impure CsDS

The Debye rings of the four purified (see 2.2.1.2, 2.2.1.3, 5.5 and 7.6.) CsDS samples and the one impure CsDS are presented next.

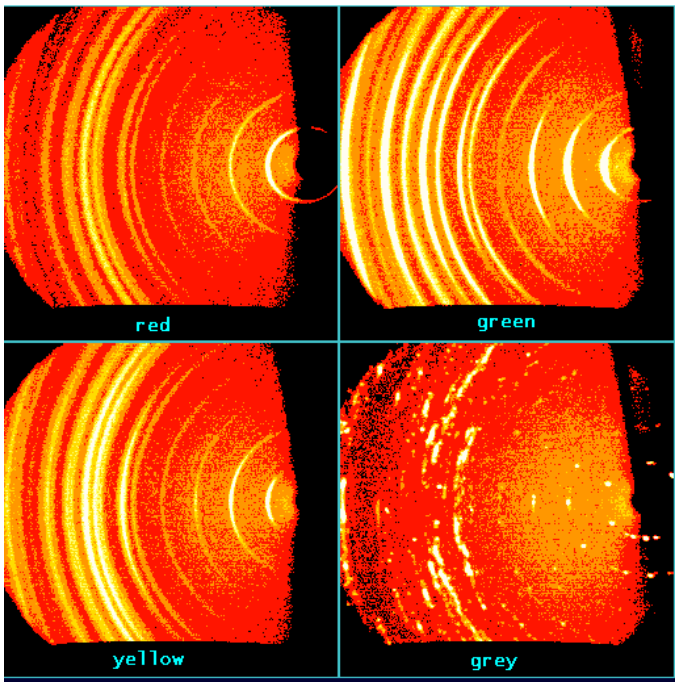

Fig.4.10. The Debye rings of the four purified (see 2.2.1.2. and 5.5.) CsDS samples at constant T, T=25 [ºC].Reproduced with permission from Torija M.J.

As can be seen in Figure 4.10, the 'grey' sample is associated with a more weakly-defined diffraction ring. A reason for that is that the crystals might have a size that does not lie within the powder limit **[75]**.This is discussed in 7.4 and 5.4.2.

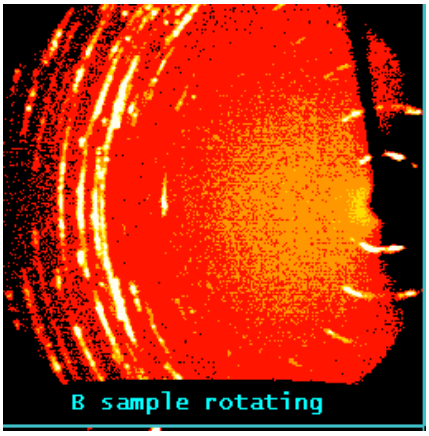

Fig.4.11. The Debye rings of the impure (see 2.2.1.2. and 5.5.) CsDS sample at T=25 [ºC]. Reproduced with permission from Torija M.J.

Similarly to the comments about Figure 4.10, the ‘B sample’ is also associated with a more weakly-defined diffraction ring. One reason for that might be that the crystal size does not lie within the powder limit **[75].**This is discussed in 7.4 and 5.4.2, as well.

Compared to the other 3 samples, the 5 wt % purified CsDS solution at T= 25 [°C] (grey) and 15 wt % impure CsDS (‘B sample’) at T= 25 [°C] do not have well - defined diffraction (Debye) rings; they provided discontinuous rings, instead.

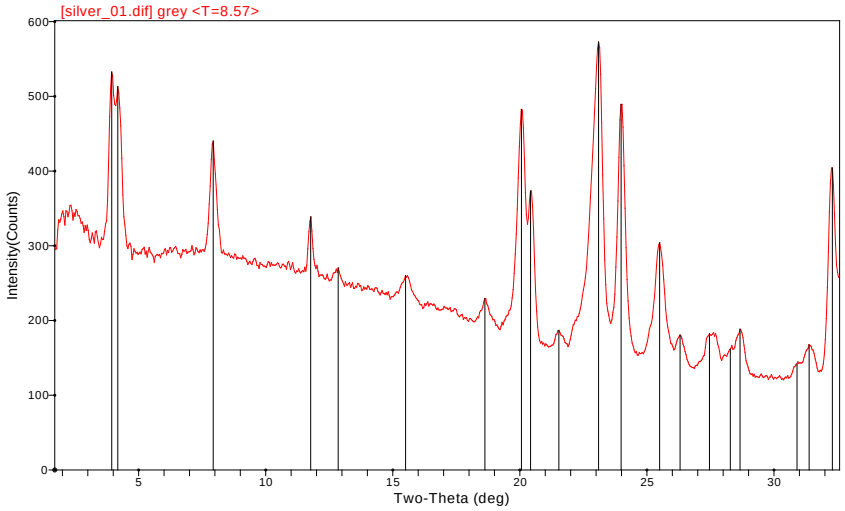

Fig.4.12. Diffractograms for the 5 wt % purified CsDS unheated sample, examined at T=25[ºC]. Reproduced with permission from Torija M.J.

Table 4.9.Raw data for the unheated 5% wt purified CsDS sample. Reproduced with permission from Torija M.J.

Peak Search Report (20 Peaks, Max P/N = 7.8)
[silver_01.dif] grey <T=8.57>
PEAK: 17(pts)/Parabolic Filter, Threshold=3.0, Cutoff=0.1%, BG=3/1.0, Peak-Top=Summit

2-Theta	d(Å)	BG	Height	H%	Area	A%	FWHM
3.943	22.3907	303	230	61.6	114.8	60.7	0.425
4.180	21.1204	300	212	57.0	114.8	60.7	0.432
7.937	11.1308	290	150	40.3	45.3	24.0	0.257
11.771	7.5119	268	71	18.9	7.7	4.1	0.092
12.851	6.8829	253	17	4.7	3.2	1.7	0.148
15.506	5.7099	227	33	8.8	16.0	8.5	0.390
18.625	4.7603	197	32	8.7	11.2	5.9	0.277
20.062	4.4224	181	302	81.0	177.3	93.9	0.499
20.422	4.3452	180	193	51.9	118.5	62.7	0.490
21.536	4.1230	169	18	4.8	4.4	2.3	0.195
23.099	3.8473	200	373	100.0	188.9	100.0	0.431
23.983	3.7074	188	301	80.9	99.2	52.5	0.280
25.499	3.4904	155	149	39.9	80.1	42.4	0.458
26.306	3.3851	158	22	6.0	4.8	2.6	0.172
27.460	3.2455	147	35	9.4	17.4	9.2	0.395
28.280	3.1532	147	14	3.8	21.7	11.5	1.220
28.663	3.1119	142	47	12.5	17.0	9.0	0.309
30.905	2.8911	127	15	3.9	19.7	10.4	1.077
31.382	2.8482	131	36	9.7	19.7	10.4	0.435
32.297	2.7696	135	269	72.2	96.1	50.9	0.286

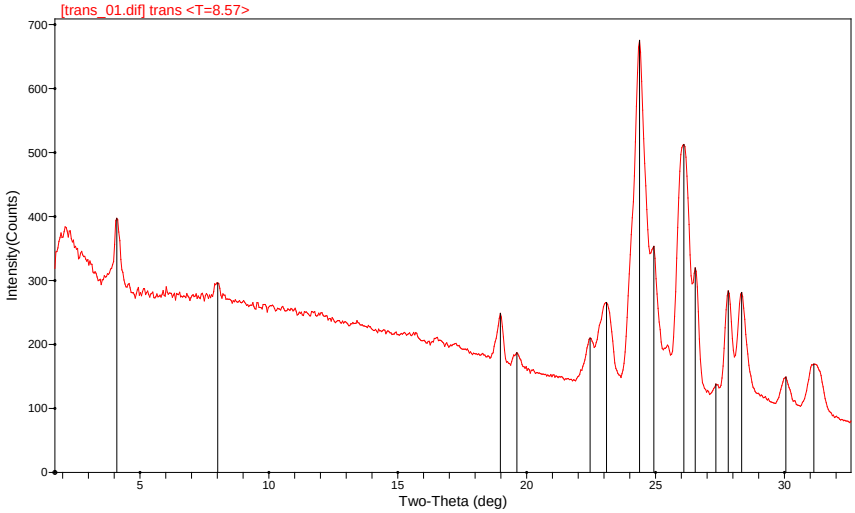

Fig.4.13. Diffractogram for the 15 wt % impure CsDS unheated sample, examined at T=25[ºC]. Reproduced with permission from Torija M.J.

Table 4.10.Raw data for the 15% wt impure CsDS sample. Reproduced with permission from Torija M.J.

Peak Search Report (15 Peaks, Max P/N = 9.6)
[trans_01.dif] trans <T=8.57>
PEAK: 19(pts)/Parabolic Filter, Threshold=3.0, Cutoff=0.1%, BG=3/1.0, Peak-Top=Summit

2-Theta	d(Å)	BG	Height	H%	Area	A%	FWHM
4.104	21.5132	301	96	19.3	19.9	6.4	0.176
8.016	11.0204	273	23	4.7	6.5	2.1	0.221
18.980	4.6720	182	66	13.3	9.6	3.1	0.123
19.623	4.5203	170	17	3.4	3.1	1.0	0.145
22.461	3.9551	152	58	11.6	79.9	25.5	1.168
23.099	3.8474	156	110	22.0	78.7	25.1	0.608
24.379	3.6481	175	500	100.0	313.4	100.0	0.533
24.934	3.5682	215	139	27.7	103.2	32.9	0.632
26.099	3.4115	125	387	77.4	265.5	84.7	0.583
26.540	3.3559	125	194	38.8	147.8	47.1	0.609
27.340	3.2594	133	5	1.0	0.4	0.1	0.323
27.821	3.2041	127	157	31.3	75.4	24.0	0.409
28.339	3.1467	126	155	30.9	76.8	24.5	0.422
30.055	2.9708	109	40	8.0	13.9	4.4	0.296
31.141	2.8697	99	71	14.1	45.3	14.5	0.545

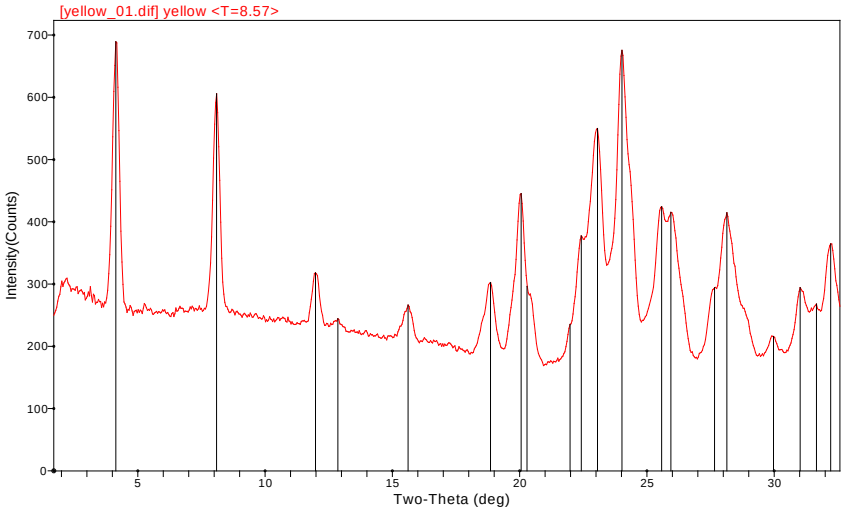

Fig.4.14. Diffractogram for the 40 wt % purified CsDS at T=25[ºC], after the completion of the following processes: superheating, followed by natural cooling to T=25[ºC] for several hours. Reproduced with permission from Torija M.J.

Table 4.11.Raw data for the 40% wt (initially superheated and then naturally cooled) purified CsDS sample. Reproduced with permission from Torija M.J.

Peak Search Report (20 Peaks, Max P/N = 9.6)
[yellow_01.dif] yellow <T=8.57>
PEAK: 23(pts)/Parabolic Filter, Threshold=3.0, Cutoff=0.1%, BG=3/1.0, Peak-Top=Summit

2-Theta	d(Å)	BG	Height	H%	Area	A%	FWHM
4.141	21.3201	264	425	85.2	136.2	37.3	0.272
8.098	10.9095	257	349	69.9	114.3	31.3	0.278
11.982	7.3804	237	81	16.3	28.5	7.8	0.297
12.860	6.8783	231	13	2.7	1.1	0.3	0.247
15.620	5.6685	215	51	10.3	17.0	4.6	0.281
18.857	4.7021	196	106	21.3	51.3	14.1	0.411
20.058	4.4233	188	257	51.5	145.8	39.9	0.482
20.291	4.3730	184	112	22.4	96.0	26.3	0.686
21.980	4.0406	233	2	0.5	0.2	0.1	0.276
22.421	3.9621	176	201	40.3	174.7	47.8	0.738
23.058	3.8540	176	374	74.8	316.5	86.7	0.720
24.020	3.7019	176	499	100.0	365.2	100.0	0.622
25.580	3.4796	176	248	49.7	287.7	78.8	0.986
25.941	3.4319	215	200	40.1	202.5	55.4	0.808
27.659	3.2226	218	76	15.2	69.1	18.9	0.728
28.139	3.1686	196	219	43.8	197.6	54.1	0.768
29.973	2.9788	189	27	5.4	9.5	2.6	0.285
31.019	2.8807	234	60	12.1	18.5	5.1	0.260
31.660	2.8238	255	13	2.7	1.1	0.3	0.377
32.219	2.7761	274	90	18.1	28.9	7.9	0.256

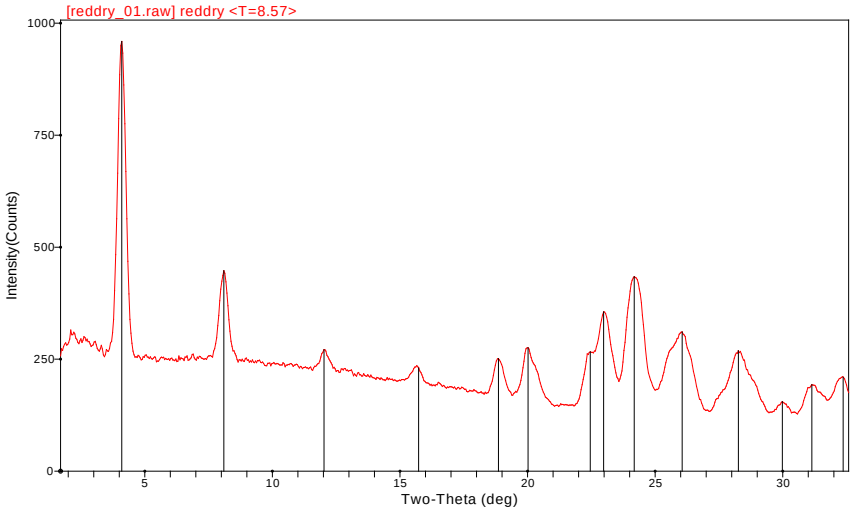

Fig.4.15. Diffractogram for the 45 wt % purified CsDS at T=25[ºC], after the completion of the following processes: initial heating, followed by natural cooling for several hours. Reproduced with permission from Torija M.J.

Table 4.12.Raw data for the 45 % wt (initially heated and then naturally cooled) purified CsDS sample. Reproduced with permission from Torija M.J.

Peak Search Report (14 Peaks, Max P/N = 11.3)
[reddry_01.raw] reddry <T=8.57>
PEAK: 17(pts)/Parabolic Filter, Threshold=3.0, Cutoff=0.1%, BG=3/1.0, Peak-Top=Summit

2-Theta	d(Å)	BG	Height	H%	Area	A%	FWHM
4.099	21.5374	261	698	100.0	271.7	100.0	0.331
8.100	10.9063	251	197	28.2	82.2	30.2	0.355
12.024	7.3547	228	43	6.2	16.5	6.1	0.306
15.731	5.6289	196	34	4.9	19.4	7.2	0.454
18.859	4.7016	175	77	11.0	33.9	12.5	0.377
20.019	4.4318	164	111	15.9	69.9	25.7	0.536
22.459	3.9555	174	92	13.2	125.5	46.2	1.160
22.981	3.8668	191	165	23.6	130.7	48.1	0.673
24.181	3.6776	200	234	33.5	161.3	59.4	0.586
26.060	3.4166	160	151	21.6	146.9	54.1	0.828
28.261	3.1553	142	126	18.1	125.7	46.3	0.845
29.983	2.9778	133	22	3.2	7.8	2.9	0.277
31.140	2.8697	147	46	6.6	26.4	9.7	0.484
32.369	2.7636	181	28	4.1	11.0	4.0	0.310

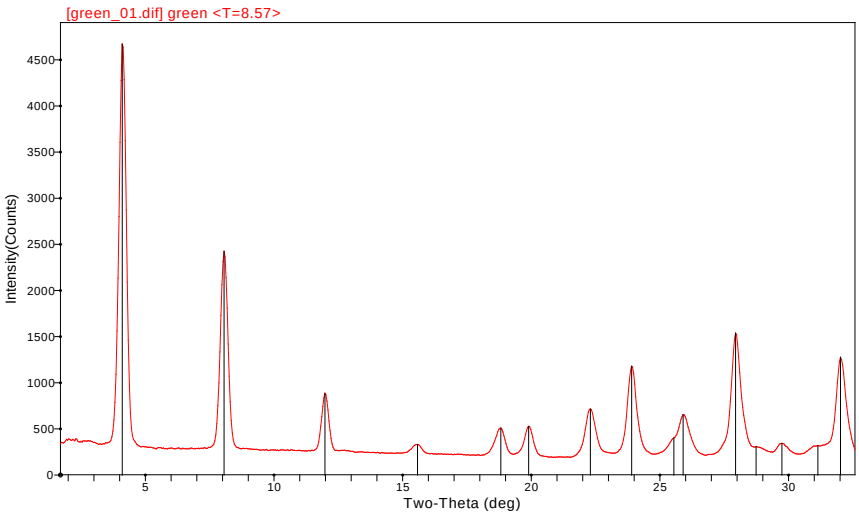

Fig. 4.16. Diffractogram for the 40 wt % purified CsDS at T=25[ºC], after the completion of the following processes: initial heating, followed by supercooling that was followed by natural warming for several hours. Reproduced with permission from Torija M.J.

Table 4.13.Raw data for the 40% wt (initially heated then supercooled and naturally warm-up) purified CsDS sample. Reproduced with permission from Torija M.J.

Peak Search Report (15 Peaks, Max P/N = 31.8)
[green_01.dif] green <T=8.57>
PEAK: 17(pts)/Parabolic Filter, Threshold=3.0, Cutoff=0.1%, BG=3/1.0, Peak-Top=Summit

2-Theta	d(Å)	BG	Height	H%	Area	A%	FWHM
4.103	21.5154	318	4349	100.0	1503.5	100.0	0.294
8.061	10.9595	283	2139	49.2	755.5	50.2	0.300
11.982	7.3802	257	628	14.4	211.3	14.1	0.286
15.579	5.6835	234	95	2.2	37.5	2.5	0.336
18.818	4.7119	224	283	6.5	126.0	8.4	0.378
19.901	4.4578	215	311	7.2	123.4	8.2	0.337
22.299	3.9835	214	500	11.5	245.1	16.3	0.417
23.901	3.7200	234	944	21.7	416.1	27.7	0.375
25.545	3.4843	231	170	3.9	149.2	9.9	0.702
25.902	3.4371	224	430	9.9	278.8	18.5	0.552
27.941	3.1906	253	1284	29.5	607.1	40.4	0.402
28.740	3.1037	302	4	0.1	0.3	0.0	0.339
29.741	3.0015	246	97	2.2	40.6	2.7	0.355
31.140	2.8698	309	10	0.2	0.8	0.1	0.370
32.021	2.7928	323	952	21.9	405.8	27.0	0.341

All five samples had stayed at T = 25[ºC] for long time (more than 24 hours the unheated samples).Their diffractograms represent crystalline (and not amorphous) materials **[81]**, as all the materials diffract at certain $2 \cdot \theta$ values only instead of a range of concentrations (which would be the case for an amorphous material).

The two unheated samples (the 5% purified CsDS and the 15% impure CsDS) exhibit

a more diffuse scattering compared to the thermally treated samples. Specifically, the unheated samples exhibit a non-zero slope of the signal at the noise level). This might be attributed to the elastic properties of the crystal in these cases. It might be possible that crystal vibrations can be related with the imperfect destructive interference between rays scattered at non Bragg angles, angles where the signal ideally should have been zero and it is non - zero).

Moreover, the ratios of the 2·θ values at the three peaks with the strongest intensity, would also be valuable information in order to identify the unit cell crystal structure of the material under examination. The diffractogram of the unknown material could be compared with the diffractogram of a known unit cell crystal structure. Table 4.9 depicts the 2·θ values for the five different samples.

Table 4.14. 2·θ values for the five CsDS samples in the 2·θ region θ - 35º); four purified CsDS samples (supercooled, superheated, heated, unheated) and one impure . Reproduced with permission from Torija M.J.

15 wt % impure CsDS unheated (degrees)	5 wt % purified CsDS unheated sample (degrees)	40 wt % purified CsDS superheated (degrees)	45 wt % purified CsDS normally heated (degrees)	40 wt % purified CsDS supercooled (degrees)
4	4	4	4	4
		7		
	8	8	8	8
	12	12	12	12
		13		
		16	16	16

19		19	19	19
	20			20
		21		
				22
			22.5	
23	23		23	
24	24	24	24	24
25.5	25.5			
26		26	26	26
		26.5		
27.5				
		28		28
28.5				
		31		
31.5				
		32		32
	32.5			

All five diffractograms exhibit similar 2·θ values and thus similar d-spacing. The d-spacing can be calculated, using Bragg's Law **[82]**:

$$n \cdot \lambda = 2 \cdot d \cdot \sin\theta$$

where θ is the diffraction angle for the incident X-ray beam, the beam which collides on the crystal pattern. For these experiments, the value of 'λ' that was used, was the principal X-ray of a copper compartment, also known as the most abundant wavelength, with a value of λ=1.54 [Aº] **[91]**. The value of n was equal to 1 - the refractive index of air. A discussion of these results follows in 5.4.

4.2.4. Results of the optical microscope

Certain figures provided by the optical microscope without using cross-polar filters are presented here. These figures give an idea about how solid crystals of CsDS looked like. In all these figures, the samples were heated from T =25 [ºC] with a heating rate larger than 1[ºC/min].

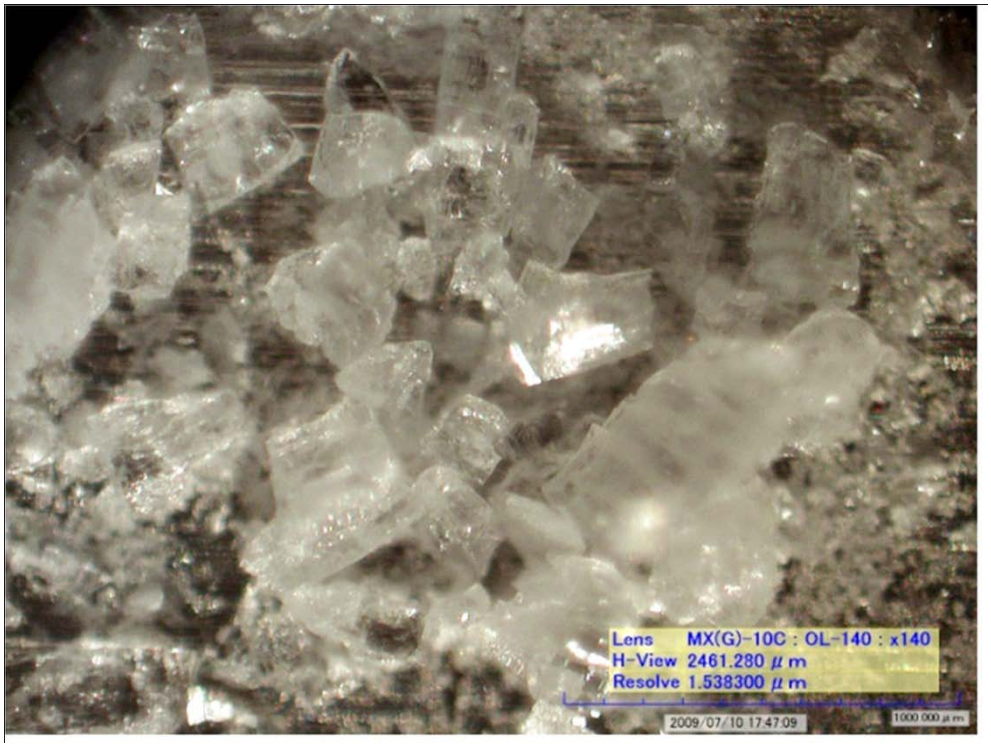

Fig.4.17. 50 wt % CsDS sample at T =50 [ºC]. Heating rate larger than 1[ºC/min] from T=25 [°C]. No cross–polarized light was used; *bottom right*, size scale: 1000 [µm].

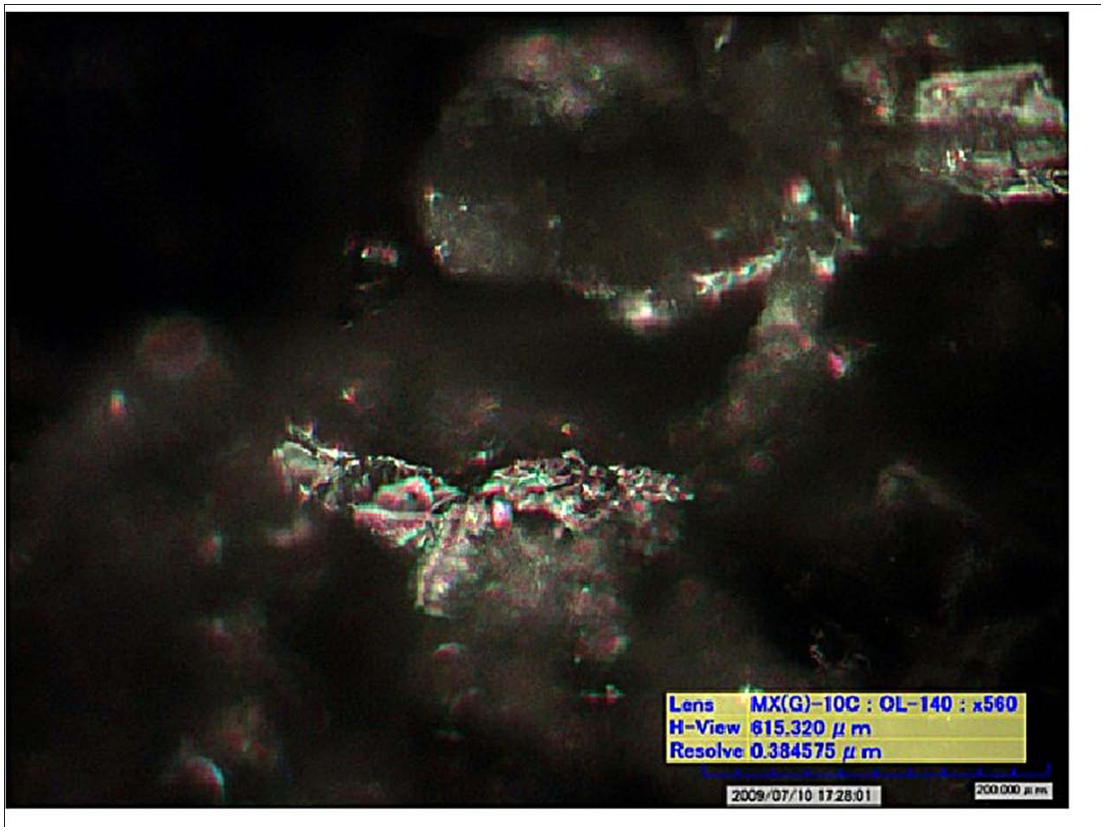

Fig.4.18. 48 wt % CsDS sample at T =50 [ºC]. Heating rate larger than 1[ºC/min] from T=25 [°C]. No cross–polarized light was used; *bottom right,* size scale: 200 [µm].

CHAPTER 5

DISCUSSIONS AND ANALYSIS

5.1. Preface

This chapter includes a discussion on the results for the CsDS/water phase behavior. For every characterization technique that was used for the CsDS/water system, it is attempted to outline the physical meaning of the results. Analogously, parts of the SDS/water system are also discussed **[2]**. The two systems are compared and a connection of the results with their physical meaning is also provided.

5.2. Discussions on the macroscopic experiments with cross-polarized light

5.2.1. The effect of the heating rate selection on the phase behavior

To connect with the methods presented in chapter 2 and the results presented in chapter 4, the experimental design was improved when the time needed for the center of the sample tube to reach the water tank temperature was taken into account. Regarding the effect of the heating rate on the temperature at the center of the glass tube, it has been hypothesized that whenever the heating rate changes, the time (needed to elapse for the temperature in the center of the glass Pyrex® tube to become the same as the temperature in the water tank environment) also changes. This time could be affected by the crystalline microstructure of the colloidal suspension (isotropy/anisotropy of the material, density of the suspension), as well as heat transfer coefficients of the glass and/or the suspension. With heating rates larger than 0.2 [ºC/min], the system would be driven faster to a new set temperature by thermal perturbation **[92]**, **[93]**, **[94]**, **[95]**. Whenever the samples were thermally treated, the following observation (which is not a proof) has been made:

When samples at different concentrations were cooled simultaneously and seed was added, the nucleation of new solid phase boundaries would be favored, as the surfactant concentration in the samples would increase. This can be related to the solubility ratio of the system. As the Cs^+ concentration in the solution increases, the solubility product of CsDS in water increases and it eventually becomes larger than the solubility constant. This resulted in

precipitation of solid CsDS, at room temperature.

The selection of lower heating and cooling rate (~0.05 to 0.1 [ºC/min]) in the case of the 2nd cycle, gives more chances for a given system (i.e. 20 wt % CsDS isotropic micellar phase) to approach thermodynamic equilibrium. Relevant studies have shown that a heating rate of 4 orders of magnitude higher (0.2 [ºC/min]) for the case of the 1st cycle, is high enough for the system to reach thermodynamic equilibrium **[94]**, **[93]** and **[95]**. For these heating rates, intermediate liquid crystals also appear (see 5.2.1.1). The higher heating rates in the 1st cycle compared to the 2nd cycle, imply that the system might have not reached thermodynamic equilibrium at each temperature **[92]**.

It should also be mentioned that the above mentioned values of the heating rates (~0.05 to 0.2 [ºC/min]) might be considered even relatively high for calorimetric studies, as relative research in phase equilibria has suggested the use of even lower heating rates **[93]**. According to these studies, a relatively "small" heating rate is a rate in the range between 0.1 and 0.5 [K/hour] **[93]**. However, it would be difficult to apply these "low" heating rates, just because of time demands. The time needed to run an experiment with a "low" heating rate (as these studies suggest), would be very long. For instance, an experiment of the 2nd cycle lasted about 19 hours, with a heating rate between 0.05 and 0.1 [ºC/min].

Concentration region 5 wt % - 20 wt % (1st cycle)

For the 1st cycle, the heating and cooling rates were in the same order of magnitude and have been relatively high, as can be compared with relative research on heating rate of systems **[93], [94]** and **[95]**. For all the experiments performed, the heating rate is defined as the measured difference $\Delta T/\Delta t$, i.e. the temperature difference for the given time of a heating cycle, over that time. This suggests that the cooling rates used have been too large for the sample to approach thermodynamic equilibrium. Within the time of an experiment (8 hours), the proper choice of heating and cooling rate is very important because (as it has been observed for a 20 wt % CsDS sample, for instance) a heating rate of 0.02 [ºC/min] will make an intermediate liquid crystal vanish. This liquid crystal might not vanish with a

heating rate larger than 0.2 [ºC/min] (see 3.2, 5.2.1.1. and 5.9).

Concentration region 5 wt % - 20 wt % (2nd cycle)

20 wt % CsDS samples, that were heated faster than 0.2 [ºC/min] from room temperature up to about 35 [ºC] and with a heating rate of 0.15 [ºC/min] in the temperature region between 35.5±0.1 [ºC] and 43.2±0.1 [ºC], would form birefringent liquid crystals (see 3.2). Another clue related with the above observation, is that the samples stayed for 60 minutes in the whole temperature range. The liquid crystals disappeared at a temperature higher than 43.5±0.1 [ºC]. 3 independent samples of 20 wt % CsDS concentration were heated with a 2nd cycle (1stheating, followed by cooling with seed addition to be followed by a next heating), a cycle that ensures thermodynamic equilibrium approach. This approach would indicate the representative phase for the system at that concentration and temperature. The thermodynamically equilibrated findings suggested that the transition temperature for the 20 wt % CsDS sample, is T= 33±1 [ºC]. Therefore, the possibility that birefringent liquid crystals are the representative structure at 20 wt % CsDS concentration was excluded.

The results of the 2nd cycle presented in Figure 3.2 suggest that the solubility curve in that concentration region is pretty flat, with Krafft temperatures at T= 33±1 [ºC]. This means that the concentration of surfactant does not affect the Krafft temperature in that concentration region. Another way to look at it could be that the 1st order transition, from an anisotropic 2 phase system of solid crystals and micelles to a 1 phase isotropic micellar solution, does not depend on the concentration of the surfactant in the system. Moreover, there is a larger deviation (between the temperatures before heating and after reheating) for the lower concentrations (i.e. 5%, 10% and 15% wt) compared to the 20 wt % CsDS. One reason for the possible offset, could be the smaller mass of seed used in these cases than in the 20 wt % sample. In any case, the 20 wt % CsDS sample has stayed long enough (~30') at temperatures close to the transition temperature, in order to relax to its thermodynamic equilibrium.

Table 5.1 includes a comparison between the 1st and 2nd experimental cycle, in the concentration region 5 wt % - 20 wt % CsDS. Certain advantages of the 2nd cycle over the 1st

cycle are mentioned.

Table 5.1. Comparison between the 1st cycle and 2nd cycle of experiments in the concentration region 5 wt % - 20 wt % CsDS

1st Cycle	2nd Cycle
(+) Observation of intermediate liquid crystals (see 4.2.3.), using relatively high heating rates (~0.2 [ºC / min] in the region 25-33 [ºC])	(+) Low heating rate (~0.1 [ºC / min] in the region 25-36 [ºC]; more chances exits to achieve thermodynamic equilibrium.
(-) Relatively high cooling rates from 37 to 33 [ºC], or, from 35 to 33 [ºC] (~0.2 [ºC / min])	(+) Low cooling rate from 38 to 32 [ºC] (~0.05 [ºC / min])
(-) No addition of seed at T=34 [ºC]	(+) Addition of seed at T=34 [ºC] (Crystals dissolved, so 34 [ºC] should not be the Krafft temperature).
(-) No addition of seed at T=32 [ºC]	(+) Addition of seed at T=32 [ºC]- crystals did not dissolve; Krafft temperature should be close.
(-) No solid crystal production at T=32 [ºC]	(+) At T=32 [ºC], the higher concentration produced more solid crystals than the lower concentrations (nucleation is favored at higher concentrations).
(+) Larger mass of CsDS (better visualization of transitions)	(-) Smaller mass of CsDS crystals
(+) Pure CsDS (no organic impurities).	(+) Pure CsDS (no organic impurities)
(+) No supercooling; the lowest temperature has been T=25 [ºC].	(+) No supercooling; the lowest temperature has been T=25 [ºC].
(-) Coarser dispersion of CsDS into water	(+) Finer dispersion of CsDS powder into water (manually ground crystal)

The importance of the proper selection of heating rate is a major concern and is depicted in the following example for the SDS/water system:

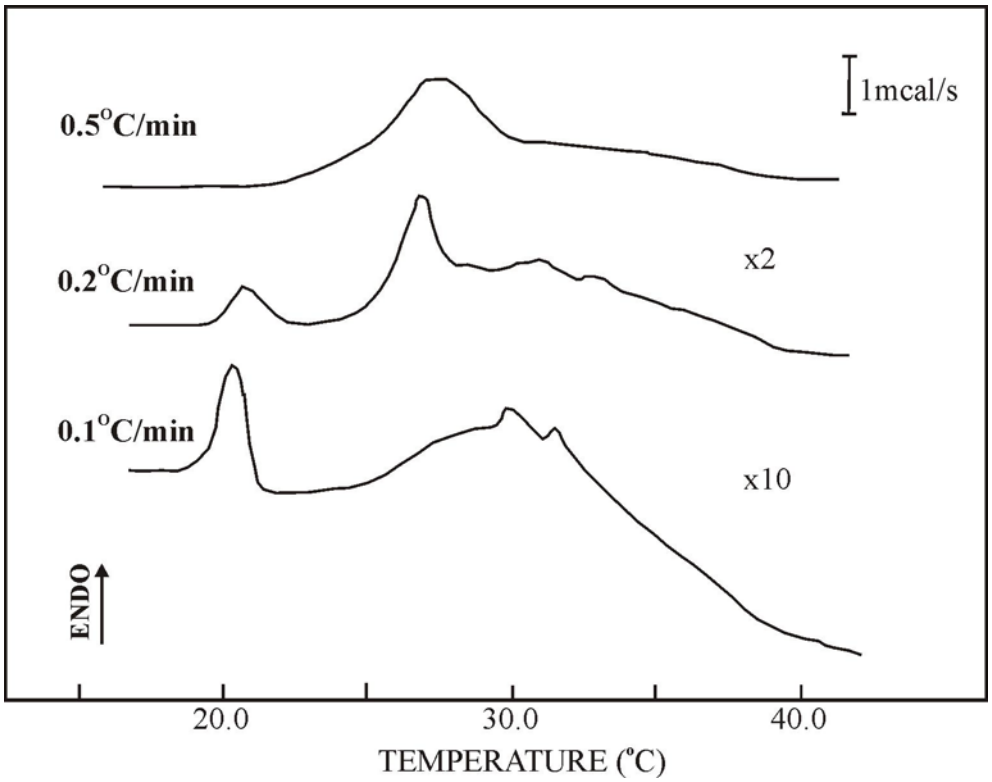

Fig.5.1. DSC Graph Intensity (Arbitrary units) vs. Temperature for the SDS / water system at 50 wt % SDS concentration, reported by Kekicheff et al. **[1]**. Figure 5.1. has been reproduced with permission that has been granted from the Copyright Clearance Center Inc. (see Appendix G for permissions).

Figure 5.1 is a DSC diagram that highlights the importance in the selection of heating rate for the thermodynamic equilibrium approach in a surfactant/water system. Specifically, this DSC graph shows the effect of heating rate on the transformations from coagel state (solid crystal and some mesophase (intermediate liquid crystal structure), or, solid crystal and micelles) to liquid crystal state, for the SDS/water system at 50 wt %. As the heating rate increases, the data become more irreproducible as far as the location (temperature), the intensity of the peak and its width. The fact that the kinetics for a transformation from a given temperature to a higher are very slow (transition from coagel state into the liquid crystal state) implies that the heating rate should be selected to be as low as possible to allow

the system to approach thermodynamic equilibrium.

The importance of the heating rate that was stressed in the SDS/water system, also applies for the case of the CsDS/water system. This diagram (Figure 5.1) indicates that the 2nd cycle experiments have more chances to have driven the system to its thermodynamic equilibrium, at a certain temperature and concentration, compared to the 1st cycle.

Concentration region 25 wt % - 40 wt % CsDS

The solubility curve exhibits a slight increase of 1-2 [°C] over that concentration region. Taking into account the results provided both by the 1st and the 2nd cycle for 3 independent runs at concentration 35 wt % and for the samples at concentrations higher than 40 wt % (heating only), one can hypothesize that the 2 phase region lies between 30 and 45 wt % CsDS.

It is suggested that more independent samples in that concentration region be examined in the future. This would help to identify precisely the concentration boundaries of the 2 phase region.

5.2.1.1. Intermediate liquid crystals

In the very first experiments, birefringent liquid crystals were observed while heating (see 3.2). It was necessary to prove that the lever rule applies for these samples. The way to prove that the lever rule applies in a two-phase system was to check if the volume fractions of the liquid crystal phase scale linearly with concentration. It had to be checked, actually, if the amount of the birefringent liquid crystal in the sample increases, as surfactant concentration increases).

This observation included 6 samples that had stayed at a certain temperature (T=44 [ºC]) for a period of few minutes, not necessarily in a simultaneous experiment. The 6 samples were at different concentrations; 18%, 20%, 28%, 30%, 38% and 40 wt % CsDS. The relative volume fraction of birefringent liquid crystals was approximated as the birefringent liquid crystal volume over the total solution volume.

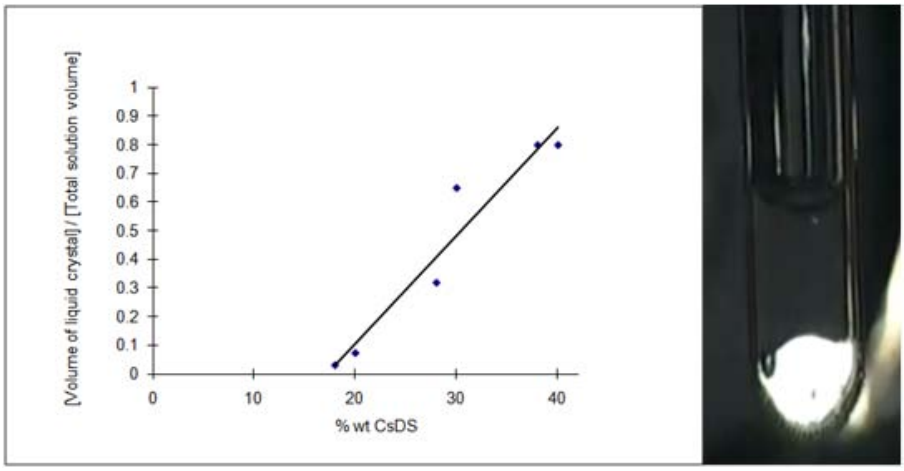

Fig.5.2. The application of the lever rule application for the coexisting phases, in a CsDS/water system in the concentration region 1 wt % - 30 wt % CsDS, at T = 44[ºC]. Figure captured at T =44 [°C]. Heating rate larger than 0.2 [ºC/min] starting from T = 25 [°C]. Cross–polarized light was used. *Size scale:* tube diameter is 15 [mm].

The threshold between relatively high and low heating rate in the macroscopic experiments was mentioned to be 0.2 [ºC/min]. Figure 5.2 is useful, in the sense that it depicts incorrect conclusions that can be drawn, when a relatively large heating rate (>0.2 [ºC/min]) is used and when an estimation of the lever rule for the sample is attempted.

This plot represents the birefringent volume fraction vs. the wt % concentration of CsDS in the samples. The samples had concentrations lower than 30 wt % CsDS at T = 44[ºC] and they were heated only (1st cycle) with relatively high heating rates (higher than 0.2 [ºC/min], about 0.5 [ºC/min]).

The coordinates seem to be related well in a linear regression curve. According to these data, the lever rule seems to hold in the concentration region 1 wt % - 30 wt % and at T = 44 [ºC]. This means that in the concentration region 1 wt % - 30 wt % and at T = 44 [ºC], birefringent liquid crystals could be expected to be the representative structure, if the samples have stayed there for a period of a few minutes (~5').A test was done to investigate whether these liquid crystals have constant volume fraction (representative phase), or they are intermediate liquid crystals that were formed during the initial runs of the experiments.

This process was followed:

1. While heating, the samples would stay at a certain temperature. The samples were checked to see which among them form liquid crystals.

2. While heating, the samples stayed for a certain period of time (about 30') at a given temperature and the liquid crystalline volume fractions among all the samples were compared. The samples were also checked to see if the liquid crystals shrink or not. If at any temperature, the liquid crystal volume fraction shrunk, then that liquid crystal would probably be an intermediate at that temperature and some thermodynamic transition would still be take place.

3. In order to strengthen the above observations, the samples have stayed at a certain temperature for longer time (8 hours). If a liquid crystal did not shrink over that time, this would practically prove that the liquid crystal structure is the representative phase at that temperature. If the liquid crystal shrunk over that time, then at that specific temperature and for the certain heating rate, the liquid crystal would be an intermediate structure.

For the low concentration region (less than 30 wt % CsDS), the conclusion is that heating rates higher than 0.2 [ºC/min] favored the formation of liquid crystalline intermediates. Heating rates between 0.05 [ºC/min] and 0.2 [ºC/min] would not result in the formation of these intermediates. During the first experiments, the crystals were introduced as chunks in the glass Pyrex® tubes. In consecutive experiments, the dispersion of the solid crystal into water was taken into account. In these (consecutive) experiments, the solid crystals would be as finely dispersed as possible, as the crystals were manually ground inside a glossy paper sheet. More than 1 sample at each concentration has been examined during the same run (2 or 3 samples).

The findings of the 2nd cycle experiments suggest that in the concentration region 5 wt % - 30 wt % and at temperatures higher than 33 [ºC], the thermodynamically equilibrated state, is a one–phase, represented by a neat micellar solution. Therefore, at 44[ºC], the thermodynamically equilibrated phase is expected to be micellar solution, as well.

Heating rates higher or equal to 0.2 [ºC/min]) in the concentration region 5 wt % - 30

wt %, will result in the formation of intermediate liquid crystals. These crystals might or might not vanish within the time of the experiment (within the 3 or 4 hours of a heating or cooling cycle, or within the 8 hours of a full heating and cooling cycle).

Here is the summary of the observations in that concentration region:

a. At concentrations lower than 30 wt % CsDS, it was observed that the liquid crystals dissolve at some temperature.

b. At concentrations higher than 30 wt % CsDS and as concentration of CsDS in the system increases, the number of independent samples where liquid crystal structure has been observed increases as well.

c. At 35 wt % CsDS concentration, for the 3 independent samples observed, liquid crystalline structure has also been observed.

d. At concentrations higher than 35 wt % CsDS, there are practically only liquid crystals in the sample.

Fig.5.3. Intermediate birefringent liquid crystals at T = 45 [ºC] for the CsDS/water system; *left*, 38 wt % CsDS; *right*, 20 wt % CsDS. Heating rate larger than 0.2 [ºC/min], starting from T = 25 [°C]. Cross–polarized light was used. *Size scale:* tube diameter is 15 [mm].

Figure 5.3 depicts how the coarse dispersion of solid crystals into water and the selection of relatively large heating rate, might influence the system to approach the representative phase (see 5.2.2). The 2nd cycle findings suggest that the sample at 20 wt %

CsDS concentration and at temperatures higher than 33 [ºC] is a neat micellar solution. For that concentration (20 wt %), no birefringent liquid crystals should be expected. The selection of a heating rate higher than 0.2 [ºC/min], however, might postpone the approach of the representative phase at the concentration mentioned, until after the 8 hours of the full experiment.

Fig.5.4. CsDS/water samples at T = 35 [ºC]; *left*, 30 wt % CsDS; *middle*, 20 wt % CsDS; *right*, 10 wt % CsDS. Heating rate higher than 0.2 [ºC/min], starting from T = 25 [°C]. Solid crystals transform. Cross–polarized light was used. *Size scale:* tube diameter is 15 [mm].

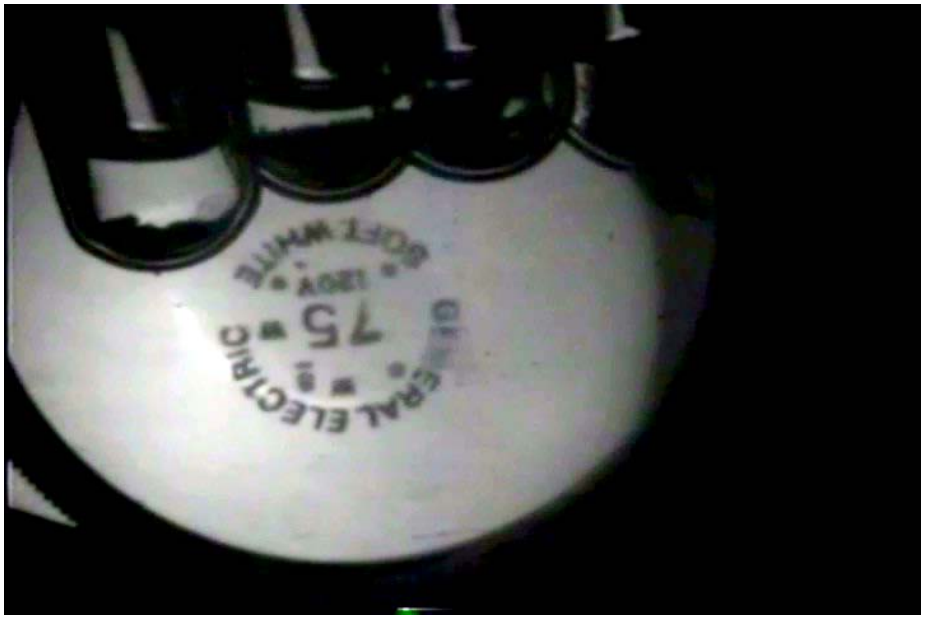

Fig.5.5. CsDS solid crystals in water at T= 25 [°C]; *left*, 40 wt % CsDS; *left to middle*, 30 wt % CsDS; *middle to right*, 20 wt % CsDS; *right*, 10 wt % CsDS. Heating rate higher than 0.2 [ºC/min], starting from T = 25 [°C]. Cross–polarized light was used. *Size scale,* tube diameter: 15 [mm].

Fig.5.6. 30 wt %, 15 wt % purified CsDS at T = 48 [ºC]. Intermediate, birefringent liquid crystals are observed in both samples. Heating rate higher than 0.2 [ºC /min], starting from T = 25 [ºC].Cross–polarized light was used. *Size scale:* tube diameter is 15 [mm].

5.2.2. The solid crystal dispersion in water

The maximum interfacial area between solute and solvent ensures maximum hydration of the surfactant (optimum interaction between solute and solvent). A finer dispersion of surfactant in water will increase the interfacial area between solid crystal and water. As the interfacial area between surfactant and water increases, the chances that the system approaches thermodynamic equilibrium are expected to increase.

5.3. Discussions on the Cryo-TEM experiments (These experiments were performed by Arunagirinathan M.A. and Bellare J.R.)

The reason why this concentration was selected for the CsDS/water solution (0.34 [M]), was to be able to be close enough to the concentration of the SDS/water system (0.3 [M]). This would help to compare the shape and size of the micellar nanostructures between the two systems, more reliably (see 5.9). This comparison would be supported by the hydrated radius effect of the alkali metal counter ion upon binding with the dodecyl sulphate chain and by the interaction of the alkali metal counterion with the negatively charged polar head groups **[53]**, **[54]** and **[56]**.

As can be observed in Figures 4.4 and 4.5 that represent the 0.34 [M] CsDS solution, both ellipsoidal and threadlike structures were observed on the same grid, in the same session. The ellipsoidal structures had a semi-major axis of 7 [nm] and a semi-minor axis 5 [nm], while the threadlike structures had a diameter of about 15 [nm] and their length varied from 200 [nm] to more than 1000 [nm]. The size of these threads (Figure 4.5.) is very large compared to the size that a rodlike micelle would have, if that rod-like micelle was composed of CsDS molecules.

It is possible that these observed nanostructures have formed, because of the heating rate selection during the sample preparation at the VITROBOT. The heating started from T = 25 [ºC] and the VITROBOT temperature was slightly higher than the Krafft temperature of the solution (Krafft temperature~33 [ºC] for a 0.34 [M] –or 12 wt % - CsDS solution, as the

macroscopic observations with cross-polarized light have shown).

(This part connects the Cryo-TEM findings with the discussion about the heating rate selection in the macroscopic experiments using cross-polarized light, as has already been discussed in section 5.2.1.) For concentrations less than 30 wt % CsDS, it was observed that heating rates higher than 0.2 [ºC/min] would result in the formation of intermediate birefringent liquid crystals in the system - during the macroscopic observations (see section 5.2.1.1). These liquid crystals would most likely dissolve either after the end of the experiment (the thermal treatment), or, at a temperature higher than the corresponding Krafft temperature. When the experiments were more carefully designed (2^{nd} cycle) and the heating rates were less than 0.2 [ºC/min], however, the system would look as a one phase isotropic solution, at the Krafft temperature.

Similarly to the observations of the macroscopic experiments, thermodynamic equilibrium approach is a necessary prerequisite in order to get and observe the representative nanostructure of the system (and not some intermediate nanostructures),when Cryo–TEM is used to characterized the structures. It is very likely that the threadlike structures are not micelles, but they are related to some intermediate liquid crystal structure (phase transition of the CsDS crystals). When heating samples with concentrations less than 30 wt % CsDS, the system moves into an intermediate liquid crystal structure, a liquid crystal structure that will eventually melt into a neat micellar solution. It is possible that these Cryo-TEM images have captured an intermediate liquid crystal structure.

5.4. Discussions on the XRD experiments (these experiments were performed by Torija M.J.)

5.4.1. Limitations

The decision to plan on XRD experiments was taken towards the end of the experiments of the Master's program. In any case, these experiments can be repeated in the future, in order to completely understand the CsDS/water phase behavior. During the sample

preparation process, two causes might have acted as limiting factors:

1. A possibility of solvent evaporation that dried the samples.

2. Some preferred orientation, because of shear forces that were induced by the action of a metallic spatula.

3. A smaller number of larger crystals, whose size that might have not satisfied the powder limit range of size **[75]**.

The screw - sealed glass Pyrex® Tubes containing CsDS solution, were brought at the XRD lab of the Characterization Facility. The samples were aqueous suspensions at T= 25 [ºC]. The diffraction took place at the same temperature (25 [ºC]. The tubes were opened, in order to deposit sample on the instrument inside the MicroDiffractometer chamber. The tubes were left open for 5', during the sample transfer onto the instrument. After that time, the samples inside the tubes looked dried. Their corresponding diffractograms are presented in the Figures 4.12 - 4.16 and their Debye rings in the Figures 4.10 and 4.11.

It is possible that during that time (5'), solvent (water) has evaporated. Some possible reasons are presented; humidity difference in the lab, or some interaction with the metallic spatula that extracted some specimen from the glass tube.

Assuming that evaporation indeed happened, and, in order to understand why evaporation in these samples happened, samples of similar concentration were prepared and reopened. A glass capillary tube scratched the bottom of the Pyrex® tubes. The tubes were left open for 15'. After 15', the supercooled sample looked more sponge – like, whereas all the other four samples were separated into two macroscopically distinct phases; an aqueous phase and a solid crystal phase.

There is no further information to connect the change in the macroscopic appearance of the samples with their resulting diffractograms (and, therefore, to question the reliability of the results with more evidence).It is not known whether the dried sample represents the same crystal structure with the sample before drying, considering the fact that there might be different hydrated crystal structures in the CsDS/water diagram.

5.4.2. Discussion about the X-ray diffractograms and the Debye rings

if solvent had evaporated during the sample preparation, the concentration of CsDS in the solution would have changed. It is useful to review the SDS/water phase diagram reported by **[2]** (see Figure 3.3). In the SDS/water phase diagram, at T = 25 [°C] and as concentration of SDS increases to more than 85 wt %, different crystal polymorphs appear **[2]**. These polymorphs also differ in the number of water molecules in their unit cell crystal structure. Therefore, it might be possible that water evaporation might have changed the concentration of CsDS in the CsDS/water system, where the CsDS would be some different crystal polymorph and the corresponding unit cell crystal structure of CsDS would also alter. That could be the treatment for the samples that lead to the X-ray diffractograms presented in Figures 4.12 to 4.16. It should be mentioned that no further data has been retrieved with the experiments of this thesis to show the crystal hydrate state where the initial (before drying) or the final (dried) of the sample have been.

'Since the samples have dried before being diffracted, the diffraction data of the dried samples cannot be used to extrapolate information about the corresponding sample in the solution', according to Torija M.J. For convention, however, a comparison between the dried byproduct X-ray diffractograms is presented below, within the range of the diffraction angle that the materials were examined. A comparison between the X-ray diffractograms (Figures 4.12 - 4.16) of the unheated samples (pure 5 wt % CsDS and impure 15 wt % CsDS), indicates that the two materials exhibit similarities in their diffraction angles ($2 \cdot \theta$). This suggests that any impurity present in CsDS (because of impurities in the reagents that were used to synthesize CsDS; see 2.2.1.2 and 2.2.1.3), does not seem to affect the CsDS crystal structure. The $2 \cdot \theta$ values of the superheated and supercooled samples are also similar with each other. Finally, the diffraction angles of all five samples examined, looked similar. According to Torija M.J, 'it is not possible to deduce conclusions about the unit cell crystal structure of the unheated sample, by trying to extrapolate conclusions from the dried diffraction byproduct'.

It is possible that both factors (thermal treatment and the possibility that impurities

might be present in some samples) do not seem to affect the diffraction angles, in the diffraction angle regime where the samples were examined by the instrument. Moreover, the loss of solvent because of evaporation has not been quantitatively analyzed. The experiment should be repeated in a wider diffraction angle regime. Keeping in mind that the diffraction data represent dried byproducts, the similarities in the $2 \cdot \theta$ values between the thermally treated and untreated samples suggest that the thermally treated samples (including the superheated and/or the supercooled sample) most likely do not represent metastable states.

Regarding the resulting Debye rings, two reasons can be mentioned to explain the stronger diffracted intensity for the thermally treated samples compared to the unheated samples; the size of the solid crystal and the concentration of CsDS in the sample (this discussion is related with the Figures 4.10 and 4.11). The fact that the crystal size should lie within the powder limit range **[75]**, is a necessary condition, in order for the Debye rings to represent accurately, crystal structure features of the material. As the size of the dispersed solid crystal increases, the size of some crystals may not lie within the powder limit range of the crystal size **[75]**. If the crystals do not lie within this size range, the diffracted intensity will be weaker and the Debye rings will become discontinuous and faint. Following Torija M.J., 'when the concentration of the sample decreases, the diffraction of the corresponding crystalline material is expected to be weaker' and the appearance of the Debye rings is going to be affected, resulting to non-uniform and weakly defined Debye rings. As one can see in Figures 4.10 and 4.11, the two unheated samples ('grey' and 'B sample') exhibit similarities in their Debye rings. These two unheated samples - purified CsDS crystal at T = 25 [ºC] (grey) and impure CsDS ("sample B") - do not have well-defined diffraction (Debye) rings, compared to the other three samples (thermally treated).

The smoothness and uniformity of the Debye rings for the thermally treated samples, means that these three samples – 40 wt % supercooled ('green'), 40 wt % superheated ('yellow') and 45 wt % heated ('red') - have a smaller grain size and more crystals are expected to satisfy the powder limit size range, compared to the samples that were not heated **[75].** It is possible that some of the crystals for the two unheated samples do not lie within

the powder limit size range **[75].** Second, the concentration of CsDS in the thermally treated samples (40% wt, 40% wt and 45% wt CsDS in CsDS/water solution) is larger compared to the unheated samples (5% wt and 15% wt). This difference in concentration can be translated as difference in CsDS crystals' presence. A larger number of CsDS crystals in the thermally treated samples means that the diffracted beam intensity will be stronger for these samples. This would result in more well-defined Debye rings for the thermally treated samples compared to the unheated samples.

Finally, a more weakly defined Debye ring can be related with presence of preferred orientation in the crystals **[80]**. This suggests that the unheated samples might exhibit some preferred orientation, while the other four samples do not.

To connect with the macroscopic observations, the thermally treated systems that have reached room temperature naturally) appeared macroscopically different than the unheated samples, probably because of difference in the way that the surfactant has been dispersed in water (see Figure 4.6).This change in the crystal size is associated with different nucleation and growth rates of the solid phase, for a sample that undergoes cooling (after it had been treated thermally, initially). This difference in the crystal size can be explained by the Ostwald Ripening **[88]**.

Ostwald ripening can describe the temporal increase in the solid crystal size, for a solid that had already been dispersed in an aqueous solution **[88]**. When the superheated and supercooled samples move to the final state (the final state macroscopically looks the same with the initial state) at T = 25 [ºC] (right image in Figure 4.8), either naturally or through solute /solvent perturbation **[35]**. The size of the dispersed crystal in water increases over time, as smaller crystals coalesce into a crystal with a larger crystal size. A finer dispersion of crystals with smaller size corresponds to a larger surface/ volume ratio (or, smaller inverse characteristic length) **[88]**. The larger crystal has a smaller solid crystal/water interface. This is true, because coarser surfactant dispersion in water is characterized by larger crystal sizes (or smaller inverse characteristic length). As the crystal size increases over time (the system moves to the final state –*right* image in Figure 4.6), the surface-to-volume ratio decreases

and the system minimizes its surface energy and moves to a more stable thermodynamic state.

There might still be some difference in the chemical potential of the system between the finely dispersed state and the coarsely dispersed state (the former case might have a higher chemical potential than the latter). This difference in chemical potentials, however, might be smaller than a difference that would discriminate a metastable and a stable state.

Taking into account both Ostwald's ripening and the fact that the diffraction angles for the thermally treated and untreated dried byproducts samples are similar, the possibility that the thermally treated samples (either superheated and/or supercooled) represent metastable states is minimized. The different macroscopic appearance is connected with difference in crystal size, when CsDS was dispersed in water).

5.4.3. Discussion about impurity in the crystals

The diffractogram of the unheated CsDS crystal (see Figure 4.15) exhibits overlapping peaks, in the $2 \cdot \theta$ range between 20º and 30º. These overlaps could be related to:

1. Some inherent feature of the CsDS diffractogram (and of the unit cell crystal structure of the pure CsDS crystal).

2. (This is more likely) the presence of impurity in the crystal, such as SDS, NaCl, or some other organic or inorganic material (discussed in 5.5.1 and 5.5.2).

Both SDS and NaCl exist in the aqueous solution during the recrystallization process (see 2.2.1.3.):

$$CsCl + SDS \rightarrow CsDS + NaCl$$

According to the stoichiometry of the aqueous recrystallization reaction (see 2.2.1.3), the CsDS is expected to be 99 wt % pure. It is possible that the 1% wt impurities may consist of SDS and/ or NaCl. Instead of having completely dissolved in water, NaCl and/ or SDS might have polluted the CsDS crystal.

A comparison between the pure CsDS X-ray diffractogram (see Figure 4.12) with the

diffractograms of SDS and NaCl suggests similarities. Both SDS and NaCl have peaks in their diffractograms at T = 25 [ºC] in the 2·θ range between 20º and 30º. The X-ray Diffractogram of SDS at T = 25 [ºC] has many peaks at 2·θ values between 20º and 25º **[96]**, while the X - Ray Diffractogram of NaCl at T = 25 [ºC] has a peak at 2·θ ~28º **[97]**.

CsDS samples were analyzed by ICP (Inductive Coupled Plasma), in order to quantitatively estimate the Cs^+ and Na^+ contents of the synthesized **[98]**. For a theoretically expected yield of a 1000 [ppm] Cs^+, the results of ICP analysis have shown that the sample had about 10 [ppm] Na^+ and more than 1000 [ppm] Cs^+ material (see Appendix A.3). For instance, 1 [g] of CsDS might contain 3 [mg] NaCl. This could be one reason behind these overlapping peaks in that 2·θ region.

5.5. Impurities and their effect in the phase behavior in the region 1 wt % - 40 wt % CsDS

5.5.1. The effect of organic impurities

Relative studies are provided, in the bibliography, about the effect of organic impurities on the surfactants. These studies include: the effect of organic impurity on the micellar behavior on SDS **[92]**, **[99]**; the effects in other surfactant systems **[100]**, **[101]**, **[102]** and **[50]**; a kinetic stability effect with presence of an organic cosolvent **[58]**; a study on surface physicochemical properties **[103]**; an investigation on the effect of organic molecules (alcohols) on cesium n-tetradecanoate/water system**[104]**.

Since CsDS is the recrystallization product of SDS, impurities possibly contained in SDS are considered major concern for CsDS. The major impurity in the SDS is considered to be dodecanol **[2]**, **[52]** and **[70]**. Dodecanol is formed after prolonged storage, according to an acid hydrolysis reaction of SDS, at temperatures higher than 40 [ºC] **[2]**, **[52]** and **[70]** .The reaction is written as:

$$SDS \rightarrow C_{12}H_{24}OH + NaH_2S$$

The SDS provided by the vendor, has a little less than 2 wt % impurities; probably

both inorganic and organic (L4509 (Product number) Sigma-Aldrich Sodium dodecyl sulfate Reagent Plus®, 98.5 wt % (GC)). The SDS, which has been used for the phase behavior experiments, was treated with ethanol to remove the organic impurities.

To connect with the description of section 2.2.1.2, the product from the desiccator after 2 days, the mass of the purified SDS was 32.2136±0.0001 [g] (corresponding yield of 80 wt %), expressed as: [SDS purified]/ [SDS non-purified]. These 20 wt % losses could be attributed to organic impurities that were dissolved in ethanol, as well as losses of SDS during both solubilization and foaming, because of vacuum filtration.

Figure 5.7 presents a comparison in the corresponding phase behavior between purified CsDS, as well as non-purified CsDS (see 2.2.1.2 and 2.2.1.3) in the concentration region 1 wt % - 40 wt % CsDS. The purpose of study is to examine if the phase behavior can change, by the presence of dodecanol as a cosurfactant in the CsDS/water system. For the concentrations 5 wt % - 20 wt %, a 2^{nd} cycle was performed, with 2 to 3 independent samples at each concentration. For the region 25 wt % - 40 wt %, a 1^{st} cycle was performed (a single heating cycle), with 1 to 2 independent samples, at each concentration.

For the impure CsDS, between 1 and 3 independent samples were examined in the concentration region 5 wt % - 20 wt % CsDS (at each concentration). Only one sample at each concentration was examined in the concentration region 25 wt % - 40 wt % CsDS. Thermal treatment of 1^{st} cycle was used (neither cooling, nor seed addition).

Fig.5.7. Solubility curve in the region 1 wt % - 40 wt % for purified and impure CsDS.

The error bar was calculated with reference to the average temperature value, at the given concentration. The error bar corresponds to concentrations, of course, at which more than 1 independent sample were examined. This means that if no error bar is seen at a certain concentration, then less than two independent measurements were examined at that concentration .The results suggest that the solubility curves (of pure and impure CsDS) in the concentration region 1 wt % - 40 wt %, seem to match well with each other and do not deviate more than 1 [ºC] (at certain concentrations, same for both systems).

Table 5.2 shows the Krafft temperatures that were estimated. When stated: “not recorded”, there was no measurement taken, because of experimental limitations.

Table 5.2 .Krafft temperature for impure CsDS in the region 1 % wt - 40% wt

% wt CsDS	Transition temperatures [ºC]		
5	32.1±0.1	31.7±0.1	31.90±0.1
10	32.5±0.1	32.5±0.1	32.50±0.1
15	33.1±0.1	33±0.1	33.05±0.1
20	33.55±0.1	33.4±0.1	33.48±0.1
25	34±0.1 (solid to micellar)	34 C±0.1	33.63±0.1
30	Not recorded	34.5±0.1	35.5±0.1
35	Not recorded	Not recorded	Not recorded
45	36±0.1	Not recorded	36.6±0.1

5.5.2. The effect of inorganic impurities

As far as inorganic impurities are concerned, it is assumed that they are removed by dissolution in deionized water, during the aqueous recrystallization process in the synthesis of CsDS (see 2.2.1.3). A qualitative and quantitative analysis of NaCl presence in the CsDS crystal should be examined in a future study. A comparison between the X-ray Diffraction pattern of pure CsDS crystal and NaCl, suggests that there are similar diffraction angles between CsDS and NaCl.

5.6. The Gibbs Phase rule, intraparticle and interparticle forces and a definition of phase transitions for both CsDS/water and SDS/water systems

5.6.1. The application of the Gibbs Phase rule in the CsDS/water system and the SDS/water system

The experiments were conducted at constant (ambient) pressure. The Gibbs Phase Rule for both systems is written as F=C-P+1. The phase rule is specified as follows, when applied

in the various regions of each phase diagram:

1. Pure component regions; P=1, F=2 (2 degrees of freedom). 2 independent variables need to be determined in order to define the system; the chemical potential of the surfactant and the temperature. An example can be a neat micellar solution (2-dimensional curves).

2. Two-phase regions; P=2, F=1 (1 independent variable, 1 degree of freedom). The temperature that represents a field variable (for example, concentration) is the same for each phase, at the boundaries of the 2 phase region. An example can be a two-phase region of micelles coexisting with hexagonal phase H_α) .The 1–dimensional curve is represented by the tie-line.

3. Three-phase regions; P=3, F=0, (no independent variables, completely defined regions in the phase diagram). An example can be the coexistence of three phases; micelles, hexagonal phase H_α and solid crystals C_2. This is represented by a point in the phase diagram.

5.6.2. Interparticle and intraparticle forces in the two systems

Any difference in the phase behavior between the 2 systems is expected to have been caused by a difference in the alkali metal ionic radius. A change in the counter ion radius would correspond to different interactions (electrostatic and steric forces) between the solvent molecules, the polar head groups and the dodecyl sulphate chain (see 5.8.2) **[56]**. These different interactions would result in different interactions within the aggregate units, as well as between different aggregates. The forces that are present in either system can be:

- Repulsive, due to excluded volume effects (because of the change in the alkali metal radii) and/or electrostatic stabilization. A change in the charge density of the alkali metal ions would correspond to different interaction between the colloidal particles.
- Attractive, due to Van der Waals forces between polar head groups, water molecules and alkali metal counterions

At the intraaggregate level, excluded volume effects, electrostatic and steric forces, as well as Van der Waals forces again exist, but now between larger multimolecular

compartments of hydrated surfactant molecules. These compartments can be micelles and/or more ordered structures. Favorable and unfavorable coexistence between phases can be explained as the net result between the Van der Waals forces and repulsive forces that exist among these aggregates.

5.7. Discussion on the CsDS/water system

The discussion refers to Figure 3.1. Macroscopic observation with the use of cross-polarized light has provided the solubility curve in the concentration region 5 wt % - 30 wt % CsDS. The curve is relatively flat, represented by Krafft temperatures at a constant value of 33 [ºC]. This flatness of the solubility curve in that concentration region, can suggest that the 1st order thermodynamic transition (from solid crystals and micelles (anisotropic system) to one-phase isotropic micellar solution) does not depend on the surfactant concentration.

At temperatures between 25 [ºC] and 33[ºC] in the concentration region 5 wt % - 30 wt % CsDS, the system is represented by the (solid crystal and micellar coexistence) two-phase region (blue caption). At temperatures higher than 33 [ºC] and in the concentration region 5 wt %-30 wt %, the system forms a one-phase micellar solution (bright pink caption) **[16]**. Cryo–TEM was used to examine the nanostructures formed in a 0.34 [M] CsDS/water solution (~ 12 wt % CsDS) at T = 35 [°C] (by permission of Arunagirinathan M.A.; Bellare J.R.) **[16]**. The reason why this concentration and temperature has been selected, was to compare the dimensions of the resulting CsDS nanostructures with both the dimensions of CsDS nanostructures reported by certain studies **[53]**, **[54]** and with the analogous nanostructures formed by the SDS/water system, at identical phase diagram coordinates; similar Krafft temperature and its corresponding critical micelle concentration (0.3 [M]) **[16]**.

In the same session, both threadlike and ellipsoidal nanostructures were observed on the same grid for the CsDS/water system (see Figures 4.4 and 4.5). The ellipsoidal CsDS

structures had a semi-major axis of 7 [nm] and a semi-minor axis of 5 [nm]. The threadlike structures had a diameter of about 15 [nm] and their length varied from 200 [nm] to more than 1000 [nm]. The size of the threadlike structures is too large to be related with a rod like micelle. Compared with relevant studies on alkali metal surfactants **[53]**, **[54]** the ellipsoidal structures have similar dimensions, but the threadlike structures have not been reported before.

Certain reasons can explain why both ellipsoidal and threadlike CsDS structures have been observed on the same grid. Firstly, the sample preparation temperature (T = 35 [ºC]) was very close to the measured Krafft temperature for the 12 wt % CsDS solution (T ~ 33 [ºC]). Secondly, the heating rate that was used during sample preparation could have been very high (see 5.2.1). The importance of the heating rate selection was stressed in the macroscopic observations with cross–polarized light, where intermediate liquid crystals have been observed when a heating rate larger than 0.2 [°C/min] was used (see 3.2, 5.2.1.1 and 5.9). These factors (the sample preparation temperature and the heating rate selection) might have prevented the CsDS crystals to completely dissolve in water. Therefore, these threadlike structures might be related with a transition of solid crystals into intermediate birefringent liquid crystals, before the system becomes a neat micellar solution.

As concentration of CsDS in the system increases from 30 wt % to 40 wt %, the Krafft temperature slightly increases from 33 [ºC] to 34 [ºC]. At temperatures lower than 34 [ºC], the system macroscopically appears as a two-phase system of micelles and solid crystals. At temperatures higher than 34 [ºC] and in the concentration region 30 wt % - 45 wt % CsDS, the results suggest that the system is represented by a two-phase region of micelles coexisting with some liquid crystal phase. The exact boundaries have not been determined and these could be identified in a future study (see chapter 7).

At 40 wt % CsDS concentration, the following observations have been made: At T > 37 [°C], the system most likely lies in a two-phase region of micelles and liquid crystals. Heating rates larger than 0.2 [ºC/min] from 25 [°C] to 55 [°C], result in the formation of superheated samples. After these samples have been naturally cooled and the system is at T =

25 [°C] again, these samples look relatively viscous (yellow legend in Figure 3.1.). A cooling rate larger than 0.2 [ºC/min], from 55 [°C] to 0 [°C], will result in supercooling. When the superheated and supercooled samples are naturally cooled and warmed (to T = 25 [°C]), respectively, they look macroscopically different than the unheated samples of the same concentration. The thermally treated samples will look like that for several days, if solute or solvent seed is not inserted (brown legend in Figure 3.1). It had been investigated if these samples represent some metastable state and X–ray Diffraction experiments took place, to confirm or reject that.

The XRD results of the dried byproducts suggest that the superheated and supercooled (dried) samples have similar $2 \cdot \theta$ values with the unheated, purified CsDS crystals. This means that the thermally treated samples most likely exhibit similarities compared to the unheated samples Therefore, it is very likely that the thermally treated samples do not represent some metastable state.

Macroscopic observation with cross–polarized light suggests that at concentrations higher than 40 wt % and at temperatures higher than 37 [°C], the system is most likely represented by some birefringent liquid crystal phase region (green caption in Figure 3.1).

Macroscopic observation with cross–polarized light was also used to check the effect of impurities in the phase behavior of the CsDS/water system, in the concentration region 1 wt % – 40 wt %. The results have shown that impurities possibly present in CsDS do not change the location of the solubility curve, compared to the solubility curve location of the purified CsDS (see 2.2.1.2 and 2.2.1.3).

5.8. An analysis of the SDS/water system

This analysis is based on the findings for the SDS/ water system that have been reported by **[1]**, **[2]**, **[3] and [96]** (see Figures 3.2 and 3.3). In the concentration region 5 wt % - 35 wt % SDS, the solubility curve (transition of solid crystals and micelles to neat micellar solution) has a positive inclination, with an increase of 12 [°C] over the

concentration region 5 wt % - 38 wt % SDS. This suggests that the temperature of this 1st order thermodynamic transition depends on the surfactant concentration. In the same concentration region, as temperature is increased higher than the Krafft temperature, the system moves from an anisotropic two-phase region (solid crystals and micelles) to an isotropic micellar region (single phase). The Critical Micelle Concentration of SDS at T = 25 [ºC] is 8 [mM] **[28]**.

Between 35 wt % and 40 wt % SDS and at temperatures lower than T = 25 [ºC], the system lies in a two-phase region of solid crystal coexisting with micelles. As the temperature increases, the system moves into another two-phase region where micelles coexist with hexagonal phase of liquid-like core (H_α & micelles) **[2]**. As both temperature and surfactant concentration in water (to more than 40 wt % SDS) increase, the SDS micelles organize themselves into the less ordered mesophase, the hexagonal, H_α **[2]**.The Hexagonal H_α (compared to all other intermediate mesophases) is the next more favorable configuration for the surfactant molecules after the micellar region, as it is the less packed structure (more open) than all the other mesophases **[105]**. At short distances, the repulsive forces within the charges within a colloidal aggregate, as well as between colloidal aggregates are stronger in the hexagonal structure. This conformation provides more freedom for the surfactant molecules to arrange in space.

For surfactant concentrations between 55 wt % and 70 wt % and as temperature rises higher than 40 [ºC], intermediate mesophases appear; cubic, tetrahedral, mesomorphic **[2]**. With even larger increase in concentration and in temperature, the system moves to the next more ordered mesophase, the lamellar phase, L_α **[2]**.

Finally, the solid crystal transformations are discussed. These correspond to transformations between different unit cell crystal structures (polymorphs) of SDS with variable degree of hydration in the crystal structure **[2]**. The first solid crystal transformation is located at about 30 wt % SDS and at T = 20 [ºC]. No other solid crystal transformation is reported, until 85 wt % SDS **[2]**. At concentrations of surfactant higher than 85 wt % SDS, isoplethal transitions, from T = 0 [ºC] to higher temperatures, indicate that the SDS unit cell

undergoes solid crystal transformations. At lower temperatures, two different crystalline polymorphs coexist in thermodynamic equilibrium (C' with C''). As temperature increases, the system moves into a two-phase region, where liquid crystals coexist in thermodynamic equilibrium with solid crystals (i.e. lamellar phases exist in equilibrium with a crystal hydrate).

5.9. A comparison between the CsDS/water and the SDS/water systems

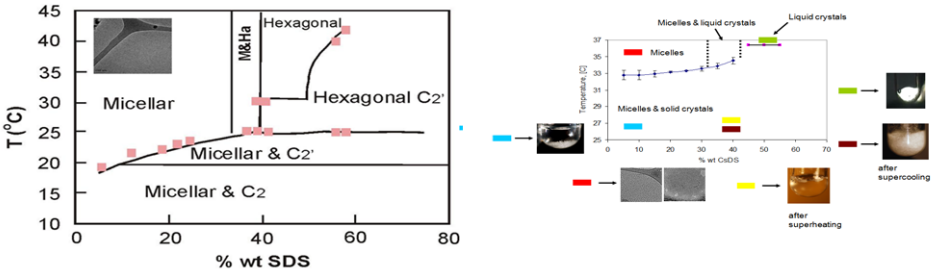

Fig.5.8. The SDS/water phase diagram (left) that has been reported by Fontell et al. **[1]** and Kekicheff et al.**[2].** The pink squares (points) of the SDS/water phase diagram have been reproduced with permission that has been granted from that has been granted from the Copyright Clearance Center Inc. (see Appendix G for permissions). The Cryo-TEM image of the SDS/water system has been reported by Arunagirinathan M.A. and Bellare J.R. and has been reproduced with their permission. The CsDS/water phase diagram (right).

The major differences between the two phase diagrams:

1. Solubility curves and temperature width of the two-phase region (solid crystal and micelles) in the region 5 wt % -30 wt %

In the CsDS/water system, the solubility curve is relatively flat in that concentration region, with corresponding Krafft temperatures at T = 33±1 [ºC]. This flatness of the solubility curve can suggest that the 1st order thermodynamic transition, from solid crystals

and micelles (anisotropic system) to one-phase isotropic micellar solution, does not depend on the surfactant concentration. On the contrary, the solubility curve of the SDS/water system in the concentration region 5%wt - 30% wt is not flat. The SDS solubility curve increases about 12 [°C] over the concentration region 5% wt -38% wt **[1], [2]**.

An explanation of why the solubility curve of CsDS lies at higher temperatures compared to SDS, can be provided starting with the Hofmeister series for the alkali metals **[56]**, **[106]**. These series can explain the changes in the interaction between the corresponding colloidal particles. Before their dissolution in water, Cs^+ has a larger ionic radius compared to Na^+. When the alkali metal cations are dissolved in water, the water molecules in the solution can be attracted easier by the smaller ionic radius of Na^+, compared to the bulkier ion of Cs^+. Therefore, the Van der Waals (attractive) forces between the water molecules and Na^+ are stronger. The distance between the center of charge of the hydrated radius of Cs^+ and the negatively charged polar head groups (SO_4^{2-}) is smaller, compared to the case of Na^+. This means that the hydrated counterion of Na^+ will have more difficulty to bind with the anionic polar head groups, as the steric repulsions will become larger. Regarding the electrostatic repulsions, the larger, hydrated Na^+ counterion (which, after dissolution, becomes the bulkier cation) screens less effectively the electrostatic repulsions between the anionic polar head groups than the hydrated Cs^+ **[53]**, **[54]**, **[56]**, **[106]** and **[23]**. Likewise, the smaller hydrated radius of Cs^+ corresponds to a higher cation charge density. For the reasons mentioned above, the hydrated Na^+ cation is more lyophilic than the hydrated Cs^+ cation.

In order to describe fully the solubility differences, the differences in the hydration of the counter ion radii can be connected with differences on the corresponding micelles of the two salts. Since Na^+ counter ions are bulkier, a smaller number of these counter ions can condense on the hydrophilic outside layer of the SDS micelles and the degree of counterion condensation on the micelle will be smaller in the case of SDS, compared to CsDS **[53]**, **[54]**, **[106]** and **[23]**.

The CsDS micelles have a smaller net charge, because the smaller hydrated counterion

of Cs^+ can reduce more effectively the electrostatic screening of the polar head group repulsions. Therefore, Cs^+ has a higher degree of counter ion binding on the corresponding CsDS micelles and the net charge of the CsDS micelles is expected to be smaller. This difference in the degree of the counter ion binding on the surfactant micelles means that the SDS micelles will have a larger net charge than the CsDS micelles which would correspond to a larger surface charge on the micellar surface. From the viewpoint of colloidal particles, the less charged CsDS micelles can electrostatically stabilize with each other less easily than the corresponding SDS micelle. This would indicate that coagulation of the micelles into a solid crystal phase is favored more for the CsDS micelles, compared to the SDS micelles.

The solubility differences between the 2 sulfate salts can be viewed as the net result of 2 types of competitive interactions among the counter ions, the polar head groups and the water molecules; hydrophilic forces and crystalline free energy (thermodynamically driven) forces **[23]**. The larger hydrated Na^+ counterion can be related with stronger hydration of the anionic polar head groups, or stronger hydration effects, compared to Cs^+ **[23]**. Without having calculated the crystal free energy of either surfactant, the observations suggest that the hydration forces for the SDS/water system are stronger compared to the strength of the thermodynamically driven forces of the SDS crystal phase (weaker crystal energy) **[23]**. The opposite seems to hold for the CsDS/water system (stronger crystal energy and weaker hydration of the polar head groups) **[23]**.

Finally, apart from having been explained as temperatures that represent 1^{st} order thermodynamic transitions, the Krafft temperatures can be related with the kinetic stability of colloidal particles. The kinetic stability is expressed by means of the system's energy barrier height against coagulation. The Krafft temperatures for the CsDS/water system are higher than for the SDS/water system. This means that the energy barrier against coagulation (energy penalty) seems to be larger for the SDS/water system compared to the CsDS/water system. SDS seems to be more resistant against coagulation and thus more kinetically stable at that concentration region, compared to CsDS [107].

The above analysis has examined how the differences in the hydrated metal ionic radii

can affect the interactions between alkali metal counterions, water molecules and anionic polar head groups. This discussion conforms to the results of the CsDS/water system and the SDS/water system, as it (SDS/water system) has been reported by **[1]** and **[2]**.The observations suggest that differences in these interactions affect the Krafft temperatures by an order of 8 [°C], in the concentration region 5 wt % - 30 wt %. These differences are related with different electrostatic and steric forces that can be interparticle (polar head group repulsions) and intraparticle. This Krafft point difference may be also related to the competitive action between thermodynamically driven forces and hydration forces. Apart from these descriptions, there is also an attempt to connect the Krafft temperature differences with kinetic stability differences between the colloidal systems.

2. Location and concentration width of the coexistence region of liquid crystals and micelles. A comparison between the micellar structures

The two-phase region of hexagonal phase and micelles in the SDS/water system spans the concentration region from 35% to 40 wt %. Its concentration width is narrower than the analogous phase of the CsDS/water system, where this phase lies between 30% and 40 wt %. The transition temperature of the SDS/water system is much lower compared to the CsDS/water system; T = 25±1 [ºC] for the SDS/water system **[2]** and T = 34±1 [ºC] for the CsDS/water system.

Regarding the CsDS/water system, the results of the macroscopic experiments with cross-polarized light have shown that liquid crystals can be the representative structure at CsDS concentrations higher than 30 wt % but lower than 45 wt % when the system is heated to temperatures higher than 35[°C] (see 3.2 and 5.2.1.1). At concentrations of about 45 wt % CsDS and at temperatures larger than 35 [ºC], the system gets completely transformed into a liquid crystal structure. Therefore, the two-phase region of micelles and liquid crystals in the CsDS/water system should probably lie at temperatures higher than 35 [°C] and in the concentration region between 30 wt % and 45 wt %. The exact boundaries of the coexistence region of liquid crystals and micelles for the case of CsDS/water have not yet been

determined.

The larger concentration width in the case of CsDS, corresponds to a more favorable coexistence (stronger Van der Waals forces) between the two corresponding phases (micelles with liquid crystals), compared to the SDS/water system.

The reasoning for that can also begin through the Hofmeister series **[56]**, **[106]** and conclude at the level of forces between the colloidal particles. As has already been mentioned in the 1st difference regarding the solubility curve locations (above), the larger hydrated ionic radius for Na^+ compared to Cs^+ corresponds to an increased hydrophilicity of the SDS surfactant compared to CsDS **[56]**. This is why CsDS appears less soluble in water than SDS. Order is favored more in the CsDS/water system compared to the SDS/water system.

It is attempted to connect this width in concentration with the difference in order between the two surfactant/water systems. The smaller hydrated radius of Cs^+ reduces more effectively the screening of the polar head group repulsions **[53]**, **[54]**. Therefore, Cs^+ can be attracted easier by the polar head groups compared to Na^+. The favored polar head group/Cs^+ attractions reduce more effectively the screening of the polar head group repulsions. Consequently, a higher degree of counterion binding on the CsDS micelle is expected **[106]**. Moreover, the reduced repulsions between the polar head groups in the CsDS/water system result in a larger degree of counterion condensation on the CsDS micelles. The differences in the counter ion binding degrees and in the counter ion condensation constants can explain why the CsDS/water system exhibits a lower critical micelle concentration compared to SDS, at the same temperature **[67]**. The lower critical micelle concentration at the same temperature for CsDS in water, is a first indication that order is favored more in the CsDS/water system compared to the SDS/water system.

Using Cryo-TEM, the CsDS ellipsoidal structures that were observed were larger compared to the SDS micelles. Both samples were examined at similar temperature and concentration by (by permission of Arunagirinathan M.A.; Bellare J.R.) **[16]**. For the CsDS structures, the semi–major axis and semi–minor axis were 7[nm] and 5[nm], respectively.

The SDS micelles had a diameter of 5 [nm] **[16]**.

The differences in the size can be related with larger aggregation numbers for the CsDS micelles. Both the increase in the counter ion condensation and the decrease in the polar head group repulsions can explain the larger aggregation numbers for the CsDS, compared to SDS **[106]**.This is also a difference in order at the micellar level.

The reduction of the polar head group repulsions reduces more effectively the curvature of the CsDS micellar nanostructures, compared to Na^+ **[53]**, **[54]**. As this curvature is decreased, the CsDS/water interaction will also decrease and surfactant molecules will arrange easier from micelles into more ordered liquid crystal mesophases. The decrease in curvature and increase in order is depicted in the following order; spherical micelle, rod-like micelle, hexagonal liquid crystal phase, lamellar liquid crystal phase (see Critical Packing Parameter in 1.3.5). This can explain the fact that the CsDS structures are larger.

Assuming that the actual concentration width for the two-phase region conforms to the observations, an explanation for the difference in width can be based on the interparticle and intraparticle interactions. The smaller net charge that the CsDS micelles experience (for the reasons mentioned above; larger degree of counterion condensation on the micelles) reduces the electrostatic repulsions within a micelle (polar head group repulsions) as well as between micelles. Therefore, Van der Waals forces between the micelles become more significant than the repulsive forces. Therefore, aggregation between the colloidal particles in the suspension compared to the SDS/water system. Since aggregation of structures is favored more in the CsDS/water system, liquid crystal phase (aggregated micelles) and micellar phase can coexist over a wider concentration range for the CsDS/water system compared to the SDS/water system.

To connect with the discussion about more ordered mesophases and with the results of the Cryo–TEM experiments in a 0.34 [M] CsDS/water solution (by permission of Arunagirinathan M.A.; Bellare J.R.), the threadlike structures that were observed (diameter of about 15 [nm] and a length varying from 200 [nm] to more than 1000 [nm]), were too large to be related with a rod like micelle **[16]**. Instead, they could probably represent some

intermediate liquid crystal before the dissolution of the solid crystals into a neat micellar solution at that temperature and concentration.

In the concentration region between 30 wt % and 45 wt % and at T = 25 [ºC], the CsDS/water system lies in a 2 phase region of solid crystal and micelles. On the other hand, the SDS/water system is represented by the following transition; solid crystals and micelles to liquid crystals and micelles. The liquid crystal phase is a less ordered phase than the solid crystal phase.

The analysis is also related with the Hofmeister series for the alkali metal ionic radius interaction with the solvent molecules **[56]**. The explanation is similar with the explanation for the difference in the solubility curves in the concentration region 5 wt % - 30 wt %, as has been explained before (1^{st} difference). The larger hydrated ionic radius for Na^+ is larger compared to Cs^+ increases the hydrophilicity of the surfactant. The liquid crystal structure favors more the interaction with the solvent molecules, compared to the solid crystal structure. Since the CsDS is less soluble than SDS, this difference seems to make sense.

3. X-ray Diffractograms

Regarding the CsDS crystals, as seen in Figures 4.12 to 4.16, the diffractograms of all five (dried) CsDS samples examined at T = 25 [°C] (thermally treated and untreated) have peaks at similar $2\cdot\theta$ values with each other, in the $2\cdot\theta$ range that the CsDS samples were examined (between 0° and 30°). The CsDS diffractograms, however, represent dried byproduct and not the actual solutions.

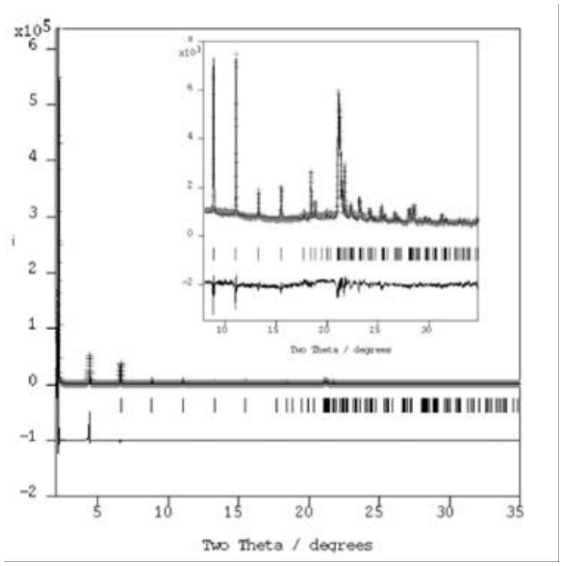

Fig.5.9. X-ray Diffraction Analysis for SDS crystals at T = 25 [ºC], reported by L.A. Smith et al. **[96]**. The Figure has been reproduced with permission that has been granted from the Copyright Clearance Center Inc. (See Appendix G for permission).

An attempt was also made to figure out the unit cell crystal structure for the CsDS crystal, using the materials database Jade at the Characterization Facility of the University of Minnesota. A computer database has unit cell crystal structures for many materials. An already known material data sheet is selected and the diffractograms of the known material with the unknown material are compared. The parameters in the saved diffractogram are modified, until the diffractogram of a selected material and the known diffractogram match.

Using the following information for the anhydrous SDS crystal structure provided by L. A. Smith et al. **[96]**: unit cell parameters, dimensions, unit cell volume, unit cell density, space group, crystal structure, unit cell angles and lengths, as well as bond lengths, already saved diffractogram were selected and compared.

The dried byproduct diffractograms of the unheated, pure CsDS (Figure 4.12) and the unheated, pure SDS (Figure 5.9) at T =25 [°C] exhibit similarities in their 2·θ values, in the 2·θ range that the CsDS sample was examined (between 0° and 30°). In that range, many diffraction peaks between the two systems match with each other. The diffractogram of the dried byproduct cannot be used, however, to deduce conclusions about the unit cell crystal structure of CsDS in the solution, if the sample had not dried.

In order to be more confident in the crystal structure comparison between SDS and

CsDS, the experiment for CsDS should be repeated in a wider 2·θ diffraction regime (between 0° and 100°). This can strengthen the comparison between the unit cell crystal structure of the two surfactants; CsDS and SDS.

4. Intermediate birefringent crystal behavior; the comparison between CsDS/water and SDS/water systems

Macroscopic experiments with cross-polarized light have taken place in order to investigate simultaneously, the effect of the counterion hydrated ionic radius in the appearance of intermediate birefringent liquid crystals (at concentrations where the intermediate liquid crystal is not the representative phase) and the time for the dissolution of these intermediate liquid crystals (see 3.2 and 5.2.1.1). The comparison was done at the same molar concentration for both cesium dodecyl sulphate and sodium dodecyl sulphate aqueous solutions and at a temperature higher than the Krafft temperature of either system, for the same absolute temperature difference for both systems (ΔT = 6 [ºC]).The reason why this temperature difference and the molar concentration were the same in both systems was to focus on the effect of the different counterion radius only on the time needed for the following 1st order phase transition; crystals and micelles to a neat micellar solution.

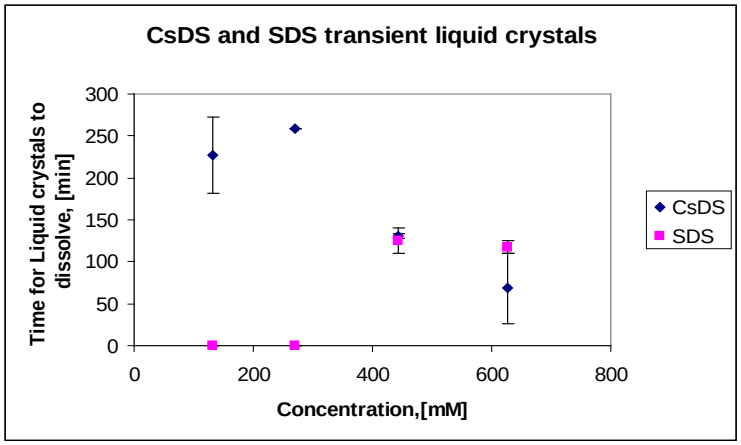

Fig.5.10. Time for the dissolution of intermediate liquid crystals vs. surfactant concentration; same heating rate.

Figure 5.10 presents the time needed for the intermediate liquid crystals to dissolve

versus the molar concentration of surfactant in water. The comparison was done at the same molar concentration, for either surfactant. The CsDS crystals were synthesized according to the method describes in 2.2.1.2 and 2.2.1.3 and aqueous suspensions were prepared. Starting from T =25 [°C], the samples were heated with the same heating rate (larger than 0.2 [ºC/min]) and, as mentioned above, with the same temperature difference from their corresponding Krafft temperatures, ΔT=6 [ºC], where the temperature of each sample was 6 degrees Celsius higher than the Krafft temperature of the corresponding concentration. (It can be mentioned that this experiment can also check the time for dissolution of these birefringent crystals, when the water tank is at a temperature 6 degrees Celsius higher than the Krafft temperature, for the corresponding concentration. The standard deviation (indicated with the error bar in the CsDS/water system, as shown in Figure 5.10) is measured with respect to the average temperature value for the same set of independent samples, at each molar concentration. More experiments with CsDS should take place, to minimize the error bar.

A first comparison between the 2 systems shows that with increasing molar concentration of surfactant in water, shows the following:

i. At concentrations less than 300 [mM], the 2 systems show opposing trends, where the Na^+ system does not form liquid crystals, while the Cs^+ system exhibits liquid crystals.

ii. At concentrations higher than 300 [mM], the 2 systems exhibit similar times for dissolution of the liquid crystals.

By chance, the surfactant concentration of 300 [mM], is at about the concentration region where the Cryo-TEM experiments for both systems (Cs^+ and Na^+) were done.

5. Thermodynamic transitions

Both systems exhibit 1^{st} order transitions, as has been mentioned above, in the cases where the system moves from an anisotropic system (2 phase system of micelles and solid crystals) to an isotropic solution (neat micellar solution).The lines in each diagram that indicate the following phase changes, correspond to 1^{st} order thermodynamic transitions:

i. For both Cs^+ and Na^+ systems, any isoplethal transition of crystals and micelles (two-phase region, anisotropic system) to neat micellar solution (one-phase region, isotropic solution) that crosses the solubility curve.

ii. For the Na^+ system, the isothermal transition of hexagonal phase and micellar phase (two– phase region) to neat micellar phase

iii. For the Cs^+ system, the isothermal transition of liquid crystal and micelles (two-phase region of an anisotropic system with still undefined boundaries) to a neat micellar solution

Finally, another 1st order transition should be mentioned for the SDS/water system **[2]**. This is the sudden discontinuity of the transition line that separates the two-phase region of C_2 and H_α phases from a one-phase region (H_α), at 50 wt % concentration and at temperature T=30 [ºC].

Table 5.3. A summary of certain differences between SDS and CsDS

Properties	CsDS/water system	SDS/water system
Solubility in water	Lower	Higher
Krafft temperature	Higher	Lower
Width of the micellar and liquid crystal region	Larger	Smaller
Nanostructures	Threadlike (10 to 15 [nm] diameter); Ellipsoidal (~8 [nm] semi major axis; 5[nm] semi-minor axis)	Spherical micelles, 5 [nm] diameter
CMC at T= 25 [°C]	Lower	Higher
Unit cell crystal type	Undefined	Monoclinic
Space group	Undefined	P*2l/c

CHAPTER 6

CONCLUSIONS

The goal of this thesis has been to explore the phase behavior of the CsDS/water system and compare it with the already studied SDS/water system **[1]**, **[2]**, **[3]** and **[96]**. Two different methods have been investigated for the synthesis of CsDS; ion exchange (batch and continuous mode) of SDS into HDS that was followed by neutralization with CsOH, aqueous recrystallization of SDS in a CsCl solution into CsDS. For the purposes of phase behavior exploration of this thesis, the CsDS was synthesized by aqueous recrystallization.

Various experimental techniques have been used to explore the CsDS/water phase behavior, such as macroscopic observation with cross–polarized light, Cryo–TEM, SAXS, XRD and optical microscopy with cross–polarized light. A comparison between the results of the experiments for the CsDS/water phase behavior and the SDS/water phase behavior (**[1]**, **[2]** and **[3]**) can show that:

1. The solubility curve in the concentration region 1 wt % - 30 wt % CsDS is a flat line at T = 33±1 [ºC]. This slope of this curve slightly increases to from T = 33±1 [ºC] to T = 34±1 [ºC], as concentration of CsDS in the system increases from 30 wt % CsDS to 40 wt % CsDS. On the other hand, the solubility curve in the concentration region 1 wt %-30 wt % for the SDS/water system has a nonzero slope. This slope increases at about 12 [°C] in the concentration region between 5 wt %–30 wt % SDS. The solubility curve of SDS ranges between 20[ºC] and 25[ºC], at lower temperatures compared to the Cs^+ system **[2]**. The lower Krafft temperature for the Cs^+ system compared to the Na^+ system, at the same concentration region, is fundamentally related to the smaller hydrated cationic radius of Cs^+ compared to Na^+. Na^+ exhibits a stronger hydrophilic character compared to Cs^+ **[56]**.

2. The concentration boundaries for the micellar and liquid crystal (two-phase) region in the case of CsDS/water have not been verified. Macroscopic observations suggest, however, that the regime should lie between 30 wt % and 45 wt % at T = 34 [ºC]. For the same range of concentrations (between 30% and 40 wt %), the micellar and liquid crystal two-phase region is wider for CsDS compared to SDS **[2]**. As for the SDS/water system, the concentration boundaries for that 2 phase region lie between 35% and 40%, at T > 25 [ºC] **[2]**.The fact that liquid crystals comprise representative nanostructure in the Cs^+ system at

concentrations lower than the Na^+ system is also related to the lyotropic series of the alkali metals **[56]**. The smaller hydrated radius for Cs^+ compared to Na^+, indicates stronger screening of the polar head group repulsions within the surfactant molecules for Cs^+ compared to Na^+. This difference favors a reduction of the curvature and a decrease in the surfactant solubility (increase in the Krafft temperature) in the Cs^+ compared to the Na^+ system **[53]**, **[54]**. Because of smaller head group repulsions, the net charge of the CsDS micelles is lower, leading to weaker repulsions and stronger attractions between CsDS micelles. Because of these weaker repulsions, aggregation of CsDS micelles into more ordered mesophases is favored. Therefore, the larger width of this 2 phase region for the Cs^+ system signifies an increase in the Van der Waals forces between the 2 phases; micelles and liquid crystals.

3. Cryo-TEM experiments on the CsDS/water system have shown both ellipsoidal structures of semi-major axis radius = 7 [nm] and semi- minor axis radius = 5[nm], as well as threadlike structures of 15 [nm] diameter, on the same grid **[16]**. On the contrary, spherical micelles are formed in the SDS /water system at similar temperature and concentration. The SDS micelles have a diameter = 5 [nm] **[16]**. The macroscopic observations with cross-polarized light and the results of Cryo-TEM experiments can be connected. The large, threadlike nanostructures that were observed using Cryo–TEM could correspond to an intermediate, birefringent, liquid crystal aggregate that had been observed with the macroscopic observations with cross-polarized light. These intermediate liquid crystals have been formed, possibly because of two reasons. First, due to the large heating rate that was used (>0.2 [°C/min]) and also, due to the fact that the sample preparation temperature very close to the Krafft temperature of the CsDS/water system.

4. The dried byproduct diffractograms of the unheated purified CsDS crystal exhibit similarities with the diffractogram of the pure SDS in their $2 \cdot \theta$ values, in the diffraction angle regime that the CsDS sample was examined (between 0° and 30°) **[96]**.

For the same diffraction angle regime that the CsDS samples were examined (between 0° and 30°), the thermally treated CsDS samples have almost identical $2 \cdot \theta$ values in their

diffractograms. Moreover, their diffraction angle values are also very similar with the unheated pure CsDS crystal (which was also a dried byproduct). These diffraction angle similarities and the explanation of Ostwald ripening can justify the fact that the superheated and supercooled samples do not represent some type of metastable state, as was initially assumed based on their different macroscopic observation **[88]**. Ostwald ripening can describe the change in the macroscopic appearance of the superheated and supercooled samples and their reverse to the final state, a final state which macroscopically looks the same with the initial state. After long time (several weeks), whether by self–reverse, or by solvent or solute perturbation, the small crystals will coalesce into a larger crystal. This larger crystal has a smaller surface-to-volume ratio. By this solid crystal growth process, the surface energy of the system is reduced **[88]**. The thermally treated samples must probably represent the same thermodynamic state with the unheated sample. The reason for the different macroscopic appearance between the thermally treated (heated, superheated and supercooled) and the unheated samples, is the different degree of dispersion of solid crystal in water, because of larger heating and cooling rates. The cooling and heating rates for the superheated and the supercooled samples must have been large enough, so that the solid crystals have nucleated rapidly, when the samples were cooled. A faster nucleation is related with a smaller crystal size **[108]**.

For the thermally treated samples, well-defined Debye rings have formed because of smaller crystal size and/or larger concentration of CsDS in these samples, compared to the unheated samples. The unheated samples have more weakly-defined Debye rings, compared to the thermally treated samples. These weakly–defined Debye rings correspond to a smaller number of larger crystals (that diffract less) and/or smaller concentration of CsDS in the solution. The size of the crystals in the unheated samples is such, that the powder limit size for some of the crystals is not achieved **[75]**.

CHAPTER 7

ONGOING WORK AND FUTURE PERSPECTIVES

7.1. Preface

This chapter includes a discussion about experiments that have been included in the thesis at the very end. Specifically the reasons behind the lack of success for some experiments, as well as certain ways to avoid the experienced problems in the future, are provided. Some ideas are suggested to improve the reliability of these experiments (that did not work), as well as new ideas for all the experiments that have taken place. The purpose is to provide suggestions to interested experimentalists, in order to interpret the CsDS/water phase behavior as better as possible.

.

7.2. SAXS experiments

The experimental design of the sample preparation and the run were not good enough to provide a representative scattering diagram that would be the basis to interpret the mesophase that appears at 32 wt % CsDS concentration. The experiment, however, should be repeated in the future, as part of a research attempt to identify the liquid crystal structures of the CsDS/water system at intermediate concentrations (CsDS concentrations higher than 30 wt % in an aqueous solution). Some limiting factors are presented:

1. Improper sealing

Solvent evaporation from the capillary might have occurred, because of improper sealing of the capillary tube (with Teflon tape). A stronger insulator should be used, such as wax or some glue (like epoxy), that would prevent water evaporation. The heating of an improperly sealed capillary tube from T = 25 [ºC] to T = 45 [ºC], might have resulted in water evaporation. This possible evaporation might have influenced the status of the sample.

2. Sample inhomogeneity and temperature gradients

Starting at T = 25[ºC] in a capillary tube of 80 [mm] length, the sample was a two-phase system at first. The surfactant suspension was not uniformly distributed inside the capillary, but there were two distinct phases, a discreet aqueous (above) and another one

solid crystal–like (below).

Since the scattering involved heating to a temperature higher than T = 25[ºC], this heterogeneity of the system is a reason why any scattering data are considered not representative. In a future experiment, the sample should have reached the bottom of the capillary (<20 [mm]). The bottom is in contact with a copper compartment, which provides enough heat transfer to the sample. That would ensure that the temperature on the sample has reached 45 [ºC]. The upper part of the capillary is not in contact with this metallic part, so a temperature gradient would be expected.

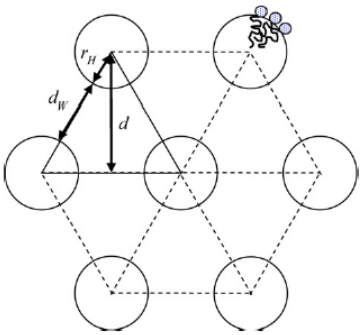

Fig.7.1. Typical hexagonal pattern with certain interstructural spacing, reported by Sakamoto K. et al. **[109]**. The Figure has been reproduced with permission that has been granted from the Copyright Clearance Center Inc. (See Appendix G for permission).

The 1st step in the attempt to identify the liquid crystal type at 32 wt % CsDS is to use available data for the SDS/water system. Data from X-ray Diffraction experiments at temperatures between 24 and 30 [ºC] for the SDS/water system at 48 wt % SDS concentration, reported by Kekicheff et al. showed that the system lies is the periodic spacing for a hexagonal phase, H_α **[3].** As far as the order of the nanostructures is concerned, the next more ordered nanostructure for the surfactant system in terms of increased packing of surfactant molecules after the micelles, is the hexagonal phase H_α.

The experiments should be repeated in order to prove that in the concentrations region between 30 wt % and 40 wt % CsDS and at T > 35 [°C], the liquid crystal phase that appears first, is the hexagonal phase. Another idea would be to run more experiments (isothermal

and/or isoplethal), in order to fully identify all the liquid crystal phases that appear in this intermediate concentration region. Scanning electron microscopy could be also used. Finally, it might be of use to check for the effect of impurities in the CsDS/water phase behavior in that concentration region, by comparing the purified CsDS and the impure CsDS phase behavior in aqueous solutions (see 2.2.1.2).

7.3. Optical microscope

The optical microscope experiments were not successful in the attempt to identify the presence of birefringent liquid crystals, as well as to double-check the Krafft temperatures found by the macroscopic observation with cross-polarized light. It is considered necessary that these experiments be repeated.

The images presented in Figures 4.17. and 4.18. were captured without the use of cross-polarized filters. No indication of anisotropic liquid crystal structure was observed, such as mosaic patterns, fan-like textures, Schlieren textures and birefringence **[42]**, **[84]**. This means that the structures presented by the Figures 4.17 and 4.18 cannot be birefringent liquid crystals. A birefringent liquid (or solid) crystal would not disappear in the cross-polarized light. Only the cubic phase that is an isotropic liquid crystal phase, however, is not birefringent and could disappear when observed using cross–polarized light **[42]**. Moreover, the crystals in Figures 4.17 and 4.18 exhibit sharp edges. Liquid crystals do not have sharp edges. Therefore, these reflections captured by the camera should have been formed by the interaction of the light beam with the edge of the surface of the solid crystals. Some limiting factors, which at the same time are reasons of why these experiments should be repeated, are indicated below:

- Accidental movement of the fiber optic tube that shines light onto the sample. This happened several times. To ensure higher reproducibility, the light source has to be mounted at a fixed position, in order to shine light from a fixed incident angle.
- Inhomogeneity in the dispersion of solid crystals in water. There was difficulty in

the production of a homogeneous dispersion of solid crystals in water in the indentations. In the case of a homogeneous dispersion, the incident light beam would scatter uniformly through the sample and any image taken from that certain indentation would be representative, for the given concentration. During the sample preparation of these experiments, the solid crystals were ground manually. This grinding process, however, cannot guarantee that the solid crystals have satisfied the powder limit (powder limit for a particle size: 0.8 [μm] - 75[μm] **[75]**). There was an observable, small (but not negligible) profile variation on the surface of the samples within the indentations. This could result in temperature gradients within the indentation. Smaller crystals that were closer to the surface only, had a more uniform temperature.

In that case, any images captured from the sample would not be representative, because of the inhomogeneity of the material, due to non - uniform crystal dispersion. The temperature measured by the thermocouple would be more representative for a measurement of a sample with finer crystal dispersion than from a sample with a coarser one. The captured images, however, were taken mostly from very small crystals, as close to the surface as possible. A future study should examine a more appropriate way of inserting the samples in the indentations, in order to increase quantitative interpretation.

- Possible water evaporation from the thin water film of the sample. When the samples had been prepared, overflow of water happened and droplets spread out, along multiple sample indentations. This made it difficult to visualize the samples. Therefore, during the same experiment, the glass slide that was covering the indentation with the samples was changed. During the time of that exchange, some water that might had spread onto the glass slide could have escaped, due to evaporation (the higher the temperature difference between the top of the sample and the environment (T_∞ - T_S), the higher the evaporation rate of water towards the environment). It was not possible to quantitatively assess the mass of water that had escaped. Again, a future study should examine how to seal the indentations properly, after the suspension has been inserted in the indentations.

These experiments should be repeated, in order to develop a method to observe phase

transitions from multiple samples at different concentration regions, simultaneously. It would be useful to record videos from the small CCD camera attached to the Hyrox microscope, in order to deduce conclusion about the time that phase transitions need to take place.

7.4. X–ray Diffraction experiments

Despite the fact that the diffractograms represent dried byproduct, the X-ray Diffraction experiments were valuable in terms of providing evidence in order to check if the thermally treated samples represent metastable states or not (as they appeared macroscopically different than the unheated samples). The $2\cdot\theta$ values between the diffractograms of all five CsDS samples were similar. This similarity between the thermally treated and untreated samples indicates that the thermally treated samples do not represent some metastable states. Moreover, the similarities in the $2\cdot\theta$ values between the diffractogram of the CsDS dried byproduct (Fig.4.12.) with the SDS diffractogram (see Fig. 5.12.) in the angle regime between 0° and 30° suggests that the crystals of the two surfactants may also have similarities in their unit cell crystal structure **[96]**.The X-ray diffraction experiments should be better designed, in order to strengthen the comparison between thermally treated and untreated CsDS samples, as well as between the CsDS and SDS crystals. More samples should be examined over a wider $2\cdot\theta$ range, than the range that was used for these experiments (0° - 30°). That would involve amelioration in the sample preparation method, especially in the transfer of the samples into the diffractometer chamber. The samples should be prepared in the same glass Pyrex® tubes and a different spatula should be used. Alternately, the samples might be prepared in glass capillary tubes that would consecutively be inserted in the diffractometer chamber. A smaller tube – maybe a capillary - might increase sample homogeneity and might be a way to avoid the spatula. The reproducibility of these measurements is very important to consider, for a future experiment.

All these ideas mentioned above would help to receive a representative diffractogram for CsDS in the future. One way to identify the XRD pattern of CsDS, is to compare the

CsDS diffractogram with already saved diffractograms of known materials (see Software Jade at the Characterization Facility of the University of Minnesota). It might be also helpful to compare the diffractogram extracted by the XRD experiments with a molecular simulation of the crystal structure of CsDS. A last idea would involve combining several XRD experiments with molecular simulations in the concentration region 0 wt %-100 wt % CsDS at various temperatures, in order to identify what –and how many- types of different crystalline polymorphs are formed in the CsDS/water system.

7.5. Macroscopic observations

More experiments should take place, in order to investigate the exact concentration boundaries for the 2 phase region of micelles coexisting with liquid crystals. It should also be verified if the transition temperature from solid crystals and micelles to some liquid crystal and micellar phase indeed exhibits a slight increase, for CsDS concentrations higher than 30 wt %.

Another idea would involve to examine if the intermediate liquid crystals that were observed using large heating rates (larger than 0.2[ºC/min]) in the concentration region 1 wt % - 30 wt % CsDS, can be related with some theory regarding the effect of alkali metal counterion upon binding with the sulfate surfactants. The study should focus on the time for a phase transition, for a given order parameter (same molar concentration), same order parameter for both Cs^+ and Na^+ systems.

7.6. Impurities in SDS and their effect in the CsDS/water phase behavior

As mentioned in 2.2.1.2. and 2.2.1.3, the reagent SDS, that was received by Sigma –Aldrich, was 98.5 wt % pure (according to gas chromatography analysis). The X–ray diffractograms have been a first step in order to investigate the presence of the impurities. It was not possible, however, to deduce qualitative conclusions about the presence of

impurities in the CsDS, by the X–ray diffractograms.

7.6.1. Organic impurities

The reason why SDS was recrystallized twice in ethanol (see 2.2.1.2.), was to remove possible organic impurities; most likely dodecanol **[2]**, **[52]**. As mentioned before and as far as the impurity effect on the phase behavior of the CsDS/water system is concerned, the experiments of this thesis have taken into account information by relative studies on the SDS / water system, regarding the effect of organic cosolvents in the micellar behavior of the SDS/ water system **[92]**,**[99]**, **[100]**, **[101]**, **[103]** – **[50]**,**[58]**.The amount of organic impurity present in SDS, should be identified by some instrumental technique (i.e. Gas Chromatography coupled with Mass Spectrometry).

7.6.2. Inorganic impurities

To connect with the description of chapter 5 regarding inorganic impurities for the SDS, it is assumed that these inorganic impurities are removed by dissolution in deionized water, during the process of aqueous recrystallization to synthesize CsDS (see 2.2.1.2.). The X-ray Diffraction pattern of the pure CsDS crystal, however, suggests that there might be presence of NaCl or SDS in the examined CsDS crystal, as the materials have peaks at similar $2 \cdot \theta$ values **[96]**, **[97]**.

A next step should involve the examination of all possible impurities in SDS, qualitatively and quantitatively. Some techniques that can be used are referred in table 7.1.

Table 7.1. Instrumental methods used for analysis of the impurity in the sample

Gas Chromatography	Qualitative assessment of the organic impurities
Gas Chromatography with Mass Spectrometry	Qualitative and quantitative assessment of the organic impurities
Spectroscopy (IR, Raman)	Quantitative and qualitative identification of solid state composition
X-ray Diffraction analysis	Identification of solid state structure
Inductive Coupled Plasma	Qualitative and quantitative assessment of the inorganic species
Inductive Coupled Plasma with Mass Spectrometry	Identification and quantification of inorganics-(cation concentration with ICP) and organics-mass spectrometry

Having identified these impurities, the next step would involve:

1. To repeat steps 2.2.1.2. and 2.2.1.3 - ethanolic recrystallization of SDS for the purification of SDS and aqueous recrystallization of SDS in a CsCl solution for the synthesis of CsDS, respectively, in order to make sure that the retrieved CsDS does not contain any significant amount of impurities.

2. To compare the phase behavior of the CsDS/water system between the purified and the impure CsDS.

7.7. CsDS micellar nanostructures at 0.34 [M] concentration and comparison with existing studies

In order to compare the shape and size of the CsDS micellar nanostructures with the findings of relative studies (**[53]**, **[54]**), the following protocol should be followed:

1. Synthesis of CsDS by ion exchange, using a continuous ion exchange column (as

described in **[53]**). The protocol for producing CsDS crystals by the continuous ion exchange experiment (see Figure 2.1.) is the following:

a. The resin is rinsed with deionized water initially (water as feed, in Tank 2)

b. A 5 wt % SDS solution is passed through the column, to rinse again (10') (solution is pumped from Tank 2).

c. An HCl 0.779 [M] solution is passed through the column to activate the resin into the H^+-form (30') (solution is pumped from Tank 2).

d. The resin is rinsed again with deionized water (45') (water is pumped from Tank 2).

e. A CsOH 0.779 [M] solution is passed through the column to neutralize the bed. (30') (solution is pumped from Tank 2).

f. The resin is rinsed with deionized water, until the base is removed. (45') (water is pumped from Tank 2).

g. A 5 wt % SDS solution is passed through the resin (10') (solution is pumped from Tank 2).

h. The solution is vacuum filtered at 0 [ºC] to receive the pure CsDS crystals.

i. The purified CsDS crystals are stored in the desiccator for several days.

2. A next set of experiments using Cryo–TEM should take place, in order to observe the nanostructures formed in the micellar region. In that set, the heating rate of the samples from T = 25 [ºC] to the VITROBOT temperature (a temperature higher than the Krafft temperature of the system) should be as low as possible (lower than 0.2 [ºC/min]), so that the chances that the system approaches thermodynamic equilibrium are maximized. It is necessary to use these heating rates to observe the representative nanostructures – and not some intermediate liquid crystal nanostructures - for the CsDS/water system at that concentration and VITROBOT parameters.

BIBLIOGRAPHY

[1] Fontell, K., 1981. 'Liquid crystallinity in lipid-water systems'. Molecular Crystals and Liquid Crystals Vol. 63, 59.

[2] Kekicheff, P., Grabielle – Madelmont, C., Ollivon, M., 1987. 'Phase Diagram of SDS- A Calorimetric study'. Journal of Colloid and Interface Science 131, 112 - 132.

[3] Kekicheff, P., 1989. 'Complementary Isoplethal and Isothermal Phase Studies- Phase Diagram of Sodium Dodecyl Sulphate/Water System'. Journal of Colloid and Interface Science 131, 14 - 28.

[4] Jonsson, B., Wennerstrom, H.J., 1981. 'Thermodynamics of ionic amphiphile/water systems', Journal of Colloid and Interface Science 80, 482 - 496

[5] Wilhelm Norde, 2005. 'Colloids and Interfaces in Life Sciences', Marcel Dekker Incorporation, New York, p.5.

[6] Peter Kelley Kilpatrick, 1983. 'Phase behavior, thermodynamic modeling and fluid microstructure in amphiphile-oil-water mixtures', PhD Thesis, University of Minnesota.

[7] Paul C. Hiemenz, Raj Rajagopalan, 1997. 'Principles of colloid and surface chemistry', CRC, Taylor & Francis Group, 3rd edition, p.1

[8] Mukerjee, P., 1967. 'The nature of the association equilibria and hydrophobic bonding in aqueous solutions of association colloids'. Advances in Colloid and Interface Science, Elsevier Publishing Company, Amsterdam, Vol. 1, 241 - 275.

[9] Zuchen Lin, 1993. 'Microstructure and Phase behavior of surfactants in aqueous solution', PhD Thesis, University of Minnesota.

[10] Rieger, M.M., Rhein, L.D., 1997. “Surfactants in Cosmetics”, 1997, Marcel Dekker, 2nd Edition

[11] Sinko, P. J., Martin, A.N., 2006. ‘Martin's physical pharmacy and pharmaceutical sciences’. Lippincott Williams and Wilkins, 5th Edition, p.494.

[12] Malmsten, M., 2002. ‘Surfactants and polymers in drug delivery’. Marcel Dekker Incorporation, Vol. 122, p.80.

[13] American Water Works Association, 2005. ‘Microfiltration and Ultra-filtration membranes for drinking water”’, Glacier Publishing Services, 1st Edition, p.175.

[14] Schwarz, J.A., Contescu, C.I., Putyera, K.I., 2004. ‘Dekker encyclopedia of nanoscience and nanotechnology’, Marcel Dekker Incorporation, Vol. 3rd, p.1833.

[15] Tadros, T.F., 2005. ‘Applied Surfactants: Principles & Applications’, Wiley VCH – Verlag GmbH & Co., Weinheim, Germany, 1st Edition, p.2.

[16] Vagias A.N., Arunagirinathan M.A., Davis, H.T., Mc Cormick, A., Bellare J.R. ‘Cryo-TEM of surfactant nanostructures in aqueous solutions’, I-PRIME, Minneapolis, University of Minnesota, May 2009.

[17] http://pubchem.ncbi.nlm.nih.gov/summary/summary.cgi?cid=5974

[18] Holmberg, K., Jonsson, B., Kronberg, B., Lindman, B., 2003. ‘Surfactants and Polymers in aqueous solutions’, John Wiley & Sons Ltd., West Sussex, England, 2nd Edition, p.22.

[19] Kalfayan, L, 2001. ‘Product enhancement with acid stimulation’, Penn Well Corporation, Tulsa, Oklahoma, 2nd Edition, p.242.

[20] Makievski, A.V., Grigoriev, D.O., 1998. ‘Adsorption of alkyl dimethyl phosphine oxides at the solution/air interface’. Colloids and Surfaces A: Physicochemical and Engineering Aspects, Vol. 143, 233 – 242.

[21] http://en.wikipedia.org/wiki/Sodium_lauryl_sulfate

[22] Erh – Lin C., Chen M.-J., Huang H.-C., Chen H.-W., 2001. ‘Capillary electrophoresis study on the micellization and critical micelle concentration of sodium dodecyl sulfate: Influence of solubilized solutes’. Journal of Chromatography A 924, 83 - 91.

[23] Lin, B., McCormick, A., Davis, H.T., Strey, R., 2005, ‘Solubility of sodium soaps in aqueous solutions’. Journal of Colloid and Interface Science, Vol.291, p.543 -549

[24] Laughlin R.G., 1994, ‘The aqueous phase behavior of surfactants’. Academic Press, San Diego

[25] Milton J. Rosen, 2004. ‘Surfactants and interfacial phenomena”, Wiley Inter Science, New Jersey, 3rd Edition, p.106.

[26] Candau, F., Ottewill, R. H., 1990. ‘Scientific methods for the study of polymer colloids and their applications’. Kluwer Academic Publishers, Dordrecht, The Netherlands, p.18.

[27] Hiemenz, P. C., Rajagopalan, R., 1997. ‘Principles of colloid and surface chemistry’, Taylor & Francis Group, 3rd edition, CRC, p. 357 - 359.

[28] Shah, S.S., Jamroz, N.U., Sharif, Q.M., 2001. ‘Micellization parameters and electrostatic interactions in micellar solution of sodium dodecyl sulfate (SDS) at different temperatures’. Colloids and Surfaces A: Physicochemical and Engineering Aspects 178, 199 –206.

[29] Hiemenz, P. C., Rajagopalan, R., 1997. 'Principles of colloid and surface chemistry', CRC, Taylor & Francis Group, 3rd edition, p.537.

[30] Linder, B., 2004. 'Thermodynamics and introductory statistical mechanics'. Wiley Inter Science, p.119.

[31] http://www.bio.brandeis.edu/classes/biochem104/hydrophobic_effect.pdf

[32] Alberts, B., 1989. 'Molecular Biology of the Cell'. Garland Publishing Incorporation, 2nd Edition, Vol. 1, p.91.

[33] Evans D. F., Yamauchi A., Roman R., Casassa E. Z., 1982. J. Colloid Interface Science 88, 89 - 96.

[34] Evans D. F., Yamauchi A., Wei G. J., Bloomfield V. A., 1983. Journal of Physical Chemistry 87, 3537 - 3541.

[35] Sagui, C., Desai, R.C., 1995. Phys. Rev. Lett. 74, 1119.

[36] Aniansson, E.A.G., Wall S., 1974. 'On the kinetics of step-wise micelle association'. J. Phys. Chem. 78, 1024.

[37] Lang J., Zana R., In Surfactant Solutions. New Methods of Investigation; Zana R., Ed., New York, 1987, M. Dekker Inc. Edition.

[38] Rosevear, F. B., 1954. J. Am. Oil Chem. Soc. 31, 628 - 638.

[39] Tardieu, A., Luzzati, V., Reman, F.C., 1973. ‘Structure and Polymorphism of the Hydrocarbon Chains of Lipids: A Study of Lecithin-Water Phases’, 1973. J. Mol. Biol. 75, 711 - 733.

[40] Stegemeyer, H., 1994. ‘Liquid Crystals’. Deutscher Bundes-Gesellschaft fuer Physikalische Chemie, Dr. Dietrich Steinkopff Verlag GmbH & Co. KG, Darmstadt, Germany, p.3.

[41] Ranck, J. L., Mateu, L., Sadler, D. M., Tardieu, A., Gulik-Krzywicki, T., Vittorio Luzzati, 1974. ‘Order-disorder conformational transitions of the hydrocarbon chains of lipids’. Journal of Molecular Biology 85, 249 - 260.

[42] Stegemeyer, H., 1994. ‘Liquid Crystals’. Deutscher Bundes-Gesellschaft fuer Physikalische Chemie, Dr. Dietrich Steinkopff Verlag GmbH & Co. KG, Darmstadt, p.157 - 159.

[43] Wang, H., Zhang, G., Du, Z., Li, Q., Wang, W., Liu, D., Zhang, X., 2006. ‘Effect of temperature on dynamic rheological behavior of discontinuous cubic liquid crystal’. Journal of Colloid and Interface Science, Vol. 300, 348 – 353.

[44] Yao, H., Hatta, I. Koynova, R. Tenchov, B., 1992. ‘Time-resolved x-ray diffraction and calorimetric studies at low scan rates -II. On the fine structure of the phase transitions in hydrated dipalmitoylphosphatidylethanolamine’. Biophysics, Journal of Biophysical Society 61, 683 - 693.

[45] Israelachvili, J. N., 1992. ‘Intermolecular and surface forces’. Academic Press London, 2nd edition.

[46] Stølen, S., Grande, T., 2004. ‘Chemical thermodynamics of materials: macroscopic and microscopic aspects’. John Wiley &Sons Ltd., West Sussex, England, p.29 - 37

[47] Lavis, D.A., McDonald Bell, G., 1999. 'Statistical Mechanics of Lattice Systems: Exact, series, and renormalization group methods', 1999. Springer-Verlag, Berlin-Heidelberg, Vol. 2, p.15.

[48] Vinson, P.K., Bellare, J.R., Davis, H.T., Miller, W.G., Scriven, L.E., 1991. 'Direct imaging of surfactant micelles, vesicles, discs, and ripple phase structures by Cryo-transmission electron microscopy'. Journal of Colloid and Interface Science 142, 74 - 91.

[49] Stølen, S. Grande, T., 2004. 'Chemical thermodynamics of materials: macroscopic and microscopic aspects'. John Wiley &Sons Ltd., West Sussex, England, p.29 - 31.

[50] Bordes, R. Tropsch, J., Holmberg, K., 2009. 'Counterion specificity of surfactants based on dicarboxylic amino acids'. Journal of Colloid and Interface Science 338, 529 - 536

[51] http://chemistry.about.com/od/chemistryhowtoguide/ss/recrystallize.htm

[52] Muramatsu, M., Inoue, M., 1976. 'A radiotracer study on slow hydrolysis of sodium dodecylsulfate in aqueous solution'. Journal of Colloid and Interface Science 55, 80 - 84.

[53] Bales, B.L., Benrraou, M., Zana, R., 2002. 'Krafft Temperature and Micelle Ionization of Aqueous Solutions of Cesium Dodecyl Sulfate', J. Phys. Chem. B. 106, 9033 – 9035.

[54] Joshi, J.V., Aswal, V.K., Goyal, P.S., 2007. **'**Combined SANS and SAXS studies on alkali metal dodecyl sulphate micelles'. Journal of Physics: Condensed matter, 19, 196-219.

[55] Harland, C.E., 1994, 'Ion exchange: Theory and Practice, 2nd Edition, p.161.

[56] Vlachy, N., Arteaga, A.F., Klaus, A., Touraud, D., Drechsler, M., Kunz, W., 2009. 'Influence of additives and cation chain length on the kinetic stability of supersaturated catanionic systems'. Colloids and Surfaces A: Physicochemical Engineering Aspects 338, 135 –141.

[57] Hinrichs, R.L., Snoeyink, V.L., 1976. 'Sorption of benzenesulfonates by weak base anion exchange resins'. Water Research 10, 79 - 87.

[58] Rana, S., Dubuc, J., Bradley, M., White, P., 2000. 'The synthesis of the cyclic antibacterial peptide Kawaguchipeptin B on 11 different DVB cross-linked PS resins'. Tetrahedron Letters 41, 5135 - 5139.

[59] Sundararaj, U., Dori Y., Macosko, C.W., 1995. 'Sheet formation in immiscible polymer blends: model experiments on initial blend morphology'. Polymer 36, 1957 - 1968.

[60] Siril, P.F., Cross, H.E., Brown, D.R., 2008. 'New polystyrene sulfonic acid resin catalysts with enhanced acidic and catalytic properties'. Journal of Molecular Catalysis A: Chemical 279, 63 – 68.

[61] Grady, C.P.L., Daigger, G.T., Lim, H.C., 1999. 'Biological wastewater treatment'. Marcel Dekker Incorporation, 2nd Edition, p.134

[62] 'Amberlyst 15-wet Ion exchange Resin', Product Data Sheet, Rohm and Haas Company, July 2003.

[63] Wittrup, K.D., 2007. Course materials for 10.37 Chemical and Biological Reaction Engineering, Spring 2007, Massachusetts Open Course Ware [http;//ocw.mit.edu], MIT

[64] http://www.answers.com/topic/peristaltic-pump

[65] http://www.answers.com/topic/tygon-tubing

[66] Errede, L.A., 1992. 'Polymer swelling: 11. A molecular interpretation of association in polystyrene-liquid systems'. Polymer 33, 2168 - 2176.

[67] Mukerjee, P., 1967. Adv. Colloid Interface Sci., Vol. 1, p.24.

[68] Hafner, R., 2007. TEM Primer Characterization Facility, University of Minnesota.

[69] Hansen M.A., Slavin, S.E.M., 1993. 'Visualizing dispersion morphology via ultra-rapid freezing/transmission electron microscopy'. Progress in Organic Coatings 22, 201 - 210.

[70] Pickover, C.A., 2008. 'Archimedes to Hawking: laws of science and the great minds behind them'. Oxford Press, p.65.

[71] Putnis Andrew, "Introduction to mineral sciences", Cambridge University Press, Cambridge U.K., 1992, p.35

[72] Laszlo Solymar, D. J. Webb, A. Grunnet-Jepsen, "The physics and applications of photorefractive materials", Oxford University Press Incorporation, New York, 2002, p.274

[73] M. J. Katz *et al*., 2007, Angew. Chem. Int. Ed., **46**, 8804 (DOI: 10.1002/anie.200702885)

[74] http://www.microscopyu.com/articles/polarized/polarizedintro.html

[75] Alen, T., 'Powder Sampling and Particle size determination', Elsevier, 146.

[76] Cho, Y.I., Irvine, T.F. Bioengineering Heat Transfer, Vol. 22, 162.

[77] http://en.wikipedia.org/wiki/Properties_of_water

[78] http://en.wikipedia.org/wiki/Thermal_diffusivity

[79] http://www.charfac.umn.edu/InstDesc/microdifdesc.html

[80] Bramfitt, B.L., Benscoter, A.O., 2002. 'Metallographer's Guide: Practices and procedures for irons and steels'. ASM International, USA, 1st edition, p.258.

[81] Cullity, B.D. 'Elements of X-ray Diffraction', 2nd Edition, p.105.

[82] http://reference.iucr.org/dictionary/Bragg's_law

[83] Lipson, H., Tannhauser, D.S., 'Optical Physics', Cambridge University Press, UK, p.26.

[84] Figueiredo Neto, A.M., Salinas, S.R., 2005. 'The physics of lyotropic liquid crystals-Phase transitions and structural properties', Oxford Science Publications, Oxford University Press, p.45.

[85] Fewster, P.F., 2003. 'X-ray scattering from semiconductors', Imperial College Press, 2nd Edition, p.117.

[86] http://www.charfac.umn.edu/InstDesc/6mSAXSdesc.html#Equipment

[87] Schelly, Z.A., Chao, D.Y., Sumdani, G., 1979. 'Relaxation Amplitude of Non-Ionic Micelle systems perturbed by Solvent Jump', 1979. Solution Chemistry of Surfactants, Plenum Press Vol. 1, 323 - 335.

[88] http://en.wikipedia.org/wiki/Ostwald_ripening

[89] Ostwald, W.Z., 1901. Phys. Chem. 37, 385.

[90] Kahlweit M., 1981. Journal of Colloid and Interface Science 90, 92-99.

[91] Koleske, J.V., 1995. 'Paint and Coating Testing Manual: 14th edition of the Gardner-Sward'. American Society for Testing and Materials, p.872.

[92] Mc Nicoll, B., Sangster, J. Schreiber, H.P., 1979. 'Some observations on the micellar behavior of surfactants in water and aqueous systems'. Solution Chemistry of Surfactants, Plenum Press Vol. 1, 367 - 376.

[93] Schroedle, S., Buchner R., Kunz, W., 2004. 'Automated apparatus for the rapid determination of liquid–liquid and solid–liquid phase transitions'. Fluid Phase Equilibria 216, 175 –182.

[94] Gnanadurai, P., Soundararajan, N., Sooriamoorthi, C.E., 2005. 'Influence of heating rate on the hysteresis in the phase transition in silver selenide thin films'. Vacuum 78, 33 - 36.

[95] Hecht E., Hoffmann H., 1995. Colloids and Surfaces A: Physicochemical Engineering Aspects 96, 181.

[96] Smith, L.A., Hammond, R.B., Roberts, K.J., Machin, D., McLeod, G., 2000. 'Determination of the crystal structure of anhydrous sodium dodecyl sulphate using a combination of synchrotron radiation powder diffraction and molecular modeling techniques'. Journal of Molecular Structure 554, 173 - 182.

[97] http://www.uiowa.edu/~c004206/hand9.pdf

[98] Lipták, B.G. ‘Instrument Engineers' Handbook: Process measurement and analysis’, CRC Press, 4th edition, p.1343 - 1344.

[99] Meguro, K., Shoji, N., 1979. ‘Application of keto-enol tautomerism to the study of micellar property of surfactants’. Solution Chemistry of Surfactants, Plenum Press Vol. 1, 407 - 424.

[100] Tomlinson, E., Davis, S.S., Mukhayer, G.I., 1979. ‘Ionic interaction and phase stability’. Solution Chemistry of Surfactants, Plenum Press Vol. 1, 3 - 47.

[101] Farinato, R.S., Rowell, R. L., 1979. ‘Pre-Micellar Maximum in the Light Scattering from Cetyltrimethyl-ammonium bromide and chloride’. Solution Chemistry of Surfactants, Plenum Press Vol. 1, 311 - 322.

[102] Huang, J.B., Mao, M., Zhu, B.Y., 1999. ‘The surface physicochemical properties of surfactants in ethanol–water mixtures’. Colloids and Surfaces A: Physicochemical and Engineering Aspects 155, 339 – 348.

[103] Vlachy, N., Jagoda-Cwiklik, B., Vácha, R., Touraud, D., Jungwirth, P., Kunz, W., 2009. ‘Hofmeister series and specific interactions of charged head groups with aqueous ions’, Advances in Colloid and Interface Science 146, 42-.

[104] John C. Blackburn, J.C., Kilpatrick, P.K. 1992. ‘Lyotropic liquid crystalline phase behavior and structure of cesium n-tetradecanoate-water mixtures’. Journal of Colloid and Interface Science 149, 450 - 471.

[105] Myers, D., 2006. ‘Surfactant Science and Technology’, John Wiley and Sons, 2006, 3rd edition, p.168.

[106] Kim D.H., Oh S. G., Oh C.G., 2001, 'Effect of Cs^+ and Na^+ ions on the interfacial properties of dodecyl sulfate solutions' .Colloid Polym. Sci., Springer Verlag, 279, p.39 – 45

[107] Hiemenz, P. C., Rajagopalan, R., 1997. 'Principles of colloid and surface chemistry', CRC, Taylor & Francis Group, 1997, 3rd edition, p.15

[108] Ciobanu, A., Lasku, G., Bercescu, V., Nicolescu, L., 1976. 'Cooling technology in the food industry'. Abacus Press 1976, 1st edition, p.30.

[109] Yamashita, Y., Kunieda, H., Oshimura, E., Sakamoto, K., 2007. 'Formation of intermediate micellar phase between hexagonal and discontinuous cubic liquid crystals in brine/*N*-acylamino acid surfactant/*N*-acylamino acid oil system'. Journal of Colloid and Interface Science 312, 178-.

[110] 'Amberlyst 15 –Wet, Strongly Acidic Resin, Product Data Sheet'. Rohm and Haas, 2003.

[111] Taylor, J.R., 1982. 'An Introduction to Error Analysis: The Study of Uncertainties if Physical Measurements'. University Science Books.

[112] Capuzzi et al., 2000. 'Counter ion complexation by calixarene ligands in cesium and potassium dodecyl sulphate micelles. A small angle neutron scattering study'. Langmuir, 188-194

[113] http://en.wikipedia.org/wiki/Probit

[114] Hiemenz, P.C., Rajagopalan, R., 1997. 'Principles of colloid and surface chemistry', CRC, Taylor & Francis Group, 3rd edition, p.396.

APPENDIX A

SYNTHESIS RESULTS

A.1. Experimental method-Ion exchange

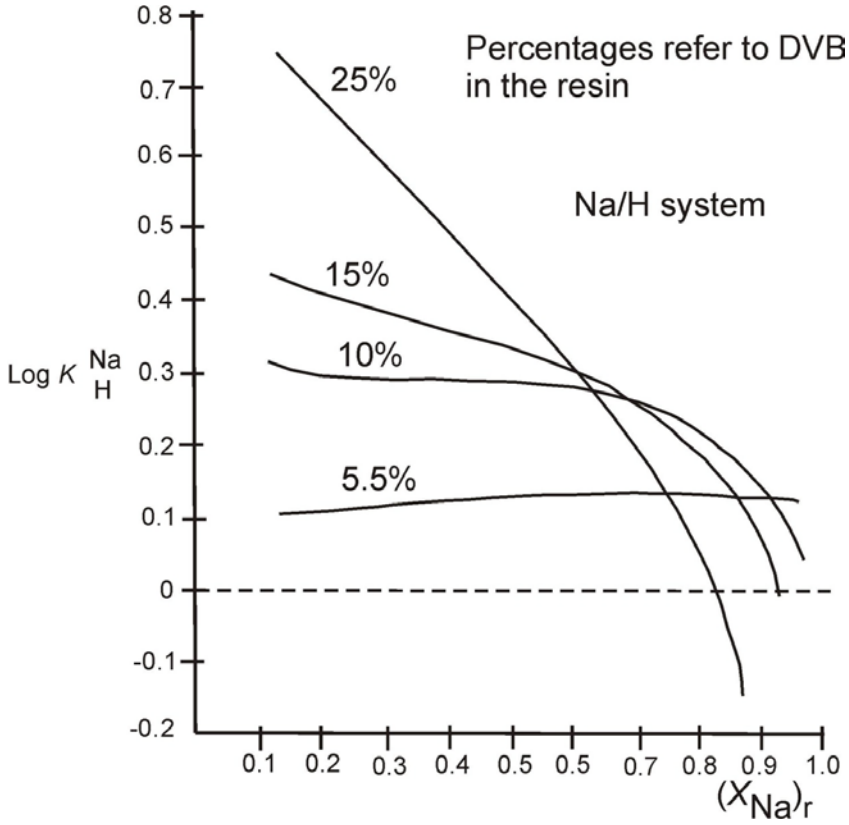

Fig.A.1. Ion exchange equilibrium constant K_H^{Na} vs. mole fraction of Na^+ in the resin for different divinylbenzene crosslinkage degrees, reported by Harland C. E. **[55]**. Figure A.1. has been reproduced with permission that has been granted from the Copyright Clearance Center Inc (See Appendix G for permission).

.

Figure A.1. depicts the relation between ion exchange equilibria constant versus the mole fraction of Na^+ on the resin, for different degrees of crosslinkage of divinylbenzene on the resin matrix. A typical composition of a resin is a polystyrene chain network (matrix) with cross-linked regions, as well as with regions of available cations (for a cationic resin, the cations would be H^+) **[110]**.

A.2. Rotameter calibration

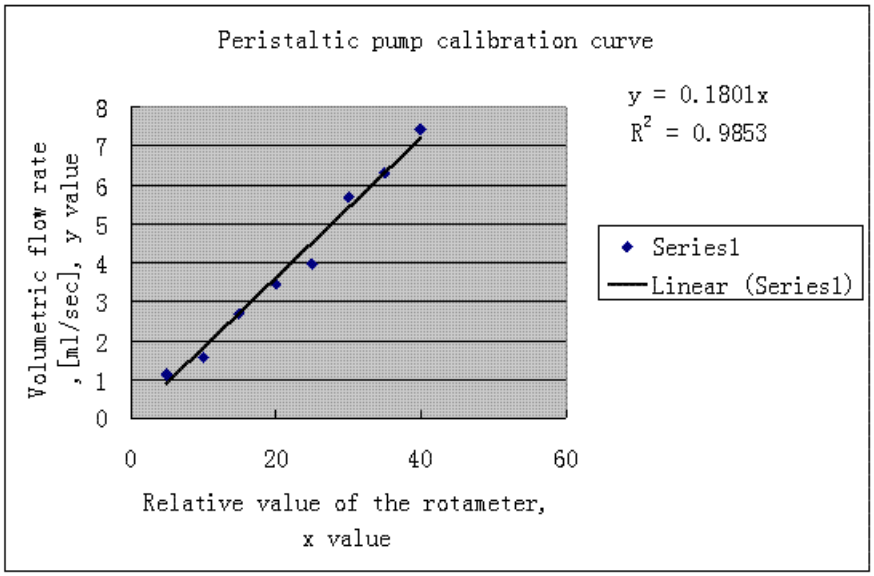

Fig.A.2. Rotameter calibration at T = 25 [ºC].

The flow rate vs. the indication of the rotameter values showed a good linear correlation. A first run was performed to investigate the resin properties for the ion exchange of a different solution (NaCl of 0.19 [M]). Sodium Chloride (NaCl) is cheap and easily available in the lab. It was assumed that the breakthrough curves that were received for the aqueous solution of NaCl 0.19 [M], would be the same for an SDS 0.19 [M] aqueous solution (as both solutions have the same cation; Na^+).

The method was the following:

a. The resin was rinsed with deionized water.

b. The resin bed was activated by passing HCl 0.779 [M] solution for 30'.

c. The bed was rinsed by passing deionized water for 45'.

d. The solution for ion exchange is passed through (NaCl 0.19 [M]) for 10'.

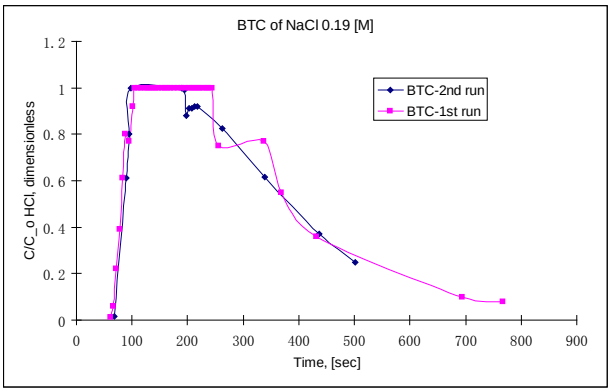

Fig.A.3. Breakthrough curves for a NaCl 0.19 [M] solution.

As was reported in chapter 2, the CsDS that was used for the phase behavior was synthesized by recrystallization.

The reason that this ion exchange experiment should be done in the future, however, is s to compare the micellar nanostructures of the CsDS/water system, following the same protocol with existing studies **[53]**, **[54]**. An experiment has provided the breakthrough curve for the $Na^{+} \rightarrow H^{+}$ exchange for a NaCl 0.19 [M] solution in the feed. This ion exchange experiment (Na^{+} to H^{+} ion exchange) has been a model study to interpret the ion exchange characteristics of the system. It is assumed that the ion exchange process of SDS to HDS, has the same breakthrough curve.

As can be seen in Figure A.3., the breakthrough curves of the 2 independent runs are in pretty good agreement with each other. The curves show a very steep increase as the operating window (100% ion exchange of Na^{+} to H^{+}) is approached. The temporal width of the operating window, is about 120 [sec] (time between 100 and 220 [sec]), followed by a smooth exponential decay. The breakthrough curve can be related with a strongly favored adsorption of Na^{+} on the resin (large K_{H}^{Na} equilibrium constant –see Figure A.1).

It is recommended that the synthesis of CsDS by the continuous ion exchange experiment should be incorporated in a future work. The corresponding protocol is described in Chapter 7.

A.3.Results

Recrystallization and ion exchange (considering only the 2 batch processes, fast and slow), were both equally successful in the production of pure CsDS, considering the Cs^+ content, Na^+ content, as well as the Cs^+/Na^+ ratio. The quantification has been done by ICP (Inductive coupled plasma elemental analysis) **[98]**. Plasma state (temperatures higher than 6000 [K]) is used to ionize all the metals and burn all the hydrocarbon molecules in the specimen, in order to produce carbon oxides and water **[98]**. The technique took place at the University of Minnesota at St. Paul, "Dept. of Soil, Water, and Climate, Soil Testing and Research Analytical Laboratory" **[98]**. Table A.1. shows the ICP results of the first analysis of samples, produced by both recrystallization, as well as ion exchange (two batch processes).

Table A.1. ICP Results of each process

Sample	Cs [ppm]	CsDS	Na	Cs/Na Ratio
Batch3 flasks, long experiment	333.110	995	3.557	93.6
Batch1 flask, fast experiment	316.360	944	11.655	27.1
Recrystallization	399.300	1193	3.125	127.8

All three methods have been efficient in producing pure CsDS, considering the Cs^+ concentration, Na^+ concentration and Cs^+/Na^+ ratio. The Na^+ content for the CsDS produced by recrystallization is slightly lower, compared to the ion exchange - batch processes. In all cases, however, the Na^+ content is at very low level compared to the Cs^+ (2 orders of magnitude lower). The recrystallization and the batch experiments are wet bench procedures. It is the first study that has been reported so far, to have produced cesium dodecyl sulfate using four independent methods of preparation (three in ion exchange and one in

recrystallization).

As Table A.2 indicates, the fastest process is the batch process with one flask (fast process) at 4 hours. Then, follows the recrystallization experiment. The slowest method is the batch process with 3 flasks (slow process). As mentioned in the chapters of the thesis, the continuous ion exchange setup has not been tested for the production of CsDS. Assuming, however, that the breakthrough curve for the exchange of Na^+ to Cs^+ is similar to an extent with the one for the exchange of Na^+ to H^+, the continuous method would be the fastest method among all in synthesizing CsDS, at about 3 hours.

Table A.2.Time for each process

Ion exchange-Continuous experiment	3 hours
Ion exchange-Batch-1 Flask, fast	4 hours
Ion exchange-Batch-3 Flasks, slow	56 hours
Recrystallization	8 hours

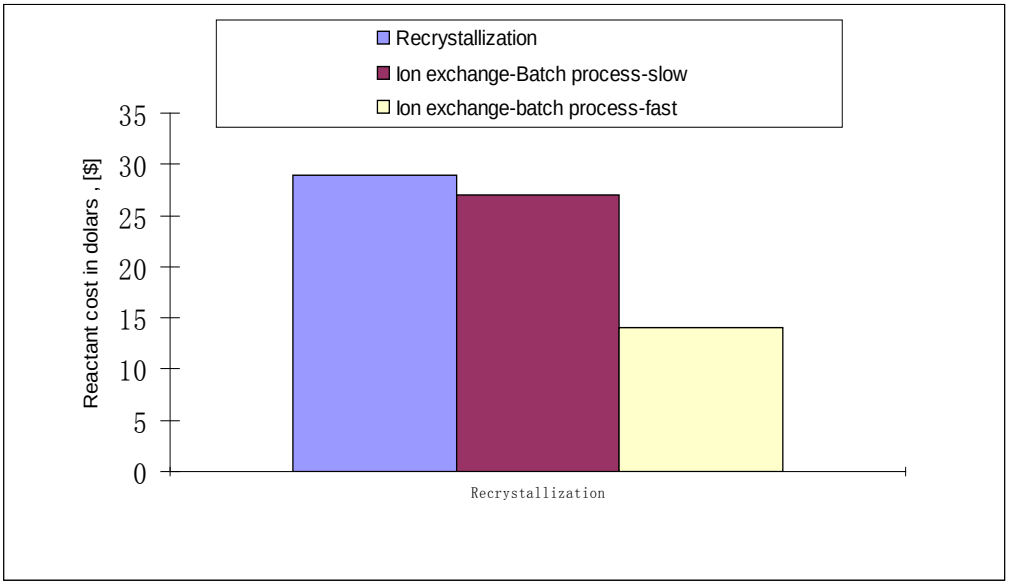

Fig.A.4. Reduced cost of CsDS produced.

.Figure A.4.shows the reduced cost per each method, expressed as cost of grams of each reagent used per gram of CsDS produced. Regarding the reagents, in the case of recrystallization involved the total cost of cesium chloride and sodium lauryl sulfate that have been used, whereas for the ion exchange, the reagents have been cesium hydroxide and sodium dodecyl sulfate. The recrystallization is more efficient process than the ion exchange (batch), as for roughly the same cost, it provides a larger yield of material. The cost for the synthesis of CsDS is provided, to compare with an estimate of a “5000 $ minimum order for CsDS in the market”, Davis (2009).

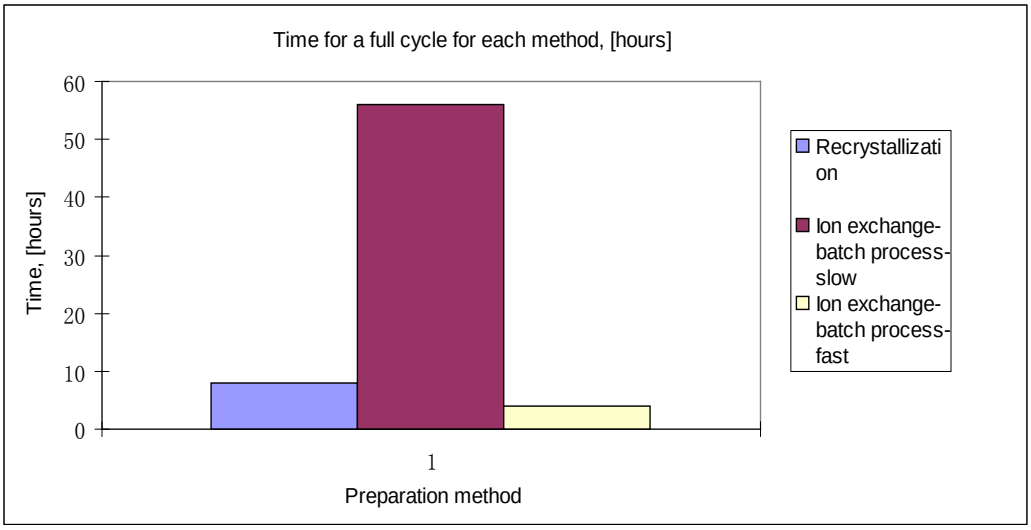

Fig.A.5. Time for every method in the production of CsDS

APPENDIX B

5 wt % - 55 wt % CsDS CONCENTRATION TABLE

Table B.1.Concentrations before and after seed insertion, 5-55 wt % CsDS, 2nd cycle

Perturbation by seed addition–solute jump, 560 % wt pure CsDS samples, 2nd cycle

	[g] crystals_after	[g] crystals_before	[g] CsDS_before	[g] CsDS_after	[g] water	conc_before	conc_after
5%	0.0210±0.000100	0.0185±0.000100	0.0207±0.000113	0.0221±0.000113	0.3863±0.0001000	0.0508±0.00246	0.05400±0.002456
5%	0.0209±0.000100	0.0199±0.000100	0.0225±0.000113	0.0236±0.000113	0.4294±0.0001000	0.0497±0.00222	0.05217±0.002213
5%	0.0274±0.000100	0.0264±0.000100	0.0298±0.000113	0.0309±0.000113	0.5762±0.0001000	0.0491±0.00165	0.05103±0.001651
10%	0.0145±0.000100	0.0135±0.000100	0.0152±0.000113	0.0163±0.000113	0.4236±0.0001000	0.0346±0.00228	0.03727±0.002276
10%	0.0190±0.000100	0.0180±0.000100	0.0203±0.000113	0.0214±0.000113	0.1806±0.0001000	0.1010±0.005027	0.1063±0.005004
10%	0.0215±0.000100	0.0205±0.000100	0.0231±0.000113	0.0243±0.000113	0.2893±0.0001000	0.0739±0.00321	0.0775±0.003208
15%	0.0273±0.000100	0.0263±0.000100	0.0297±0.000113	0.0308±0.000113	0.1704±0.0001000	0.1484±0.005106	0.1534±0.005084
15%	0.0156±0.000100	0.0146±0.000100	0.0167±0.000113	0.0176±0.000113	0.097±0.000100	0.1468±0.008983	0.1538±0.008927
25%	0.0263±0.000100	0.0253±0.000100	0.0286±0.000113	0.0298±0.000113	0.0856±0.000100	0.2505±0.009027	0.2578±0.009049
25%	0.0329±0.000100	0.0319±0.000100	0.0361±0.000113	0.0372±0.000113	0.1098±0.0001000	0.2473±0.007062	0.2531±0.007075
25%	0.0301±0.000100	0.0291±0.000100	0.0329±0.000113	0.0340±0.000113	0.0997±0.000100	0.2482±0.007700	0.2545±0.007785
30%	0.0214±0.000100	0.0204±0.000100	0.0230±0.000113	0.0242±0.000113	0.0533±0.000100	0.3021±0.01368	0.3122±0.01374
30%	0.0208±0.000100	0.0198±0.000100	0.0224±0.000113	0.0235±0.000113	0.0553±0.000100	0.2882±0.01340	0.2984±0.01344
30%	0.0289±0.000100	0.0279±0.000100	0.0316±0.000113	0.0327±0.000113	0.0713±0.000100	0.3068±0.01017	0.3143±0.01020
35%	0.0304±0.000100	0.0294±0.000100	0.0333±0.000113	0.0343±0.000113	0.0613±0.000100	0.3517±0.01121	0.3593±0.01125
35%	0.0225±0.000100	0.0215±0.000100	0.0243±0.000113	0.0254±0.000113	0.0448±0.000100	0.3518±0.01534	0.3622±0.01541
40%	0.0194±0.000100	0.0184±0.000100	0.0208±0.000113	0.0219±0.000113	0.0298±0.000100	0.4112±0.02137	0.4240±0.02153
40%	0.0186±0.000100	0.0176±0.000100	0.0199±0.000113	0.0210±0.000113	0.0283±0.000100	0.4129±0.02245	0.4264±0.02263
40%	0.0299±0.000100	0.0289±0.000100	0.0327±0.000113	0.0338±0.000113	0.0465±0.000100	0.4128±0.01366	0.4210±0.01373
45%	0.0157±0.000100	0.0147±0.000100	0.0167±0.000113	0.0178±0.000113	0.0204±0.000100	0.4501±0.01742	0.4659±0.01750
45%	0.0147±0.000100	0.0137±0.000100	0.0155±0.000113	0.0166±0.000113	0.0189±0.000100	0.4505±0.01881	0.4679±0.01889
45%	0.0112±0.000100	0.0103±0.000100	0.0116±0.000113	0.0126±0.000113	0.0138±0.000100	0.4566±0.02581	0.4786±0.02592
50%	0.00913±0.000100	0.00813±0.000100	0.00920±0.000113	0.0103±0.000113	0.0098±0.00010	0.4842±0.03652	0.5122±0.03649
50%	0.00469±0.000100	0.00459±0.000100	0.00520±0.000113	0.00530±0.000113	0.0066±0.00010	0.4406±0.05367	0.4455±0.05378
50%	0.0101±0.000100	0.00919±0.000100	0.0104±0.000113	0.0114±0.000113	0.0098±0.00010	0.5148±0.03647	0.5382±0.03625
55%	0.0963±0.000100	0.0106±0.000100	0.0109±0.000113	0.0120±0.000113	0.0095±0.00010	0.5343±0.03745	0.5587±0.03707
55%	0.0963±0.000100	0.0106±0.000100	0.0109±0.000113	0.0120±0.000113	0.0095±0.00010	0.5497±0.03410	0.5707±0.03363
55%	0.0121±0.000100	0.0111±0.000100	0.0126±0.000113	0.0136±0.000113	0.0104±0.000100	0.5478±0.03404	0.5681±0.03369

Table B.1. depicts the concentration, before and after the addition of a mass of seed in the samples. There is a deviation in concentrations of the order of ±2 wt % with respect to the desired concentration, before and after seed addition. These concentration changes are indeed perturbations in concentrations.

For the error analysis, the following operations have been used:

$$A=B+C,\ (\Delta A)^2=(\Delta B)^2+(\Delta C)^2$$

$$Z=B/A,\ (\Delta Z/Z)^2=(\Delta A/A)^2+(\Delta B/B)^2 \textbf{ [111]}$$

In our case, B= [Mass of CsDS, g]

A= [Mass of CsDS, g] + [Mass of Water, g] (Denominator)

Z= [Mass of CsDS, g]/A = [wt % CsDS Concentration]

APPENDIX C

5 wt % - 40 wt % IMPURE and PURIFIED CsDS/WATER CONCENTRATIONS & CERTAIN FIGURES

Impure CsDS/water phase behavior - Concentration region 5-20 wt % (2nd cycle)

Three independent samples were examined at each concentration and heated according to 2nd cycle heating (heating, cooling with seed addition, and heating again).The average of these samples at each concentration provided a candidate Krafft temperature, during the 1st heating. The same process was repeated for the 2nd heating process. The total average between the two heating processes was calculated. The standard deviation was measured with respect to the total average temperature for the set of 6 independent temperature values (3 during the 1st heating and 3 for the 2nd heating process). A certain reference for the ethanol recrystallization procedure is the study of Kapuzzi et al. [112]

Table C.1. Weighed concentrations for the impure samples in the region 5 wt % - 20 wt % CsDS

Perturbation by seed addition –solute jump 5-20% wt samples (impure), three samples

	[g] crystals_after	[g] crystals_before	[g] CsDS_before	[g]CsDS_after	[g] water	concentration_before	concentration_ after
5%	0.0162±0.000100	0.0152±0.000100	0.01662±0.0001131	0.01772±0.0001131	0.2848±0.000100	**0.05516±0.003762**	**0.05858±0.004018**
5%	0.0215±0.000100	0.0205±0.000100	0.02242±0.0001131	0.02352±0.0001131	0.3873±0.0001000	**0.05473±0.002764**	**0.05725±0.00311585**
5%	0.0119±0.000100	0.0109±0.000100	0.01193±0.0001131	0.01302±0.0001131	0.1988±0.000100	**0.05659±0.005382**	**0.06146±0.0055453515**
10%	0.0155±0.000100	0.0145±0.000100	0.01586±0.0001131	0.01695±0.0001131	0.133±0.000100	**0.1065±0.007680**	**0.1130±0.00768**
10%	0.0096±0.00010	0.0086±0.00010	0.0094±0.0001131	0.01050±0.0001131	0.0801±0.000100	**0.1051±0.01276**	**0.1159±0.01257**
10%	0.0174±0.000100	0.0164±0.000100	0.0179±0.0001131	0.01903±0.0001131	0.1417±0.000100	**0.1123±0.007171**	**0.1184±0.007189**
15%	0.00968±0.000100	0.00868±0.000100	0.00950±0.0001131	0.01059±0.0001131	0.0484±0.000100	**0.1640±0.02008**	**0.1795±0.01923**
15%	0.0121±0.000100	0.0111±0.000100	0.0122±0.0001131	0.01324±0.0001131	0.0631±0.000100	**0.1615±0.01544**	**0.1735±0.01489**
15%	0.01078±0.0001000	0.00978±0.000100	0.0107±0.0001131	0.01179±0.0001131	0.0554±0.000100	**0.1618±0.01758**	**0.1755±0.01690**
20%	0.0108±0.000100	0.0098±0.00010	0.0107±0.0001131	0.01181±0.0001131	0.039±0.000100	**0.2156±0.02398**	**0.2325±0.02230**
20%	0.0082±0.00010	0.0072±0.00010	0.0079±0.0001131	0.008971±0.0001131	0.0287±0.000100	**0.2154±0.03256**	**0.2381±0.03006**
20%	0.0106±0.000100	0.0096±0.00010	0.0105±0.0001131	0.01159±0.0001131	0.0352±0.000100	**0.2298±0.02631**	**0.2478±0.02421**

Table C.2. Weighed concentrations for the impure samples in the region 25 wt % - 40 wt % CsDS.

wt%	g crystals	g CsDS	g water	concentration
25%	0.0105±0.000100	0.01148±0.0001131	0.0856±0.000100	**0.2716±0.02824**
25%	0.0099±0.000100	0.01083±0.0001131	0.1098±0.0001000	**0.28215±0.03129**
25%	0.0096±0.000100	0.01050±0.0001131	0.0997±0.000100	**0.1411±0.01543**
30%	0.0113±0.000100	0.01236±0.0001131	0.0533±0.000100	**0.3247±0.03207**
30%	0.01±0.00010	0.01094±0.0001131	0.0553±0.000100	**0.2969±0.03274**
30%	0.0196±0.000100	0.02144±0.0001131	0.0713±0.000100	**0.3014±0.01698**
35%	0.0085±0.000100	0.009299±0.000 1131	0.0613±0.000100	**0.3780±0.05085**
35%	0.0095±0.000100	0.01039±0.0001131	0.0448±0.000100	**0.3752±0.04511**
35%	0.0092±0.0001000	0.01006±0.0001131	0.0298±0.000100	**0.3876±0.04840**
40%	0.0102±0.000100	0.01115±0.0001131	0.0283±0.000100	**0.4417±0.05115**
40%	0.0124±0.000100	0.01356±0.0001131	0.0352±0.000100	**0.4512±0.04319**

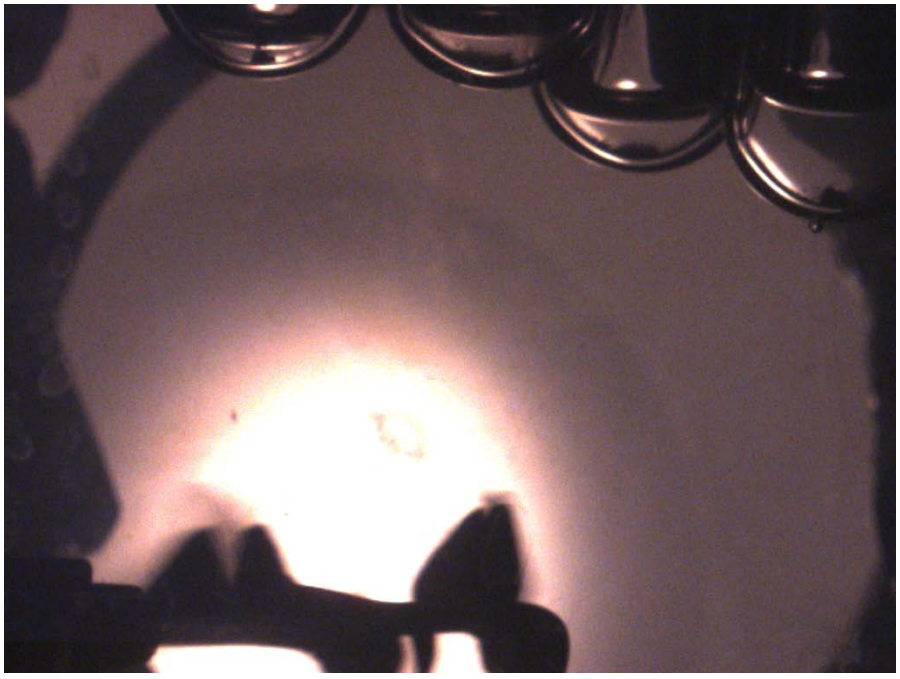

Fig.C.1. 5%, 10%, 15%, 20 wt % impure CsDS seeded, at T = 30.1 [ºC]. Heating started at T = 25 [ºC] with heating rate 0.2 [ºC/min]. No cross–polarization. *Size scale:* the tube diameter is 15[mm].

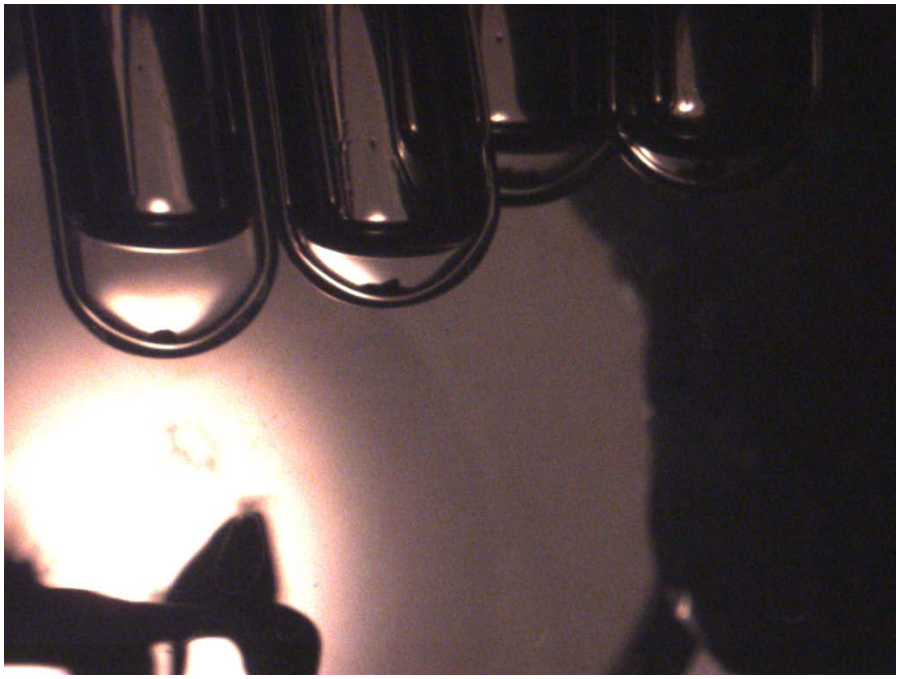

Fig.C.2. 5%, 10%, 15%, 20 wt % impure CsDS at T = 31.7 [ºC] (12') - 2nd heating cycle. Heating started at T = 25 [ºC] with heating rate 0.2 [ºC/min]. No cross–polarization. *Size scale: the t*ube diameter is 15[mm].

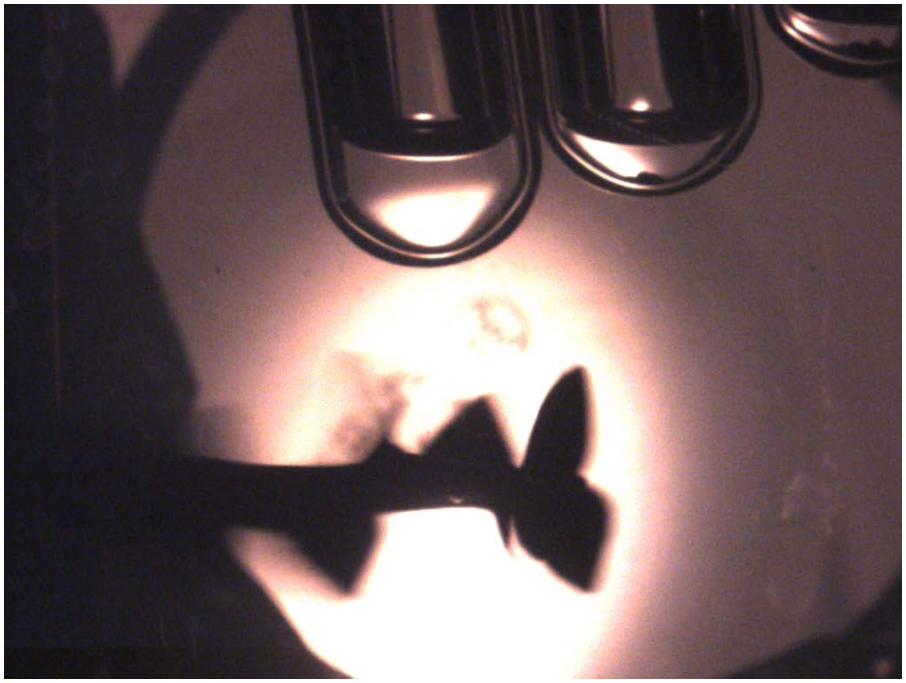

Fig.C.3. 5 wt % and 10 wt % impure CsDS at T = 32.1 [ºC] - seed is melting. Heating started at T = 25 [ºC] with heating rate 0.2 [ºC/min]. No cross–polarization. *Size scale: the t*ube diameter is 15[mm].

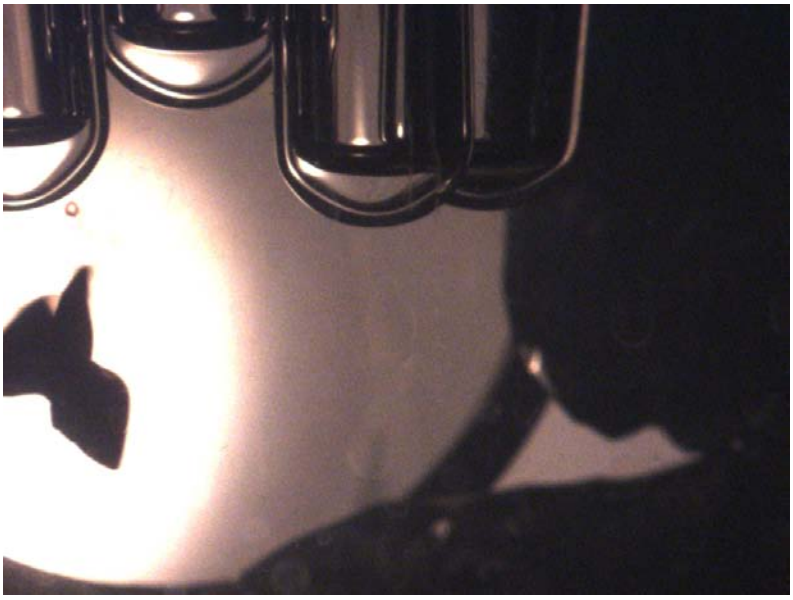

Fig.C.4. 5%, 10%, 15%, 20 wt % impure CsDS at T = 32.4 [ºC], (2nd from right) is a 15% CsDS micellar solution. Heating started at T = 25 [ºC] with heating rate 0.2 [ºC/min]. No cross–polarization. *Size scale: the t*ube diameter is 15[mm].

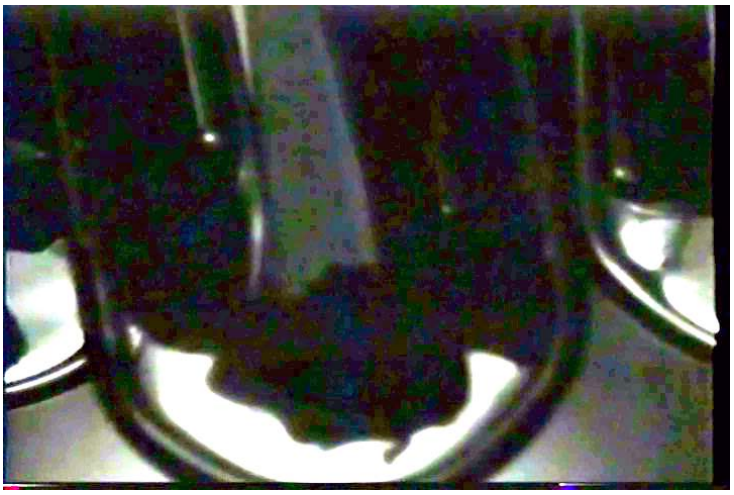

Fig.C.5. Liquid crystals in a 60 wt % purified (see 5.5, 7.6, 2.2.1.2 and 2.2.1.3) CsDS at T > 35 [ºC] - ongoing melting of solid crystals to liquid crystals. Heating started at T = 25 [ºC] with heating rate 0.2 [ºC/min]. Cross–polarized light was used. *Size scale: the t*ube diameter is 15[mm].

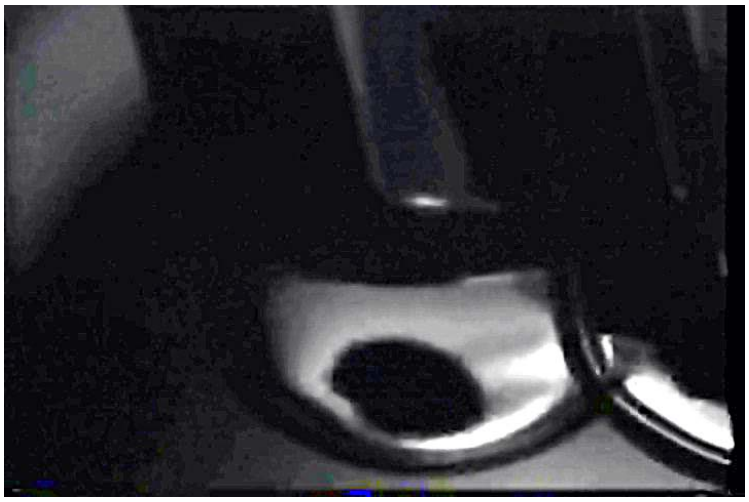

Fig.C.6. 45 wt % impure CsDS with ongoing transition from solid to liquid crystals at T > 35 [ºC]. Heating started at T = 25 [ºC] with heating rate 0.2 [ºC/min]. Cross–polarized light was used. *Size scale: the t*ube diameter is 15[mm].

Fig.C.7. Solid crystals (stable state) that have been created at T = 25 [ºC] by solute or solvent jump in a 10 wt % CsDS solution (see solvent jump in **[87]**, **[35]**, **[36]**, **[37]**, **[90])**. Figure captured at T = 25 [ºC]. No cross–polarized light was used. *Size scale: the t*ube diameter is 15[mm].

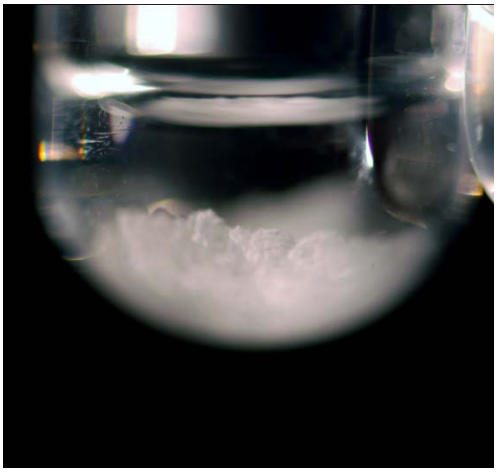

Fig.C.8. Solid crystals (stable state) created by solute or solvent jump in a 20 wt % purified CsDS solution after heating, at T = 25 [ºC] (see solvent jump in **[87]**, **[35]**, **[36]**, **[37]**, **[90])**. Figure captured at T = 25 [ºC]. No cross–polarized light was used. *Size scale: the t*ube diameter is 15[mm].

APPENDIX D

CsDS/WATER CONCENTRATIONS FOR THE EXPERIMENT OF INTERMEDIATE LIQUID CRYSTALS

Tables D.1 and D.2. depict the exact concentrations. At each concentration, 2 to 3 independent samples 3 were examined in the case of CsDS and 3 independent samples for the case of SDS.

Table D.1. CsDS concentrations in water – intermediate liquid crystal experiment

[mM]	%wt	[g] crystals	[g] CsDS	[g] water	conc.
132	5%	0.1308±0.0001000	0.1479±0.0001131	2.7784±0.0001000	**0.05054**±0.001211
132	5%	0.1303±0.0001000	0.1473±0.0001131	2.6277±0.0001000	**0.05308**±0.001303
132	5%	0.1271±0.0001000	0.1437±0.0001131	2.8355±0.0001000	**0.04823**±0.001150
270	10%	0.1585±0.0001000	0.1794±0.0001131	1.6459±0.0001000	**0.09828**±0.002894
270	10%	0.1552±0.0001000	0.1755±0.0001131	1.6137±0.0001000	**0.09808**±0.002919
270	10%	0.1485±0.0001000	0.1679±0.0001131	1.4986±0.0001000	**0.10075**±0.0031074
443	15%	0.1201±0.0001000	0..1358±0.0001131	0.7663±0.0001000	**0.15053**±0.0062846
443	15%	0.1099±0.0001000	0.1242±0.0001131	0.7868±0.0001000	**0.13633**±0.0056871
443	15%	0.1055±0.0001000	0.1193±0.0001131	0.6518±0.0001000	**0.15471**±0.0070011
627	20%	0.0963±0.0001000	0.1089±0.0001131	0.0399±0.0001000	**0.21441**±0.011899
627	20%	0.0309±0.0001000	0.0361±0.0001131	0.1408±0.0001000	**0.20407**±0.019906

Table D.2. SDS concentrations in water - intermediate liquid crystal experiment

[mM]	%wt	[g] SDS	[g] water	conc.
132	4%	0.0583±0.0001	1.5475±0.0001000	**0.03631**±0.0006236
132	4%	0.0553±0.0001	1.4641±0.0001000	**0.03639**±0.0006590
132	4%	0.0518±0.0001	1.3700±0.0001000	**0.03643**±0.0007042
270	7%	0.0718±0.0001	0.9503±0.0001000	**0.07024**±0.0007832
270	7%	0.0905±0.0001	1.1990±0.0001000	**0.07018**±0.0007793
270	7%	0.1180±0.0001	1.5519±0.0001000	**0.07066**±0.0006018
443	11%	0.1823±0.0001	1.4850±0.0001000	**0.10933**±0.00060690
443	11%	0.1940±0.0001	1.1580±0.0001000	**0.11124**±0.00060707
443	11%	0.1855±0.0001	1.482±0.0001000	**0.14349**±0.00075472
627	15%	0.2016±0.0001	1.1596±0.0001000	**0.14811**±0.00075058
627	15%	0.1985±0.0001	1.1305±0.0001000	**0.14936**±0.00076904

APPENDIX E

STATISTICAL TOOL

Number of independent samples needed - Statistical tool

A statistical test would show the number of independent samples that are needed, in order for the measured temperatures to have a deviation of ± 0.5 [ºC] from the actual value of the Krafft Temperature.

The test is called: “Type 1-Error Rate A” [111].

μ is the deviation of a measured Krafft temperature from the actual Krafft temperature of the sample,

σ is the standard deviation of the data set

H_o: $\mu=0$ (zero hypothesis)

H_α: $\mu=\mu^*=0.5$ (alternative hypothesis)

H_o is rejected:

i . With a probability $1-\beta$, when H_α is true

$P(x_{average} > (Z_\alpha * \sigma/\sqrt{n})/ H_\alpha \text{ true}) = 1-\beta$

ii. With a probability α, when H_o is true

$P(x_{average} > (Z_\alpha * \sigma/\sqrt{n})/ H_o \text{ true}) = \alpha$

Acceptable size of measurements:

If the upper α% point of the standard normal distribution function is Z_α, the least minimum number of samples that are needed, will be given by the equation:

$n \geq [(\Phi^{-1} (1-\beta) + Z_\alpha) * \sigma/\mu]^{\wedge 2}$, where Φ is the cumulative normal distribution function and Φ^{-1} is the probit function **[113].**

For example, starting with a data set with the following numbers:

$\sigma = 0.69$ (a standard deviation of an initial set of samples)

$\beta=0.95$

$\alpha=1$

$$Z\_\alpha=1.01*0.5=0.505$$

$\Phi^{-1}(0.05)=1.83$

$n\geq 11$ (independent samples needed)

In these studies, 3 independent samples have been used. These are less than 11.The findings with 3 samples, though, could represent a first approach of the actual Krafft temperature.

APPENDIX F

BILAYERS

Bilayers are double-layered surfactant aggregates. The bilayers are formed by the assembly of two surfactant monolayers. The two monolayers are separated by penetrating water molecules. This conformation results in the formation of a thin water film of constant density. The hydrophobic domains (hydrocarbon chains) form an inner film that is separated by an outside hydrophilic film. This hydrophilic film, which lies on the outside, is formed by the polar head groups that are bound with the hydrated counterion and with solvent molecules that diffuse freely through the bilayer (hydrophilic part) **[38]**, **[114]**.

According to Israelachvili J.N. (1992), a surfactant molecule is possible to form bilayers if the CPP is above 0.5 and less or equal to 1 **[45]**, [**114]**. Curved bilayers form vesicular structures. An example can be the case of lecithin aggregates in aqueous solutions **[16]**.

In the case of bilayers, the optimal polar head group area is reduced, compared to a spherical micelle of the same solution. This reduces the mean structure curvature. This reduction of the optimal head group area favors the arrangement of more surfactant molecules into a larger colloidal aggregate in the case of bilayers compared to the micelles. Therefore, following Israelachvili J.N. (1992), the bilayered lamellar structure is a more ordered structure, compared to the micelles **[45]**.

APPENDIX G

PERMISSIONS AND LICENSE AGREEMENTS

G.1. Permission for Figure 1.1.

- **Subject:** **RE: Permission request in order to reproduce a figure of the CTAB molecule from your website**
- From: Pechous, Steve (NIH/NLM/NCBI) [C] <pechous@ncbi.nlm.nih.gov> +
- Date: Tue, 19 Jan 2010 20:29:46-0500
- To: vagia001@umn.edu <vagia001@umn.edu> +
- Report this message as spam

Dear Colleague,

I apologize for the delay in response to your email. You can use these images for your academic endeavors as long as you acknowledge the source (the URL of the page where you obtain the image is fine).

Regards,

Steve Pechous, Ph.D.
NCBI Public Services

From: vagia001@umn.edu [vagia001@umn.edu]
Sent: Friday, January 15, 2010 8:53 AM
To: NLM/NCBI Info
Subject: Permission request in order to reproduce a figure of the CTAB molecule from your website

Dear Sir/Madam:

Good afternoon.I have been the last graduate student of Professor H.Ted Davis at the Chemical Engineering and Materials Science Department at the Univeristy of Minnesota. I would like to request permission from you (the copyright holder), in order to reproduce with permission, an original Figure that represents the CTAB molecule in the website:
http://pubchem.ncbi.nlm.nih.gov/summary/summary.cgi?cid=5974

After your permission is granted, the figure will serve as part of the theoretical background of my Masters Thesis at the Chemical Engineering and Materials Science Department at the University of Minnesota. The title of my thesis is 'Cesium dodecyl sulphate phase behavior in aqueous solutions and it comparison with the SDS/water phase diagram'. Upon your request,I can send to you and to the article's authors my thesis so that you can review it.
The time is stringent, regarding the deadline of the submission of my thesis to the Graduate School for this Spring semester.I would appreciate if you could reply to me within the next few days.

Waiting for your prompt attention,
Apostolos Vagias

G.2.Permission (as license agreement between Apostolos Nikolaou Vagias and Elsevier Inc.– Copyright Clearance Company Inc.) for Figure 1.3.

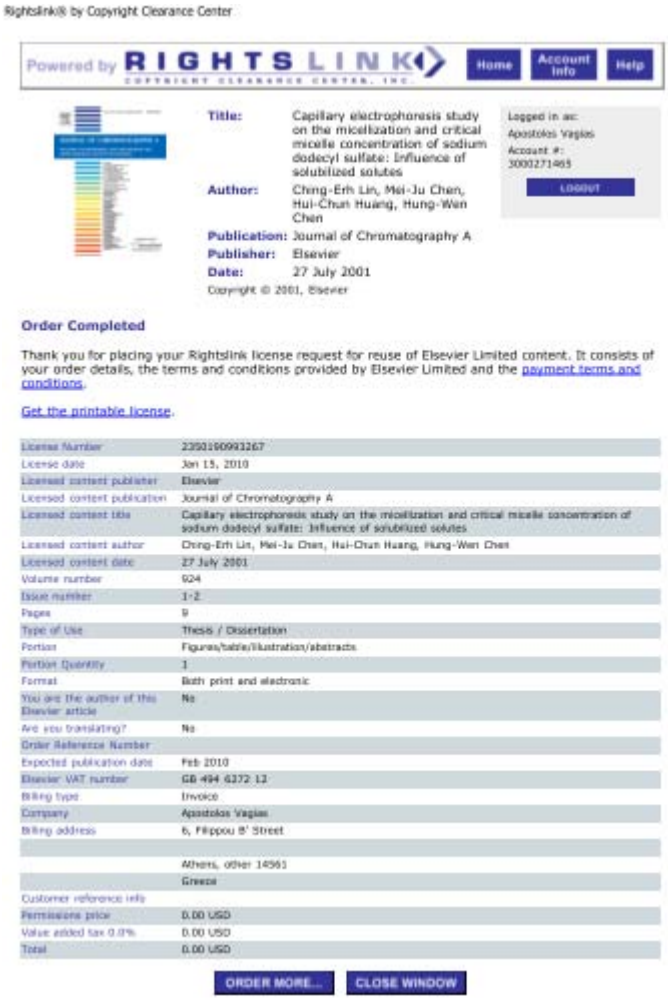

Rightslink® by Copyright Clearance Center

Powered by RIGHTSLINK

Home | Account Info | Help

Title: Capillary electrophoresis study on the micellization and critical micelle concentration of sodium dodecyl sulfate: Influence of solubilized solutes

Author: Ching-Erh Lin, Mei-Ju Chen, Hui-Chun Huang, Hung-Wen Chen

Publication: Journal of Chromatography A

Publisher: Elsevier

Date: 27 July 2001

Copyright © 2001, Elsevier

Logged in as: Apostolos Vagias
Account #: 3000271465
LOGOUT

Order Completed

Thank you for placing your Rightslink license request for reuse of Elsevier Limited content. It consists of your order details, the terms and conditions provided by Elsevier Limited and the payment terms and conditions.

Get the printable license.

License Number	2350190993267
License date	Jan 15, 2010
Licensed content publisher	Elsevier
Licensed content publication	Journal of Chromatography A
Licensed content title	Capillary electrophoresis study on the micellization and critical micelle concentration of sodium dodecyl sulfate: Influence of solubilized solutes
Licensed content author	Ching-Erh Lin, Mei-Ju Chen, Hui-Chun Huang, Hung-Wen Chen
Licensed content date	27 July 2001
Volume number	924
Issue number	1-2
Pages	9
Type of Use	Thesis / Dissertation
Portion	Figures/table/illustration/abstracts
Portion Quantity	1
Format	Both print and electronic
You are the author of this Elsevier article	No
Are you translating?	No
Order Reference Number	
Expected publication date	Feb 2010
Elsevier VAT number	GB 494 6272 12
Billing type	Invoice
Company	Apostolos Vagias
Billing address	6, Filippou B' Street
	Athens, other 14561
	Greece
Customer reference info	
Permissions price	0.00 USD
Value added tax 0.0%	0.00 USD
Total	0.00 USD

ORDER MORE... | CLOSE WINDOW

ELSEVIER LICENSE
TERMS AND CONDITIONS

Jan 15, 2010

This is a License Agreement between Apostolos Vagias ("You") and Elsevier ("Elsevier") provided by Copyright Clearance Center ("CCC"). The license consists of your order details, the terms and conditions provided by Elsevier, and the payment terms and conditions.

All payments must be made in full to CCC. For payment instructions, please see information listed at the bottom of this form.

Supplier	Elsevier Limited The Boulevard,Langford Lane Kidlington,Oxford,OX5 1GB,UK
Registered Company Number	1982084
Customer name	Apostolos Vagias
Customer address	6, Filippou B' Street Athens, other 14561
License Number	2350190993267
License date	Jan 15, 2010
Licensed content publisher	Elsevier
Licensed content publication	Journal of Chromatography A
Licensed content title	Capillary electrophoresis study on the micellization and critical micelle concentration of sodium dodecyl sulfate: Influence of solubilized solutes
Licensed content author	Ching-Erh Lin, Mei-Ju Chen, Hui-Chun Huang, Hung-Wen Chen
Licensed content date	27 July 2001
Volume number	924
Issue number	1-2
Pages	9
Type of Use	Thesis / Dissertation
Portion	Figures/table/illustration/abstracts
Portion Quantity	1
Format	Both print and electronic
You are an author of the Elsevier article	No
Are you translating?	No
Order Reference Number	
Expected publication date	Feb 2010
Elsevier VAT number	GB 494 6272 12
Permissions price	0.00 USD
Value added tax 0.0%	0.00 USD

Total 0.00 USD

Terms and Conditions

INTRODUCTION

1. The publisher for this copyrighted material is Elsevier. By clicking "accept" in connection with completing this licensing transaction, you agree that the following terms and conditions apply to this transaction (along with the Billing and Payment terms and conditions established by Copyright Clearance Center, Inc. ("CCC"), at the time that you opened your Rightslink account and that are available at any time at http://myaccount.copyright.com).

GENERAL TERMS

2. Elsevier hereby grants you permission to reproduce the aforementioned material subject to the terms and conditions indicated.

3. Acknowledgement: If any part of the material to be used (for example, figures) has appeared in our publication with credit or acknowledgement to another source, permission must also be sought from that source. If such permission is not obtained then that material may not be included in your publication/copies. Suitable acknowledgement to the source must be made, either as a footnote or in a reference list at the end of your publication, as follows:

"Reprinted from Publication title, Vol /edition number, Author(s), Title of article / title of chapter, Pages No., Copyright (Year), with permission from Elsevier [OR APPLICABLE SOCIETY COPYRIGHT OWNER]." Also Lancet special credit - "Reprinted from The Lancet, Vol. number, Author(s), Title of article, Pages No., Copyright (Year), with permission from Elsevier."

4. Reproduction of this material is confined to the purpose and/or media for which permission is hereby given.

5. Altering/Modifying Material: Not Permitted. However figures and illustrations may be altered/adapted minimally to serve your work. Any other abbreviations, additions, deletions and/or any other alterations shall be made only with prior written authorization of Elsevier Ltd. (Please contact Elsevier at permissions@elsevier.com)

6. If the permission fee for the requested use of our material is waived in this instance, please be advised that your future requests for Elsevier materials may attract a fee.

7. Reservation of Rights: Publisher reserves all rights not specifically granted in the combination of (i) the license details provided by you and accepted in the course of this licensing transaction, (ii) these terms and conditions and (iii) CCC's Billing and Payment terms and conditions.

8. License Contingent Upon Payment: While you may exercise the rights licensed immediately upon issuance of the license at the end of the licensing process for the transaction, provided that you have disclosed complete and accurate details of your proposed use, no license is finally effective unless and until full payment is received from you (either by publisher or by CCC) as provided in CCC's Billing and Payment terms and conditions. If full payment is not received on a timely basis, then any license preliminarily granted shall be deemed automatically revoked and shall be void as if never granted. Further, in the event that you breach any of these terms and conditions or any of CCC's Billing and Payment

terms and conditions, the license is automatically revoked and shall be void as if never granted. Use of materials as described in a revoked license, as well as any use of the materials beyond the scope of an unrevoked license, may constitute copyright infringement and publisher reserves the right to take any and all action to protect its copyright in the materials.

9. Warranties: Publisher makes no representations or warranties with respect to the licensed material.

10. Indemnity: You hereby indemnify and agree to hold harmless publisher and CCC, and their respective officers, directors, employees and agents, from and against any and all claims arising out of your use of the licensed material other than as specifically authorized pursuant to this license.

11. No Transfer of License: This license is personal to you and may not be sublicensed, assigned, or transferred by you to any other person without publisher's written permission.

12. No Amendment Except in Writing: This license may not be amended except in a writing signed by both parties (or, in the case of publisher, by CCC on publisher's behalf).

13. Objection to Contrary Terms: Publisher hereby objects to any terms contained in any purchase order, acknowledgment, check endorsement or other writing prepared by you, which terms are inconsistent with these terms and conditions or CCC's Billing and Payment terms and conditions. These terms and conditions, together with CCC's Billing and Payment terms and conditions (which are incorporated herein), comprise the entire agreement between you and publisher (and CCC) concerning this licensing transaction. In the event of any conflict between your obligations established by these terms and conditions and those established by CCC's Billing and Payment terms and conditions, these terms and conditions shall control.

14. Revocation: Elsevier or Copyright Clearance Center may deny the permissions described in this License at their sole discretion, for any reason or no reason, with a full refund payable to you. Notice of such denial will be made using the contact information provided by you. Failure to receive such notice will not alter or invalidate the denial. In no event will Elsevier or Copyright Clearance Center be responsible or liable for any costs, expenses or damage incurred by you as a result of a denial of your permission request, other than a refund of the amount(s) paid by you to Elsevier and/or Copyright Clearance Center for denied permissions.

LIMITED LICENSE

The following terms and conditions apply only to specific license types:

15. **Translation:** This permission is granted for non-exclusive world **English** rights only unless your license was granted for translation rights. If you licensed translation rights you may only translate this content into the languages you requested. A professional translator must perform all translations and reproduce the content word for word preserving the integrity of the article. If this license is to reuse 1 or 2 figures then permission is granted for non-exclusive world rights in all languages.

16. **Website:** The following terms and conditions apply to electronic reserve and author websites:
Electronic reserve: If licensed material is to be posted to website, the web site is to be password-protected and made available only to bona fide students registered on a relevant

course if:
This license was made in connection with a course,
This permission is granted for 1 year only. You may obtain a license for future website posting,
All content posted to the web site must maintain the copyright information line on the bottom of each image,
A hyper-text must be included to the Homepage of the journal from which you are licensing at http://www.sciencedirect.com/science/journal/xxxxx or the Elsevier homepage for books at http://www.elsevier.com, and
Central Storage: This license does not include permission for a scanned version of the material to be stored in a central repository such as that provided by Heron/XanEdu.

17. **Author website** for journals with the following additional clauses:

All content posted to the web site must maintain the copyright information line on the bottom of each image, and
he permission granted is limited to the personal version of your paper. You are not allowed to download and post the published electronic version of your article (whether PDF or HTML, proof or final version), nor may you scan the printed edition to create an electronic version,
A hyper-text must be included to the Homepage of the journal from which you are licensing at http://www.sciencedirect.com/science/journal/xxxxx, As part of our normal production process, you will receive an e-mail notice when your article appears on Elsevier's online service ScienceDirect (www.sciencedirect.com). That e-mail will include the article's Digital Object Identifier (DOI). This number provides the electronic link to the published article and should be included in the posting of your personal version. We ask that you wait until you receive this e-mail and have the DOI to do any posting.
Central Storage: This license does not include permission for a scanned version of the material to be stored in a central repository such as that provided by Heron/XanEdu.

18. **Author website** for books with the following additional clauses:
Authors are permitted to place a brief summary of their work online only.
A hyper-text must be included to the Elsevier homepage at http://www.elsevier.com

All content posted to the web site must maintain the copyright information line on the bottom of each image
You are not allowed to download and post the published electronic version of your chapter, nor may you scan the printed edition to create an electronic version.
Central Storage: This license does not include permission for a scanned version of the material to be stored in a central repository such as that provided by Heron/XanEdu.

19. **Website** (regular and for author): A hyper-text must be included to the Homepage of the journal from which you are licensing at http://www.sciencedirect.com/science/journal/xxxxx. or for books to the Elsevier homepage at http://www.elsevier.com

20. **Thesis/Dissertation:** If your license is for use in a thesis/dissertation your thesis may be submitted to your institution in either print or electronic form. Should your thesis be published commercially, please reapply for permission. These requirements include permission for the Library and Archives of Canada to supply single copies, on demand, of the complete thesis and include permission for UMI to supply single copies, on demand, of the complete thesis. Should your thesis be published commercially, please reapply for

permission.

21. **Other Conditions**: None

v1.6

Gratis licenses (referencing $0 in the Total field) are free. Please retain this printable license for your reference. No payment is required.

If you would like to pay for this license now, please remit this license along with your payment made payable to "COPYRIGHT CLEARANCE CENTER" otherwise you will be invoiced within 30 days of the license date. Payment should be in the form of a check or money order referencing your account number and this license number 2350190993267.
If you would prefer to pay for this license by credit card, please go to http://www.copyright.com/creditcard to download our credit card payment authorization form.

Make Payment To:
Copyright Clearance Center
Dept 001
P.O. Box 843006
Boston, MA 02284-3006

If you find copyrighted material related to this license will not be used and wish to cancel, please contact us referencing this license number 2350190993267 and noting the reason for cancellation.

Questions? customercare@copyright.com or +1-877-622-5543 (toll free in the US) or +1-978-646-2777.

G.3.Permission for Figure 1.4.

You have my permission. I don't need to see the thesis.

Gregory A. Petsko
Gyula and Katica Tauber Professor of Biochemistry and Chemistry and
Chair,
Department of Biochemistry, Brandeis University;
Adjunct Professor, Department of Neurology and Center for Neurologic
Diseases, Harvard Medical School

Address: Rosenstiel Center
Brandeis University MS 029
415 South Street
Waltham, MA 02454-9110 USA
Phone: 781-736-4903
FAX: 781-736-2405
E-mail: petsko@brandeis.edu
Web site: http://www.rose.brandeis.edu/PSlab/main.html
Administrative assistant: Ann Killeen Phone: 781-736-4905
E-mail: killeen@brandeis.edu

On Jan 15, 2010, at 6:18 AM, vagia001@umn.edu wrote:

> Dear Professor Petsko,
>
> Good afternoon from Athens, Greece.I have been the last graduate
> student of Professor H.Ted Davis at the Chemical Engineering and
> Materials Science Department at the Univeristy of Minnesota. I would
> like to request permission from you (possibly you can refer me to
> the actual copyright holder), in order to reproduce with permission,
> an original Figure that represents the tetrahedral conformation of a
> water molecule in a network of water molecules. This figure is in
> the class 104: 'Physical Chemistry of Macromolecules'.This class is
> taught at Brandeis University.
> After your permission is granted, the figure will serve as part of
> the theoretical background of my Masters Thesis at the Chemical
> Engineering
> and Materials Science Department at the University of Minnesota. The
> title of my thesis is 'Cesium dodecyl sulphate phase behavior in
> aqueous solutions and it comparison with the SDS/water phase
> diagram'. Upon your request,I can send to you and to the article's
> authors my thesis so that you can review it.
> The time is stringent, regarding the deadline of the submission of

> my thesis to the Graduate School for this Spring semester.I would
> appreciate if you could reply to me within the next few days.
>
> Waiting for your prompt attention,
> Apostolos Vagias
>

G.4.Permission for Figure 1.5.

- **Subject:** **RE: Permission request for reproduction of a figure from your article**
- From: Jacob Israelachvili <jacob@engineering.ucsb.edu>
- Date: Thu, 14 Jan 2010 14:04:36-0800
- To: vagia001@umn.edu
- Report this message as spam

Permission granted.

-Jacob Israelachvili.

Professor Jacob Israelachvili, FRS, FAA, NAE, NAS
Department of Chemical Engineering and
the Materials Department
University of California
3357 Engineering II
Santa Barbara, CA 93106-5080

Ph. 805-893-8407
Fax 805-893-7870

-----Original Message-----
From: vagia001@umn.edu [mailto:vagia001@umn.edu]
Sent: Thursday, January 14, 2010 4:36 AM
To: jacob@engineering.ucsb.edu
Subject: Permission request for reproduction of a figure from your article

Dear Professor Israelachvili:

It is my pleasure to be contacting you.I have been the last graduate student
of Regents Prof. H.Ted Davis at the University of Minnesota, at the
Chemical Engineering and Materials Science Department.I would like to
request your permission, in order to reproduce with permission the Figure
of your article of 1992 with title: 'Intermolecular and surface forces'.
Academic Press London, 2nd edition,
where the critical packing parameter is related with certain structures,
starting from spherical micelles up to the inverted micellas.
Only with your permission granted, the figure will serve as part of the
theoretical background of my masters thesis at the Chemical engineering and
Materials Science Department at the University of Minnesota. The title of
my thesis is 'Cesium dodecyl sulphate phase behavior in aqueous solutions
and it comparison with the SDS/water phase diagram'. Upon your request,I
can send you the thesis so that you can review it.

Waiting for your prompt attention,

Apostolos Vagias

Gophermail: Message Display Page 2 of 2

Waiting for your prompt attention,
Apostolos Vagias

G.5.Permission (as license agreement between Apostolos Nikolaou Vagias and Elsevier Inc. - Copyright Clearance Company Inc.) for Figure 2.5.

Rightslink® by Copyright Clearance Center

Powered by RIGHTSLINK — Home | Account Info | Help

ELSEVIER

Chapter: Chapter 1 Powder sampling
Book: Powder Sampling and Particle Size Determination
Author: Terence Allen
Publisher: Elsevier
Date: 2003
Copyright © 2003, Elsevier

Logged in as:
Apostolos Vagias
Account #:
3000271465
LOGOUT

Permission Request Placed

Thank you for placing your Rightslink license request for reuse of Elsevier Limited content.

You will receive three e-mails. The first, confirming this request which is not a license grant. You will not be charged. The second, within approximately fifteen business days, containing a link to Rightslink. Rightslink will display the custom terms and conditions and price for you to accept and finalize the order. The third, confirming the order, if placed.

PLEASE NOTE: **Licenses granted involve a fifteen-day processing period. Your permission to reuse has not yet been granted.**

Need more information about order processing?

Get the printable order details.

Order number	500553848
Order date	Jan 15, 2010 08:28 AM
Licensed Chapter Title	Chapter 1 Powder sampling
Licensed Chapter ID	9978044451564350036
Licensed content publisher	Elsevier
Licensed content publication	Elsevier Books
Book title	Powder Sampling and Particle Size Determination
Book author	Terence Allen
Publication date	2003
Type of Use	Thesis / Dissertation
Portion	Figures/table/illustration/abstracts
Portion Quantity	1
Format	Both print and electronic
You are an author of this Elsevier book?	No
Are you translating?	No
Purchase order number	
Expected publication date	
Elsevier VAT number	GB 494 6272 12
Permissions price	Not Available
Value added tax 15%	Not Available
Total	Not Available

ORDER MORE... CLOSE WINDOW

Copyright © 2010 Copyright Clearance Center, Inc. All Rights Reserved. Privacy statement.
Comments? We would like to hear from you. E-mail us at customercare@copyright.com

McAfee SECURE TESTED DAILY 15-JAN

G.6.Permission for Figure 2.7.

Date: Thu, 21 Jan 2010 10:58:54 +0800
From: Ning Tu <ntu@wspc.com.sg>
To: vagia001@umn.edu
Subject: Re: Permission request in order to reproduce a figure from the book
 of Paul F.Fewster

Dear Apostolos Vagias

Thanks for your email to us. We will be pleased to grant you the
permission provided that full acknowledgment given to the original
source. Kindly be noted that permission is granted on a non-exclusive
and one-time basis only.

With regards

Tu Ning

vagia001@umn.edu wrote:
>
> Good afternoon:
>
> Please see the forwarded message regarding my request for permission
> to reproduce a figure.
>
> Thank you,
> Apostolos Vagias
>
> ---------- Forwarded message ----------
> From: vagia001@umn.edu
> To: info@copyright.com
> Subject: Permission request in order to reproduce a figure from the
> book of Paul F.Fewster
> Date: 15 Jan 2010 07:41:27 -0600
>
>
> Dear Sir/Madam:
>
> Good morning.I have been the last graduate student of Professor H.Ted
> Davis at the Chemical Engineering and Materials Science Department at
> the Univeristy of Minnesota. I would like to request permission from
> you (the copyright holder), in order to reproduce with permission, an
> original Figure that represents the X-Ray scattering concept. This
> figure is in the book
> of Paul F.Fewster with title: 'X-ray scattering from semiconductorsâ€™,
> Imperial College Press, 2nd Edition, p.117.
> After your permission is granted, the figure will serve as part of the
> theoretical background of my Masters Thesis at the Chemical Engineering
> and Materials Science Department at the University of Minnesota. The
> title of my thesis is 'Cesium dodecyl sulphate phase behavior in
> aqueous solutions
> and it comparison with the SDS/water phase diagram'. Upon your
> request,I can send to you and to the article's authors my thesis so
> that you can review it.
> The time is stringent, regarding the deadline of the submission of my
> thesis to the Graduate School for this Spring semester.I would
> appreciate if you could reply to me within the next few days.
>
> Waiting for your prompt attention,
> Apostolos Vagias

G.7.Permission (as license agreement between Apostolos Nikolaou Vagias and Taylor Francis Group) for the Figures 3.1.(For the data of the SDS/water phase diagram that have initially been reported by Fontell et al.(1981) and 3.2.

G.8.Permission (as license agreement between Apostolos Nikolaou Vagias and Elsevier Inc.- Copyright Clearance Company Inc.) for the Figures: 3.1.(For the data of the SDS/water phase diagram that have initially been reported by Kekicheff et al.(1988) and Fontell et al.(1981), 3.3. and 5.1.

RightsLink® by Copyright Clearance Center

Powered by RIGHTSLINK — Home | Account Info | Help

Title: Phase diagram of sodium dodecyl sulfate-water system: 1. A calorimetric study
Author: P Kékicheff, C Grabielle-Madelmont, M Ollivon
Publication: Journal of Colloid and Interface Science
Publisher: Elsevier
Date: August 1989
Copyright © 1989, Elsevier

Logged in as: Apostolos Vagias
Account #: 3000271465
LOGOUT

Order Completed

Thank you for placing your Rightslink license request for reuse of Elsevier Limited content. It consists of your order details, the terms and conditions provided by Elsevier Limited and the payment terms and conditions.

Get the printable license.

License Number	2350181011901
License date	Jan 15, 2010
Licensed content publisher	Elsevier
Licensed content publication	Journal of Colloid and Interface Science
Licensed content title	Phase diagram of sodium dodecyl sulfate-water system: 1. A calorimetric study
Licensed content author	P Kékicheff, C Grabielle-Madelmont, M Ollivon
Licensed content date	August 1989
Volume number	131
Issue number	1
Pages	21
Type of Use	Thesis / Dissertation
Portion	Figures/table/illustration/abstracts
Portion Quantity	3
Format	Both print and electronic
You are the author of this Elsevier article	No
Are you translating?	No
Order Reference Number	
Expected publication date	Feb 2010
Elsevier VAT number	GB 494 6272 12
Billing type	Invoice
Company	Apostolos Vagias
Billing address	6, Filippou B' Street
	Athens, other 14561
	Greece
Customer reference info	
Permissions price	0.00 USD
Value added tax 0.0%	0.00 USD
Total	0.00 USD

ORDER MORE... | CLOSE WINDOW

Copyright © 2010 Copyright Clearance Center, Inc. All Rights Reserved. Privacy statement.
Comments? We would like to hear from you. E-mail us at customercare@copyright.com

G.9.Permission (as license agreement between Apostolos Nikolaou Vagias and Elsevier Inc.- Copyright Clearance Company Inc.) for the Figure 5.9.

Rightslink - Your Account

Powered by RIGHTSLINK

Home Help

Logged in as:
Apostolos Vagias
Account #:
3000271465
LOGOUT

License Details

Thank you for placing your Rightslink license request for reuse of Elsevier Limited content.

Get the printable license.

License Number	2350180382359
License date	Jan 15, 2010
Licensed content publisher	Elsevier
Licensed content publication	Journal of Molecular Structure
Licensed content title	Determination of the crystal structure of anhydrous sodium dodecyl sulphate using a combination of synchrotron radiation powder diffraction and molecular modelling techniques
Licensed content author	L. A. Smith, R. B. Hammond, K. J. Roberts, D. Machin, G. McLeod
Licensed content date	7 November 2000
Volume number	
Issue number	
Pages	0
Type of Use	Thesis / Dissertation
Portion	Figures/table/illustration/abstracts
Portion Quantity	1
Format	Both print and electronic
You are the author of this Elsevier article	No
Are you translating?	No
Order Reference Number	
Expected publication date	Feb 2010
Elsevier VAT number	GB 494 6272 12
Billing type	Invoice
Company	Apostolos Vagias
Billing address	6, Filippou B' Street
	Athens, other 14561
	Greece
Customer reference info	
Permissions price	0.00 USD
Value added tax 0.0%	0.00 USD
Total	0.00 USD

BACK

ELSEVIER LICENSE
TERMS AND CONDITIONS

Jan 15, 2010

This is a License Agreement between Apostolos Vagias ("You") and Elsevier ("Elsevier") provided by Copyright Clearance Center ("CCC"). The license consists of your order details, the terms and conditions provided by Elsevier, and the payment terms and conditions.

All payments must be made in full to CCC. For payment instructions, please see information listed at the bottom of this form.

Supplier	Elsevier Limited The Boulevard,Langford Lane Kidlington,Oxford,OX5 1GB,UK
Registered Company Number	1982084
Customer name	Apostolos Vagias
Customer address	6, Filippou B' Street Athens, other 14561
License Number	2350180382359
License date	Jan 15, 2010
Licensed content publisher	Elsevier
Licensed content publication	Journal of Molecular Structure
Licensed content title	Determination of the crystal structure of anhydrous sodium dodecyl sulphate using a combination of synchrotron radiation powder diffraction and molecular modelling techniques
Licensed content author	L. A. Smith, R. B. Hammond, K. J. Roberts, D. Machin, G. McLeod
Licensed content date	7 November 2000
Volume number	
Issue number	
Pages	0
Type of Use	Thesis / Dissertation
Portion	Figures/table/illustration/abstracts
Portion Quantity	1
Format	Both print and electronic
You are an author of the Elsevier article	No
Are you translating?	No
Order Reference Number	
Expected publication date	Feb 2010
Elsevier VAT number	GB 494 6272 12
Permissions price	0.00 USD
Value added tax 0.0%	0.00 USD

Total 0.00 USD

Terms and Conditions

INTRODUCTION

1. The publisher for this copyrighted material is Elsevier. By clicking "accept" in connection with completing this licensing transaction, you agree that the following terms and conditions apply to this transaction (along with the Billing and Payment terms and conditions established by Copyright Clearance Center, Inc. ("CCC"), at the time that you opened your Rightslink account and that are available at any time at http://myaccount.copyright.com).

GENERAL TERMS

2. Elsevier hereby grants you permission to reproduce the aforementioned material subject to the terms and conditions indicated.

3. Acknowledgement: If any part of the material to be used (for example, figures) has appeared in our publication with credit or acknowledgement to another source, permission must also be sought from that source. If such permission is not obtained then that material may not be included in your publication/copies. Suitable acknowledgement to the source must be made, either as a footnote or in a reference list at the end of your publication, as follows:

"Reprinted from Publication title, Vol /edition number, Author(s), Title of article / title of chapter, Pages No., Copyright (Year), with permission from Elsevier [OR APPLICABLE SOCIETY COPYRIGHT OWNER]." Also Lancet special credit - "Reprinted from The Lancet, Vol. number, Author(s), Title of article, Pages No., Copyright (Year), with permission from Elsevier."

4. Reproduction of this material is confined to the purpose and/or media for which permission is hereby given.

5. Altering/Modifying Material: Not Permitted. However figures and illustrations may be altered/adapted minimally to serve your work. Any other abbreviations, additions, deletions and/or any other alterations shall be made only with prior written authorization of Elsevier Ltd. (Please contact Elsevier at permissions@elsevier.com)

6. If the permission fee for the requested use of our material is waived in this instance, please be advised that your future requests for Elsevier materials may attract a fee.

7. Reservation of Rights: Publisher reserves all rights not specifically granted in the combination of (i) the license details provided by you and accepted in the course of this licensing transaction, (ii) these terms and conditions and (iii) CCC's Billing and Payment terms and conditions.

8. License Contingent Upon Payment: While you may exercise the rights licensed immediately upon issuance of the license at the end of the licensing process for the transaction, provided that you have disclosed complete and accurate details of your proposed use, no license is finally effective unless and until full payment is received from you (either by publisher or by CCC) as provided in CCC's Billing and Payment terms and conditions. If full payment is not received on a timely basis, then any license preliminarily granted shall be

that you breach any of these terms and conditions or any of CCC's Billing and Payment terms and conditions, the license is automatically revoked and shall be void as if never granted. Use of materials as described in a revoked license, as well as any use of the materials beyond the scope of an unrevoked license, may constitute copyright infringement and publisher reserves the right to take any and all action to protect its copyright in the materials.

9. Warranties: Publisher makes no representations or warranties with respect to the licensed material.

10. Indemnity: You hereby indemnify and agree to hold harmless publisher and CCC, and their respective officers, directors, employees and agents, from and against any and all claims arising out of your use of the licensed material other than as specifically authorized pursuant to this license.

11. No Transfer of License: This license is personal to you and may not be sublicensed, assigned, or transferred by you to any other person without publisher's written permission.

12. No Amendment Except in Writing: This license may not be amended except in a writing signed by both parties (or, in the case of publisher, by CCC on publisher's behalf).

13. Objection to Contrary Terms: Publisher hereby objects to any terms contained in any purchase order, acknowledgment, check endorsement or other writing prepared by you, which terms are inconsistent with these terms and conditions or CCC's Billing and Payment terms and conditions. These terms and conditions, together with CCC's Billing and Payment terms and conditions (which are incorporated herein), comprise the entire agreement between you and publisher (and CCC) concerning this licensing transaction. In the event of any conflict between your obligations established by these terms and conditions and those established by CCC's Billing and Payment terms and conditions, these terms and conditions shall control.

14. Revocation: Elsevier or Copyright Clearance Center may deny the permissions described in this License at their sole discretion, for any reason or no reason, with a full refund payable to you. Notice of such denial will be made using the contact information provided by you. Failure to receive such notice will not alter or invalidate the denial. In no event will Elsevier or Copyright Clearance Center be responsible or liable for any costs, expenses or damage incurred by you as a result of a denial of your permission request, other than a refund of the amount(s) paid by you to Elsevier and/or Copyright Clearance Center for denied permissions.

LIMITED LICENSE

The following terms and conditions apply only to specific license types:

15. **Translation:** This permission is granted for non-exclusive world **English** rights only unless your license was granted for translation rights. If you licensed translation rights you may only translate this content into the languages you requested. A professional translator must perform all translations and reproduce the content word for word preserving the integrity of the article. If this license is to re-use 1 or 2 figures then permission is granted for non-exclusive world rights in all languages.

16. **Website:** The following terms and conditions apply to electronic reserve and author websites:
Electronic reserve: If licensed material is to be posted to website, the web site is to be

password-protected and made available only to bona fide students registered on a relevant course if:
This license was made in connection with a course,
This permission is granted for 1 year only. You may obtain a license for future website posting,
All content posted to the web site must maintain the copyright information line on the bottom of each image,
A hyper-text must be included to the Homepage of the journal from which you are licensing at http://www.sciencedirect.com/science/journal/xxxxx or the Elsevier homepage for books at http://www.elsevier.com, and
Central Storage: This license does not include permission for a scanned version of the material to be stored in a central repository such as that provided by Heron/XanEdu.

17. **Author website** for journals with the following additional clauses:

All content posted to the web site must maintain the copyright information line on the bottom of each image, and
he permission granted is limited to the personal version of your paper. You are not allowed to download and post the published electronic version of your article (whether PDF or HTML, proof or final version), nor may you scan the printed edition to create an electronic version,
A hyper-text must be included to the Homepage of the journal from which you are licensing at http://www.sciencedirect.com/science/journal/xxxxx. As part of our normal production process, you will receive an e-mail notice when your article appears on Elsevier's online service ScienceDirect (www.sciencedirect.com). That e-mail will include the article's Digital Object Identifier (DOI). This number provides the electronic link to the published article and should be included in the posting of your personal version. We ask that you wait until you receive this e-mail and have the DOI to do any posting.
Central Storage: This license does not include permission for a scanned version of the material to be stored in a central repository such as that provided by Heron/XanEdu.

18. **Author website** for books with the following additional clauses:
Authors are permitted to place a brief summary of their work online only.
A hyper-text must be included to the Elsevier homepage at http://www.elsevier.com

All content posted to the web site must maintain the copyright information line on the bottom of each image
You are not allowed to download and post the published electronic version of your chapter, nor may you scan the printed edition to create an electronic version.
Central Storage: This license does not include permission for a scanned version of the material to be stored in a central repository such as that provided by Heron/XanEdu.

19. **Website** (regular and for author): A hyper-text must be included to the Homepage of the journal from which you are licensing at http://www.sciencedirect.com/science/journal/xxxxx. or for books to the Elsevier homepage at http://www.elsevier.com

20. **Thesis/Dissertation**: If your license is for use in a thesis/dissertation your thesis may be submitted to your institution in either print or electronic form. Should your thesis be published commercially, please reapply for permission. These requirements include permission for the Library and Archives of Canada to supply single copies, on demand, of

the complete thesis. Should your thesis be published commercially, please reapply for permission.

21. **Other Conditions**: None

v1.6

Gratis licenses (referencing $0 in the Total field) are free. Please retain this printable license for your reference. No payment is required.

If you would like to pay for this license now, please remit this license along with your payment made payable to "COPYRIGHT CLEARANCE CENTER" otherwise you will be invoiced within 30 days of the license date. Payment should be in the form of a check or money order referencing your account number and this license number 2350180382359.
If you would prefer to pay for this license by credit card, please go to http://www.copyright.com/creditcard to download our credit card payment authorization form.

Make Payment To:
Copyright Clearance Center
Dept 001
P.O. Box 843006
Boston, MA 02284-3006

If you find copyrighted material related to this license will not be used and wish to cancel, please contact us referencing this license number 2350180382359 and noting the reason for cancellation.

Questions? customercare@copyright.com or +1-877-622-5543 (toll free in the US) or +1-978-646-2777.

G.10.Permission (as license agreement between Apostolos Nikolaou Vagias and Elsevier Inc.- Copyright Clearance Company Inc.) for the Figure 7.1.

Rightslink® by Copyright Clearance Center

Powered by RIGHTSLINK

Home | Account Info | Help

Title: Formation of intermediate micellar phase between hexagonal and discontinuous cubic liquid crystals in brine/N-acylamino acid surfactant/N-acylamino acid oil system

Author: Yuji Yamashita, Hironobu Kunieda, Eiko Oshimura, Kazutami Sakamoto

Publication: Journal of Colloid and Interface Science

Publisher: Elsevier

Date: 1 August 2007

Copyright © 2007, Elsevier

Logged in as:
Apostolos Vagias
Account #:
3000271465

LOGOUT

Order Completed

Thank you for placing your Rightslink license request for reuse of Elsevier Limited content. It consists of your order details, the terms and conditions provided by Elsevier Limited and the payment terms and conditions.

Get the printable license.

License Number	2390190127335
License date	Jan 15, 2010
Licensed content publisher	Elsevier
Licensed content publication	Journal of Colloid and Interface Science
Licensed content title	Formation of intermediate micellar phase between hexagonal and discontinuous cubic liquid crystals in brine/N-acylamino acid surfactant/N-acylamino acid oil system
Licensed content author	Yuji Yamashita, Hironobu Kunieda, Eiko Oshimura, Kazutami Sakamoto
Licensed content date	1 August 2007
Volume number	312
Issue number	1
Pages	7
Type of Use	Thesis / Dissertation
Portion	Figures/table/illustration/abstracts
Portion Quantity	1
Format	Both print and electronic
You are the author of this Elsevier article	No
Are you translating?	No
Order Reference Number	
Expected publication date	Feb 2010
Elsevier VAT number	GB 494 6272 12
Billing type	Invoice
Company	Apostolos Vagias
Billing address	6, Filippou B' Street
	Athens, other 14561
	Greece
Customer reference info	
Permissions price	0.00 USD
Value added tax 0.0%	0.00 USD
Total	0.00 USD

https://s100.copyright.com/AppDispatchServlet[15/1/2010 3:01:25 μμ]

ELSEVIER LICENSE
TERMS AND CONDITIONS

Jan 15, 2010

This is a License Agreement between Apostolos Vagias ("You") and Elsevier ("Elsevier") provided by Copyright Clearance Center ("CCC"). The license consists of your order details, the terms and conditions provided by Elsevier, and the payment terms and conditions.

All payments must be made in full to CCC. For payment instructions, please see information listed at the bottom of this form.

Supplier	Elsevier Limited The Boulevard,Langford Lane Kidlington,Oxford,OX5 1GB,UK
Registered Company Number	1982084
Customer name	Apostolos Vagias
Customer address	6, Filippou B' Street
	Athens, other 14561
License Number	2350190127335
License date	Jan 15, 2010
Licensed content publisher	Elsevier
Licensed content publication	Journal of Colloid and Interface Science
Licensed content title	Formation of intermediate micellar phase between hexagonal and discontinuous cubic liquid crystals in brine/N-acylamino acid surfactant/N-acylamino acid oil system
Licensed content author	Yuji Yamashita, Hironobu Kunieda, Eiko Oshimura, Kazutami Sakamoto
Licensed content date	1 August 2007
Volume number	312
Issue number	1
Pages	7
Type of Use	Thesis / Dissertation
Portion	Figures/table/illustration/abstracts
Portion Quantity	1
Format	Both print and electronic
You are an author of the Elsevier article	No
Are you translating?	No
Order Reference Number	
Expected publication date	Feb 2010
Elsevier VAT number	GB 494 6272 12
Permissions price	0.00 USD

Value added tax 0.0%	0.00 USD
Total	0.00 USD

Terms and Conditions

INTRODUCTION

1. The publisher for this copyrighted material is Elsevier. By clicking "accept" in connection with completing this licensing transaction, you agree that the following terms and conditions apply to this transaction (along with the Billing and Payment terms and conditions established by Copyright Clearance Center, Inc. ("CCC"), at the time that you opened your Rightslink account and that are available at any time at http://myaccount.copyright.com).

GENERAL TERMS

2. Elsevier hereby grants you permission to reproduce the aforementioned material subject to the terms and conditions indicated.

3. Acknowledgement: If any part of the material to be used (for example, figures) has appeared in our publication with credit or acknowledgement to another source, permission must also be sought from that source. If such permission is not obtained then that material may not be included in your publication/copies. Suitable acknowledgement to the source must be made, either as a footnote or in a reference list at the end of your publication, as follows:

"Reprinted from Publication title, Vol /edition number, Author(s), Title of article / title of chapter, Pages No., Copyright (Year), with permission from Elsevier [OR APPLICABLE SOCIETY COPYRIGHT OWNER]." Also Lancet special credit - "Reprinted from The Lancet, Vol. number, Author(s), Title of article, Pages No., Copyright (Year), with permission from Elsevier."

4. Reproduction of this material is confined to the purpose and/or media for which permission is hereby given.

5. Altering/Modifying Material: Not Permitted. However figures and illustrations may be altered/adapted minimally to serve your work. Any other abbreviations, additions, deletions and/or any other alterations shall be made only with prior written authorization of Elsevier Ltd. (Please contact Elsevier at permissions@elsevier.com)

6. If the permission fee for the requested use of our material is waived in this instance, please be advised that your future requests for Elsevier materials may attract a fee.

7. Reservation of Rights: Publisher reserves all rights not specifically granted in the combination of (i) the license details provided by you and accepted in the course of this licensing transaction, (ii) these terms and conditions and (iii) CCC's Billing and Payment terms and conditions.

8. License Contingent Upon Payment: While you may exercise the rights licensed immediately upon issuance of the license at the end of the licensing process for the transaction, provided that you have disclosed complete and accurate details of your proposed use, no license is finally effective unless and until full payment is received from you (either by publisher or by CCC) as provided in CCC's Billing and Payment terms and conditions. If

full payment is not received on a timely basis, then any license preliminarily granted shall be deemed automatically revoked and shall be void as if never granted. Further, in the event that you breach any of these terms and conditions or any of CCC's Billing and Payment terms and conditions, the license is automatically revoked and shall be void as if never granted. Use of materials as described in a revoked license, as well as any use of the materials beyond the scope of an unrevoked license, may constitute copyright infringement and publisher reserves the right to take any and all action to protect its copyright in the materials.

9. Warranties: Publisher makes no representations or warranties with respect to the licensed material.

10. Indemnity: You hereby indemnify and agree to hold harmless publisher and CCC, and their respective officers, directors, employees and agents, from and against any and all claims arising out of your use of the licensed material other than as specifically authorized pursuant to this license.

11. No Transfer of License: This license is personal to you and may not be sublicensed, assigned, or transferred by you to any other person without publisher's written permission.

12. No Amendment Except in Writing: This license may not be amended except in a writing signed by both parties (or, in the case of publisher, by CCC on publisher's behalf).

13. Objection to Contrary Terms: Publisher hereby objects to any terms contained in any purchase order, acknowledgment, check endorsement or other writing prepared by you, which terms are inconsistent with these terms and conditions or CCC's Billing and Payment terms and conditions. These terms and conditions, together with CCC's Billing and Payment terms and conditions (which are incorporated herein), comprise the entire agreement between you and publisher (and CCC) concerning this licensing transaction. In the event of any conflict between your obligations established by these terms and conditions and those established by CCC's Billing and Payment terms and conditions, these terms and conditions shall control.

14. Revocation: Elsevier or Copyright Clearance Center may deny the permissions described in this License at their sole discretion, for any reason or no reason, with a full refund payable to you. Notice of such denial will be made using the contact information provided by you. Failure to receive such notice will not alter or invalidate the denial. In no event will Elsevier or Copyright Clearance Center be responsible or liable for any costs, expenses or damage incurred by you as a result of a denial of your permission request, other than a refund of the amount(s) paid by you to Elsevier and/or Copyright Clearance Center for denied permissions.

LIMITED LICENSE

The following terms and conditions apply only to specific license types:

15. **Translation:** This permission is granted for non-exclusive world **English** rights only unless your license was granted for translation rights. If you licensed translation rights you may only translate this content into the languages you requested. A professional translator must perform all translations and reproduce the content word for word preserving the integrity of the article. If this license is to re-use 1 or 2 figures then permission is granted for non-exclusive world rights in all languages.

16. **Website:** The following terms and conditions apply to electronic reserve and author

websites:
Electronic reserve: If licensed material is to be posted to website, the web site is to be password-protected and made available only to bona fide students registered on a relevant course if:
This license was made in connection with a course,
This permission is granted for 1 year only. You may obtain a license for future website posting,
All content posted to the web site must maintain the copyright information line on the bottom of each image,
A hyper-text must be included to the Homepage of the journal from which you are licensing at http://www.sciencedirect.com/science/journal/xxxxx or the Elsevier homepage for books at http://www.elsevier.com, and
Central Storage: This license does not include permission for a scanned version of the material to be stored in a central repository such as that provided by Heron/XanEdu.

17. **Author website** for journals with the following additional clauses:

All content posted to the web site must maintain the copyright information line on the bottom of each image, and
he permission granted is limited to the personal version of your paper. You are not allowed to download and post the published electronic version of your article (whether PDF or HTML, proof or final version), nor may you scan the printed edition to create an electronic version,
A hyper-text must be included to the Homepage of the journal from which you are licensing at http://www.sciencedirect.com/science/journal/xxxxx, As part of our normal production process, you will receive an e-mail notice when your article appears on Elsevier's online service ScienceDirect (www.sciencedirect.com). That e-mail will include the article's Digital Object Identifier (DOI). This number provides the electronic link to the published article and should be included in the posting of your personal version. We ask that you wait until you receive this e-mail and have the DOI to do any posting.
Central Storage: This license does not include permission for a scanned version of the material to be stored in a central repository such as that provided by Heron/XanEdu.

18. **Author website** for books with the following additional clauses:
Authors are permitted to place a brief summary of their work online only.
A hyper-text must be included to the Elsevier homepage at http://www.elsevier.com

All content posted to the web site must maintain the copyright information line on the bottom of each image
You are not allowed to download and post the published electronic version of your chapter, nor may you scan the printed edition to create an electronic version.
Central Storage: This license does not include permission for a scanned version of the material to be stored in a central repository such as that provided by Heron/XanEdu.

19. **Website** (regular and for author): A hyper-text must be included to the Homepage of the journal from which you are licensing at http://www.sciencedirect.com/science/journal/xxxxx. or for books to the Elsevier homepage at http://www.elsevier.com

20. **Thesis/Dissertation:** If your license is for use in a thesis/dissertation your thesis may be submitted to your institution in either print or electronic form. Should your thesis be published commercially, please reapply for permission. These requirements include

permission for the Library and Archives of Canada to supply single copies, on demand, of the complete thesis and include permission for UMI to supply single copies, on demand, of the complete thesis. Should your thesis be published commercially, please reapply for permission.

21. **Other Conditions**: None

v1.6

Gratis licenses (referencing $0 in the Total field) are free. Please retain this printable license for your reference. No payment is required.

If you would like to pay for this license now, please remit this license along with your payment made payable to "COPYRIGHT CLEARANCE CENTER" otherwise you will be invoiced within 30 days of the license date. Payment should be in the form of a check or money order referencing your account number and this license number 2350190127335.
If you would prefer to pay for this license by credit card, please go to http://www.copyright.com/creditcard to download our credit card payment authorization form.

Make Payment To:
Copyright Clearance Center
Dept 001
P.O. Box 843006
Boston, MA 02284-3006

If you find copyrighted material related to this license will not be used and wish to cancel, please contact us referencing this license number 2350190127335 and noting the reason for cancellation.

Questions? customercare@copyright.com or +1-877-622-5543 (toll free in the US) or +1-978-646-2777.

G.11.Permission (as license agreement between Apostolos Nikolaou Vagias and Elsevier Inc.- Copyright Clearance Company Inc.) for the Figure A.1.

Rightslink® by Copyright Clearance Center

Powered by RIGHTSLINK

Account Info | Help

Title: Ion-exchange — Theory and Practice : C.E. Harland, 2 edn., Royal society of chemistry, Cambridge, 1994 (ISBN 0-85186-484-8). xv + 285 pp. price £ 16.95
Author: Alan Dyer
Publication: Analytica Chimica Acta
Publisher: Elsevier
Date: May 10, 1995
Copyright © 1995, Elsevier

Logged in as:
Apostolos Vagias
Account #:
3000271465
LOGOUT

Order Completed

Thank you very much for your order.

This is a License Agreement between Apostolos Vagias ("You") and Elsevier ("Elsevier"). The license consists of your order details, the terms and conditions provided by Elsevier, and the payment terms and conditions.

License number	Reference confirmation email for license number
License date	Jan 14, 2010
Licensed content publisher	Elsevier
Licensed content publication	Analytica Chimica Acta
Licensed content title	Ion-exchange — Theory and Practice : C.E. Harland, 2 edn., Royal society of chemistry, Cambridge, 1994 (ISBN 0-85186-484-8). xv + 285 pp. price £ 16.95
Licensed content author	Alan Dyer
Licensed content date	10 May 1995
Volume number	306
Issue number	2-3
Pages	1
Type of Use	Thesis / Dissertation
Portion	Figures/table/illustration/abstracts
Portion Quantity	1
Format	Both print and electronic
You are the author of this Elsevier article	No
Are you translating?	No
Order Reference Number	
Expected publication date	
Elsevier VAT number	GB 494 6272 12
Billing type	Invoice
Billing address	6, Filippou B' Street
	Athens, other 14561
	Greece
Customer reference info	
Permissions price	0.00 USD
Value added tax 15%	0.00 USD
Total	0.00 USD

CLOSE WINDOW

Copyright © 2010 Copyright Clearance Center, Inc. All Rights Reserved. Privacy statement.
Comments? We would like to hear from you. E-mail us at customercare@copyright.com